The Dissertation Committee for Kris Wilcox Haggard Certifies that this is the approved version of the following dissertation:

Observations and Thermodynamic Interpretations of Polymer Blend Phase Behavior

Committee:

Donald R. Paul, Supervisor

Peter F. Green

Peter Rossky

Isaac C. Sanchez

Grant C. Willson

Observations and Thermodynamic Interpretations of Polymer Blend Phase Behavior

by

Kris Wilcox Haggard, BSE

Dissertation

Presented to the Faculty of the Graduate School of

The University of Texas at Austin

in Partial Fulfillment

of the Requirements

for the Degree of

Doctor of Philosophy

The University of Texas at Austin

December 2005

Observations and Thermodynamic Interpretations of Polymer Blend Phase Behavior

Publication No._____

Kris Wilcox Haggard, Ph.D.

The University of Texas at Austin, 2005

Supervisor: Donald R. Paul

The phase behavior of binary mixtures of several different homopolymers and copolymers was investigated and compared to the phase behavior predicted while using the Flory-Huggins theory, mean field approximation, and Sanchez-Lacombe Equation of State. Blends were prepared by a variety of methods to achieve equilibrium phase behavior and to simulate critical point miscibility criteria. The resulting blend phase behavior was evaluated by observation of glass transitions and scattered light. Collected blend phase behavior was used to characterize the enthalpic interaction between various polymer repeat units based on styrene, acrylonitrile, maleic anhydride, n-alkyl acrylates, benzyl acrylate, pentabromobenzyl acrylate, and polycarbonates. These interactions were

analyzed for consistency with related polymer miscibility regions, suggested binary interactions reported by other researchers, and predicted interactions obtained through regular solution theory. Of special interest were interactions with poly(styrene-co-acrylonitrile), which appears to contain a substantially larger intramolecular repulsion than some researchers have suggested. The implied styrene-acrylonitrile interaction and the interactions derived while using that interaction were closer to their predicted values than previous estimates. Interactions derived from blends with poly(styrene-co-maleic anhydride) were consistent when the alternating nature of the copolymer was accounted for. The phase behavior and optical properties of blends of poly(styrene-stat-acrylonitrile) and a polycarbonate copolymer were studied. These blends were not miscible, but appeared clear in certain conditions of composition and temperature. The light scattering behavior of these blends as a function of temperature was investigated. The phase behavior of blends containing copolymers made from benzyl acrylate and pentabromobenzyl acrylate was investigated. A set of interactions between styrene, methyl methacrylate, benzyl acrylate, pentabrombenzyl acrylate, and acrylonitrile was determined that could be used to predict the phase behavior in blends of copolymers.

Table of Contents

List of Tables

List of Figures

Chapter 1: Introduction

Polymer mixtures are commonly used to tailor material properties, minimize cost, or alter required processing conditions. Single-phase mixtures are often more desirable due to a gradual transition between constituent material properties as well as optical transparency. The thermodynamic interactions between blend components dictate the state of equilibrium phase behavior, and interfacial thickness and adhesion in the case of multiphase blends. Therefore, the design of polymer blends with useful properties requires an understanding of polymer-polymer interactions. Several theoretical frameworks have evolved to describe the thermodynamic interactions in terms intrinsic to the chemical character of the polymers being mixed[1-8]. One major accomplishment of these theories is the description of the phase behavior of blends with respect to molecular weight, mixture composition, and temperature. The thermodynamic framework has also been used to describe material properties such as permeability, solubility, interfacial tension and thickness, and diffusion.

The accurate description of polymer solution thermodynamics began with the Flory-Huggins theory[1, 2]. This theory describes the free energy of mixing for an incompressible lattice. Further adaptation of this model through incorporation of equation of state behavior has allowed the prediction of demixing in the case of increasing temperature[9]. This was an important improvement since lower critical solution behavior is predicted to occur in many polymer blends, although sometimes not observed due to thermal degradation of the polymer prior to the demixing temperature. The Flory-Huggins model was also later expanded to describe more than two enthalpic mer-mer interactions as in the case of copolymer blends[3-5]. Since the entropy of mixing is small for large polymer molecules, there are few examples of miscible

homopolymers. Copolymers often have large repulsive intramolecular interactions that act to induce miscibility. Observations of miscibility in copolymer blends, coupled with the use of the mean field theory, have facilitated the quantification of many other mer-mer interactions[10]. Analysis of the various mer-mer interactions allows an understanding of structural influences on blend thermodynamics[11-14]. A complete understanding of structure-interaction relationships would facilitate the design of new polymer structures suited to induce miscibility, control phase domain size, vary interfacial thickness and adhesion, control diffusion and permeability, and suit many other engineering needs.

The methods and accuracy of probing mer-mer interactions has also evolved over years of study. In addition to studying phase behavior of polymer blends, researchers have attempted to extract information about polymer interactions from interfacial distance studies, heats of mixing, crystallization temperatures, and equation of state behavior with limited success. The analysis of polymer blend phase behavior remains the most consistent method of extracting information about mer-mer interactions. This method has also undergone changes. Many new polymers and copolymers have had regions of miscibility with existing polymers and each other, allowing an expanded database of structure-interaction properties. Early miscibility studies often involved copolymer-copolymer blends whose phase behavior is based on six pair-wise interactions. Availability of monodisperse homopolymers in a range of molecular weights has allowed the investigation of miscibility boundaries dependent on only a single pair-wise interaction. Details of the theory and methods used to extract binary interactions are discussed in Chapters 2 and 3.

Copolymers containing styrene (S) and acrylonitrile (AN) have a large intramolecular repulsion, which has induced miscibility with many other polymers and

copolymers. The large intramolecular repulsion coupled with the availability of a range of copolymer compositions without composition drift has made these materials very useful in extracting information about binary interactions. Chapter 4 offers new experimental evidence that the S-AN interaction is much more repulsive than previously thought. Other research projects are then reviewed to determine if the more repulsive interaction is feasible.

The feasibility and implications of a larger S/AN interaction are explored in Chapter 5 by looking at phase behavior in blends of poly(styrene-co-acrylonitrile) and poly(n-alkyl acrylate-co-methyl methacrylate). The interaction between AN and the n-alkyl acrylates inferred while using the larger S/AN interaction is compared to previous estimates and predicted values.

An analysis of the poly(styrene-co-maleic anhydride)/poly(styrene-co-acrylonitrile blend system is presented in Chapter 6, which was used to extract a commonly used S/AN interaction. Interactions inferred from independent analyses of polystyrene/poly(styrene-co-maleic anhydride) blends and the S/AN interaction determined in Chapter 4 were used to predict the phase behavior of poly(styrene-co-maleic anhydride)/poly(styrene-co-acrylonitrile) blends.

An investigation of blends of SAN copolymers and a polycarbonate copolymer is provided in Chapter 7. While no region of miscibility exists in those materials studied, the light scattering behavior of these blends is extensively evaluated. Thermodynamic interactions involving the polycarbonate copolymers are discussed in Chapter 8.

Conclusions and recommendations are provided in Chapter 9. Equation of State data is provided in Appendix A.

REFERENCES

1. Flory, P.J., J. Chem. Phys. 1942;10:51.
2. Huggins, M.L., J. Chem. Phys. 1941;9:440.
3. Kambour, R.P., Bendler, J.T., and Bopp, R.C., Macromolecules 1983;16:753.
4. Paul, D.R. and Barlow, J.W. Polymer 1984;25:487.
5. Brinke, G.T., Karasz, F.E., and MacKnight, W.J. Macromolecules 1983;1:1827.
6. Lacombe, R.H. and Sanchez, I.C. J. Phys. Chem. 1976;80:2568.
7. Sanchez, I.C. and Lacombe, R.H. J. Chem. Phys. 1976;80:2353.
8. Sanchez, I.C. and Lacombe, R.H. J. Polym. Sci., Polym. Lett. Ed. 1977;15:71.
9. Sanchez, I.C. and Lacombe, R.H. Macromolecules 1978;1:1145.
10. Paul, D.R. and Bucknall, C.B. eds. 'Polymer Blends' 2 ed. Volume 1, Vol. 1. John Wiley & Sons, Inc., New York, 2000.
11. Van Krevelen, D.E., 'Properties of polymers'. 3 ed., Elsevier Pub. Co., Amsterdam, 1990.
12. Bicerano, J., 'Prediction of Polymer Properties' Marcel Dekker, Inc., New York, 2002.
13. Prausnitz, J.M., Lichtenthaler, R.N., and Gomez de Azevedo, E. 'Molecular Thermodynamics of Fluid-Phase Equilibria' 2nd Ed., Pretence Hall, 1986.
14. Zhu, S. and Paul, D.R., Polymer 2003;44:5671.
15. Merfeld, G.D., et al. Polymer 1999;41:663.

Chapter 2: Background and Theory

BLEND STABILITY CRITERIA

A polymer blend is miscible if the free energy of mixing is negative:

$$\Delta g_{mix} = \Delta h_{mix} - T\Delta s_{mix} < 0 \tag{2.1}$$

and cannot be lowered by phase separation:

$$\left(\frac{\partial^2 \Delta g_{mix}}{\partial \phi_i^2}\right)_{T,P} > 0 \tag{2.2}$$

The Gibb's free energy density is described by the Flory-Huggins equation[1, 2]:

$$\Delta g_{mix} = B_{12}\phi_1\phi_2 + RT\left[\frac{\rho_1\phi_1 \ln\phi_1}{M_1} + \frac{\rho_2\phi_2 \ln\phi_2}{M_2}\right] \tag{2.3}$$

where ϕ_1, ρ_1, and M_1 refer to the volume fraction, density, and molecular weight of species 1 respectively. The quantity B_{12} is the energy density of the 1-2 interaction[3-5]. The other term on the right hand side of Equation 2.3 accounts for the incompressible lattice entropy of mixing.

COMPRESSIBILITY

The Flory-Huggins theory is unable to predict the phase separation of a polymer solution upon heating, known as lower critical solution temperature (LCST) behavior, without expanding the enthalpic energy density term. This is an important limitation of the Flory-Huggins model since most miscible polymers should phase separate upon heating, if they do not thermally degrade first. The LCST behavior is caused the compressibility of the mixture in the absence of specific interactions[6]. The Gibbs free energy that describes the spinodal condition can be expanded to the form

$$\left(\frac{\partial^2 \Delta g_{mix}}{\partial \phi_i^2}\right)_{T,P} = \left(\frac{\partial^2 g}{\partial \phi_i^2}\right)_{v} - \left(\frac{\partial v}{\partial P}\right)_{T,\phi_i}\left(\frac{\partial^2 g}{\partial \phi \partial v}\right)^2 \tag{2.4}$$

The first term on the right hand side of Equation 2.4 is invariant with pressure. The term $\left(\frac{\partial v}{\partial P}\right)_{T,\phi_i}$ typically increases exponentially with temperature, while the term $\left(\frac{\partial^2 g}{\partial \phi \partial v}\right)$ is a positive quantity whose magnitude depends on the difference in equation of state characteristics between the polymers being mixed. Overall, the second term on the right hand side of Equation 2.4 always lowers the Gibbs free energy of mixing. At higher temperatures, this term will typically become larger than the incompressible contribution, causing LCST behavior.

The compressibility of the solution can be accounted for by using equation of state properties of the polymers and mixing rules. A lattice fluid equation of state has been established by Sanchez and Lacombe[7-9]:

$$\tilde{\rho}^2 + \tilde{P} + \tilde{T}\left[\ln\left(1-\tilde{\rho}\right) + \left(1-\frac{1}{r}\right)\tilde{\rho}\right] = 0 \tag{2.5}$$

where r is the chain length which has little effect on the equation of state for large polymers. The other parameters have been reduced by critical constants specific to polymer type $\tilde{\rho} = \rho/\rho^* = 1/\tilde{v} = v^*/v$, $\tilde{T} = T/T^*$, $\tilde{P} = P/P^*$. Sanchez and Lacombe have also established mixing rules[7, 9]:

$$P^* = \varepsilon^*/v^* \tag{2.6}$$

$$v^* = \sum \phi_i^o v_i^* \tag{2.7}$$

$$T^* = \varepsilon^*/k = \sum_i^m \phi_i^* \varepsilon_{ii}^* + \sum_{i<j}^m \sum_{i<j}^m \phi_i^* \phi_j^* kT\chi_{ij} \tag{2.8}$$

where $\phi_i = \dfrac{m_i/\rho_i^*}{\sum m_i/\rho_i^*}$, $\phi_i^o = \dfrac{m_i/\rho_i^* v_i^*}{\sum m_i/\rho_i^* v_i^*}$, and $\chi_{ij} = \left(\varepsilon_{ii}^* + \varepsilon_{jj}^* - 2\varepsilon_{ij}^*\right)/kT$. The quantity ΔP^* is known as the bare interaction energy since it is dependent only upon the polymer repeat unit interaction. This bare interaction energy may be related to the B_{12} term in the Flory-Huggins equation (Equation 2.3) under the spinodal condition given the following relation[6, 10, 11]:

$$B_{12}^{SC} = \tilde{\rho}\Delta P^* + \frac{\left\{\begin{array}{l}\left[P_2^* - P_1^* + (\phi_2 - \phi_1)\Delta P^*\right] + \dfrac{RT}{\tilde{\rho}}\left(\dfrac{1}{r_1^o v_1^*} - \dfrac{1}{r_2^o v_2^*}\right) \\ - RT\left(\dfrac{\ln(1-\tilde{\rho})}{\tilde{\rho}^2} + \dfrac{1}{\tilde{\rho}^2}\right)\left(\dfrac{1}{v_1^*} - \dfrac{1}{v_2^*}\right)\end{array}\right\}^2}{\left\{\dfrac{2RT}{v^*}\left[\dfrac{2\ln(1-\tilde{\rho})}{\tilde{\rho}^3} + \dfrac{1}{\tilde{\rho}^2(1-\tilde{\rho})} + \dfrac{(1-1/r)}{\tilde{\rho}^2}\right]\right\}} \tag{2.9}$$

where $r_i^o = r_i\left(\frac{v^*}{v_i^*}\right)$.

MEAN FIELD THEORY

A useful adaptation of the Flory-Huggins type analysis is its extension to account for more than two polymer repeat units being mixed as in the case of a statistical copolymer. The interactions of the various repeat units can be described using a mean field approximation of the following form[3-5]:

$$B = \overset{\text{Intermolecular}}{\sum_{i\neq j} B_{ij}\phi_i\phi_j} - \overset{\text{Intramolecular}}{\sum_{i\neq j} B_{ij}\phi_i\phi_j} \qquad (2.10)$$

where ϕ_i refers to the volume fraction of monomer units in the copolymer, and the notation of the summations prevents double counting of interactions.

Four common applications of Equation 2.10 are as follows: for two copolymers containing four unique monomers,

$$B = B_{13}\phi_1\phi_3 + B_{14}\phi_1\phi_4 + B_{23}\phi_2\phi_3 + B_{24}\phi_2\phi_4 - B_{12}\phi_1\phi_2 - B_{34}\phi_3\phi_4 \qquad (2.11)$$

for a copolymer containing repeat units 1 and 2 with a homopolymer containing repeat unit 3,

$$B = B_{13}\phi_1 + B_{23}\phi_2 - B_{12}\phi_1\phi_2 \qquad (2.12)$$

for a copolymer and homopolymer where the copolymer and homopolymer both contain repeat unit 1,

$$B = B_{12}\phi_2^2 \tag{2.13}$$

and for a blend of two copolymers which have the same two monomers, but different compositions

$$B = B_{12}\left(\Delta\phi_1\right)^2 \tag{2.14}$$

where $\Delta\phi_1$ is the difference between volume fractions of component 1 between the two copolymers.

EXPERIMENTAL DETERMINATION OF BINARY INTERACTIONS

Observations of polymer blend phase behavior with respect to copolymer composition, temperature, and molecular weights can be used to extract information about the enthalpic interaction, B, if the type of demixing responsible for the observed phase behavior is known. Phase separation may occur either spontaneously as in the case of spinodal demixing, or by nucleation and growth. The spinodal condition occurs when the second derivative of the free energy of mixing with respect to composition is set to zero. Nucleation and growth is a metastable (binodal) phase separation mechanism where the second partial free energy change with respect to concentration must be positive. Calculation of the binodal curve requires many calculations, and is made more complicated by the effects of polydispersity [12, 13]. It is typical to assume that the observed phase behavior for high molecular weight, equal weight polymer blends is represented by the critical point, which is a special case of spinodal demixing.

.

If we assume that B is not a function of temperature or composition, differentiation of Equation 2.3 yields the following spinodal condition for the interaction energy[1, 2]

$$B_S = \frac{RT}{2}\left[\frac{\rho_A}{(\overline{Mw})_A \phi_A} + \frac{\rho_B}{(\overline{Mw})_B \phi_B}\right] \tag{2.15}$$

where $(\overline{\mathbf{Mw}})_i$ represents the weight average molecular weight of component i. The critical point is a point along the spinodal curve defined by setting the third derivative of Gibbs free energy of mixing to zero. The resulting interaction energy is shown in Equation 2.16.

$$B_C = \frac{RT}{2}\left[\sqrt{\frac{\rho_A}{(\overline{Mw})_A}} + \sqrt{\frac{\rho_B}{(\overline{Mw})_B}}\right]^2 \tag{2.16}$$

Once an experimental map of phase behavior with respect to composition or molecular weight is obtained, information about binary interactions can be obtained by a best fit of these experimental observations. The phase behavior can be predicted by equating the estimated entropy of mixing to the enthalpy of mixing from the appropriate case of Equation 2.10.

In the case of a copolymer-copolymer blend with four unique monomer pairs, six binary interactions are required to fit the experimentally observed phase behavior. Often, information is known about several of the binary interactions involved in a blend system, such that not all six binary interactions have to be determined concurrently. However, the more degrees of freedom allowed in the fit of the experimental data, the less assured the resulting individual binary interaction values will be.

There are a few methods that allow extraction of single binary interactions at a time from experimentally observed phase behavior. One method is to vary the molecular weights of two homopolymers, and observe changes in phase behavior. However, few homopolymers are known to be miscible with one another. Another method of extracting single interaction energies would be to observe the miscibility limits of two copolymers containing the same repeat units, but different compositions. Equation 2.14 describes the resulting enthalpy of mixing in this case. To experimentally observe a phase boundary in this situation, the monomer pairs must be easily separated on the basis of their individual component glass transitions or refractive indices such that separate phases containing similar copolymers can be differentiated from one another. Also, if the mer-mer interaction is largely repulsive, the phase boundary will exist between similar copolymer pairs whose separate phases cannot be easily distinguished from one another. In some cases, it would be difficult to determine if one was observing a true phase boundary or a changing ability to distinguish between the two phases. In addition to these limitations, the effects of polydispersity and compositional variation may become important factors in the resulting phase behavior of these systems[12, 13].

Another option for determining single interactions at a time is by observing phase behavior resulting from copolymer and homopolymers that share a common monomer. In this case, equation 2.13 is set equal to the appropriate entropy of mixing. By rearranging Equation 2.13 to read $\phi_2 = \sqrt{B_{entropic} / B_{12}}$, it is apparent that a plot of the volume fraction of the monomer unique to the copolymer ($\boldsymbol{\phi_2}$) versus $\sqrt{B_{entropic}}$ yields a line whose slope is $\sqrt{1/B_{12}}$ [14]. Analysis of the experimental phase behavior is made easier by knowing that the phase boundary must pass through the origin and exist in a straight line. The confidence in data fitting coupled with an expanding availability of homopolymers standards has made this approach an attractive one.

PREDICTION OF BINARY INTERACTIONS

Binary interactions can be estimated using solubility parameters and the regular solution theory of Hildebrand in the van Laar form as shown in Equation 2.17[4, 15, 16]

$$B_{ij} = \left(\delta_i - \delta_j\right)^2 \tag{2.17}$$

The solubility parameters for polymers can be estimated through group contribution methods within the accuracy of the reported experimentally determined solubility parameters[17].

The component solubility parameters are a function of the cohesive energy and the molar volume of the polymer repeat unit as shown

$$\delta = \left(C/V\right)^{1/2} \tag{2.18}$$

Since the molar volume is a function of temperature, the solubility parameters are also a function of temperature. The difference between component solubility parameters between two liquids is mostly independent of temperature since the molar volumes of most liquids change with temperature in a similar way. The regular solution theory assumes that the excess entropy of mixing is negligible, and therefore the binary interactions will be compared to the bare interaction parameters from Equation 2.9 that are independent of excess entropy of mixing effects when possible[18].

The predictive ability of regular solution theory is limited by London's formula that approximates the cohesive attraction between unlike pairs as the geometric mean of the like-pair cohesive energy density.

$$C_{ij} = \left(C_{ii}C_{jj}\right)^{1/2} = \delta_i\delta_j \tag{2.19}$$

The error in this approximation may be quantified by the introduction of the term k_{ij}, which is related to the observed binary interaction in the following way[18]

$$B_{ij} = \left(\delta_i - \delta_j\right)^2 + 2k_{ij}\delta_i\delta_j \tag{2.20}$$

The k_{ij} term allows a comparison of predictive capability between interactions of different magnitudes.

REFERENCES

1. Flory, P.J. J. Chem. Phys. 1942;10:51.
2. Huggins, M.L. J. Chem. Phys. 1941;9:440.
3. Kambour, R.P., Bendler, J.T., and Bopp, R.C. Macromolecules 1983;16:753.
4. Paul, D.R. and Barlow, J.W. Polymer 1984;25:487.
5. Brinke, G.T., Karasz, F.E.,and MacKnight, W.J. Macromolecules 1983;16:1827.
6. Paul, D.R. and Bucknall, C.B. eds. 'Polymer Blends' 2 ed. Volume 1, Vol. 1. John Wiley & Sons, Inc., New York, 2000.
7. Lacombe, R.H. and Sanchez, I.C. J. Phys. Chem. 1976;80:2568.
8. Sanchez, I.C. and Lacombe, R.H. J. Chem. Phys. 1976;80:2353.
9. Bidkar, U.R. and Sanchez, I.C. Macromolecules 1995;28:3963.
10. Callaghan, T.A., PhD Dissertation, 1992, The University of Texas at Austin.
11. Kim, C.K. and Paul, D.R. Polymer 1992;33;1630.
12. Koningsveld, R. and Kleintjens, L.A. J. Polym. Sci., Polym. Sym. 1977;61:221.
13. Vanhee, S., et al. Macromolecules 2000;33:3924.
14. Chu, J.H., Tilakaratne, H.K., and Paul, D.R. Polymer, 2000;41:5393.
15. Hildebrand, J.H. and Scott, R.L., 'The Solubility of Nonelectrolytes'. 3 ed. 1950.
16. van Laar, J.J. Baarn. Z. physik. Chem. 1910;72:723.
17. van Krevelen, D.E., 'Properties of polymers'. 3 ed., Elsevier Pub. Co., Amsterdam, 1990.
18. Prausnitz, J.M., Lichtenthaler, R.N. and Gomez de Azevedo, E., 'Molecular Thermodynamics of Fluid-Phase Equilibria' 2 Ed. Prentice-Hall, Englewood Cliffs, N.J., 1986.

Chapter 3: Experimental Methods

HOMOPOLYMER AND COPOLYMER SYNTHESIS

Some polymers were synthesized for this work by addition polymerization using 2,2-azo-bis-isobutyronitrile(AIBN) as the free radical initiator. Monomers were washed with 5 weight% NaOH aqueous solutions to remove inhibitors. Polymerization was carried out either in bulk or in para-dioxane solutions at 60°C. Copolymer synthesis reaction time was limited such that conversion did not exceed 10%. This was done to prevent composition drift. The reactions were quenched by the addition of an excess of methanol. The precipitated polymer was dissolved in dichloromethane or tetrahydrofuran and then reprecipitated in methanol to remove residual monomer.

The mole fraction of a monomer copolymerized into a polymer can be estimated by

$$f_1 = \frac{F_1\left(1+\left[r_1-1\right]F_1\right)}{\left(r_1+r_2-2\right)F_1^2+2\left(1-r_2\right)F_1+r_2} \qquad (3.1)$$

where f_1 and F_1 are the mole fraction of monomer 1 in the copolymer and reactant mixture respectively, and r_1 and r_2 are the reactivity ratios. When series of copolymers of varying compositions are made and characterized with respect to composition, these reactivity ratios can be estimated. Comparison of predicted and actual

polymer compositions using the experimentally determined reactivity ratios can be useful in identifying problems during synthesis.

CHARACTERIZATION

The compositions of the copolymers were characterized by ^{1}H-NMR at 500 MHz. Deuterated chloroform or dichloromethane was used as the solvent, which contained tetramethylsilane for establishing the shift reference. The composition of the copolymers was determined by comparing ratios of hydrogen shift areas, which can be attributed to the various monomer structures.

Molecular weight information was obtained by gel permeation chromatography using a Polymer Laboratories 5 micron column, a Waters 515 HPLC pump, and a Viscotek model 250 refractive index detector. Crosslinked polystyrene was used as the fixed phase and tetrahydrofuran was the carrier phase. The column was calibrated with polystyrene standards.

Polymer density was obtained using either a pycnometer, or a density gradient column. The gradient column was used with aqueous calcium nitrate solutions and calibrated with standards.

Calorimetric information was obtained with a Perkin Elmer DSC7, where scans and calibrations were performed at 20 °C per minute. Glass transition temperatures are defined here as the onset of the transition.

Equation of state properties of the copolymers were determined with a Gnomix mercury dilatometer. The resulting data were fitted using the Sanchez-Lacombe

Equation of State to extract the corresponding characteristic parameters P*, T* and ρ*[1, 2].

BLEND PREPARATION

Blends were mostly made by casting from a common solvent due to the limited size of polymer samples. Solution cast blends were cast from approximately 10 weight % solutions using various solvents. The most common solvents used were dichloromethane and tetrahydrofuran. The residual solvent was removed from the cast blends in a vacuum oven held at a temperature above the glass transitions of the constituent polymers for a period of at least 12 hours.

In several instances, the conditions of casting and the annealing time in the vacuum oven were found to affect the phase behavior of the blends. Rapid solvent removal by casting at elevated temperatures, or by using a low boiling point solvent, or by precipitation into a non-solvent can trap the blend in a homogenous non-equilibrium state[3]. Alternatively, polymers that are thermodynamically miscible could become trapped in a two phase state by the "$\Delta\chi$" effect[4-6]. This situation occurs when the solvent preferentially interacts with one of the blend constituents. An elevated temperature during solvent removal was found to facilitate transesterification reactions in some cases, which induced phase homogenization.

The Flory-Huggins free energy model can only describe equilibrium blend behavior, and it is, therefore, important to set up experiments that will achieve that condition. Therefore, the effects of solvent type and rate of solvent removal was investigated when appropriate.

PHASE BEHAVIOR ASSESSMENT

There are many methods that can provide insight into the number of coexisting phases such as observing scattered radiation, dynamic mechanical analysis, dielectric relaxation, and calorimetry. The work presented here relies on observation of scattered light and observation of glass transitions by calorimetry.

A two-phase polymer blend will scatter a significant amount of light if the two polymers possess an index of refraction difference of 0.01 or greater[7]. This will cause the sample to appear cloudy when visually inspected. At times, scattered light was further quantified by recording the intensity and angular position of the scattered light. Our light scattering device uses a polarized 632nm He-Ne LASER, focusing and collimating lenses, and a 512 pixel array detector. Neutral density filters and the adjustment of sample times are used to obtain a strong signal without over saturating the detector. Temperature jump experiments were conducted by placing a glass slide on a heated brass block. Temperature ramp experiments were performed with a Mettler FP82HT Hot Stage with a Mettler FP80HT Central Processor. Nitrogen purge gas was used to prevent sample degradation.

Polymers possess a second order phase transition known as the glass transition where the polymer gains segmental mobility. The temperature of the glass transition is dependent on many factors such as backbone stiffness, pendant side chain length, and electron distribution that form a relaxation environment. The glass transition observed by differential calorimetry is defined here as the onset of the step change in heat capacity for the transition. If a polymer blend is miscible, it will possess a single relaxation environment and therefore a single glass transition. If the blend system possesses two phases then two glass transitions will usually be observed. In practice, glass transitions

must be at least 5°C different from one another to distinguish them as separate transitions while analyzing calorimetric scans. More than one temperature scan was usually performed to remove non-equilibrium energy due to processing and to make sure phase morphology is an equilibrium condition. Scans and calibrations were performed at 20°C/min.

EFFECTS OF BLEND COMPOSITION

As mentioned in Chapter 2, several interaction energies have been extracted by the observation of phase behavior in blends of monodisperse homopolymers with copolymers of varying composition[8-11]. These studies have typically observed the phase behavior in blends with equal weights of their components. The interactions were extracted by assuming that the equal weight blend entropy of mixing was equal to that of the critical point. This is a good approximation for blends whose components possess similar molecular weights. However, when the disparity between molecular weights becomes large, analysis of Equation 2.16 indicates the critical point occurs at a composition with a larger amount of the low molecular weight component.

Once the disparity between molecular weights becomes large enough, a difference in phase behavior between equal weight blends and those of the critical composition can be observed. Figure 3.1 shows calorimetric curves for three blend compositions of polystyrene having a molecular weight of 7,000 Da and poly(styrene-co-benzyl acrylate) having an approximate molecular weight of 202,500 Da. These blends were cast from dichloromethane and annealed at 150 °C for 48 hours. The equal weight blend exhibits a single glass transition, while the blends containing 65 and 80 wt% polystyrene exhibit two glass transitions.

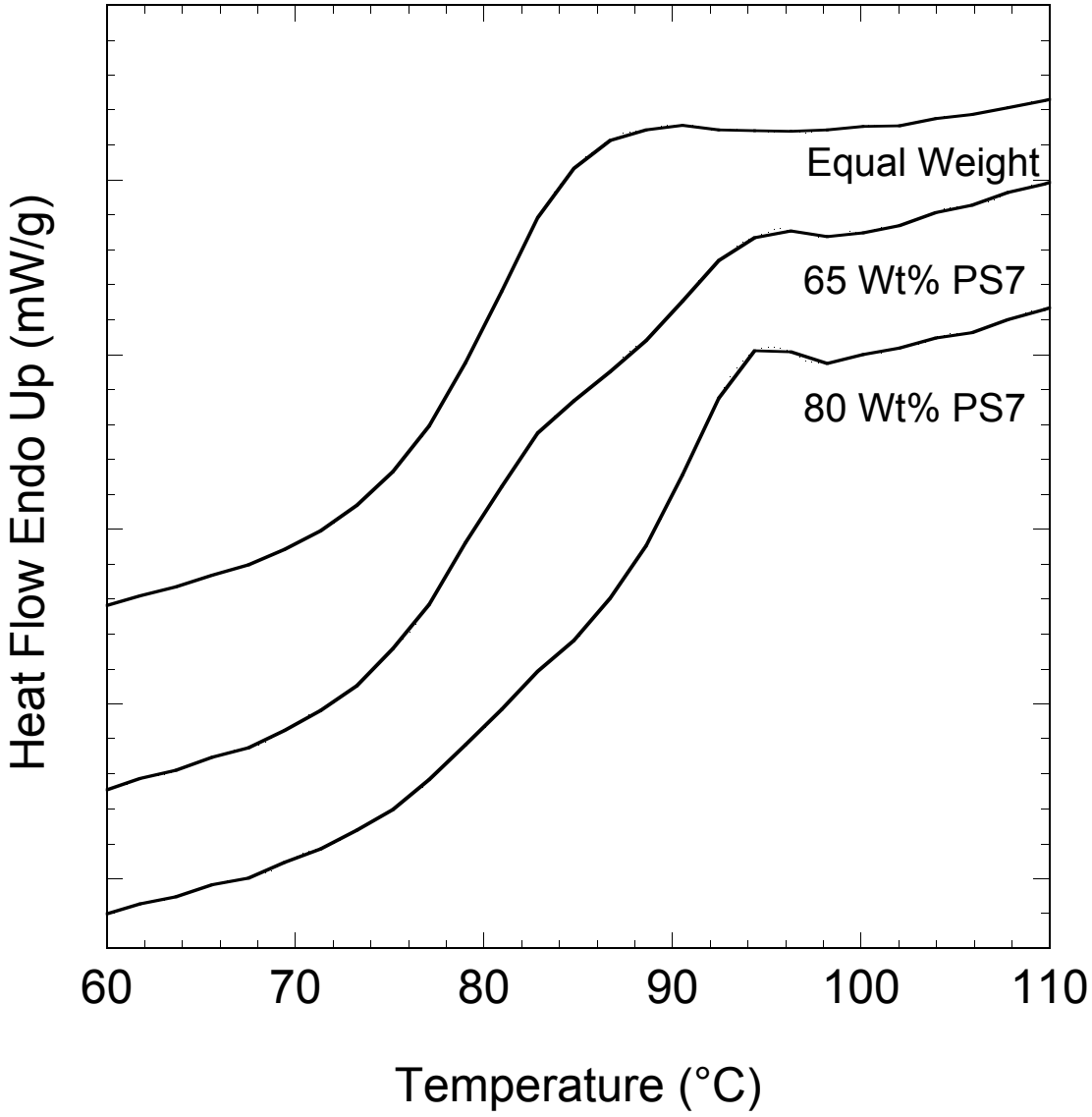

Figure 3.1 - DSC scans for blends of poly(styrene-stat-benzyl acrylate) and monodisperse polystyrene having different blend compositions.

The curve in Figure 3.2 shows the composition of the blends shown in Figure 3.1 relative to the estimated spinodal entropy of mixing determined using Equation 2.16 at 150 °C. The minimum in the curve, which is the critical point entropy of mixing, occurs at 84 wt % polystyrene. The solid circles represent the two phase blends while the open circle represents the single phase, equal weight blend. The blend compositions are placed along a line that intersects the y-axis at 0.095 cal/cm^3. This energy corresponds to the enthalpy of mixing between the polymers, determined from Equation 2.14 and the experimentally determined binary interaction between styrene and benzyl acrylate repeat units. If the phase behavior were due to spinodal phase separation, only blend compositions having between 92 and 67 wt% polystyrene would be immiscible. It is likely that the actual of phase separation mechanism for these blends was a binodal mechanism. The binodal curve, which is prohibitively difficult to predict due to polydispersity, apparently intersects the enthalpy of mixing line somewhere between 75 and 50 wt% polystyrene. Binodal phase separation induces two phase behavior outside of the predicted spinodal curve. This improves the assumption that equal weight blends exhibit critical point phase behavior. However, in the case of the polymers shown in Figure 3.1, this is not a good assumption.

To avoid problems associated with calculating the entropy of mixing between equal weight blends having large molecular weight disparities, all blends made with monodisperse polymers of varying molecular weights were made to approximate the predicted critical point composition. The critical point is defined by setting the third derivative of the Gibbs free energy of mixing with respect to composition equal to zero. If we assume the system is incompressible and neglect the effects of polydispersity[12], Equation 3.2 defines the composition of the critical point.

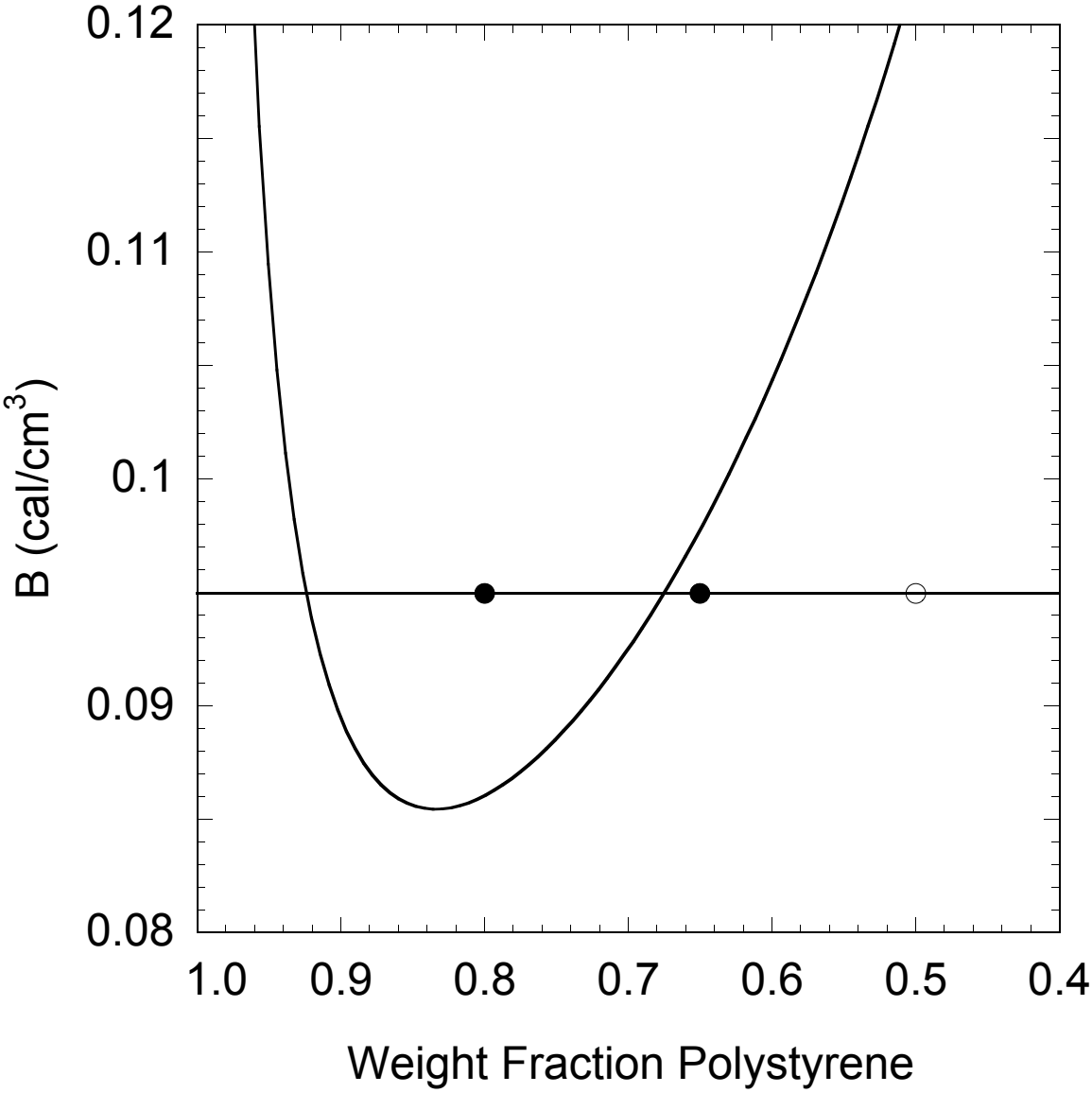

Figure 3.2 – Predicted entropy of mixing for the spinodal condition versus blend composition. The closed and open circles represent the two phase and single phase blends whose DSC scans are shown in Figure 3.1. The line indicates the enthalpic interaction between the polymer pairs.

$$\phi_1 = 1/\left(1+\sqrt{\left(M_{W1}\rho_2/M_{W2}\rho_1\right)}\right) \qquad 3.2$$

The critical point blend concentration for very large disparities sometimes requires a large excess of the lower molecular weight blend component. It becomes difficult to observe a second phase by calorimetry or observation of light scattering when its total weight fraction is below 20%. The curve corresponding to the blend containing 80 wt% polystyrene in Figure 3.1 illustrates this difficulty. Because of this difficulty, very low molecular weight oligimers were not used.

REFERENCES

1. Lacombe, R.H. and Sanchez, I.C. J. Phys. Chem. 1976;80:2568.
2. Sanchez, I.C. and Lacombe, R.H. J. Polym. Sci., Polym. Lett. Ed. 1977;15:71.
3. Nishimoto, M., Keskkula, H., and Paul, D.R. Polymer 1991;32:272.
4. Zeman, L. and D. Patterson, Macromolecules, 1972. 5: p. 513.
5. Nandi, A.K., Mandal, B.M. and Bhattacharyya, S.N. Macromolecules 1985;18:1454.
6. Woo, E.M., Barlow, J.W. and Paul, D.R. J. Polym. Sci., Polym. Symp. 1984;71:137.
7. Bohn, L., 'Compatible Polymers', in 'Polymer Handbook', Brandrup J. and Immergut, E.H. eds, Wiley, New York, 1975.
8. Merfeld, G.D. and D.R. Paul, Polymer, 1998. 39:1999.
9. Chu, J.H., Tilakaratne, H.K., and Paul, D.R. Polymer 2000;41:5393.
10. Zhu, S. and Paul, D.R. Macromolecules 2002;35:2078.
11. Zhu, S. and Paul, D.R. Polymer 2003;44:3009.
12. Koningsveld, R. and Kleintjens, L.A. J. Polym. Sci., Polym. Sym., 1977. 61:221.

Chapter 4: Interactions with Poly(styrene-co-acrylonitrile)

Copolymers containing poly(styrene-co-acrylonitrile) (SAN) repeat units are commercially successful due in part to their relatively large intramolecular repulsion, which induces miscibility or near miscibility with other polymers. This large intramolecular repulsion coupled with the existence of numerous SAN compositions facilitates the observation of a phase boundary in blends of SANs of varying composition with other polymers and copolymers. These phase boundaries have been used to extract information about many thermodynamic interactions between polymers. These research efforts involving SAN materials have contributed greatly to the number experimentally determined polymer-polymer interactions. Therefore, the S/AN interaction is important to the understanding of polymer-polymer interactions and to structure-property relations in polymers.

Previous analysis of polymer miscibility boundaries has resulted in a wide range of reported styrene/acrylonitrile interactions typically ranging between 4.99 and 8.4 calories/cm^3 [1-9] An extensive study on SAN copolymer/ polystyrene miscibility was recently conducted that concluded the interaction is between 6.35 and 7.03 cal/cm^3 depending on the observation temperature[7]. New data presented here using those same polymers suggest the S/AN interaction is 11.7 cal/cm^3 at 200 °C. This interaction value is much higher than many other studies have indicated, yet it is consistent with predictions using group contribution methods and similar to one estimate from analog calorimetry as shown in Table 4.1[10, 11].

Table 4.1 Predicted and experimental interaction energies

Method of Determination	S/AN (cal/cm^3)	Source
Hoftyzer & van Krevelen Prediction*	9.64	[10]
Small Prediction*	12.8	[10]
Hoy Prediction*	12.3	[10]
Analog Calorimetry (Isopropyl-cyanide)	7.63	[11]
Analog Calorimetry (n-Pentyl-cyanide)	6.62	[11]
Analog Calorimetry (n-Octyl-cyanide)	11.2	[11]
Copolymer/Homopolymer miscibility	11.7	This Study
Copolymer/Homopolymer miscibility	6.35-7.03	[12]
Copolymer-copolymer miscibility	6.80	[5]
Copolymer-Copolymer miscibility	4.99-5.45	[1-4]
Copolymer-Copolymer miscibility	8.41	[9]
Copolymer-Copolymer miscibility	8.41	[8]

*Predicted using molar volumes at 200°C

The purpose of this chapter is to present new evidence for the larger SAN interaction, and to begin to show how the larger S/AN interaction can be used to accurately fit existing copolymer-copolymer miscibility data sets.

MATERIALS AND PROCEDURES

The polymers used in this study, shown in Tables 4.2 and 4.3, were used as received from the indicated source. The copolymer compositions and molecular weights of all polymers were determined previously[13, 14].

Polymer blends were made by solution casting 10 wt% polymer in dichloromethane onto glass slides heated to 40°C. Blends were heated to 200 °C in less than a 24 hour period and held at that temperature for 48 hours.

EXPERIMENTAL PHASE BEHAVIOR OF CRITICAL COMPOSITION BLENDS

The critical point compositions were calculated for blends of SAN copolymers and S homopolymers using Equation 3.2. The resulting phase behavior after annealing is shown in Figure 4.1. The open and closed circles in Figure 4.1 refer to single and two phase blends respectively. As outlined in Chapter 2, the slope of a line that passes through the origin and separates miscible from immiscible regions is related to the S/AN binary interaction. The two blend compositions indicated by arrows suggest slightly conflicting S/AN interaction values. The immiscible blend indicated by the arrow suggests the S/AN interaction is greater than 11.9 cal/cm^3, and the miscible blend

Table 4.2 SAN copolymers

Polymer	Wt%AN	M_W	M_W/M_N	Source
SAN9.5	10	195,600	2.07	Asahi Chemical
SAN11.5	12.9	151,400	2.22	Asahi Chemical
SAN14.7	14.7	182,000	2.19	Asahi Chemical
SAN13.5	15.2	149,300	2.65	Asahi Chemical
SAN15.5	17.7	144,300	2.21	Asahi Chemical
SAN19.5	20.8	178,700	2.12	Asahi Chemical
SAN23	23	117,500	2.71	Daicel Chemical Ind. Ltd.
SAN25	25	152,000	1.97	Dow Chemical Co.
SAN28	28.4	143,800	2.72	Asahi Chemical
SAN30	30	168,000	2.07	Dow Chemical Co.
SAN33	33	146,000	2.15	Monsanto Co.
SAN40	40	122,000	2.00	Asahi Chemical

Table 4.3 PS homopolymers

Polymer	M_W	M_W/M_N	Source
PS1.35	1,350	1.07	Polymer Laboratories
PS2	2,000	1.06	Pressure Chemical
PS4	4,000	<1.06	Pressure Chemical
PS7	7,000	1.03	Polymer Laboratories
PS9	9,000	<1.06	Pressure Chemical
PS12.9	12,900	1.02	Polymer Laboratories
PS17.5	17,500	1.04	Pressure Chemical
PS22	22,000	1.03	Polymer Laboratories

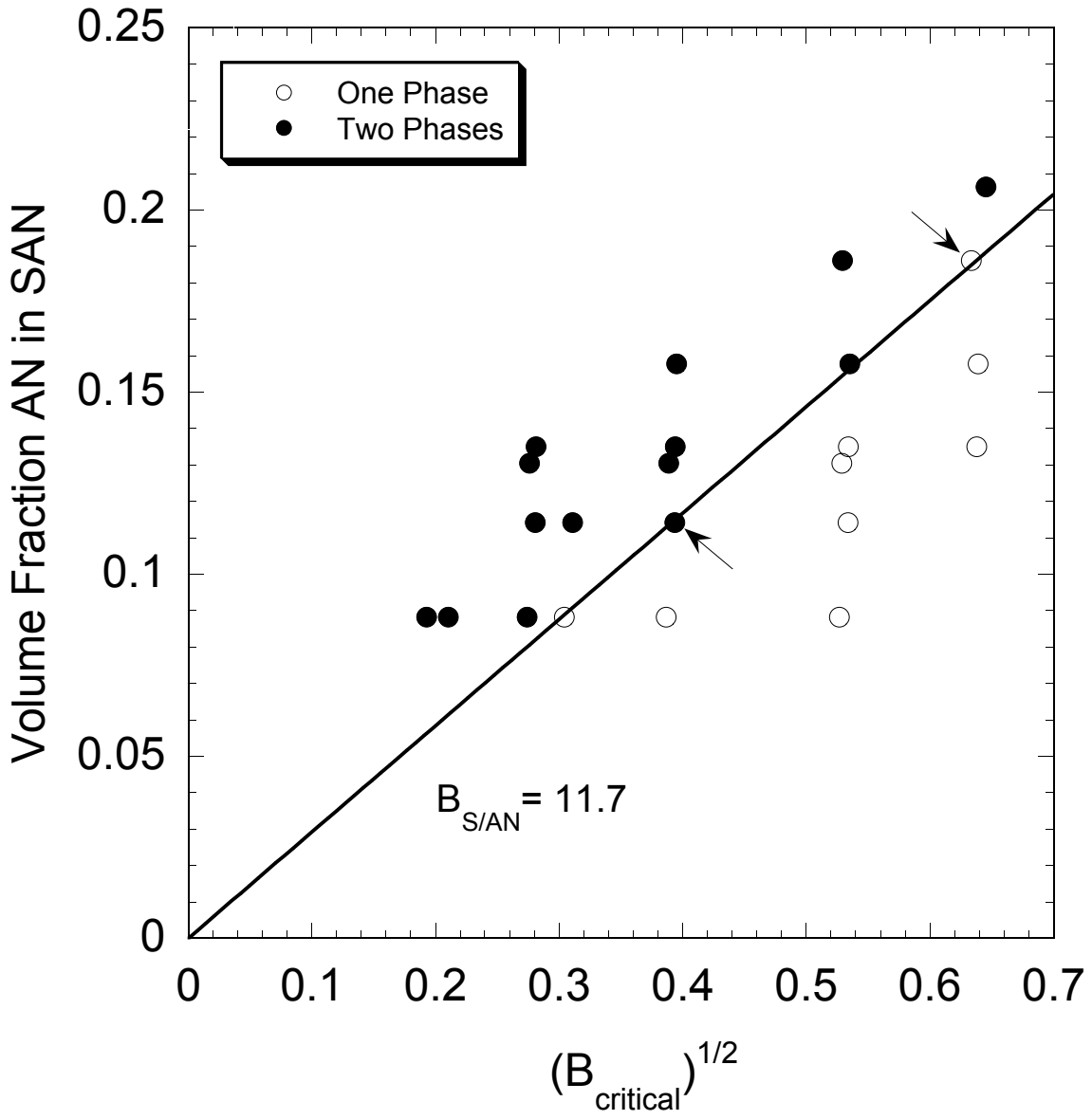

Figure 4.1 Blend phase behavior for SAN/PS critical composition blends at 200°C.

indicated by the arrow suggests that the S/AN interaction must be less than 11.59 cal/cm^3. Therefore, an average of the two points, 11.74 cal/cm^3, is used to describe the S/AN interaction. This S/AN interaction was used to construct the line shown in Figure 4.1. The phase behavior of the other two points near the line drawn is consistent with the S/AN interaction of 11.7 cal/cm^3. Using the equation of state parameters listed in Appendix A with Equations 2.5-9, the binary interaction parameter can be converted into a bare interaction of $\Delta P_{S/AN}$=13.0 cal/cm^3.

EXPERIMENTAL PHASE BEHAVIOR OF EQUAL WEIGHT BLENDS

A recent study concluded that the S/AN interaction at 200 °C is 6.65 cal/cm^3[7]. The blends used in this study were made from equal weight portions of SAN copolymers and S homopolymers. The blends were cast from dichloromethane at room temperature. The blends were then dried under vacuum while raising the annealing temperature 20 °C per day until 200 °C. The blends were maintained at 200 °C for an unspecified time at which thermodynamic equilibrium was said to have been established.

To extract information about the S/AN interaction from the observed phase behavior, the entropy of mixing must be estimated. The analysis used in the previous study assumed the phase behavior was representative of critical point behavior. The critical point entropy of mixing for the points was calculated using Equation 2.16 and used to construct Figure 4.2. The volume fractions of the SAN components were calculated using S and AN densities at 200 °C to be consistent with the method used to construct Figure 4.1. These densities were calculated using Equation 2.5 and the characteristic parameters shown in Appendix A. As a result of using densities at 200 °C,

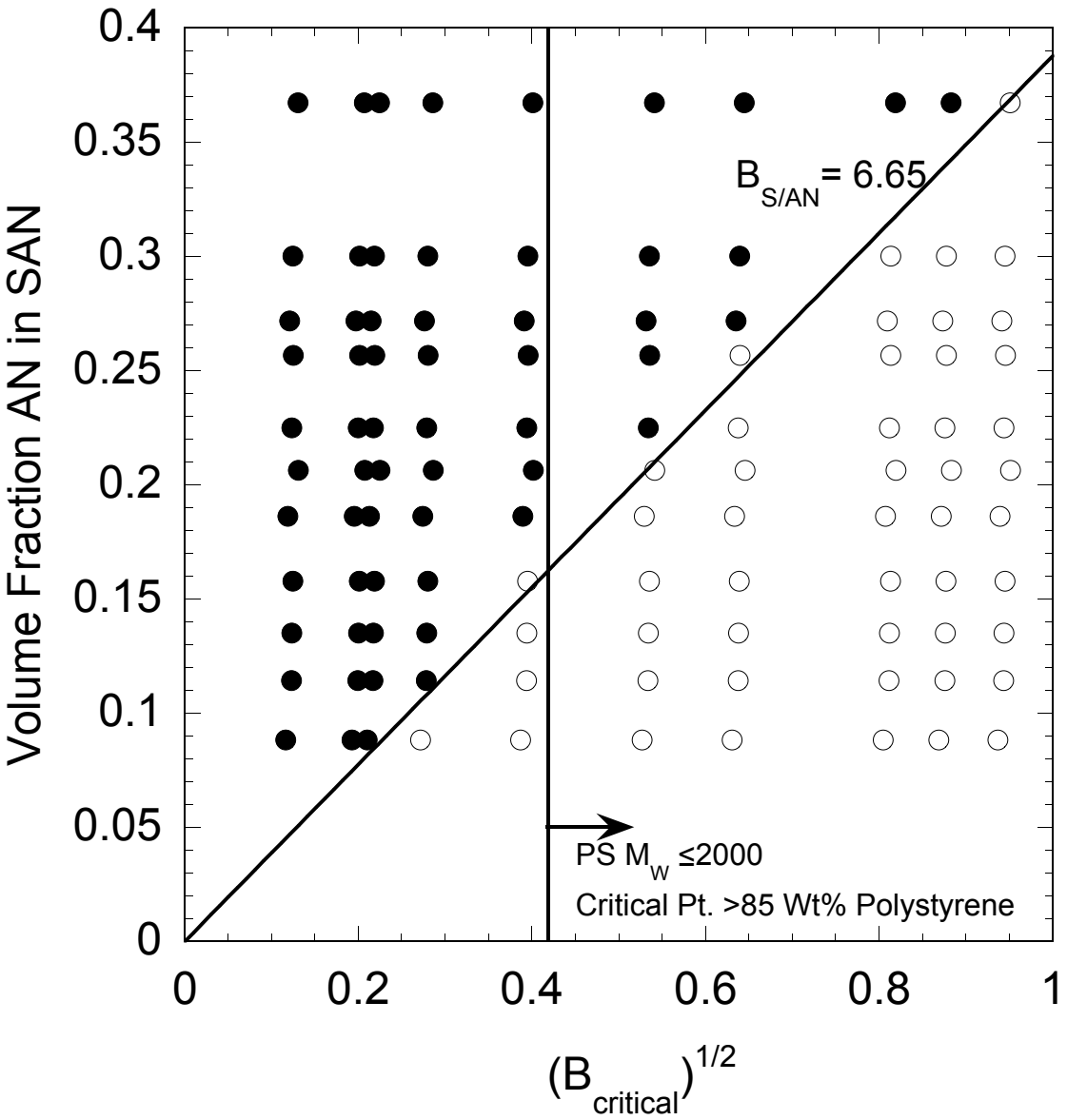

Figure 4.2 Phase behavior of equal weight SAN/PS blends at 200°C plotted relative to critical point entropy of mixing. Open and closed circles represent one and two phase blends respectively.

the data shown in Figure 4.2 is slightly different than that originally published.

By analysis of Equation 3.2, large disparities in molecular weights between blend components shifts the predicted composition of the critical point towards the lower molecular weight blend component. As shown in Chapter 3, equal weight blends may be miscible while the critical point compositions are immiscible. This was true for a blend whose critical point was predicted to contain 84 wt% polystyrene. This would cause the enthalpic interaction to be under-represented when interpreting the data using the critical point entropy of mixing. All of the blend compositions to the right of the line in Figure 4.2 were made with polystyrenes having molecular weights of 2000 or less and have predicted critical points containing more than 85 wt% polystyrene.

Figure 4.3 was constructed using the phase behavior shown in Figure 4.2, converted to the spinodal entropy of mixing using Equation 2.15. This is not done to assert that the mode of demixing could be a spinodal one, but to establish an upper limit of possible binary interactions responsible for the equal weight blend phase behavior shown in Figure 4.2. The data in Figure 4.3 indicates the S/AN interaction is bounded between the interpretations of 6.65 and 11.7. It would seem that the difference between the data shown here and that shown in the previous paper could only partially be explained by the assumption that equal weight blends represent the spinodal point.

The phase behavior of several equal weight blends near the miscibility boundary shown in Figure 4.2 were investigated. These blends were prepared under the same conditions as the blends made to represent the critical point. The DSC thermal scans of some selected equal weight blends near the phase boundary are shown in Figure 4.4. These blends were found to possess two phases whether the blends had equal weights of constituents, or represented the critical compositions. The same equal weight compositions shown in Figure 4.4 were described as having a single phase in the previous

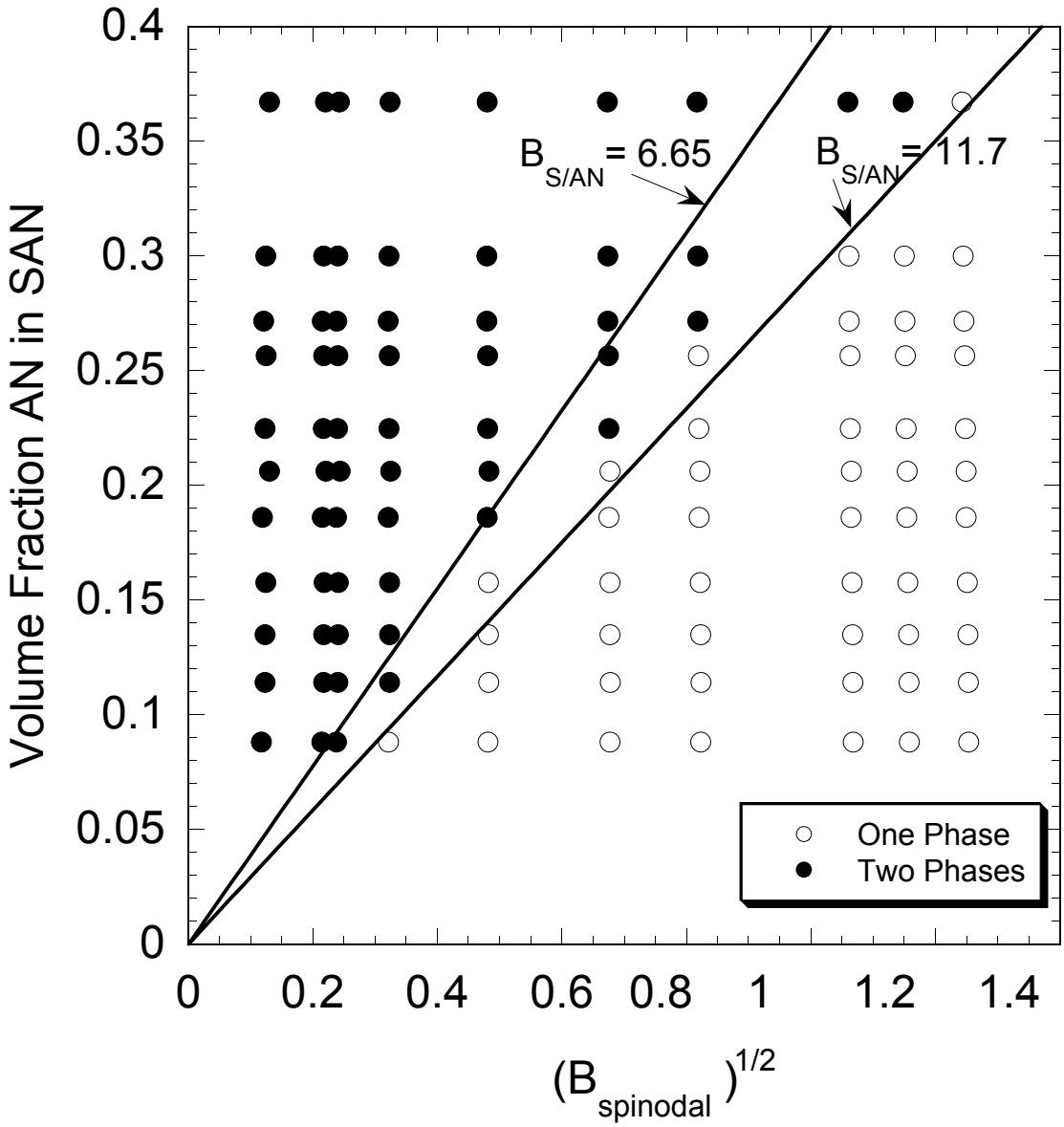

Figure4.3 Phase behavior data from Figure 4.2 versus spinodal entropy of mixing.

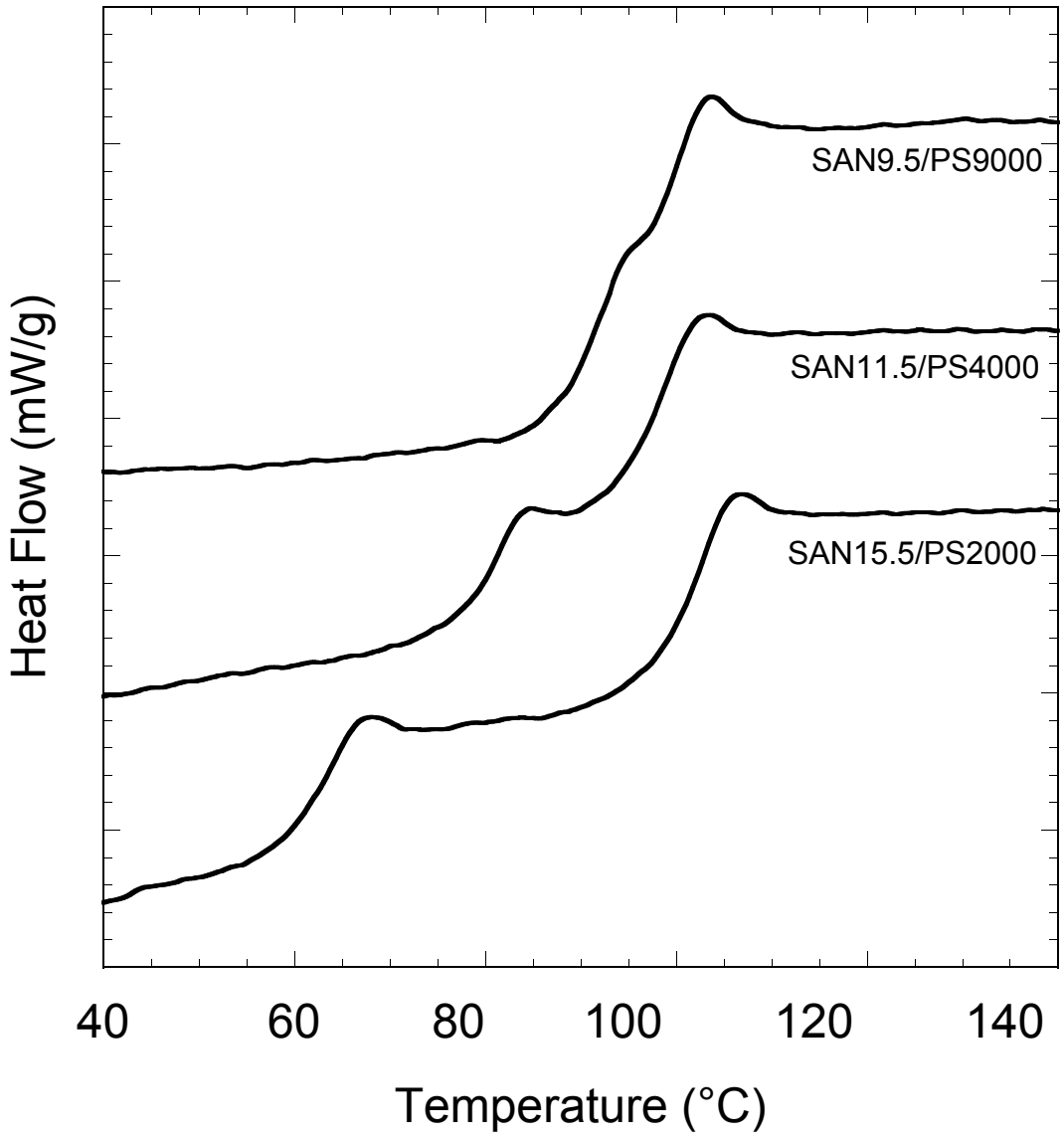

Figure 4.4 DSC scans for selected equal weight SAN/PS blends.

study, as shown in Figure 4.2. Figure 4.5 shows Figure 4.2 redrawn with the location of these three compositions represented as black squares.

It is unknown why these equal weight blends were judged as being miscible in the previous study. The higher temperature casting conditions of the current study are more likely to produce single phase blends during casting than by casting at room temperature. However, more two phase blends were observed in this study relative to the previous one. One of the equal weight blends that were evaluated as being miscible in the previous study had two phases immediately after casting at 40 °C, and after the 48/hour annealing period. If this blend were truly physically miscible as reported in the previous study, then phase homogenization must occur at some time greater than the 48/hour period. The only insight into the previous study's annealing time was the statement that intramolecular cyclization, indicated by sample yellowing, was avoided. After 48 hours at 200 °C, blends containing polystyrenes with a molecular weight of 800 become yellow. Since polystyrenes having molecular weights of 800, 680, and 580 were used in the previous study, the annealing times for those blends should not have been longer than annealing time used in the current study.

EVALUATION OF SELF-COMPATIBILITY EXPERIMENTS

One method used to estimate the S/AN interaction has been the interpretation of the miscibility limit observed when mixing SANs of different composition, referred to here as self-miscibility. One of the reasons this method is misleading is due to the inability to distinguish between miscible and immiscible blends which have similar AN contents. The miscibility of blends is typically judged by optical or calorimetric

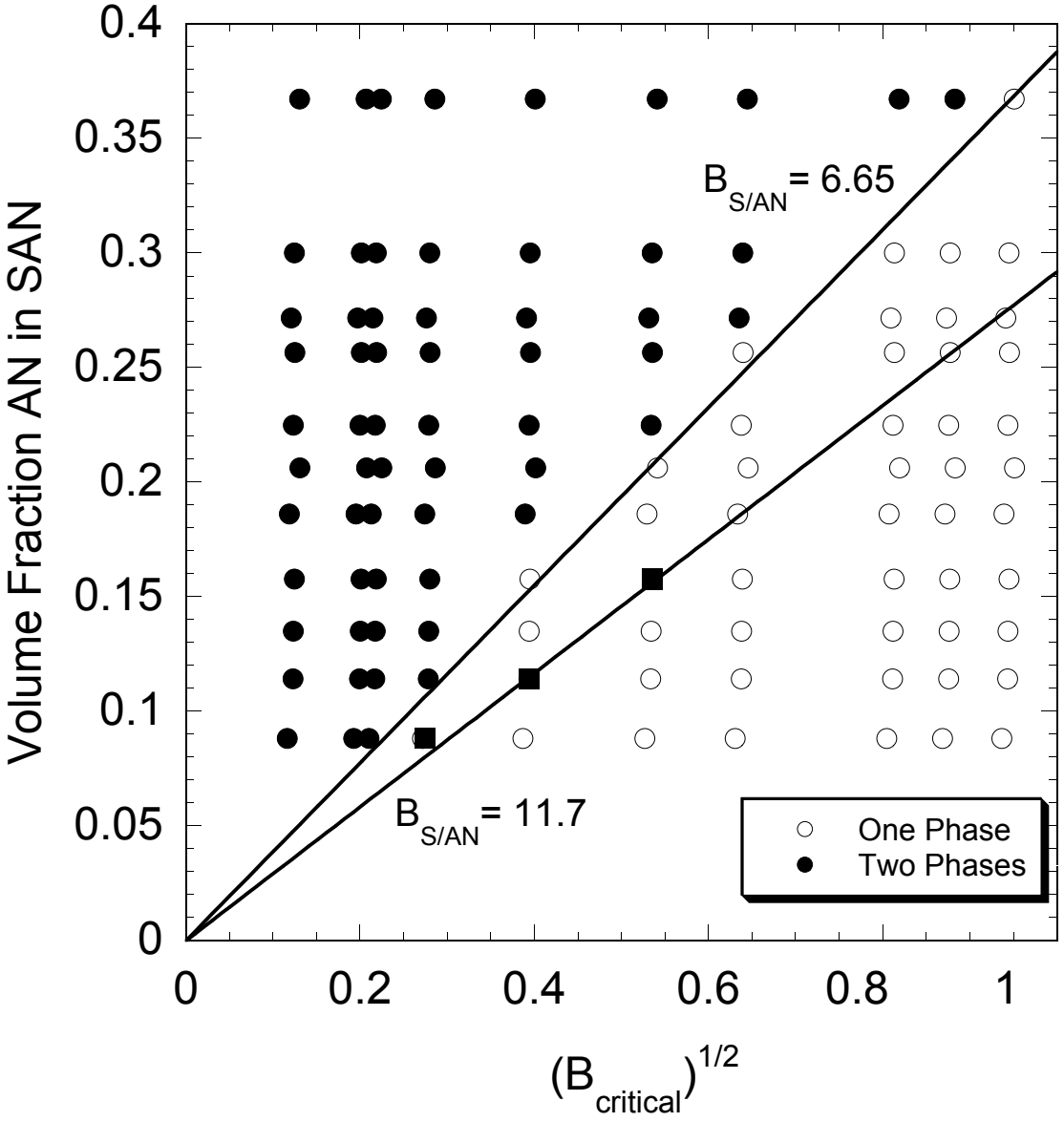

Figure 4.5 Locations of immiscible equal weight bends shown in Figure 4.4 with respect to critical point entropy of mixing.

methods. Polystyrene and polyacrylonitrile do not possess a relatively large contrast between their respective refractive indices or glass transition temperatures. The self compatibility of SAN is predicted to be 3 weight percent using the combinations of Equations 2.16 and 2.14, $B_{S/AN}$ = 11.7 cal/cm^3, and the average SAN molecular weight of polymers used in this study of 172,000 Da. The 3 weight percent composition difference would correspond to a refractive index difference of 0.002 between SAN blend components. The refractive index difference must be approximately 0.01 for the determination of miscibility[15]. An increase in SAN composition by 3 weight percent would correspond to less than a single degree Celsius change in glass transition. Differential scanning calorimetry cannot be used to identify two overlapping glass transition signatures that are one degree Celsius apart from one another. It is likely that these studies mistakenly evaluate the limits of phase contrast rather than limits of phase behavior. This would result in an underestimation of the S/AN interaction. Therefore, observations of high molecular weight SAN/SAN blends using optical and calorimetric methods cannot be converted into a meaningful S/AN interaction.

ANALYSIS OF COPOLYMER-COPOLYMER STUDIES

The analysis of copolymer/copolymer phase behavior to extract binary interaction energies is made difficult by the number of binary interactions responsible for the phase behavior. Yet much of the information previously gathered about the S/AN interaction has been deduced through copolymer/copolymer studies.

Blends of Poly(styrene-co-maleic anhydride) and Poly(styrene-stat-acrylonitrile)

Several researchers have observed the phase behavior of blends of SAN and poly(styrene-co-maleic anhydride) (SMA) [5, 9, 16-18]. Gan and Paul inferred a S/AN interaction energy of 6.8 cal/cm^3 from one of these studies[5]. Aokj performed an independent experimental and analytical study of SAN/SMA blends and reported that the interaction parameter suggested by regular solution theory and the predicted solubility parameters of Hoy at 23°C (8.4 cal/cm^3) fit the observed data well. These studies are mentioned here since their conclusions about the S/AN interaction have been cited and used often.

A re-analysis of the SAN/SMA blend phase behavior and accompanying analysis of possible binary interaction energies requires extensive analysis, and therefore it will be the subject of Chapter 6. That chapter will show that consistency between the interactions derived from PS/SMA and SAN/SMA blend phase behavior can only be achieved with the larger S/AN interaction inferred from the PS/SAN phase behavior.

Blends of Poly(styrene-co-acrylonitrile) with Poly(butadiene-co-acrylonitrile)

Cowie et al. have reported several values for the S-AN enthalpic interaction ranging from 4.99 to 5.45 cal/cm^3 [1-4]. Since these interactions are much lower than even those reported by Zhu, the accompanying studies of miscibility are of special interest in determining the predictive capability of the larger S/AN interaction.

Miscibility information from one of Cowie's newer publications involving SAN and poly(butadiene-co-acrylonitrile) (BAN) copolymers is represented in Figure 4.8[2]. This particular study was chosen due to its low number of binary interactions (three) responsible for creating the phase behavior, as opposed to other studies such as those involving ternary polymer blends. In Cowie et al.'s extraction of binary interactions, the

intramolecular interactions are allowed different values than intermolecular interactions involving the same pair identities. The subsequently reported value of a particular interaction is then taken as the average of the intermolecular and intramolecular interactions. The average binary interactions reported as describing the data in Figure 4.6 were $B_{S/AN}$ = 5.30 $B_{B/AN}$ = 8.43 $B_{S/B}$ = 0.67 cal/cm^3. The inner curve in Figure 4.6 was calculated using these average interactions and Cowie et al.'s entropy of mixing of 0.015 cal/cm^3. This curve does not fit the data as well as that shown in the paper in which the results were published since multiple values of binary interactions were not used simultaneously to fit the data.

To determine if the larger value of the S/AN determined here can be used to fit the data in Figure 4.6, estimations for the B/AN and B/S interactions are required. The temperature to assign to the phase behavior observations is a subjective one since the blends were precipitated from solution at room temperature, but analyzed by their glass transitions, which occur at an elevated temperature. The phase behavior was analyzed for reproducibility, indicating there was no change in phase behavior after thermal scans above the location of blend component glass transitions. An observation temperature of 150 °C is chosen for this analysis, since it corresponds to a temperature above all of the SAN copolymer glass transitions used in the study. The solubility parameters for butadiene, acrylonitrile, and styrene groups were estimated using the predicted molar volumes at 150 °C[10]. The solubility parameters were converted into predicted binary interactions as outlined in Chapter 2. The average interactions from the solubility parameters calculated by the methods of Hoy, Small, and Hoftyzer and van Krevelen suggest interactions of $B_{B/AN}$ = 21 and $B_{B/S}$ = 1.1 cal/cm^3. The second curve in Figure 4.6 was drawn using the same entropic contribution to mixing as before and with $B_{S/AN}$ =

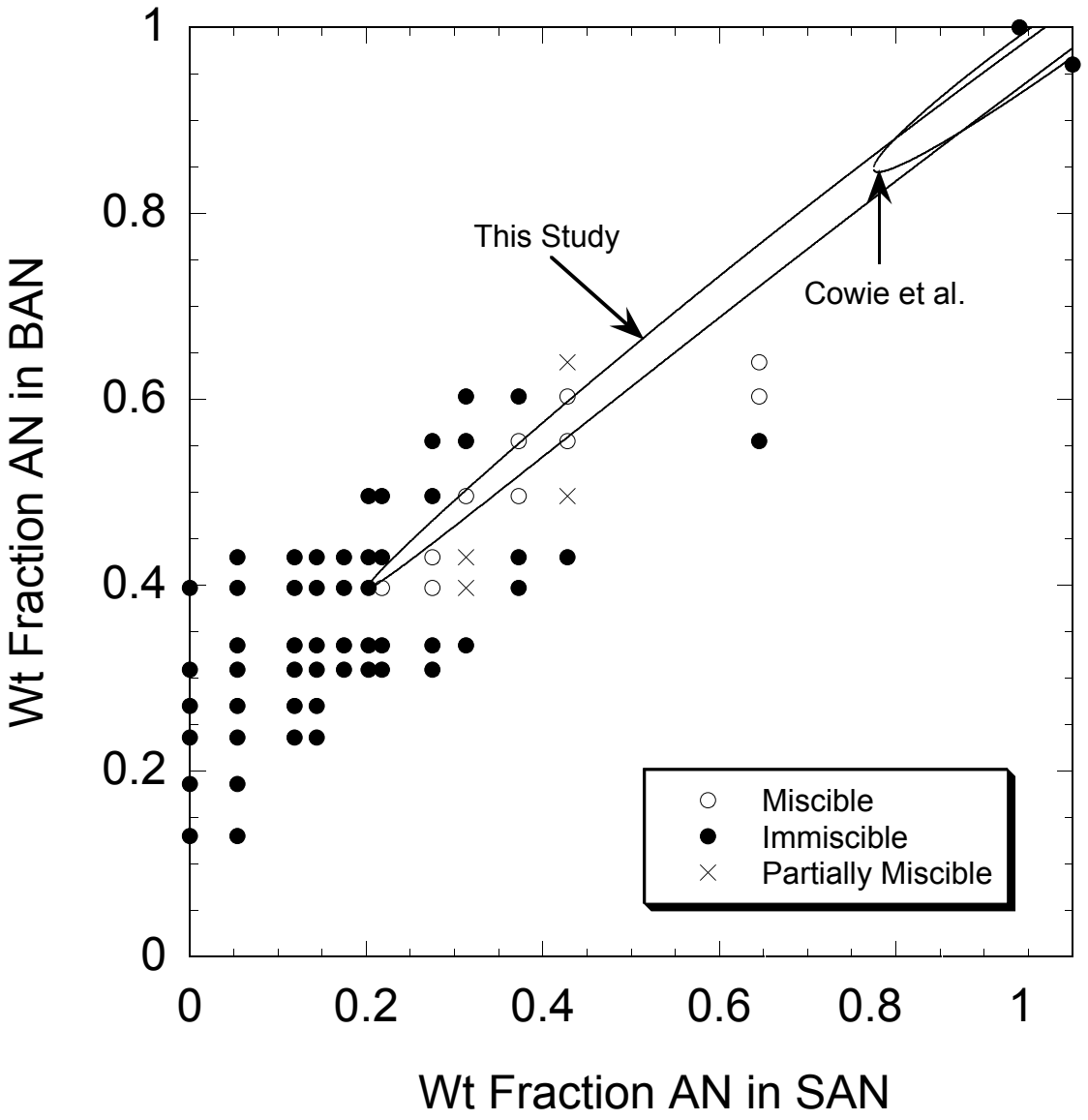

Figure 4.6 Phase behavior of SAN/BAN blends.

12.1 $B_{B/AN}$ = 19.0 $B_{S/B}$ = 0.815 cal/cm^3. This value of $B_{S/AN}$ corresponds to the bare interaction parameter of 13.0 cal/cm^3. The difference between the average predicted interactions and those used to predict the larger area shown in Figure 4.6 correspond to $k_{S/AN}$=0.002, $k_{B/AN}$=0.01, and $k_{S/B}$=0.002, while the difference between the average previously reported and predicted values correspond to $k_{S/AN}$=0.03, $k_{B/AN}$=0.06, and $k_{S/B}$=0.003.

The interactions for the SAN/BAN blend system estimated in this study provide a better qualitative approximation of the observed phase behavior, and the associated value of $k_{B/AN}$ is reduced by a factor of 6 over that of the previously estimated binary interactions. If intermolecular and intramolecular interactions are considered equivalent, the larger value of the S/AN interaction appears to be more useful in predicting the experimentally determined SAN/BAN blend phase behavior than the S/AN interaction value reported by Cowie et al.

MOLECULAR ANALOGS

Ziaee and Paul studied several analogs of styrene and acrylonitrile in order to estimate the S/AN interaction through analog calorimetry[11]. They found that the orientation of the CN dipole in the acrylonitrile analog greatly effects interactions with other molecules. In addition, they found that some analogs had specific interactions that prevented analysis of interactions by group contributions. They ultimately reported three S/AN interactions as shown in Table 4.1.

The S/AN interaction at 25 °C is 12.2 cal/cm^3 based on the 13.0 cal/cm^3 bare interaction energy. This value is 8% different than the interaction of 11.2 cal/cm^3 that was determined while using the n-Octyl-cyanide analog. Given the difficulties in using analog calorimetry to assess the S/AN interaction noted by Ziaee, and the relatively close agreement between the larger S/AN value reported here and the interaction estimated

using one of the acrylonitrile analogs, the conclusions of the analog calorimetry study do not appear to definitively conflict with the conclusions of this study.

CONCLUSIONS

New experimental evidence is presented here which indicates that the S/AN interaction is 11.74 cal/cm^3 at 200 °C. This interaction is much larger than has been reported in the past, but is consistent with estimations using solubility parameters. Several methods used to extract information about the S/AN interaction have been reviewed in the context of the larger interaction. None of the studies reviewed negated the existence of the larger interaction.

A previous study that used the same materials and a similar method to extract the S/AN interaction was re-evaluated. Several equal weight blends made by casting at elevated temperatures had two phases after annealing, while the previous study asserted that the same blends possessed a single phase after annealing. The results of this previous study agree perfectly with an earlier study of SAN/SMA blend phase behavior. However, analysis in Chapter 6 will show that agreement between interactions inferred from PS/SMA, PS/SAN and SAN/SMA blend phase behavior requires the use of the larger S/AN interaction presented in this study.

The low values for the S/AN interaction have been accepted and used following the analysis of the SAN/SMA blend study, while other polymer interactions were subsequently adjusted such that predicted phase behavior would match experimental observations. This has caused many binary interactions extracted from experimental observations of blend phase behavior involving SAN to be directly related to the lower S/AN interaction, resulting in estimated interactions that are far lower than their predicted values. This was illustrated by the analysis of the SAN/BAN blend study, and will also be illustrated in the following chapter.

REFERENCES

1. Bell, S.Y., Cowie, J.M.G. and McEwen, I.J. Polymer 1994;35:786.
2. Cowie, J.M.G., Harris, J.H. and McEwen, I.J. Macromolecules 1992;25:5287.
3. Cowie, J.M.G., et al. Polym. Comm. 1991;32:293.
4. Cowie, J.M.G. and D. Lath, Makromol. Chem. Macromol. Symp. 1988;16;103.
5. Gan, P.P. and Paul, D.R. J. of App. Polym. Sci. 1994;54:317.
6. Brannock, G.R., Barlow, J.W. and D.R. Paul, D.R. J. Polym. Sci. Polym. Phys. 1990;28:871.
7. Zhu, S. and Paul, D.R. Macromolecules 2002;35:2078.
8. Bogdanic, G., et al., Fluid Phase Equilibria 1997;139:277.
9. Aokj, Y., Macromolecules 1988;21:1277.
10. van Krevelen, D.E., 'Properties of polymers' 3 ed., Elsevier Pub. Co., Amsterdam, 1990.
11. Ziaee, PhD Dissertation, 1995, The University of Texas at Austin.
12. Zhu, S. and Paul, D.R. Macromolecules 2002;35:8227.
13. Chu, J. and Paul, D.R. Polymer 2000;41:7193.
14. Merfeld, G.D., Chan, K. and Paul, D.R. Macromolecules 1999;32:429.
15. Bohn, L., 'Compatible Polymers', in 'Polymer Handbook', Brandrup, J.and Immergut, E.H. Eds., Wiley, New York,1975.
16. Hall, W.J., et al., Prepr. Am. Chem. Soc. Div. Org. Coatings Plast. Chem., 1982;47:298.

17. Hall, W.J., et al., Am. Chem. Soc. Symp. Ser. 1983;49:229.

18. Kim, J.H., Barlow, J.W., and Paul, D.R. J. Polym. Sci. Polym. Phys. 1989;27:223.

Chapter 5: Interactions in Blends of Poly(styrene-stat-acrylonitrile) and Poly(n-alkyl acrylate-co-methyl methacrylate)

If the styrene-acrylonitrile (S-AN) interaction is nearly double what researchers have previously thought as discussed in Chapter 4, then the extraction of other interaction energies during the analysis of polymer blend phase behavior involving AN have also been misrepresented. Chu and Paul, and later Zhu and Paul, observed phase behavior in blends of Poly(styrene-stat-acrylonitrile) (SAN) with copolymers of Poly(n-alkyl acrylate –co-methyl methacrylate) (nAA), where n refers to the variable length of the hydrocarbon chain in the alkyl acrylate[1, 2]. A reanalysis of the copolymer blend miscibility presented in this study will show that the larger S-AN can be used to predict the phase behavior in these blends well.

When predicting copolymer-copolymer phase behavior using the Flory Huggins Theory combined with the mean field approximation, there are six interactions that must be represented. New data will be presented in this chapter that will establish a relationship between the S-AN, S-MMA and MMA-AN interactions. Since these interactions were present in all six of the n-alkyl copolymer/ SAN blends previously studied, there are only three interactions that are variable between those blend systems. The previous study provided independent analysis that bounded the range of nAA/MMA and nAA/S interactions, leaving the nAA/AN interaction as the only true unknown when predicting the nAA-co-MMA/ SAN blend phase behavior. This chapter will show that increasing the nAA/AN interaction when predicting the copolymer-copolymer blend phase behavior compensates for the larger S-AN interaction. The higher implied values of the nAA/AN interactions are shown to compare favorably with predicted interactions.

SAN/ MONODISPERSE PMMA BLENDS

Monodisperse PMMA shown in Table 5.1 was blended with the SAN copolymers shown in Table 4.2 in the predicted critical point compositions. The blends were cast from approximately 10 wt% polymer in dichloromethane onto glass slides at 40 °C. The blends were then annealed for 48 hours at 150 °C. Figure 5.1 shows the resulting assessment of phase state behavior. The Y-axis of Figure 5.1 corresponds to the critical point entropy of mixing calculated using Equation 2.16. The curves in Figure 5.1 were made using Equation 2.12 for the enthalpy of mixing.

The solid lines in Figure 5.1 represent interaction parameters of $B_{S/AN}$=12.0, $B_{S/MMA}$=0.301, and $B_{AN/MMA}$=7.93 cal/cm^3. This S-AN interaction represents the bare interaction parameter determined in Chapter 4 adjusted to 150 °C through the use of Equation 2.9 and the Sanchez Lacombe Equation of State parameters in Appendix A. The S-MMA interaction represents the bare interaction parameter of 0.32 cal/cm^3 determined by Callaghan through the observation of monodisperse PS and PMMA blend phase behavior[3]. The AN-MMA interaction was varied to fit the observed phase behavior. The resulting bare interaction parameter for the AN-MMA pair is 8.32 cal/cm^3. The solid curve indicates that the SAN9.5/PMMA265.6 and SAN33/PMMA13 blends are close to the miscibility boundary. The SAN33/PMMA13 blend was miscible when cast, but became phase separated after annealing at 150 °C. This indicates that this blend is in fact close to the actual boundary of thermodynamic phase equilibrium. The SAN9.5/PMMA265.6 blend appeared cloudy after being cast, but became clear and possessed a single glass transition temperature after annealing. Zhu reported that the polydisperse PMMA homopolymer (MW=442,000) used in his study was immiscible with SAN9.5[4]. Zhu's annealing temperature was 120 °C, which is 2 °C above the onset

Table 5.1 PMMA homopolymers.

Polymer	M_W	M_W/M_N	Source
PMMA2.4	2,400	1.08	Polymer Laboratories
PMMA4.9	4,910	1.10	Polymer Laboratories
PMMA13	13,000	1.03	Polymer Laboratories
PMMA27.5	27,500	1.10	Polymer Source, Inc.
PMMA48.4	48,400	1.10	Polymer Source, Inc.
PMMA60	60,000	1.07	Polymer Laboratories
PMMA105.4	105,400	1.04	Polymer Source, Inc.
PMMA265.6	265,600	1.14	Pressure Chemcial

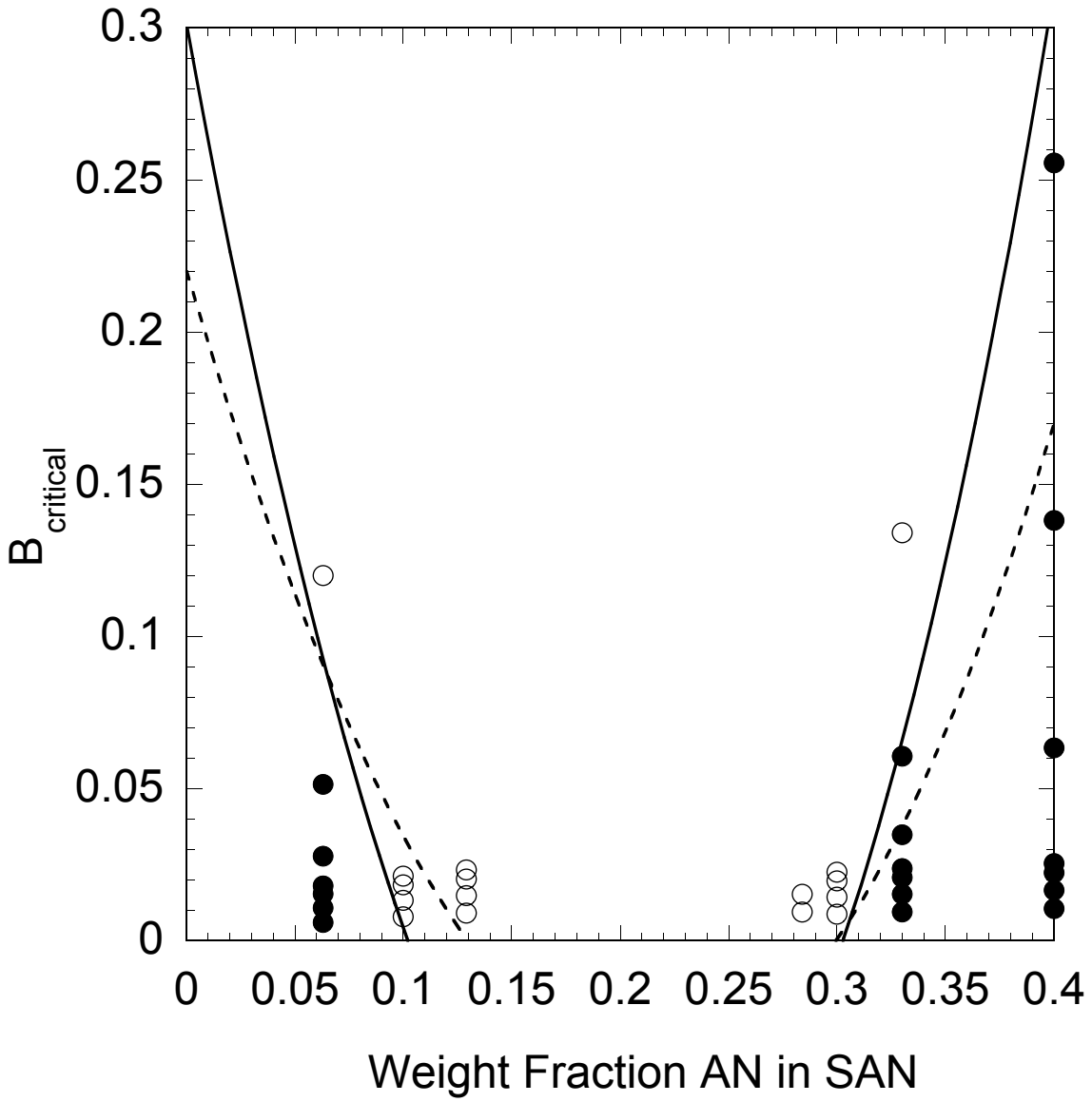

Figure 5.1 Phase behavior of SAN with monodisperse PMMA at 150°C. Open and closed circles represent single and two phase blends respectively. The solid lines were drawn using $B_{S/AN}$=12.0, $B_{S/MMA}$=0.301, and $B_{AN/MMA}$=7.93 cal/cm^3. The dashed lines were drawn using $B_{S/AN}$=6.98, $B_{S/MMA}$=0.22, and $B_{AN/MMA}$=4.49 cal/cm^3.

of the PMMA glass transition reported by Zhu. Other researchers have reported miscibility between SAN9.5 and PMMA [5, 6]. Brannock reported a could point temperature of 290 °C in approximately equal weight blends of SAN9.5 and PMMA with a molecular weight of 130,000[6]. It is possible that the low mobility of the SAN9.5, coupled with the negligible free energy incentive for phase homogenization, caused Zhu's PMMA/SAN blend to be in a state of non-equilibrium during his miscibility analysis. To reflect the observations made here and those of the other researchers cited, the state of miscibility of SAN9.5/PMMA is changed to indicate single phase behavior on the nAA-co-MMA/SAN isothermal phase maps. The interactions used to create the solid line shown in Figure 5.1 predict the observed PMMA/SAN blend phase behavior observed during this study well, and will be used to fit the nAA-co-MMA/SAN blend data.

The interaction parameters used to fit the nAA-co-MMA/SAN blends in the previous study are shown in Table 5.2. An average of the S-AN interaction value used by Zhu is shown in Table 5.3 since this interaction was used as an adjustable parameter in fitting the nAA-co-MMA/SAN phase behavior. These values for the interactions adjusted to 150 °C by using Equation 2.9 correspond to $B_{S/AN}$=6.98, $B_{S/MMA}$=0.22, and $B_{AN/MMA}$=4.49 cal/cm^3. These interaction values were used to construct the dashed lines shown in Figure 5.1. The phase behavior of 6 PMMA/SAN blends is not represented by the predicted phase behavior. The AN-MMA interaction cannot be varied independently such that a greater number of blend phase behavior observations are predicted accurately. If the S-AN interaction determined Zhu independently of other interactions, $B_{S/AN}$=6.8

Table5.2 Interactions used to construct curves in Figure 5.3a-f in cal/cm^3 at 120°C.

Interaction	S		MMA		Entropy of
	ΔP^*_{ij}	B_{ij}	ΔP^*_{ij}	B_{ij}	Mixing
MeA	1.12	1.20	0.07	0.19	0.0086
EA	0.57	0.80	-0.07	0.15	0.0085*
nPA	0.44	0.44	0.36	0.34	0.0083
nBa	0.12	0.35	0.43	0.56	0.0076*
nHA	0.23	0.38	0.74	0.78	0.0065
nDA	0.39	0.43	1.06	1.00	0.0064

- These interactions were presented by Chu[1], while all others except the MeA/S interaction were presented by Zhu[2].

Table 5.3 Binary interaction energies used in this study listed in cal/cm^3 at 120°C.

Interaction	Current Study		Previous study		Average Prediction	
	ΔP^*_{ij}	B_{ij}	ΔP^*_{ij}	B_{ij}	$V^{25°C}$	$V^{120°C}$
S-AN	13.0	12.2	7.42	7.06	12.1	12.5
S-MMA	0.32	0.30	0.23	0.22	0.012	0.013
MMA-AN	8.32	8.01	4.55	4.51	12.79	13.2
MeA-AN	10.2	10.2	3.71	4.2	8.49	10.8
EA-AN	11.2	11.2	4.52	5.09*	10.6	12.8
nPA-AN	11.0	10.6	5.71	5.66	12.2	12.8
nBa-AN	11.8	11.7	6.49	6.81*	13.4	14.1
nHA-AN	13.1	12.7	7.60	7.68	14.9	15.2
nDA-AN	15.0	14.3	8.67	8.47	16.8	17.4

* These interactions were presented by Chu[1], while all other previous interactions were presented by Zhu[2].

cal/cm^3, is used instead of the value used to construct the dashed lines in Figure 5.1, the PMMA/SAN phase behavior prediction becomes even less accurate[7].

nAA Interactions with S and MMA

The n-alkyl acrylate interactions with styrene and methyl methacrylate were estimated in two ways in the previous study. Monodisperse homopolymers of various PS and PMMA molecular weights were blended with n-AA homopolymers to obtain ranges of possible interactions. Unfortunately, most of the interactions obtained from the homopolymer-homopolymer miscibility studies were obtained from equal weight blends using oligomeric PS and PMMA with other high molecular weight n-alkyl acrylates. Monodisperse PS and PMMA of varying molecular weights were also blended with nAA-co-MMA and nAA-co-S copolymers. Ultimately however, the n-AA/PS and n-AA/MMA interactions were adjusted to obtain a better fit of the nAA-co-MMA/SAN blend phase behavior in the previous studies.

The nAA interactions determined by observations of copolymer versus homopolymer phase behavior in the previous study will be used to fit the nAA-co-MA/SAN with one exception. The reported phase behavior of PS-co-methyl acrylate (MeA) and polystyrene is shown in Figure 5.2. Much of the blend data is for blends whose critical points are predicted to contain more than 80wt% styrene. Chapter 3 illustrated an instance of an observable difference between equal weight and critical point phase behavior in a blend whose critical point was predicted to be 83 vol% homopolymer. The assumption that equal weight blends are equivalent to the critical point would result in a low estimation for the S/MeA interaction. Unfortunately, the PS-co-MeA copolymers used in the previous study are not available for study, and therefore the nAA/S and nAA/MMA cannot be determined using critical point composition blends.

Figure 5.2 contains a line that corresponds to the original PS/MeA interaction of 1.05 cal/cm^3, and another line that corresponds to 1.20 cal/cm^3, the value that will be used to fit the PMMA-co-MeA/SAN blend data. The line corresponding to BS/MeA=1.05 cal/cm^3 does not fit the reported phase behavior well since the reported PS-co-MeA compositions were used instead of the ones which comprised the original plot published in Zhu's dissertation[8].

The magnitude of the nAA/S and nAA/MMA interactions significantly contribute to the predicted miscible behavior in the nAA-co-MMA/SAN blends for only the lowest two n-AA chain lengths. Therefore, it was not necessary to adjust the n-AA/S and n-AA/MMA interactions to obtain good predictions of phase behavior in most of the nAA-co-MMA/SAN blends. Of the 12 nAA/S and nAA/MMA interactions determined in the previous study, only the S/MeA interaction required adjustment to allow a good prediction of the MeA-co-MMA/SAN phase behavior while using the larger S/AN and MMA/AN interactions.

Poly(nAA-co-MMA)/SAN Blends

Figure 5.3a-f shows the phase behavior of the nAA-co-MMA/SAN blends evaluated at 120 °C. The ethyl acrylate (EA) and n-butyl acrylate (nBA) blend system data was determined by Chu[1]. The MeA, n-propyl acrylate (nPA), n-hexyl acrylate (nHA), and n-decyl acrylate (nDA) blend systems miscibility data was determined by Zhu[2]. The interaction and entropy of mixing values shown in Tables 5.2-3 were used to construct the curves shown in Figures 5.3a-f. All of the entropy of mixing values were unchanged from the previous studies.

With the exception of the S/MeA interaction, all of the nAA/S and nAA/MMA interactions previously determined by copolymer/homopolymer phase behavior analysis

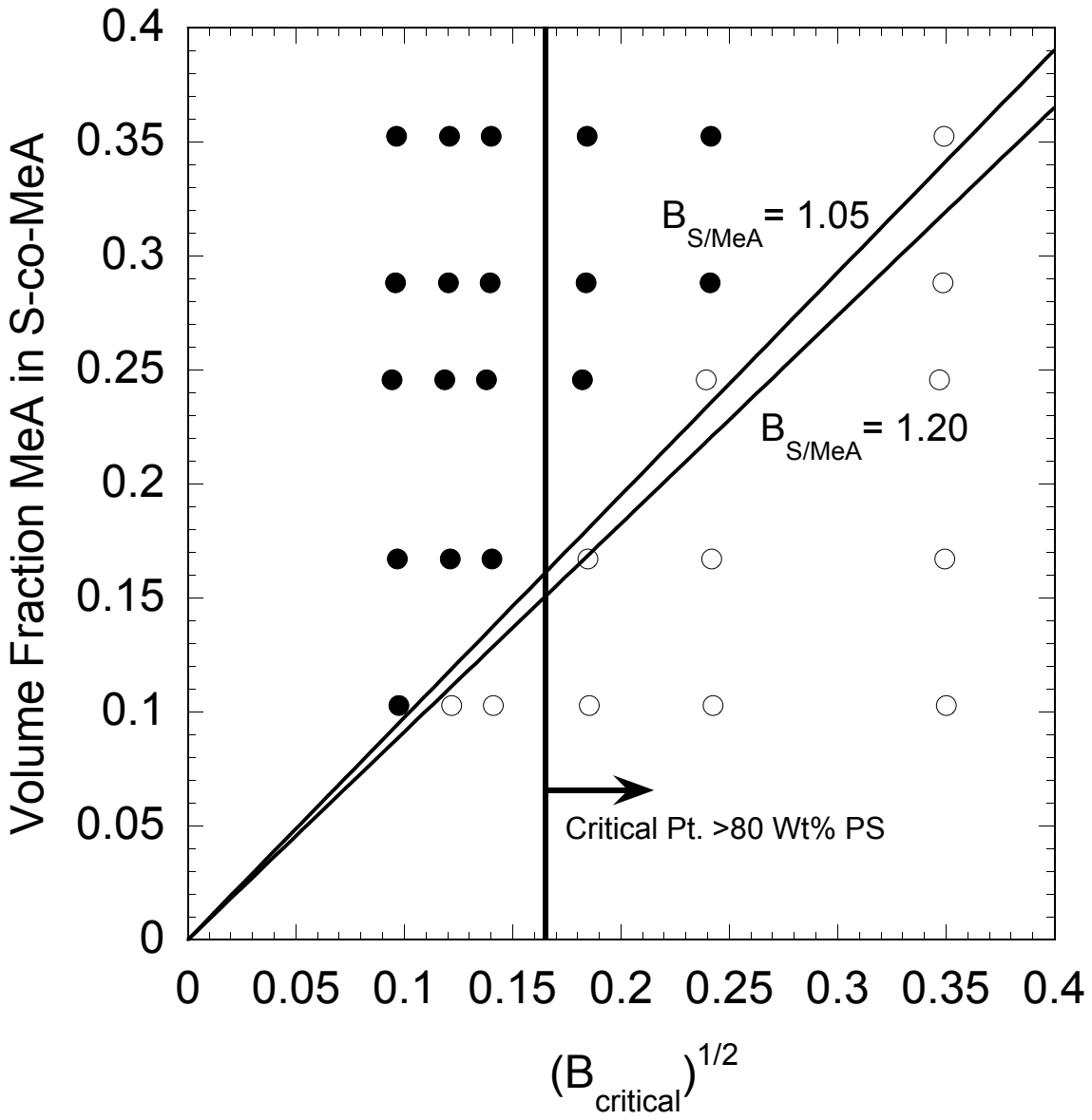

Figure 5.2 Phase behavior for equal weight S-co-MeA/PS blends at 120 °C. Open and closed circles represent single and two phase blends respectively. The previously reported interaction of 1.05 and interaction of 1.20 cal/cm^3 that will be used here are indicated by the two lines that pass through the origin.

were used to construct the curves in Figure 5.3a-f. The S/MMA, S/AN, and MMA/AN values described in the previous section were also used to construct the curves. The only variable adjusted to describe the reported phase behavior was the nAA/AN interaction. Since three fewer interactions were varied, the predicted phase behavior does not fit the observations as accurately as in the previous studies. Some of the difficulty in being able to fit the observations might also be due to non-equilibrium phase behavior like that noted in the SAN9.5/PMMA blend.

Overall, phase behavior trends in the nAA-co-MMA/SAN blends are well represented using the larger S/AN interaction discussed in Chapter 4, and the MMA/AN interaction presented in this chapter. In order to compensate for the larger S/AN and MMA/AN interactions, the nAA/AN interaction was increased to represent the experimental data.

Table 5.3 lists the nAA/AN interactions from the previous studies, the current study, and their corresponding bare interaction parameters calculated from Equations 2.5-9 and the equation of state parameters in Appenxix A. Table 5.3 also lists the predicted nAA/AN interaction estimated from Equation 2.17 and solubility parameters calculated through group contribution methods[9]. The values listed are the average of interaction values determined from the solubility parameter estimations of Small, Hoy, and Hoftyzer and van Krevelen.

Solubility parameters are determined from the cohesive energy density calculated through group contribution estimations and the molar volumes of the polymer. van Krevelin suggested using predicted molar volumes at 25 °C[9], and this was the

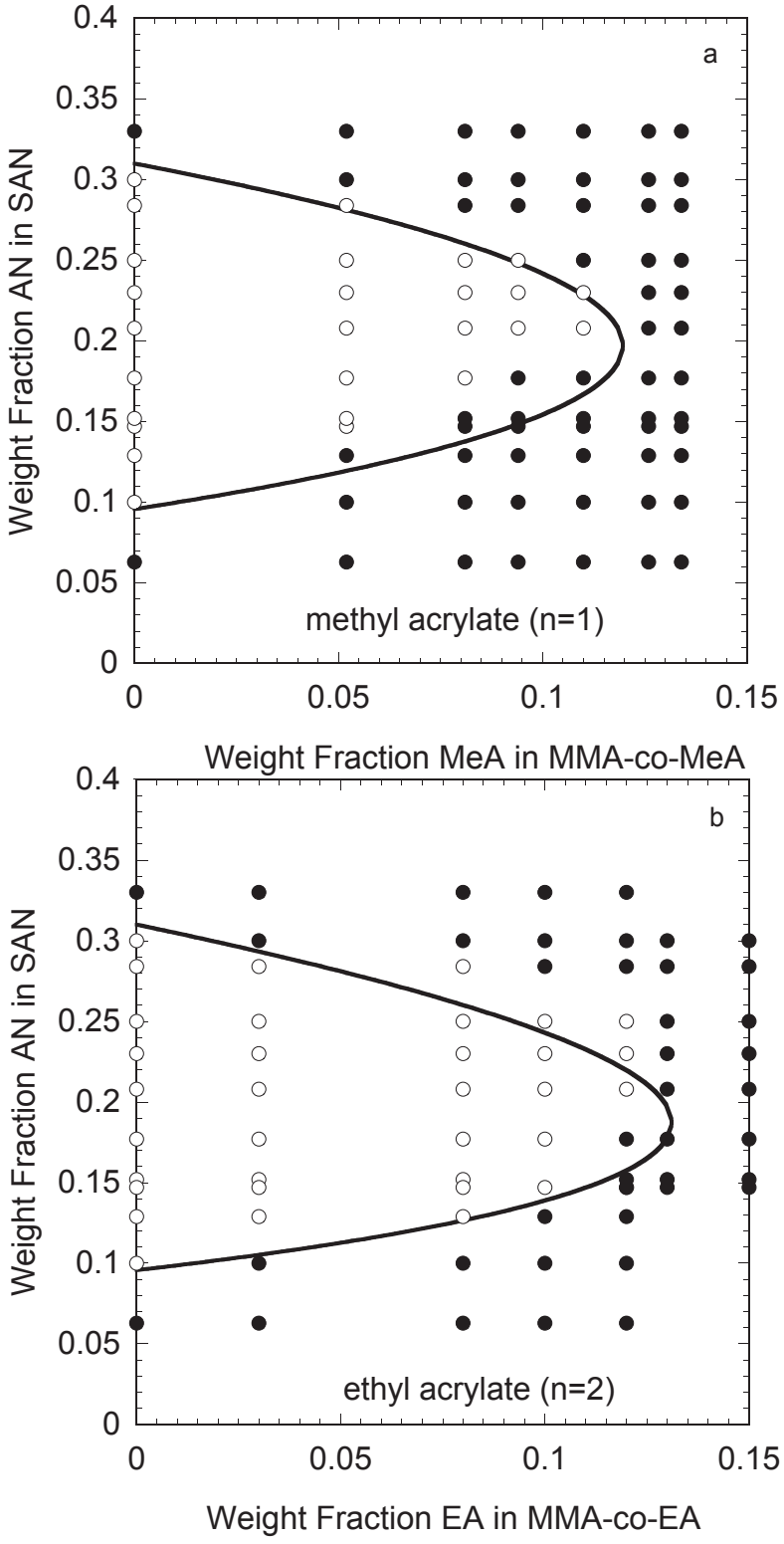
a
Weight Fraction AN in SAN
0.4
0.35
0.3
0.25
0.2
0.15
0.1
0.05
0
methyl acrylate (n=1)
0
0.05
0.1
0.15
Weight Fraction MeA in MMA-co-MeA
b
Weight Fraction AN in SAN
0.4
0.35
0.3
0.25
0.2
0.15
0.1
0.05
0
ethyl acrylate (n=2)
0
0.05
0.1
0.15
Weight Fraction EA in MMA-co-EA

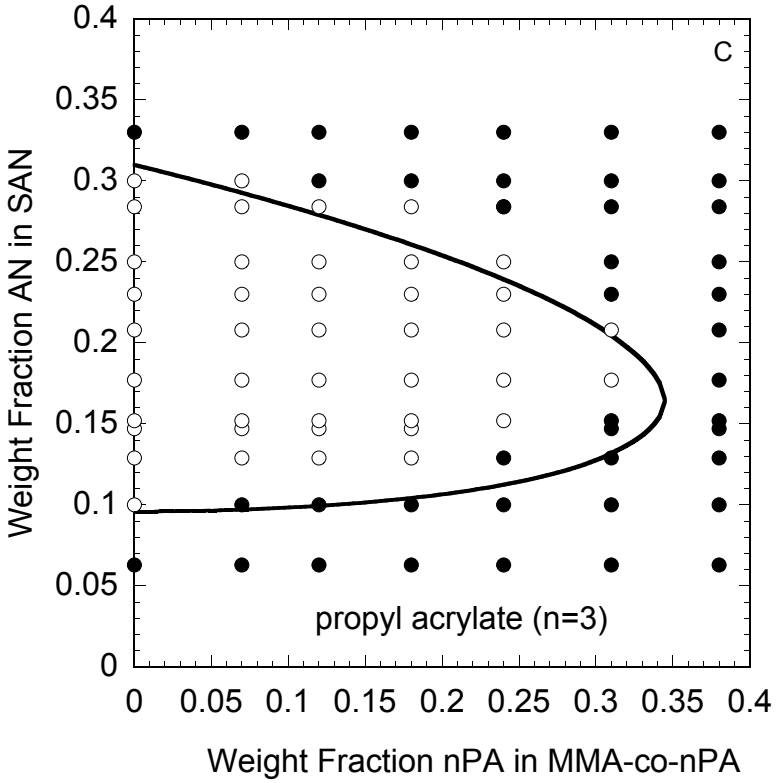
C
Weight Fraction AN in SAN
propyl acrylate (n=3)
Weight Fraction nPA in MMA-co-nPA
0
0.05
0.1
0.15
0.2
0.25
0.3
0.35
0.4

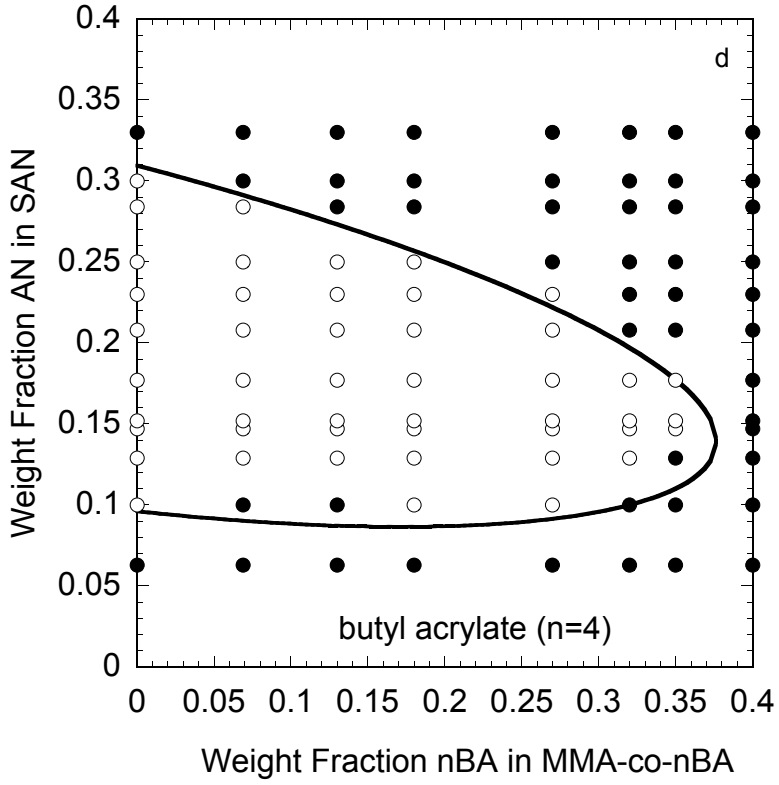
d
Weight Fraction AN in SAN
butyl acrylate (n=4)
Weight Fraction nBA in MMA-co-nBA
0
0.05
0.1
0.15
0.2
0.25
0.3
0.35
0.4

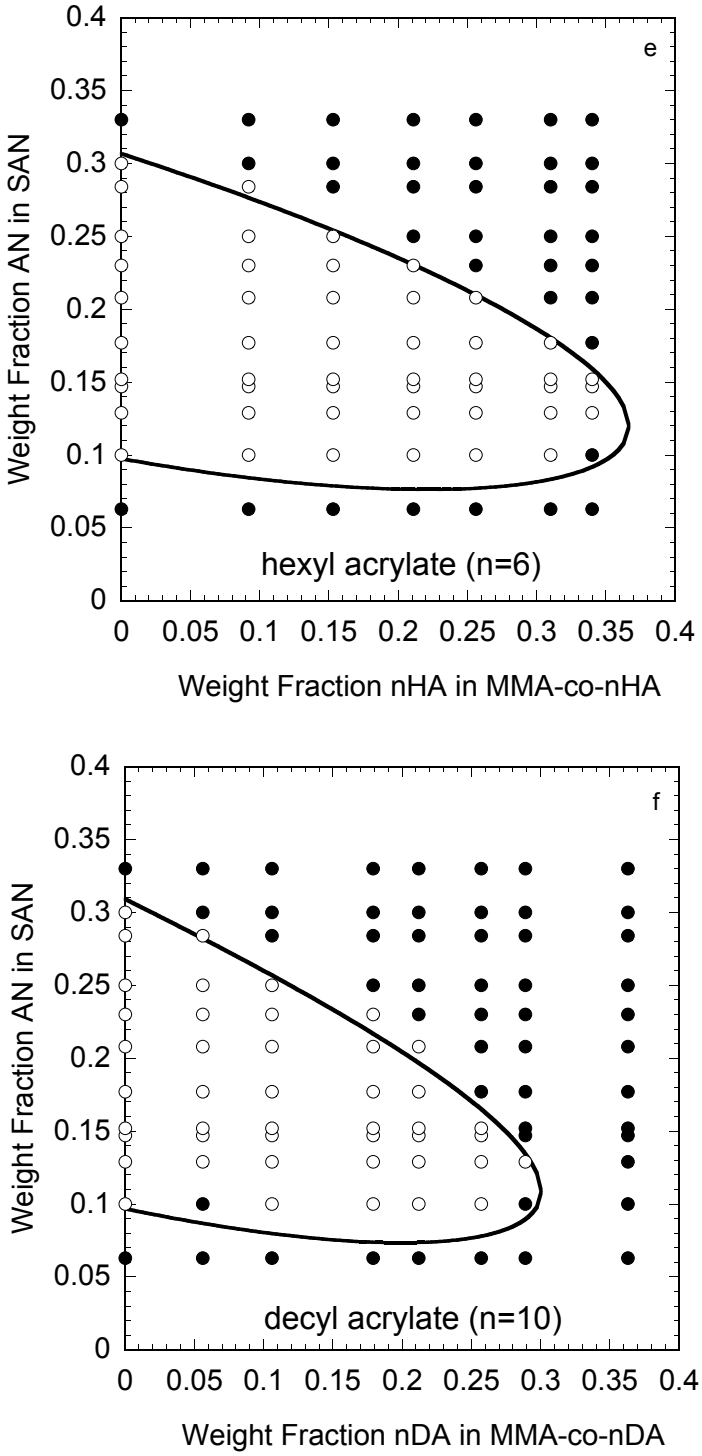

Figure 5.3 Phase behavior of equal weight nAA-co-MMA/SAN blends annealed at 120 °C. Open and closed circles represent single and two phase blends respectively. Solid lines were constructed using interactions listed in Tables 5.2-3 and Equation 2.11.

method used to estimate solubility parameters in the previous study[7]. However, equilibrium phase behavior of polymer blends is not established at 25 °C, which would correspond to the glassy state for polyacrylonitrile. Given that the glass transition temperatures of polymers are different, the differences between molar volumes at 25 °C are not likely to be equivalent to the differences between molar volumes in the melt state. The differences between molar volumes at the two temperatures would depend on the amount of excess free volume trapped in the glassy state of one or both of the polymers at 25 °C. It is therefore more intuitive to use molar volumes corresponding to the melt state. Therefore, the solubility parameters were calculated using molar volumes at 25 °C in order to compare to the previous study, and at 120 °C calculated from the equation of state parameters listed in Appendix A to represent the molar volumes in the melt state.

Figure 5.4 is a plot of the nAA/AN bare interactions and average predictions listed in Table 5.3 as a function of the n-alkyl chain length. Figure 5.4 indicates the nAA/AN interactions inferred in this study compare well to the average predicted interactions in terms of the trend of increasing energy density with n-alkyl chain length, and the magnitude of the interaction. The previous studies of Chu and Zhu infer a similar trend, but the magnitudes of their interactions are approximately half of the average predicted values. This discrepancy is equivalent to the difference between the S/AN interaction determined in Chapter 4, and the average S/AN interaction used to extract the nAA/AN interactions by Chu and Zhu.

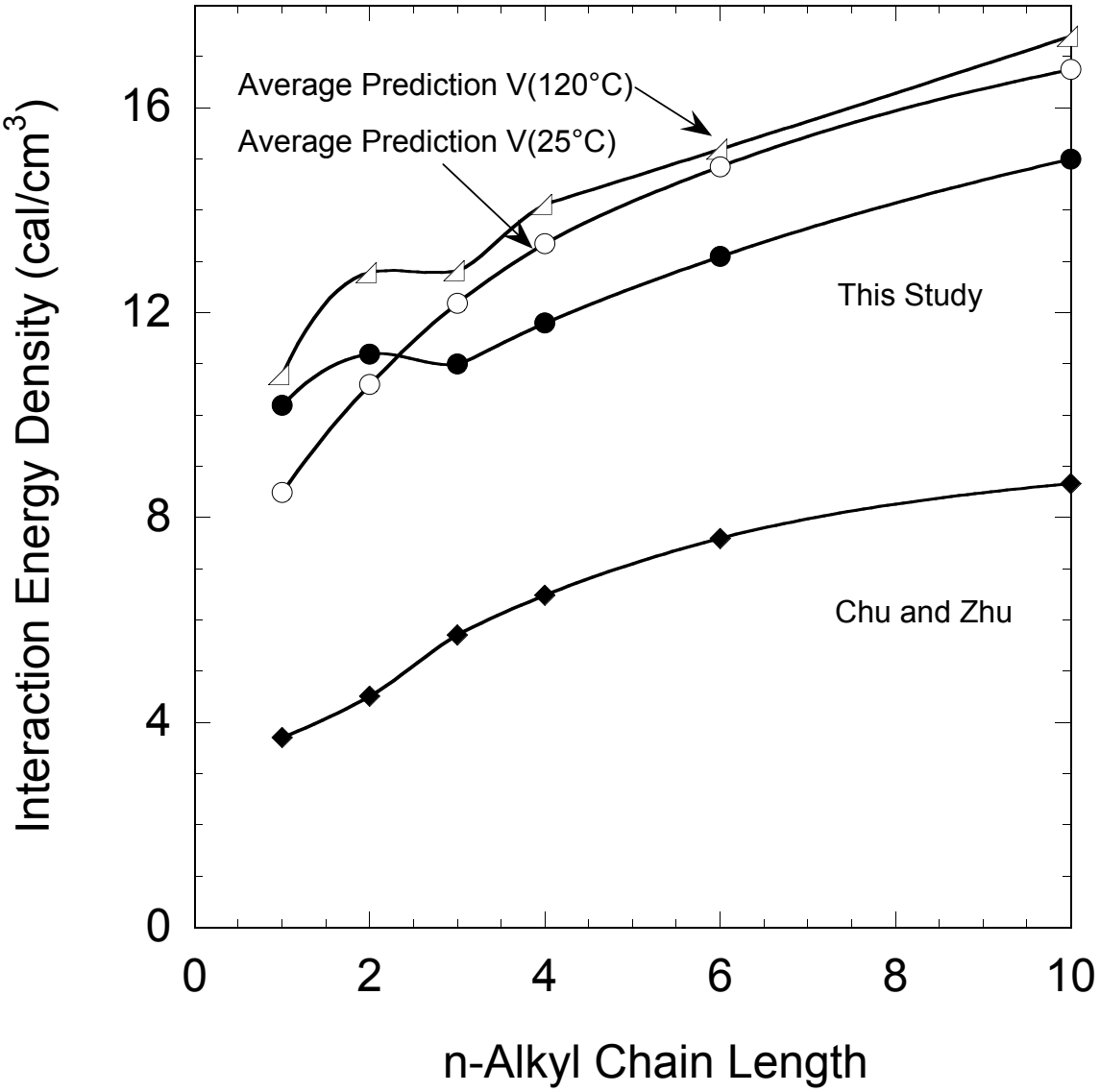

Figure 5.4 nAA/AN bare interaction parameters determined in this study and the previous ones as a function of n-alkyl chain length. The average of predicted interactions are also shown as a function of n-alkyl chain length.

The average predictions calculated using the molar volumes in the liquid state more accurately predict the trends in the experimentally determined nAA/AN bare interaction parameters than the predictions calculated using molar volumes at 25 °C. The predictions using the molar volumes at 25 °C indicate a smooth increase in nAA/AN interaction with increasing nAA chain length, while the predictions using the liquid state molar volumes predicts the nonlinear shape of the nAA/AN curve. Figure 5.5 shows the densities of the n-alkyl acrylates at 120 °C calculated from the equation of state parameters in Appendix A. The densities of poly(ethyl acrylate) and poly(propyl acrylate) diverge from the smooth trend of decreasing densities with increasing n-alkyl chain length. Figure 5.5 also shows the n-AA/AN interactions listed in Table 5.3. The deviations of the PEA and PPA densities from the general trend are mirrored by the deviations of their interactions with AN in the trend of n-AA/AN interactions.

The k_{ij} values, calculated using Equation 2.20, for the nAA/S, nAA/MMA, and nAA/AN experimentally determined bare interactions versus those predicted using the average group contribution methods and liquid molar volumes are shown in Figure 5.6. The differences between predicted and experimental binary interactions in Figure 5.4 are more apparent when put in terms of k_{ij}. The k_{ij} values calculated from Zhu and Chu's data are four times greater than the k_{ij} values associated with the nAA/AN interactions determined in this study while using the larger S/AN, MMA/AN, and S/MMA interactions.

The large negative deviation in k_{ij} values determined by Chu and Zhu suggest the existence of strongly polar or hydrogen-bonding forces involved in the nAA/AN interactions[10]. The Flory Huggins theory combined with the mean field

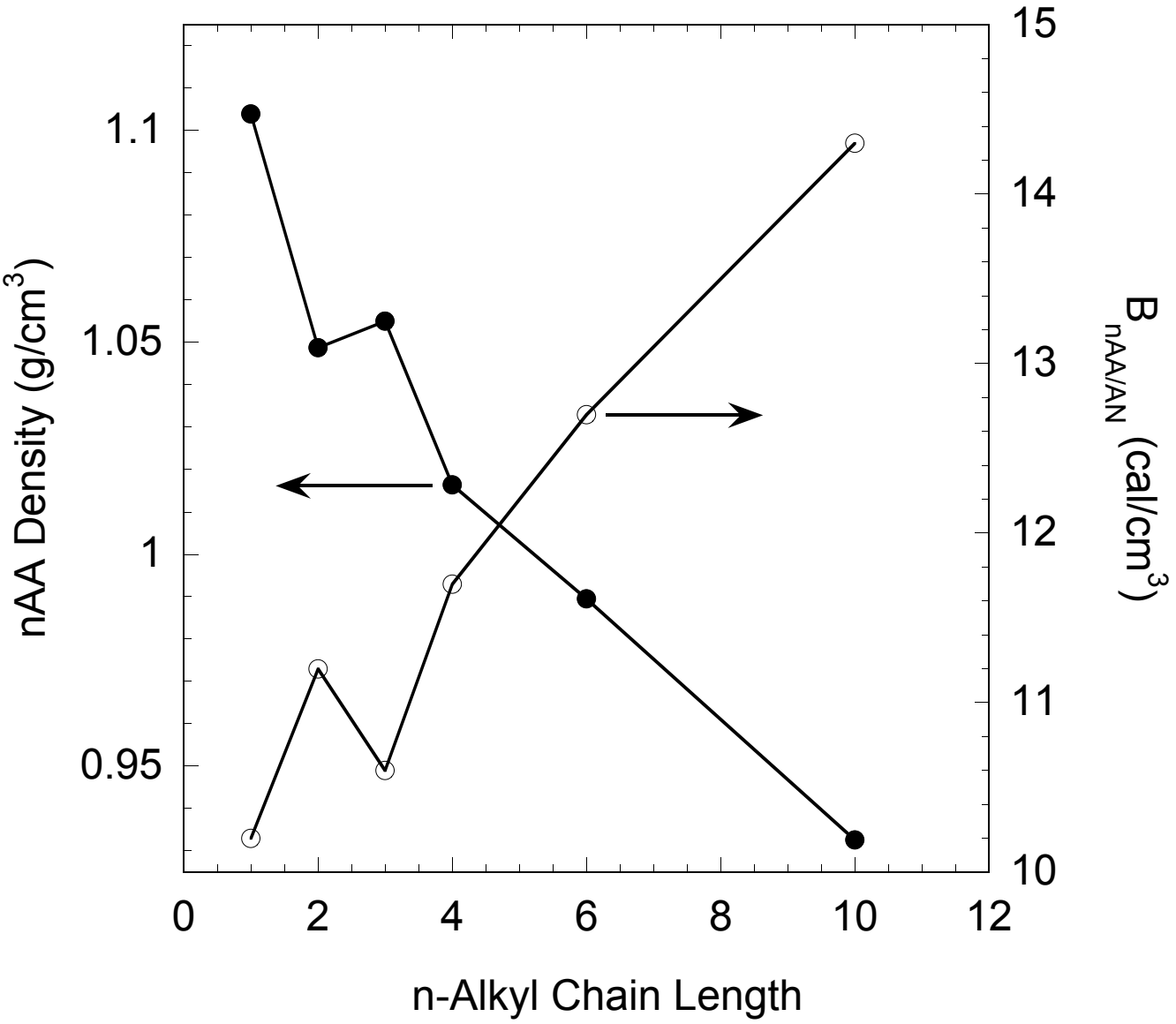

Figure 5.5 Densities of n-alkyl acrylates at 120 °C and interactions with acrylonitrile as a function of n-alkyl chain length.

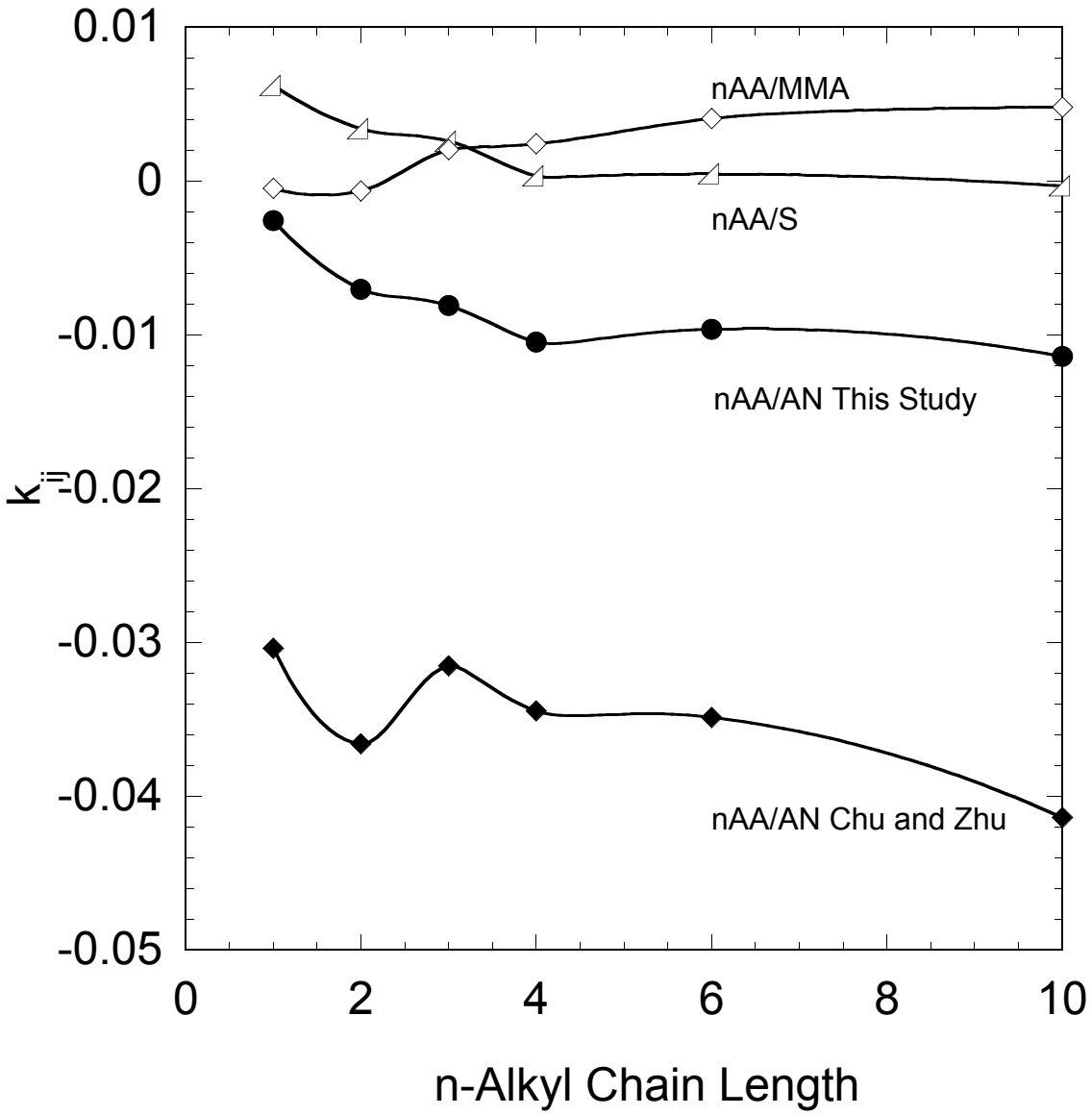

Figure 5.6 k_{ij} values as a function of n-alkyl chain length calculated from Equation 5.1 and the interaction values in Tables 5.2-3.

approximation, which has been used here and in the previous analysis of the nAA-co-MMA/SAN blends, assumes that no specific interactions exist in the blends. If these forces were present in the nAA-co-MMA/SAN blends, the Flory Huggins and mean field approximations would not be able to accurately predict the experimentally observed phase behavior over a range of nAA/AN interaction densities[11-13]. Since the nAA-co-MMA/SAN blend phase behavior was predicted well over a range of AN content in the blends as shown in Figure 5.3a-f, the presence of strong specific forces in the blends is unlikely.

Note that the curves representing the nAA/AN and nAA/PS interactions with respect to nAA chain length in Figure 5.5 are similar in shape, and are offset by a nearly constant value of 0.01. If the S/MeA interaction had not been increased by 13% from the previous study as outlined, the difference between k_{ij} values for MeA/AN and MeA/S would have been inconsistent with the overall trends.

CONCLUSIONS

The larger S/AN interaction introduced in Chapter 4 was successfully used in conjunction with the Flory Huggins theory and mean field approximation to predict phase behavior in monodisperse PMMA/SAN blends and in nAA-co-MMA/SAN blends. In order to describe the experimental nAA-co-MMA/SAN blend phase behavior, the larger S/AN interaction value was mostly compensated by larger nAA/AN and MMA/AN interactions. The resulting nAA/AN and PMMA/AN interactions agree more favorably with predicted interactions. The large difference between predicted interactions and those determined previously would suggest strong specific interactions are involved in the nAA/AN interactions. However, the success of the Flory-Huggins and mean field

theory in predicting the nAA-co-MMA/SAN blend phase behavior suggests that strong specific interactions are not present in these blends.

The ability to use the larger S/AN interaction to predict phase behavior in SAN/PMMA and nAA-co-MMA/SAN blends helps to validate its accuracy. The inability of the S/MMA, S/AN and S/MMA values used in the n-alkyl study to predict the SAN/PMMA phase behavior indicates difficulties in using smaller S/AN interaction values. In addition, this chapter has shown how interactions extracted while using the larger S/AN interaction compare much more favorably with predicted interactions than when the smaller value of the S/AN interaction is used.

A strong correlation exists between the changes in density and interaction energies of the n-alkyl acrylates with changing alkyl length. This indicates the importance of using correct molar volumes to the predictive capability of regular solution theory. Use of molar volumes corresponding to the liquid state is recommended since equilibrium phase behavior is established under those conditions, and the excess free volume is not unequally added to molar volumes based on glass transition temperatures.

REFERENCES

1. Chu, J.H. and Paul, D.R, Polymer 1999;40:2687.
2. Zhu, S. and Paul, D.R. Macromolecules 2002;35:8227.
3. Callaghan, T.A. and Paul, D.R. Macromolecules 1993;26:2439.
4. Zhu, S. and Paul, D.R. Macromolecules 2002;35:8227.
5. Gan, P.P., Paul, D.R. and Padwa, A.R. Polymer 1994;35:1487.
6. Brannock, G.R. and Paul, D.R. Macromolecules 1990;23:5240.
7. Zhu, S. and Paul, D.R. Macromolecules 2002;35:2078.
8. Zhu, S. PhD Dissertation, 2003, The University of Texas at Austin.
9. van Krevelen, D.E. 'Properties of polymers' 3 ed., Elsevier Pub. Co., Amsterdam, 1990.
10. Prausnitz, J.M., Lichtenthaler, R.N. and Gomez de Azevedo, E. 'Molecular Thermodynamics of Fluid-Phase Equilibria' 2 ed. Prentice-Hall, Englewood Cliffs, N.J., 1986.
11. Luengo, G., et al., Macromol. Chem. Phys. 1994;195:1043.
12. Panayiotou, C. and Sanchez, I.C. Polym. Pre. 1992;33:567.
13. Panayiotou, C. and Sanchez, I.C. Macromolecules 1991;24:6231.

Chapter 6: Interactions with Poly(styrene-co-maleic anhydride)

The phase behavior of poly(styrene-co-acrylonitrile)/poly(styrene-co-maleic anhydride) (SAN/SMA) blends has been assessed at several different temperatures by melt mixing and solution casting preparation methods[1-5]. One of the overall conclusions of these efforts is that a region of miscibility with respect to copolymer composition exists between the SAN and SMA materials when the AN and MA weight fractions are similar to one another. The styrene acrylonitrile interaction which was deduced from SAN/SMA blend phase behavior has been used extensively in predicting phase behavior in blends containing S/AN or S/MA interactions[4, 5]. Many miscibility studies have involved SAN or SMA copolymers since the large intramolecular interaction in both copolymers acts to induce miscibility with other polymers. The existence of a large range of available SAN and SMA copolymer compositions has allowed the observation of detailed miscibility boundaries with respect to copolymer composition. These miscibility boundaries have been used to extract information about many other binary interactions, such as in the study reviewed in Chapter 5.

The reassessment of the S/AN interaction discussed in Chapter 4 prompted a closer inspection of both the origins of the lower S/AN interaction and the ability to use the larger S/AN interaction to accurately predict blend phase behavior. This chapter presents an analysis of the SMA/SAN blend phase behavior and efforts to understand the polymer-polymer interactions that dictate the observed phase behavior.

SMA CRITICAL MOLECULAR WEIGHT EXPERIMENTS

To accurately predict phase behavior in SAN/SMA blends, it would be useful to have an independent gage of the S/MA interaction such that both the S/MA and AN/MA need not be estimated simultaneously. Following Gan's study of phase behavior in equal weight SAN/SMA blends at 170°C[4], Merfeld observed the phase behavior of equal weight blends of SMA copolymers of various compositions with monodisperse polystyrenes at 170 °C[6]. The reported miscibility behavior of these materials, and the accompanying fit of the observations are represented in Figure 6.1. Open circles in Figure 6.1 represent single phase blends and closed circles represent two phase blends that were made by solution casting and annealed at 170 °C. The squares in Figure 6.1 represent blends that were immiscible when cast from solution and annealed at 170 °C, but miscible when melt mixed in small batches. The curve in Figure 6.1 uses the reported S-MA interaction energy of 10.6 cal/cm^3, the average reported molecular weight of the SMA copolymers, and the predicted density of MA by the volumetric analysis of Gan[4].

There are several reasons why the phase behavior of the melt mixed blends cannot be directly compared to the blends made by solvent casting. Two possible explanations for the discrepancy are the degradation of the low molecular weight polystyrene, or shear induced phase homogenization[7-11]. A better understanding of this discrepancy in the blending procedures would be possible if a phase boundary in the melt mixed blends was reported. Regardless of this issue, the SAN/SMA blends that will be analyzed in this chapter were cast from solution; making the observations of melt mixed SMA/PS phase behavior of little use to this study.

In an effort to reduce this range of possible S-MA interactions, several of the SMA copolymers shown in Table 6.1 were blended with monodisperse polystyrenes

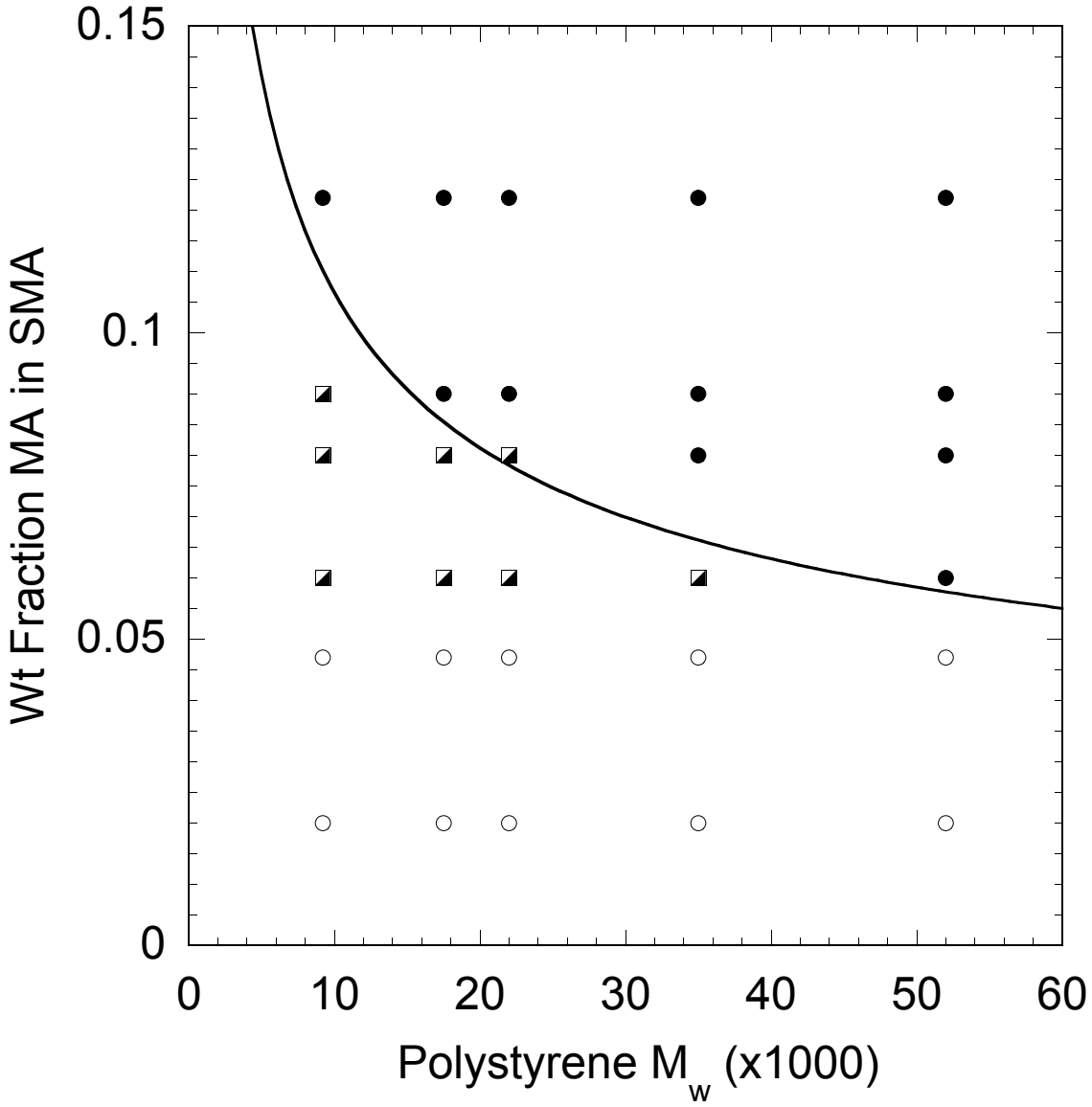

Figure 6.1 Phase behavior of equal weight SMA/PS blend phase behavior by Merfeld at 170 °C. Open and closed circles represent single and two phase blends respectively. Squares are compositions which were miscible by melt mixing, but not by solution casting. The curve corresponds to a S-MA interaction of 10.6 cal/cm^3.

.

Table 6.1 SMA copolymer properties.

Polymer	Original Wt% MA in S-MA	Wt % (MA-S) in SMA	$\overline{M}_W$	$\overline{M}_W / \overline{M}_N$	Tg (°C)	Source
SMA4.7	4.7	10	179,000	1.9	104	Dow Chemical Co.
SMA6	6	13	273,000	1.8	113	Arco Chemical Co.
SMA8	8	17	200,000	2	116	Arco Chemical Co.
SMA13	13	28	203,000	1.88	127	Arco Chemical Co.
SMA17	17	36	114,000	2.19	132	Arco Chemical Co.
SMA25*	25	53	252,000	3.62	149	Monsanto Co.

* SMA 25 contains a small amount of a third monomer[3]

shown in Table 4.3 in their estimated critical point compositions and annealed for 48 hours at 180 °C. The resulting miscibility data is shown in Figure 6.2. The volume fractions of the SMA materials were calculated using the MA density estimated by Gan[4]. The SMA/PS compositions that can be used to extract a S-MA interaction in Figure 6.2 are limited. This is because the S-MA interaction is very repulsive, and therefore low molecular weight PS is necessary to induce miscibility in SMA copolymers containing small amounts of MA. The lowest PS molecular weight used was 2000 Da since phase behavior could not be differentiated with confidence in critical point compositions using lower molecular weight polystyrenes. The line in Figure 6.2 approximates the boundary between single and two phase regions. This line corresponds to an S/MA interaction of 30 cal/cm^3. The magnitude of this implied interaction is extremely large, and not characteristic of a physical interaction. This S/MA interaction could not be used to accurately estimate the SAN/SMA blend phase behavior with either the previously reported smaller S/AN interactions or the one reported in Chapter 4.

TREATMENT OF THE MALEIC ANHYDRIDE REPEAT UNIT

The SMA/PS phase behavior shown in Figure 6.2 is consistent SAN/SMA phase behavior through an alternate treatment of the MA repeat unit. During synthesis of SMA, the styrene and maleic anhydride units form a monomer-monomer charge transfer complex before the addition to a polymer chain[12]. The resulting polymer consists of styrene and blocks of (maleic anhydride-styrene) (MA-S). In fact, the upper limit of maleic anhydride content in the SMA copolymers (48 wt%) occurs when the copolymer is completely alternating. The weight fraction of MA in the SMA copolymers can be used to calculate the weight fraction of (MA-S) repeat units. These weight fractions are shown in Table 6.1.

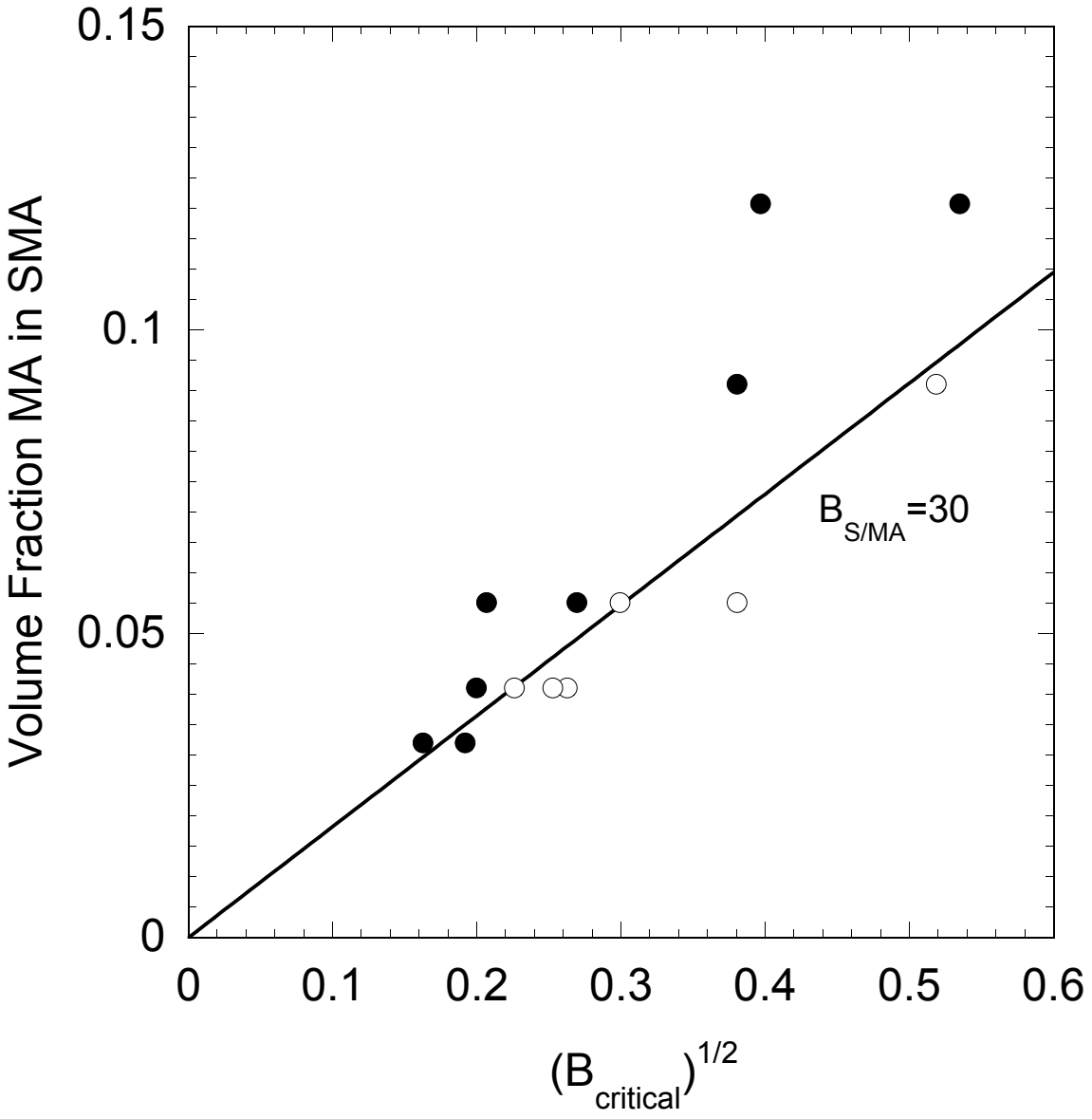

Figure 6.2 Phase behavior of SMA/PS blends at 180 °C. Open and closed circles represent observations of single and two phase character respectively. The line drawn corresponds to a S/MA interaction of 30 cal/cm^3.

Estimation of interaction energies with the (MA-S) repeating structure requires knowledge of the volume fraction of this structure in the SMA copolymers. An estimate of the Sanchez-Lacombe Equation of State (EOS) parameters for (MA-S) is desirable for calculating the density of the (MA-S) unit, and also for the conversion between bare interaction parameters and binary interaction energies as described in Chapter 2. The Sanchez-Lacombe EOS parameters for SMA copolymers containing 14, 18, and 25 wt% MA were determined by Gan, and are listed in Appendix A. These parameters could be used in conjunction with the mixing rules listed in Chapter 2 to estimate the pure (MA-S) EOS parameters. However, this procedure requires knowledge of the (MA-S) characteristic density. Instead, the (MA-S) EOS parameters were estimated by empirical means, and checked against the extrapolated densities using PS and SMA EOS parameters.

The equation of state (EOS) parameters for PS and SMA copolymers are graphed as a function of their weight fraction of (MA-S) in Figures 6.3a and 3.3b. The curves show the extrapolation used to estimate the EOS parameters for the (MA-S) repeat unit, which are listed in Appendix A. To test the predictive capability of these estimated (MA-S) EOS parameters, the predicted (MA-S) density from these parameters was compared to the individual extrapolations using the PS, SMA14, SMA18, and SMA25 EOS parameters. Figure 6.4a shows an extrapolation of the PS, SMA14, SMA18, and SMA25 densities at 180 °C and atmospheric pressure versus the weight fraction of (MA-S). Figure 6.4b shows the percent error between the densities obtained from individual extrapolations, as shown in Figure 6.4a, and the predicted (MA-S) densities using the EOS parameters listed in Appendix A for the (MA-S) repeat unit for several temperatures.

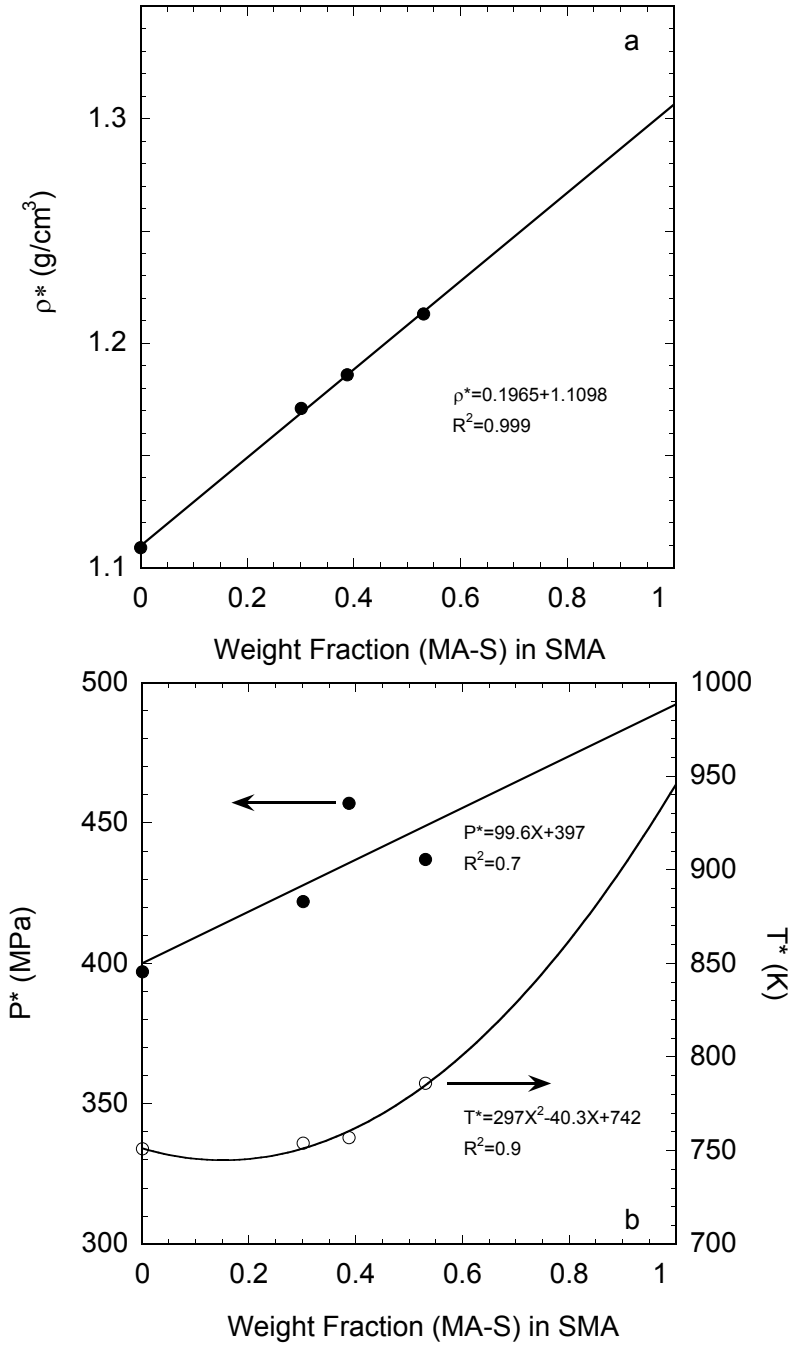

Figures 6.3 Sanchez Lacombe Equation of State parameters for PS, SMA14, SMA18, and SMA25 as a function of (MA-S) content. The curves are extrapolations used to estimate (MA-S) EOS parameters.

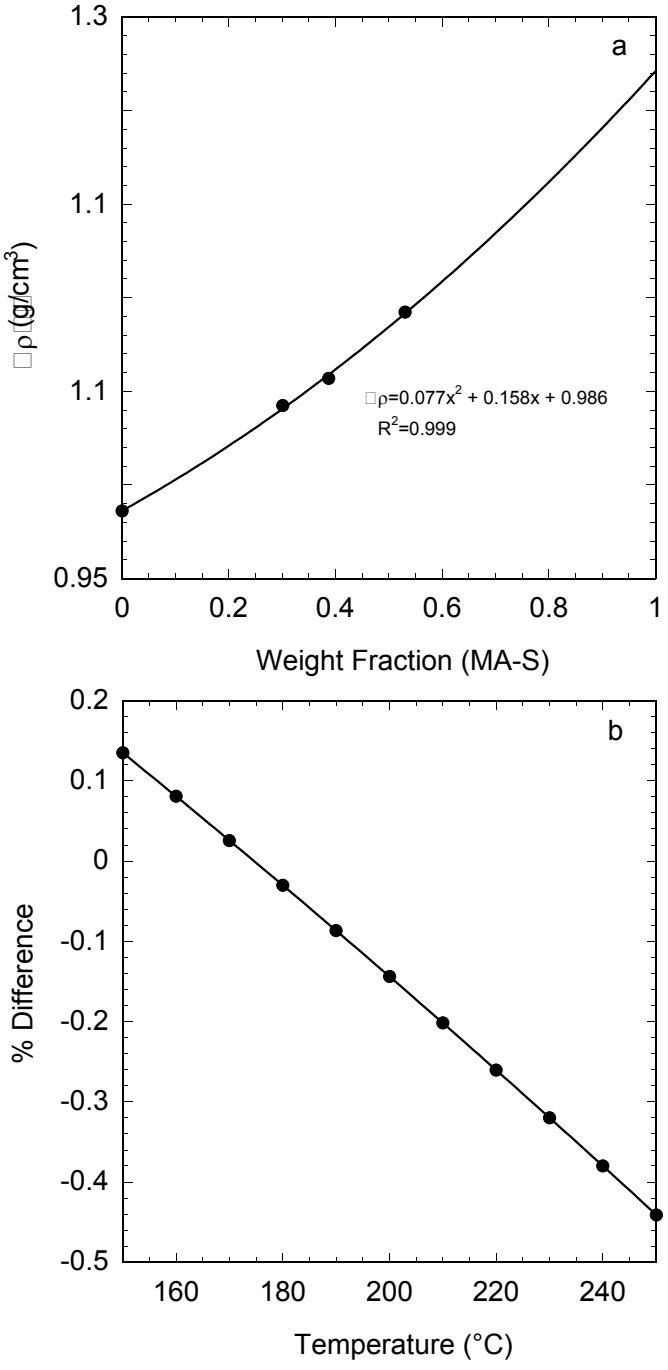

Figure 6.4 (a) Extrapolation of PS, SMA14, SMA18, and SMA25 data at 180 °C to predict (MA-S) density. (b) % difference between extrapolations as in (a) and predicted (MA-S) density from estimated EOS parameters.

Figure 6.4a indicates that an excellent correlation exists between (MA-S) content and density calculated through reported EOS parameters. This agreement is necessary or the accurate extrapolation of poly(MA-S) EOS parameters. It also suggests that the small amount of comonomer in the SMA25 copolymer is negligible. The extrapolated poly(MA-S) EOS parameters shows good agreement between predicted (MA-S) densities and those extrapolated while using individual EOS parameters, as shown in Figure 6.4a.

The PS/SMA blend phase behavior data in Figure 6.2, is shown as a function of the predicted volume fractions of the (MA-S) units in Figure 6.5. The boundary separating single and two phase blend areas in Figure 6.6 corresponds to an S/(MA-S) interaction of 3.8 cal/cm^3. This corresponds to a bare interaction parameter of 3.6 cal/cm^3, which was calculated using Equation 2.9 and the EOS parameters in Appendix A. Note that the SMA4.7/PS22 blend phase state was largely disregarded in the data fitting since its implied interaction conflicted with many observations of miscible blends.

POLY(STYRENE-STAT-ACRYLONITRILE)/POLY(STYRENE-CO-MALEIC ANHYDRIDE) BLENDS

The SAN copolymers listed in Table 4.1 were blended with the SMA copolymers listed in Table 6.1 in equal weight portions. These blends were annealed at 170 °C for 48 hours. The resulting phase behavior is shown in Figure 6.6. Open and closed circles represent single and two phase blends respectively. Half closed squares represent clear blends that had two glass transitions.

Many blends were clear and had two phases since the addition of MA or AN to styrene both act to lower the refractive index. Kim et al. measured the refractive index change with respect to MA and AN content in the styrene copolymers[3]. He determined that the refractive index decreases almost equivalently with the addition of AN or MA.

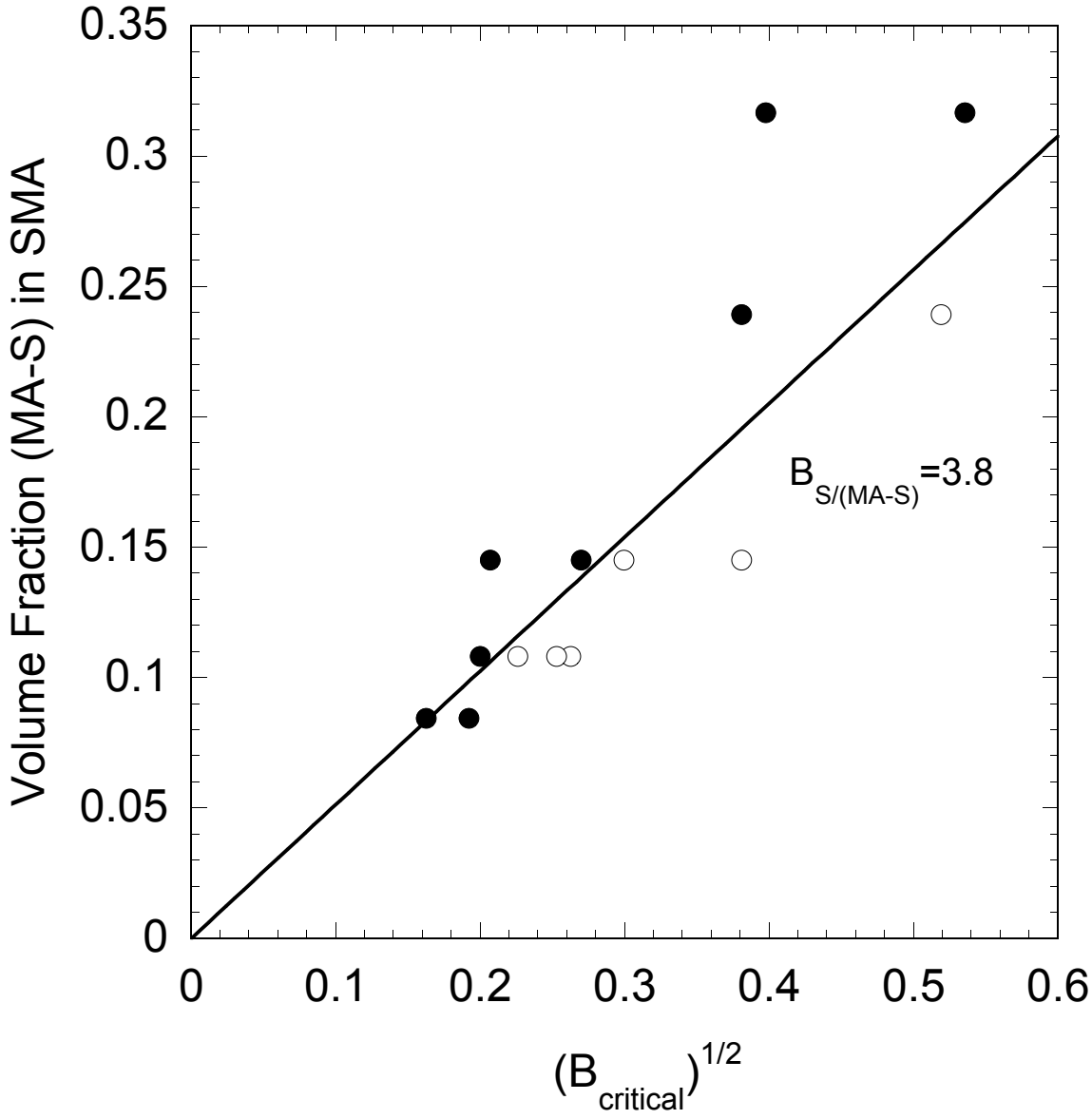

Figure 6.5 Phase behavior data for PS/SMA blends at 180 °C in terms of the (MA-S) volume fractions of SMA. Open and closed circles represent observations of single and two phase character respectively. The line drawn corresponds to a S/(MA-S) interaction of 3.8 cal/cm^3.

A refractive index difference of 0.01 is predicted to lie outside of the entire region of SAN/SMA miscibility.

Figure 6.6 displays two sets of predicted miscibility ranges based on the S/AN interaction presented in Chapter 4, and the S/MA interaction shown in Figure 6.2. The outer lines, which predict a large area of miscible compositions, are based on interactions of $B_{S/AN}$=11.9, $B_{S/MA}$=30, $B_{AN/MA}$=0, and B_{crit}=0.01 cal/cm^3. The two inner lines were constructed from the same interactions except for $B_{AN/MA}$, which was changed to 4 cal/cm^3. Neither of the predicted miscibility boundaries shown in Figure 6.6 fits the data well. Regardless of the AN/MA interaction, the predicted miscibility boundary is shifted towards the region of higher AN content due to the extremely large implied S/MA interaction.

Figure 6.7 contains the phase state data in Figure 6.6 adjusted to correspond to the (MA-S) weight fraction. The predicted miscibility boundaries correspond to $B_{S/AN}$=11.9, $B_{S/(MA-S)}$=3.8, $B_{AN/(MA-S)}$=2.05, and B_{crit}=0.01 cal/cm^3. The S/AN and S/(MA-S) interaction values correspond to those extracted from the critical molecular weight experiments, and the AN/(MA-S) interaction was used as the only adjustable parameter in fitting the observed data. The AN/(MA-S) interaction corresponds to a bare interaction parameter of 2.1 cal/cm^3.

The predicted miscibility boundary in Figure 6.7 compares favorably to the experimentally determined phase behavior with regards to the width of the allowable composition ranges and also to the slope of the miscible area with increasing MA and AN content. Consistency between the implied interactions responsible for PS/SMA, PS/SAN, and SAN/SMA blend phase behavior are possible when (MA-S) is treated as a

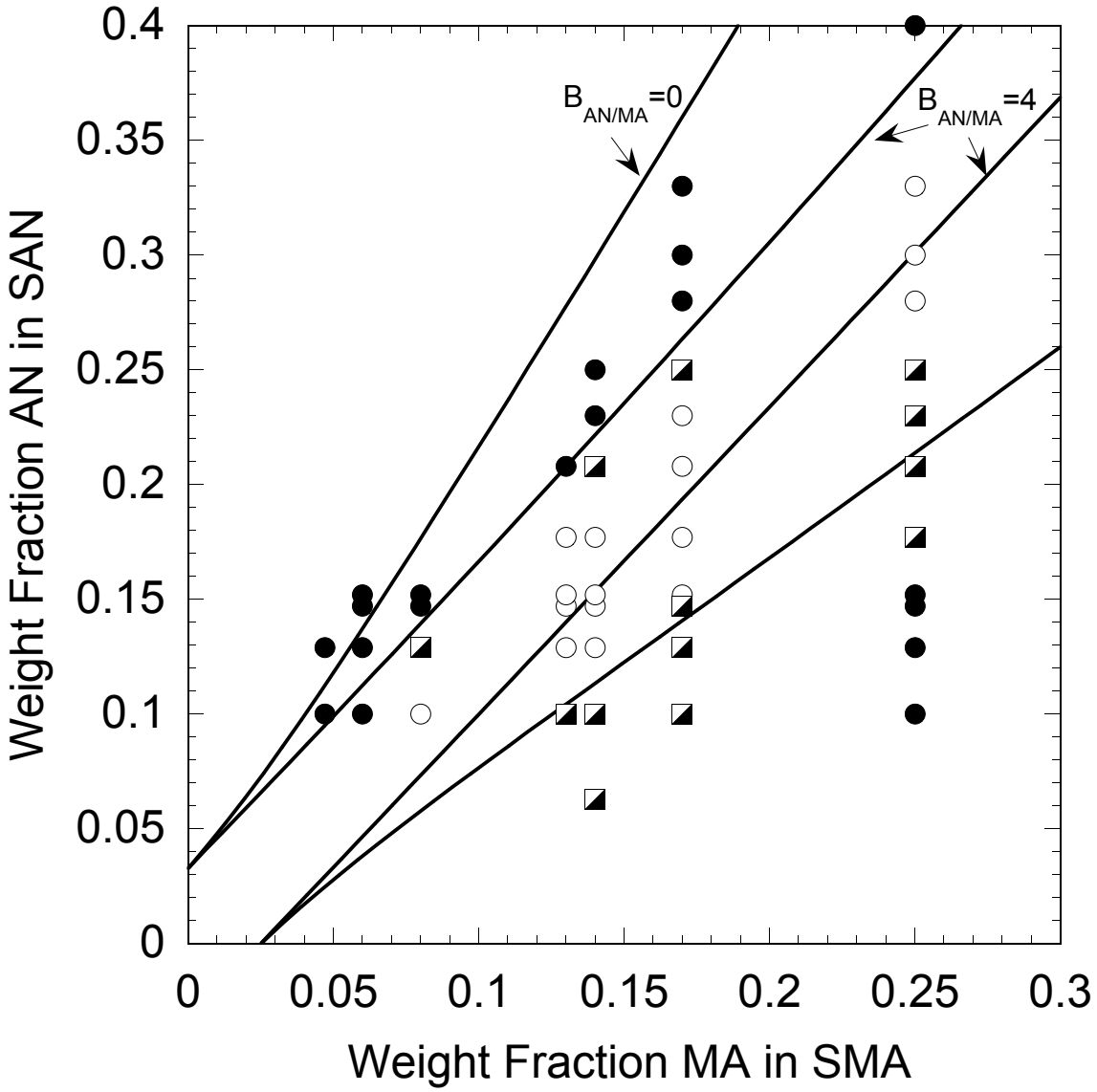

Figure 6.6 Phase behavior data for PS/SMA blends at 180 °C in terms of the (MA-S) volume fractions of SMA. Single and two phase blends are represented by open and closed circles respectively. Half closed squares represent clear, two phase blends. The predicted miscibility boundaries were created using $B_{S/AN}$=11.9, $B_{S/MA}$=30, $B_{AN/MA}$=0, B_{crit}=0.01 cal/cm^3 and the $B_{AN/MA}$ interactions indicated.

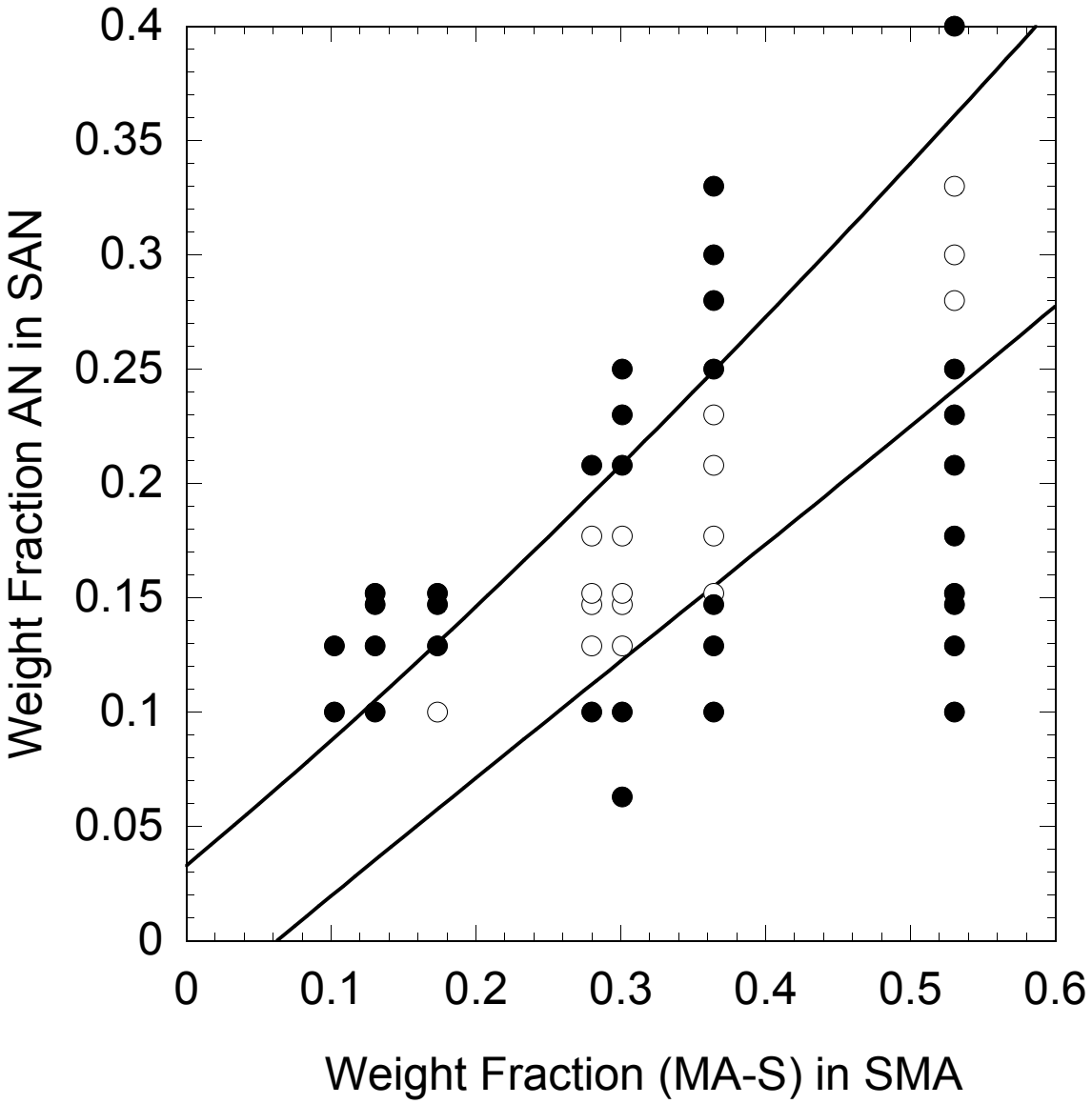

Figure 6.7 Phase behavior data for SAN/SMA blends at 170 °C in terms of the (MA-S) volume fractions of SMA. Open and closed circles represent single and two phase blends respectively. The predicted miscibility boundaries were created using $B_{S/AN}$=11.9, $B_{S/(MA-S)}$=3.8, $B_{AN/(MA-S)}$=2.05, and B_{crit}=0.01 cal/cm^3.

monomer, but not when MA is treated as though it is randomly placed throughout the SMA copolymer chain.

The S/AN interaction at 170 °C of 6.8 cal/cm^3 suggested by the work of Zhu after his observations of PS/SAN blend phase behavior[13], and also by the preceding work of Gan based on her observations of SAN/SMA phase behavior[4], cannot be used to fit the SAN/SMA blend phase behavior well while using the S/(MA-S) interaction derived from the PS/SMA phase behavior. Figure 6.8 shows the SAN/SMA phase behavior determined in this study as shown in Figure 6.7. The curves were drawn using the interactions of $B_{S/AN}$=6.8, $B_{S/(MA-S)}$=3.8, and B_{crit}=0.01 cal/cm^3. The inner curve was drawn using $B_{AN/(MA-S)}$=2.05, while the larger area was drawn using $B_{AN/(MA-S)}$=0.4 cal/cm^3. Clearly, no adjustment of the AN/(MA-S) interaction results in good agreement between the SAN/SMA phase behavior and the S/AN interaction of 6.8 cal/cm^3 while using the S/(MA-S) interaction derived from the PS/SMA phase behavior. If a similar analysis is conducted using the S/AN interaction of 6.8 and the implied S/MA interaction of 30 cal/cm^3, the predicted miscibility region is shifted even further away from the experimentally observed single phase region and towards the region of higher AN content.

Previous Observations of SAN/SMA Blend Phase Behavior

Kim et al. performed an extensive study of SAN/SMA blends[3]. Kim's study used the same SAN and SMA copolymers that were used to determine the SAN/SMA blend phase behavior in this study. Observations of phase behavior were made at temperatures "just above" the glass transition of the SMA copolymer.

Following the study of Kim et al., Gan and Paul evaluated the SAN/SMA blend phase behavior at 170 °C, which corresponds to the evaluation temperature of this

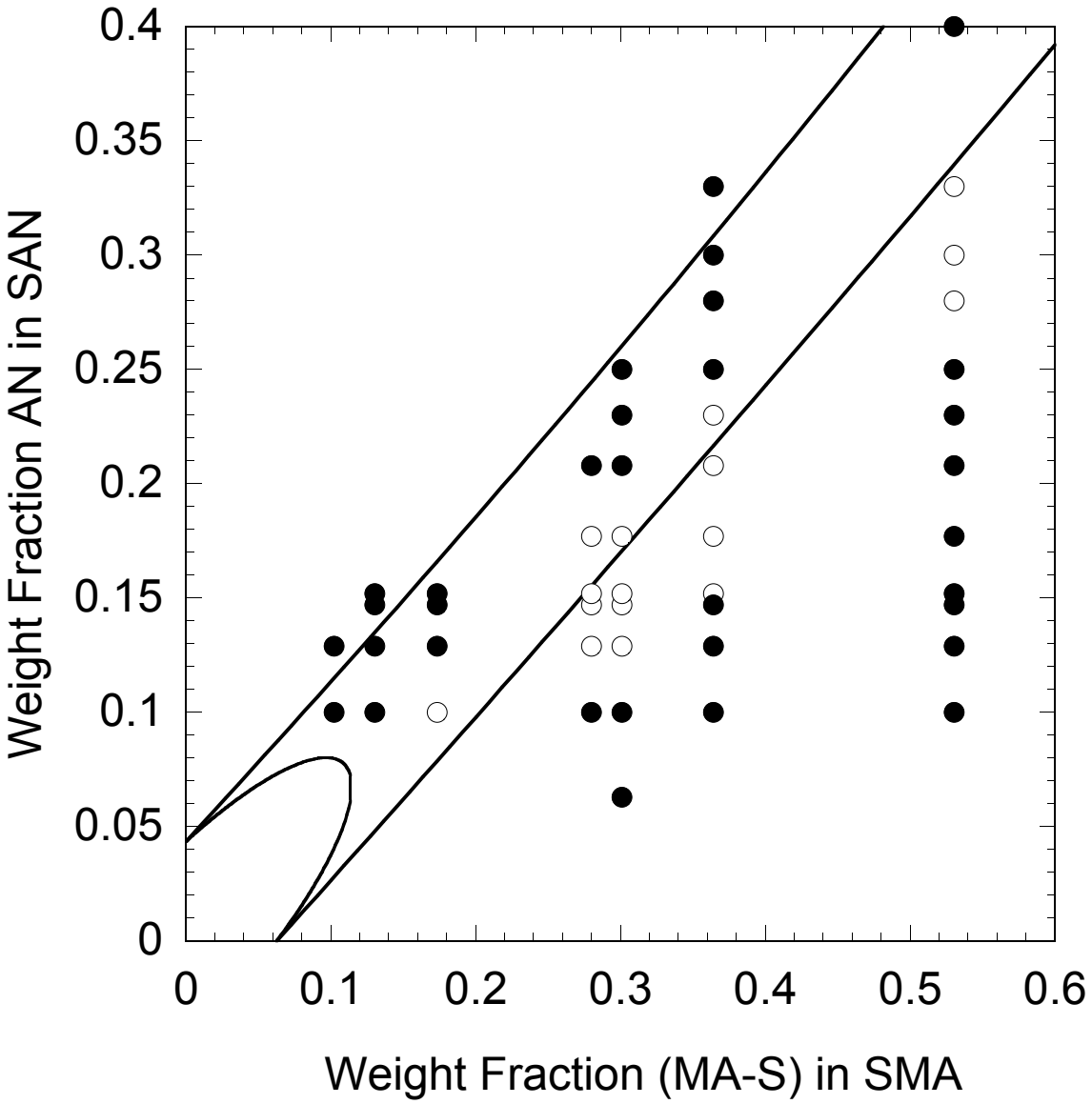

Figure 6.8 Phase behavior data for SAN/SMA blends at 170 °C in terms of the (MA-S) volume fractions of SMA. Open and closed circles represent single ant two phase blends respectively. The predicted miscibility boundaries were created using $B_{S/AN}$=6.8, $B_{S/(MA-S)}$=3.8, B_{crit}=0.01 cal/cm^3, and the $B_{AN/(MA-S)}$ values of 2.05(inner region) and 0.4(outer region).

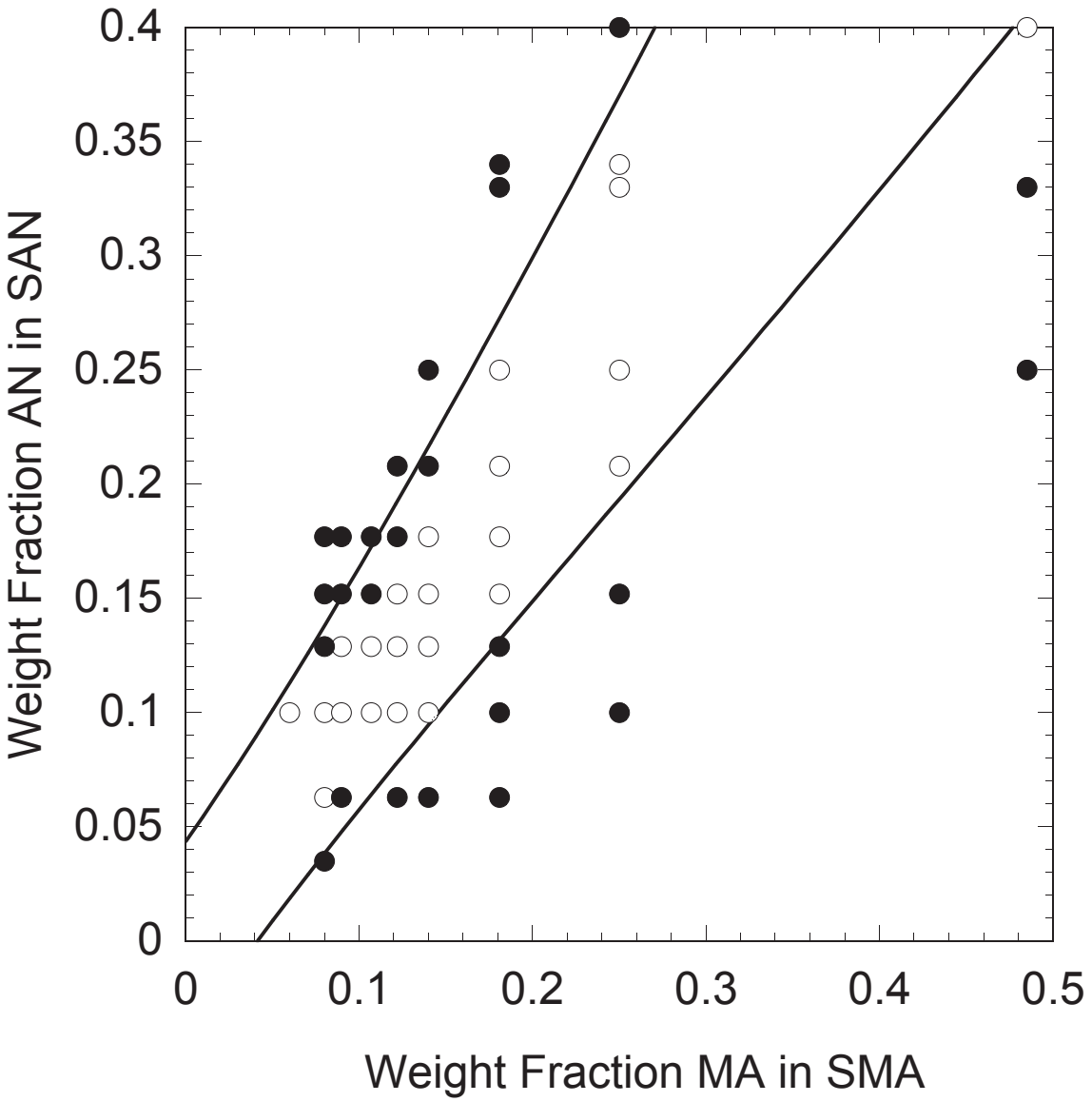

Figure 6.9 Phase behavior data for SAN/SMA blends determined by Gan at 170 °C. Open and closed circles represent single and two phase blends respectively. The predicted miscibility boundaries correspond to $B_{S/AN}$=6.8, $B_{S/MA}$=10.7, $B_{AN/MA}$= -0.31, and B_{crit}=0.01 cal/cm^3, which were reported by Gan.

study[4]. The observations of phase behavior and analysis of Gan, using the weight fraction of MA, is shown in Figure 6.9. The predicted miscibility boundaries were calculated using $B_{S/AN}$=6.8, $B_{S/MA}$=10.7, $B_{AN/MA}$= -0.31, and B_{crit}=0.01 cal/cm^3. Note that some of the SAN compositions were slightly altered to compare with a more recent analysis of the SAN compositions as discussed in Chapter 4. The adjustment of SAN compositions reduced the number of blends conflicting with Gan's prediction of miscibility from 12 to 6.

Gan's data, adjusted to reflect the weight fraction of (MA-S), is shown in Figure 6.10. The miscibility boundaries correspond to those shown in Figure 6.7, which were calculated using $B_{S/AN}$=11.9, $B_{S/(MA-S)}$=3.8, $B_{AN/(MA-S)}$=2.05, and B_{crit}=0.01 cal/cm^3. The predicted miscibility boundaries shown in Figure 6.10 represent the data well, but could be improved by adjusting the AN/(MA-S) interaction. Figure 6.11 is similar to Figure 6.10, except the miscibility region was predicted using $B_{AN/(MA-S)}$=1.8 cal/cm^3. The predicted miscibility region in Figure 6.11 is based on the interactions derived from the PS/SMA and PS/SAN phase behavior and one adjustable parameter. The prediction of phase behavior shown in Figure 6.11 is a much better representation of the data than Gan's original analysis shown in Figure 6.9, which was produced using three adjustable parameters. The number of compositions conflicting with the predicted miscibility boundary is reduced from 6 to 3, and the three remaining points lie on the boundary shown in Figure 6.11. These observations also suggest that the larger S/AN interaction, coupled with the S/(MA-S) interaction determined from PS/SMA phase behavior, can be used to accurately predict SAN/SMA blend phase behavior.

There were a few compositions of the SAN/SMA blends whose phase behavior appeared differently in the current study as opposed to the study of Gan. Figure 6.12

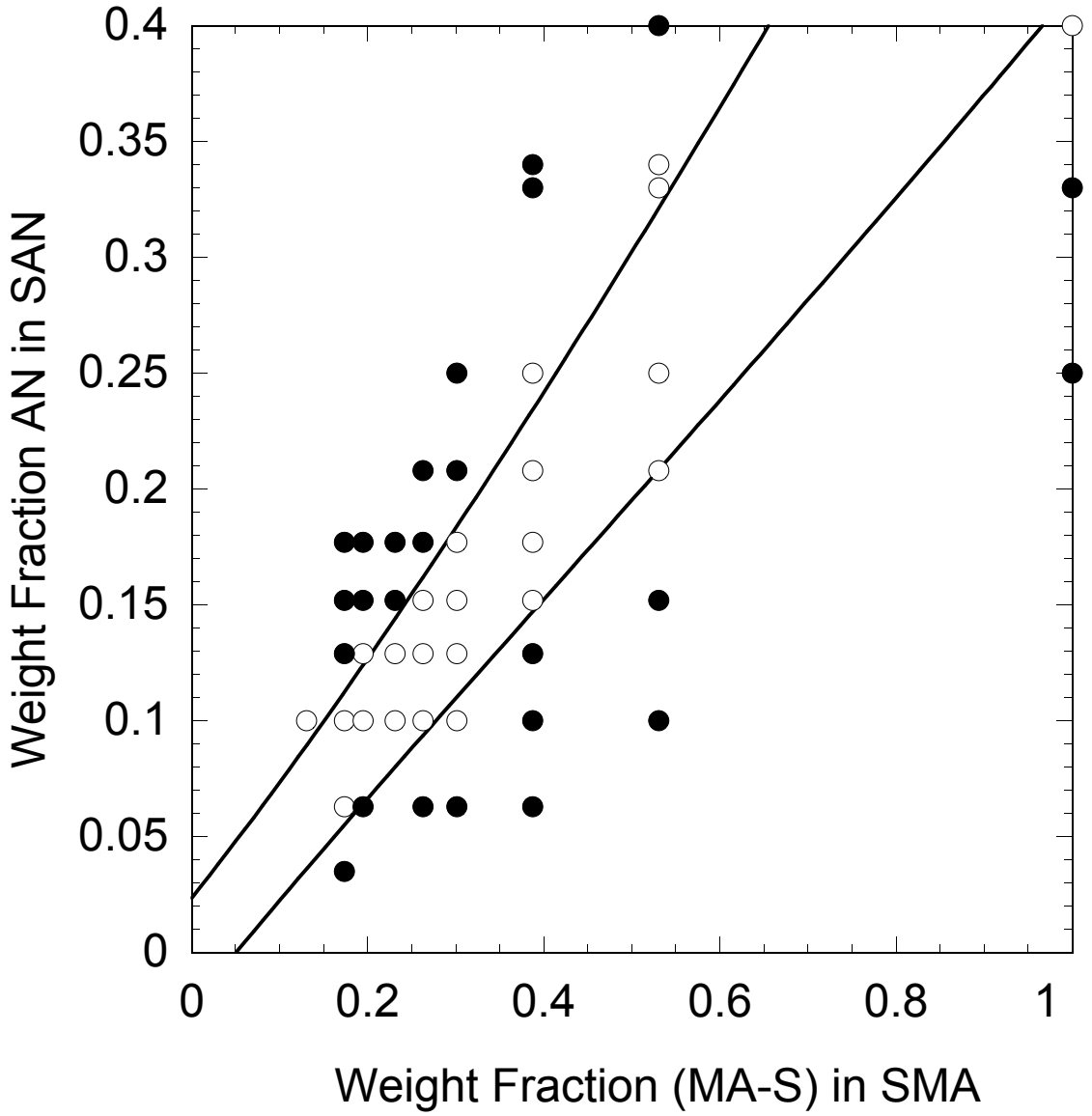

Figure 6.10 Phase behavior data for SAN/SMA blends determined by Gan at 170 °C. Open and closed circles represent single and two phase blends respectively. The predicted miscibility boundaries correspond to $B_{S/AN}$=11.9, $B_{S/(MA-S)}$=3.8, $B_{AN/(MA-S)}$=2.05, and B_{crit}=0.01 cal/cm^3, which were determined from the current study.

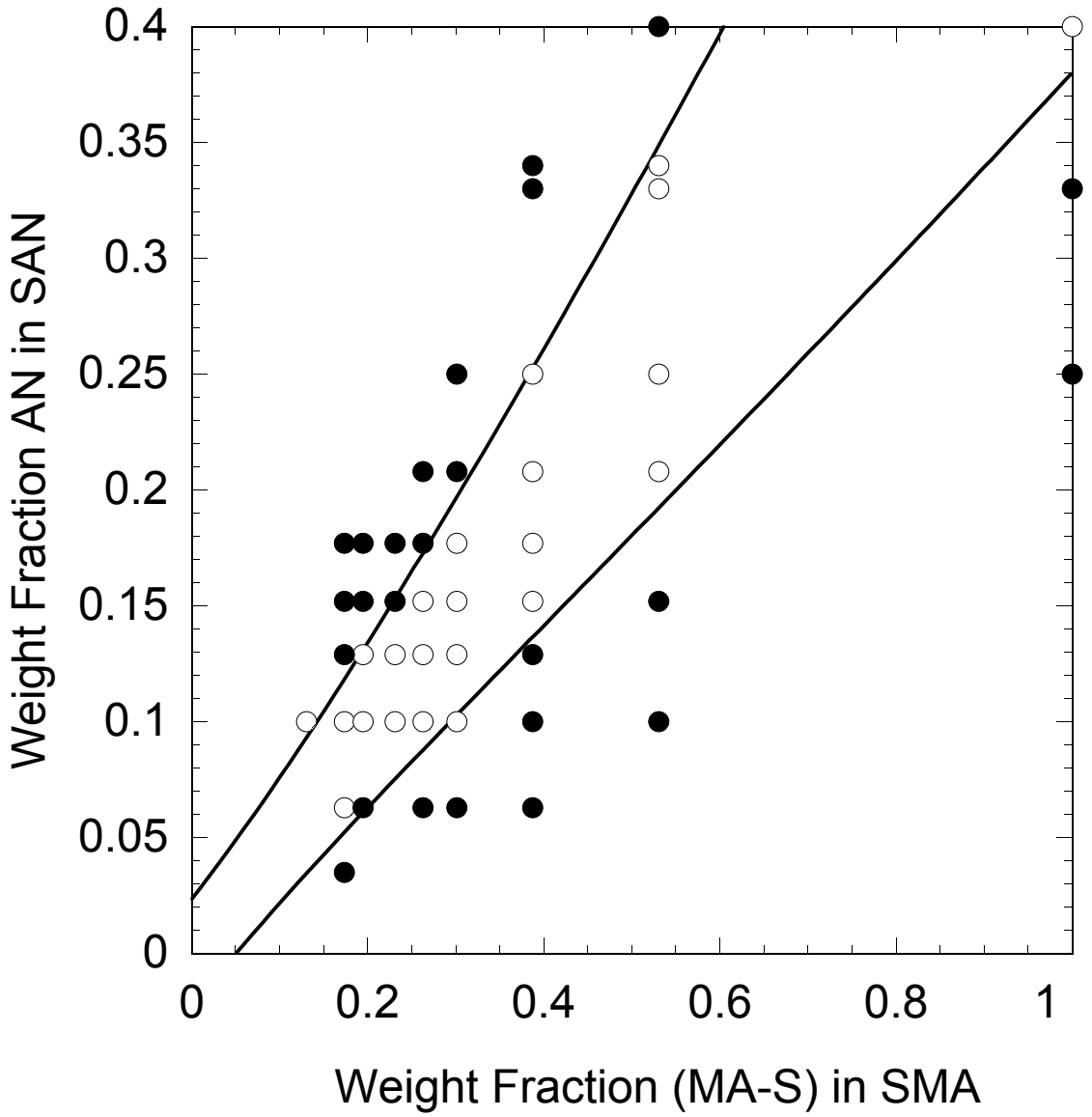

Figure 6.11 Phase behavior data for SAN/SMA blends determined by Gan at 170 °C. Open and closed circles represent single and two phase blends respectively. The predicted miscibility boundaries correspond to $B_{S/AN}$=11.9, $B_{S/(MA-S)}$=3.8, $B_{AN/(MA-S)}$=1.8, and B_{crit}=0.01 cal/cm^3.

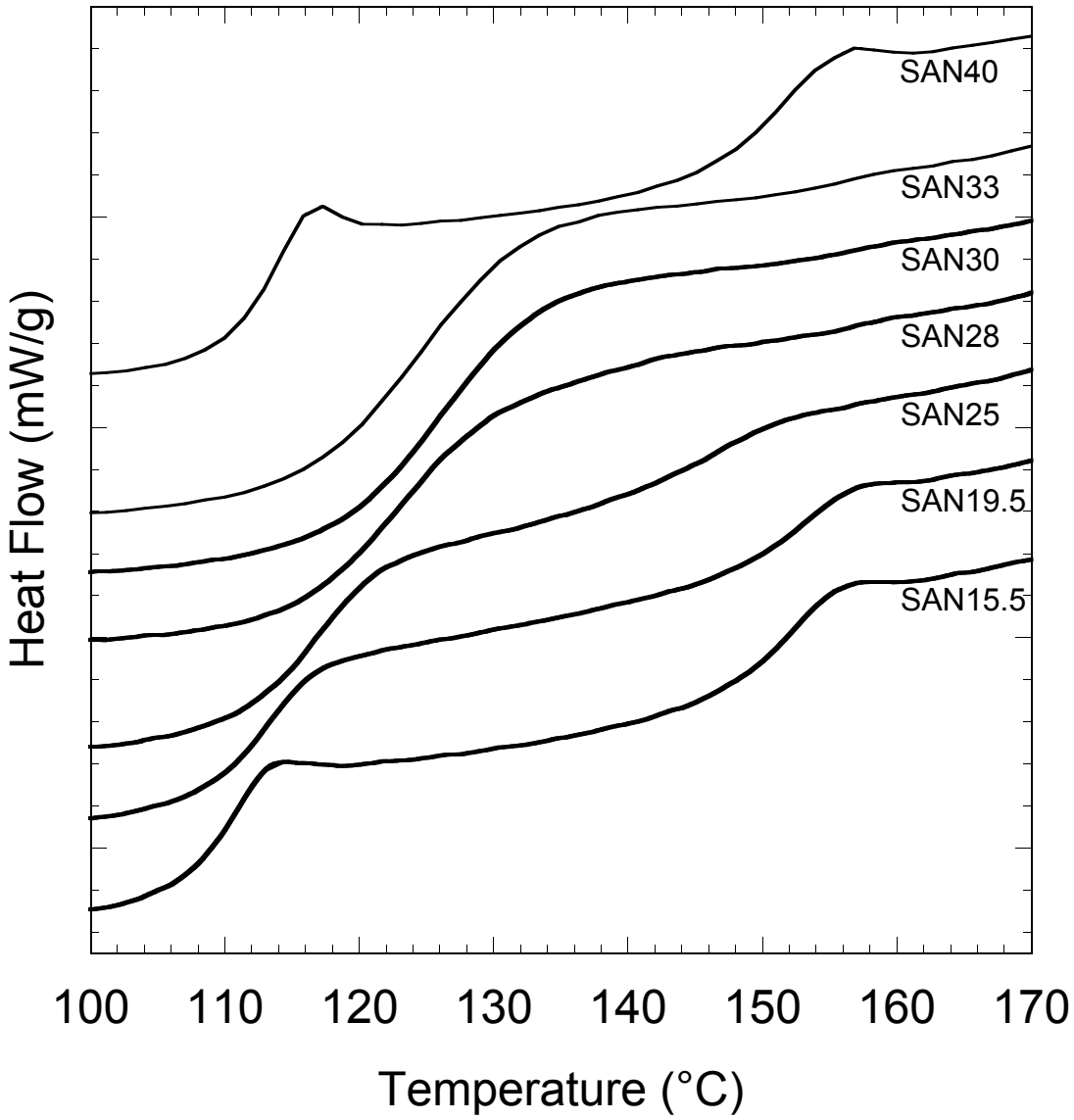

Figure 6.12 Thermal scans of selected SAN/SMA25 blends.

displays the glass transitions of selected SAN/SMA25 blends. Blends containing SAN19.5 and SAN25 were judged as having two phases in the current study, and a single phase in the study of Gan. The glass transition of the SMA rich phase become increasingly muted as the polymer-polymer repulsion is reduced. The differences noted between the studies could exist due to a difference in calorimetric data assessment. The differences between the studies are insignificant to the conclusions about the S/AN and S/(MA-S) interactions since variation of the AN/(MA-S) will result in the accurate description of the SAN/SMA blend phase behavior in either data set.

CONCLUSIONS

By treating copolymers of poly(styrene-co-maleic anhydride) (SMA) as being comprised of styrene and (maleic anhydride-styrene) (MA-S) repeat units, consistency is observed between the implied binary interactions responsible for PS/SAN, PS/SMA, and SAN/SMA blend phase behavior. The S/AN interaction at 170 °C of 6.8 cal/cm^3 reported by Gan[4], and later by Zhu[13], cannot be used in conjunction with the S/MA or S/(MA-S) interactions derived from PS/SMA phase behavior to describe the SAN/SMA phase behavior.

Interpretation of a binary interaction responsible for producing the PS/SMA phase behavior can be done by either treating the MA segment as being randomly placed throughout the polymer chain, or as being part of a repeating structure of MA coupled with S. These two treatments imply very different interactions when applied to other blend systems. This would suggest that the monomer distribution in polymer chains plays an important role in determining polymer blend phase behavior. The SMA copolymer is an extreme case with regards to alternating addition of monomers. Combining monomers with reactivity ratios less than one produces varying degrees of alternation, depending on the magnitude of the reactivity ratios. Estimation of binary

interactions through critical molecular weight experiments using copolymers such as poly(styrene-co-methyl methacrylate), which tends to form an alternating structure, may also require careful treatment of the repeating structure if the interaction is to be applied to other blend systems. Changes in the alternating character of poly(styrene-co-methyl methacrylate) with changes in composition may be responsible for the deviations between predicted and actual blend phase behavior in these copolymers while using a mean field approach[4, 14].

References

1. Hall, W.J., et al., Prepr. Am. Chem. Soc. Div. Org. Coatings Plast. Chem. 1982;47:298.
2. Hall, W.J., et al., Am. Chem. Soc. Symp. Ser. 1983;49:229.
3. Kim, J.H., Barlow, J.W. and Paul, D.R. J. Polym. Sci. Polym. Phys. 1989;27:223.
4. Gan, P.P. and Paul D.R. J. App. Polym. Sci. 1994;54:317.
5. Aokj, Y. Macromolecules 1988;21:1277.
6. Merfeld, G.D. and Paul, D.R. Polymer 1998;39:1999.
7. Aelmans, N.J.J., Reid V.M.C., and Higgins J.S. Polymer 1999;40:5051.
8. Hindawi, I.A., Higgins J.S., and. Weiss, R.A. Polymer 1991;33:2522.
9. Fernandez, M.L. and Higgins J.S., ACS Symp. Ser. 1995;597:106.
10. Fernandez, M.L., et al., Polymer 1995;36:149.
11. Chopra, D. and Vlassopoulos, D.J. Rheol. 1998;42:1227.
12. Dodgson, K. and Ebdon, J.R. Eur. Polym. J. 1977;13:791.
13. Zhu, S. and Paul, D.R. Macromolecules 2002;35:2078.
14. Hino, T., Y. Song, and Prausnitz, J.M. Macromolecules 1995;28:5709.

Chapter 7: Blends of TMC-Copolycarbonates and Poly(styrene-stat-acrylonitrile)

Callaghan et al. reported that while the interaction between poly(bisphenol-A polycarbonate), BPA-PC, and poly(styrene-stat-acrylonitrile), SAN, is unfavorable for miscibility, there is an optimal (or minimum) interaction energy density at about 25% by weight acrylonitrile in the SAN which places the blends on the verge of being miscible[1]. This near miscibility is partly responsible for the commercial success of blends of BPA-PC with ABS (i.e., rubber modified SAN) materials. A series of copolycarbonate materials based on varying ratios of bisphenol-A and 1,1-bis(4-hydroxyphenyl)-3,3,5-trimethylcyclohexanone (TMC) (Figure 7.1) have been commercialized primarily to provide higher heat resistance, relative to BPA-PC, which is demanded by some applications; note that the glass transition temperature of the TMC-PC homopolymer is 240°C versus 149°C for the BPA-PC homopolymer.

One could envision some interest in blends of these new high heat resistant copolycarbonates with ABS materials; therefore, it would then be useful to know the state of miscibility, or the interactions, of these copolycarbonates with SAN copolymers. Given the near miscibility of BPA-PC with some SANs [1] and the well-known opportunities for favorable interactions in copolymer-copolymer blends [2], it would not be surprising to find that some of these commercial copolycarbonates are miscible with SAN copolymers over some region of acrylonitrile content. Indeed, Okamoto et al. have

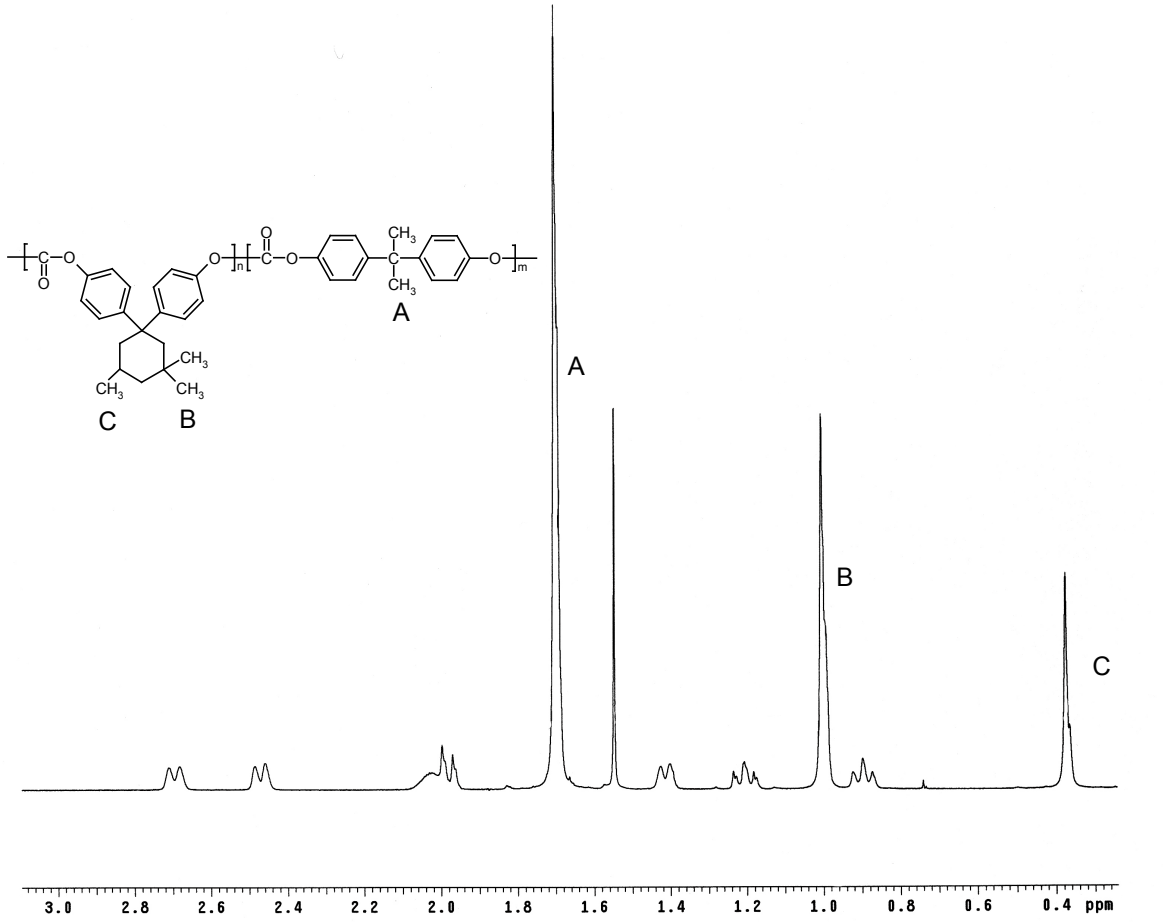

Figure 7.1 Structure and nuclear magnetic resonance spectra of a TMC-PC copolycarbonate.

reported some intriguing evidence for miscibility of one of these copolycarbonates with a particular SAN copolymer[3]. They suggested that the blend shows lower critical solution temperature (LCST) behavior and reported time-resolved light scattering results that suggest phase demixing by spinodal decomposition as a proposed phase boundary is crossed during temperature jump experiments.

Based on the reasoning outlined above and motivation from the observations of Okamoto et al., a study was initiated to broadly explore the phase behavior of copolycarbonate/SAN blends over the full range of compositions for each copolymer. The Okamoto et al. work provided reason to believe that the copolymer-copolymer composition map would contain some region of miscibility [3]. If this were the case, then it should be possible to obtain information about interactions between repeat unit pairs by analysis of the experimentally determined boundary between the regions of miscibility and immiscibility as described in the recent literature on other systems [2]. However, to our surprise, no region of miscibility could be found which left us with the responsibility of how to rationalize our findings with the observations reported by Okamoto et al. Thus, we conducted a detailed investigation of the phase behavior of the copolycarbonate/SAN blends and offer an explanation for the observations by Okamoto et al.

Table 7.1 Polymers used in TMC copolycarbonate/SAN study.

Polymer	Source	Commercial Description	Composition (wt %)	M_w	M_w/M_n
PCTMC11	Bayer	Apec 9330	11.1%TMC[a]	29,800[b]	2.4
PCTMC30	Bayer	Apec 9340	30.2%TMC[a]	33,200[b]	2.5
PCTMC40	Bayer	Apec 9358	38.9%TMC[a]	35,900[b]	2.2
PCTMC64	Bayer	Apec 9371	64.2%TMC[a]	38,300[b]	2.7
TMC-PC	Bayer	-	Homopolymer	140,200[b]	2.4
BPA-PC19	Dow Chemical Co.	-	Homopolymer	10,000	-
BPA-PC31	Dow Chemical Co.	-	Homopolymer	17,282	-
BPA-PC46	Dow Chemical Co.	-	Homopolymer	25,916	-
PS800	Pressure Chem.	-	Homopolymer	800	1.3
PS2000	Pressure Chem.	-	Homopolymer	2000	1.1
SAN6.3	Dow Chemical Co.	-	6.3%AN	343,000	2.8
SAN16	Dow Chemical Co.	-	15.9%AN	173,900	-
SAN25	Dow Chemical Co.	Tyrill	25%AN	166,800	2.2
SAN33	Monsanto Co.	-	33%AN	146,000	2.1
SAN40	Asahi Chemical	-	40%AN	122,000	2.0

[a] determined by ^{1}H-NMR
[b] determined in this study

MATERIALS AND PROCEDURES

The polymers used in this study, shown in Table 7.1, were used as received except for the TMC-PC homopolymer, which was precipitated in methanol three times from a dichloromethane solution to remove residual monomer.

The compositions of the copolycarbonates were characterized by ^{1}H-NMR at 500 MHz. Deuterated chloroform was used as the solvent, which contained tetramethylsilane for establishing the shift reference. The ^{1}H-NMR spectra for the commercial copolycarbonate designated here as PCTMC40 is shown in Figure 7.1. The composition of each copolymer was determined by comparing the area of the methyl hydrogen shifts A, B, and C. The resulting compositions are given in Table 7.1. The TMC-PC copolymers and homopolymer molecular weight information was obtained by gel permeation chromatography. Crosslinked polystyrene was used as the fixed phase and tetrahydrofuran was the carrier phase. The three BPA-PC homopolymers listed in Table 7.1, whose molecular weight information was previously collected using light scattering, were used to calibrate the column. Index of refraction values, glass transitions, and densities of the polymers used in this study are shown in Table 7.2. Property values were estimated by group contribution methods when experimental data were not available[4]. Equation of state properties of the copolymers were determined with a Gnomix mercury dilatometer. The resulting data were fitted to the Sanchez-Lacombe Equation of State to extract the corresponding characteristic parameters P*, T* and ρ* shown in Appendix A[5, 6].

Table 7.2 Polymer properties.

Polymer	Glass Transition (°C)	Density (g/cc) (30°C)	Refractive Index (25°C)
PCTMC11	156	1.180	1.582[a]
PCTMC30	167	1.169	1.576[a]
PCTMC40	180	1.161	1.573[a]
PCTMC64	203	1.137	1.565[a]
TMC-PC	237	1.110	1.554[b]
SAN6.3	104	1.057[b]	1.586[b]
SAN16	105	1.070[b]	1.579[b]
SAN25	107	1.082[b]	1.572[b]
SAN33	112	1.093[b]	1.567[b]
SAN40	113	1.102[b]	1.560[b]

[a] calculated from regression of data in product literature
[b] calculated

All polymer blends were prepared by solution casting 7 wt% solutions of polymer in dichloromethane onto glass slides at room temperature. Cast blends were dried in a vacuum oven for two days during which the temperature was slowly raised to 210°C where the temperature was maintained for 12 hours.

Miscibility was assessed by observing glass transition behavior and the amount of scattered light. The latter employed a polarized 632 nm He-Ne laser light source that was directed through a sample on a glass slide. The scattered light was focused with a set of adjustable lenses and detected by a 512 pixel photodiode array. The angle corresponding to each pixel was determined with a diffraction grating with known line widths. Temperature ramp experiments were performed with a FP 80 HT Mettler hot stage, while temperature jump experiments were performed using a heated brass block. We did not preheat the samples during temperature jump experiments. Our light scattering apparatus is described in greater detail elsewhere[7].

ASSESSMENT OF EQUILIBRIUM BLEND PHASE BEHAVIOR

The TMC-PC copolycarbonates and the TMC-PC homopolymer were blended with the various SANs listed in Table 7.1 in equal weight proportions. The blends prepared are indicated by the various points on the two dimensional compositional map (% AN in SAN vs. % TMC in copolycarbonate) shown in Figure 7.2. All of these blends exhibited two glass transitions suggesting immiscible behavior. However, several of the blends appeared transparent or were only slightly hazy as shown in Figure 7.2. The parallel lines in Figure 7.2 define a region where the blend components differ in index of

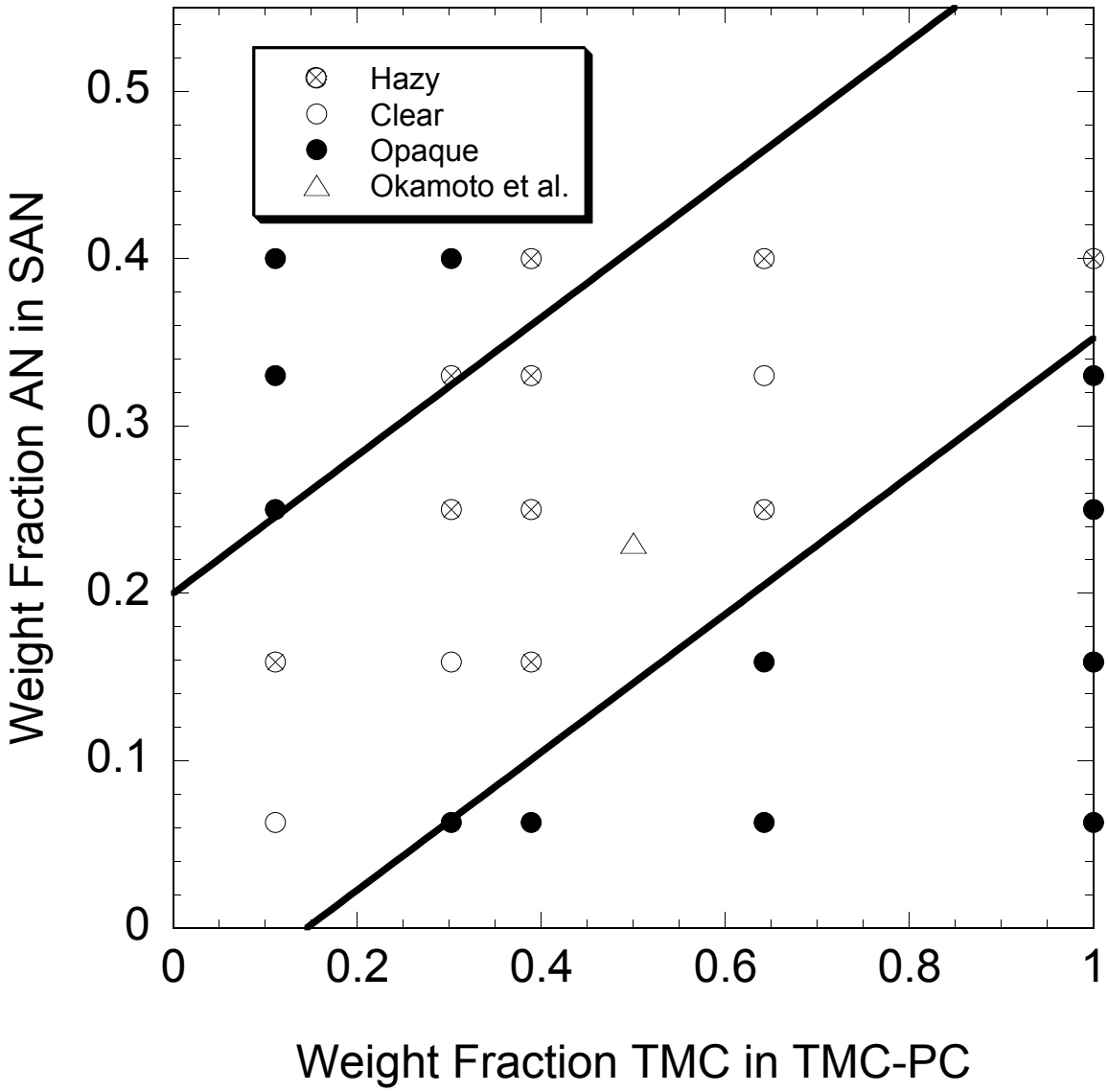

Figure 7.2 Optical appearances of TMC-PC copolycarbonate/SAN blends.

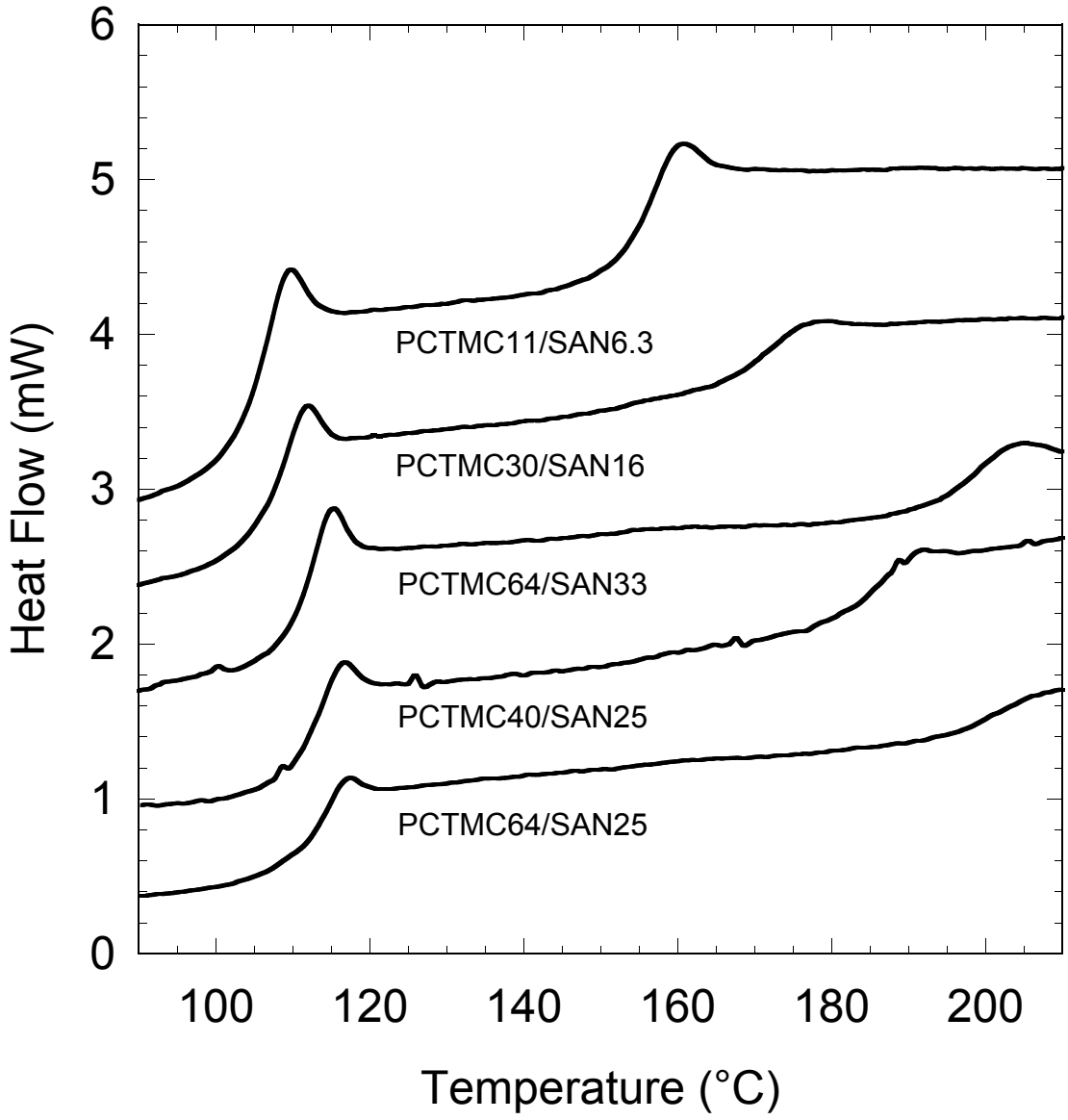

Figure 7.3 DSC scans for TMC-PC polycarbonate/SAN blends.

refraction by 0.01 or less; which is generally regarded as the critical difference necessary for assessing miscibility based on visual observation of blends[8]. The triangle in the middle of Figure 7.2 represents the blend used by Okamoto et al. based on the content of AN in the SAN and the glass transition of the TMC-PC copolycarbonate which they reported[3]. Figure 7.3 shows the DSC scans for selected blend compositions that lie within the two solid lines in Figure 7.2. Several of these blends were transparent. All of these scans show evidence of two glass transition temperatures.

The two glass transitions observed are definitive evidence of immiscibility; therefore, the observed transparency at room temperature is a result of the two components having nearly equal refractive indices. However, Okamoto et al. measured the scattered light for their blend during several temperature jump experiments and fit the resulting scattered light intensity versus time data to the Cahn-Hillard diffusion model in the classical method used to estimate a spinodal temperature[3] [9, 10]. Since their blend was melt mixed at 290°C and their estimate of a spinodal temperature was 223°C, they explained their observations in terms of an LCST phase boundary greatly perturbed by shear within the extruder. Examples of the effects of shear on phase boundaries can be found in the literature; however, lowering the spinodal temperature by 67°C seems extraordinary compared to prior literature reports[11-14].

Since blend systems with LCST-type phase diagrams are more likely to show miscibility at a given temperature at the extreme compositions, blends of PCTMC40/SAN25 and PCTMC64/SAN25 were prepared in weight fractions ranging from 10 to 90 wt%. However, none of these blends showed a single glass transition temperature.

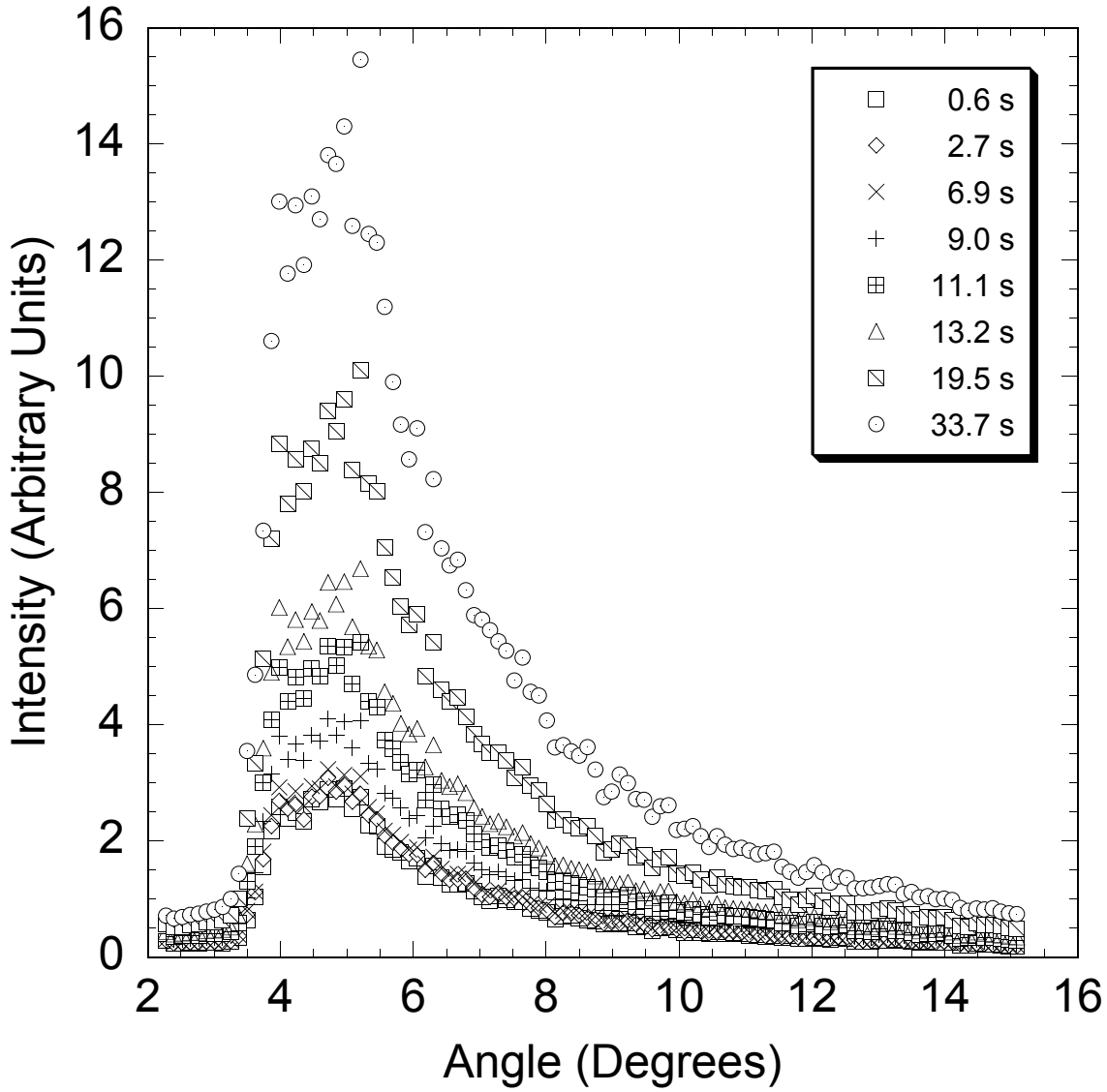

Figure 7.4 Changes in scattered light intensity as a function of scattering angle and time during a temperature jump experiment for a PCTMC40/SAN25 blend.

TIME RESOLVED LIGHT SCATTERING ANALYSIS

To determine if the clear to cloudy transitions reported by Okamoto et al. could also be observed using the current blends, the light scattered from the PCTMC40/SAN25 and PCTMC64/SAN25 blends was measured as a function of temperature. While these blends are initially hazy, they do become cloudy upon heating. An example of a temperature jump experiment using these blends is shown in Figure 7.4. While these data appear similar to those collected during spinodal decomposition, the change in scattered light intensity with time is related to the change in the temperature of the specimen with time and not a phase separation.

A clear to cloudy transition in a two-phase mixture can occur in the absence of any change in phase structure. This phenomenon has caused confusion about blend phase behavior in other systems[15, 16]. For a given morphology, the scattered light intensity is proportional to the square of the difference in indices of refraction between the phases. As the density of a material changes, so does the electron cloud density, and the associated index of refraction. Since the thermal expansion coefficient of a polymer in the melt state is approximately twice that of the glassy state in most cases, the refractive index difference between two polymers will change significantly as a function of temperature in the temperature interval between their respective glass transitions[4].

At 25 °C, the index of refraction for SAN25 is below that of the PCTMC40 and above that of PCTMC64 as shown in Table 7.2. The relationships between index of refraction and temperature were calculated by using the Lorentz-Lorenz equation and

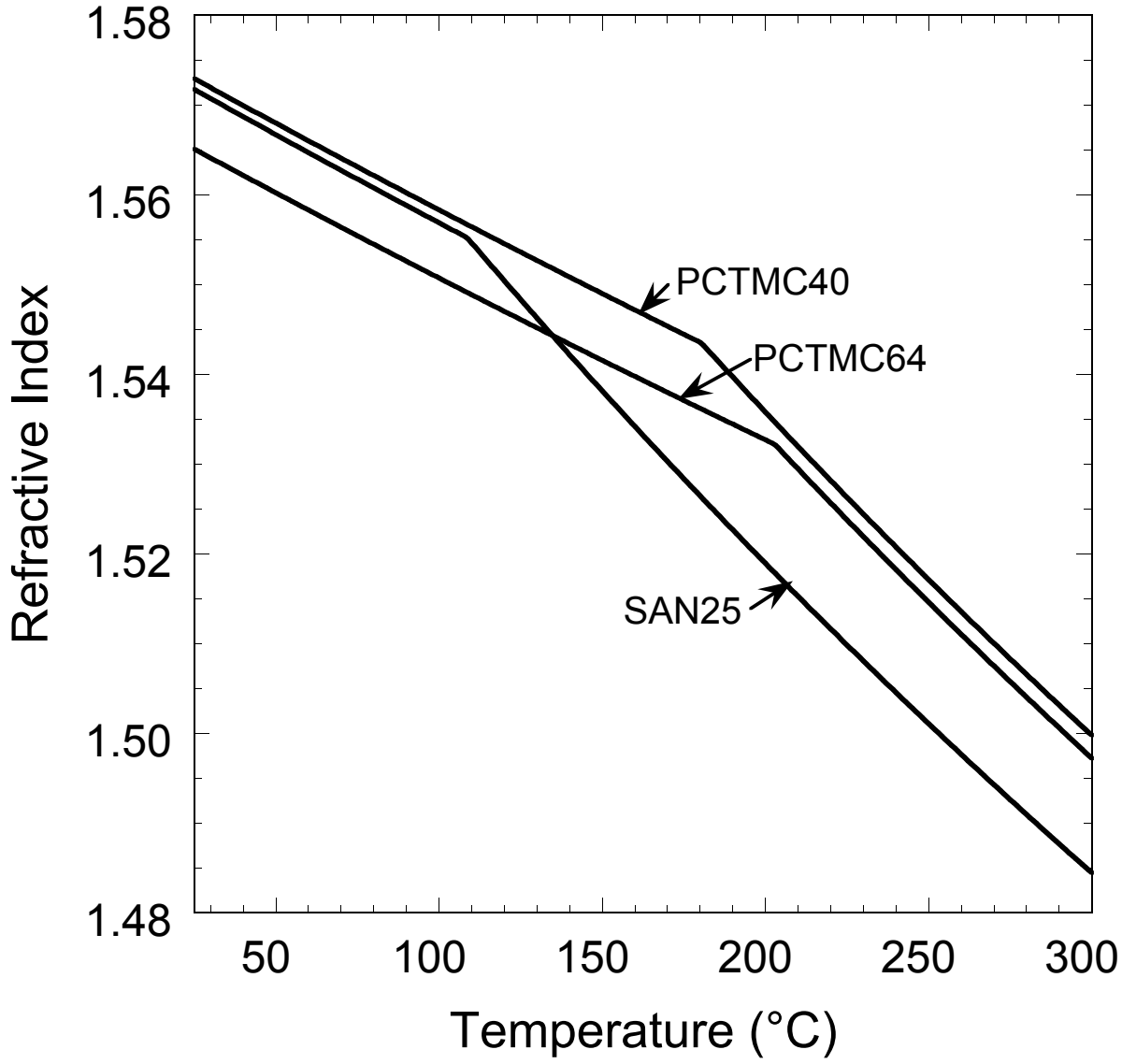

Figure 7.5 Index of refraction as a function of temperature for selected polymers calculated using a group contribution method for volume versus temperature data and the Lorentz-Lorenz equation.

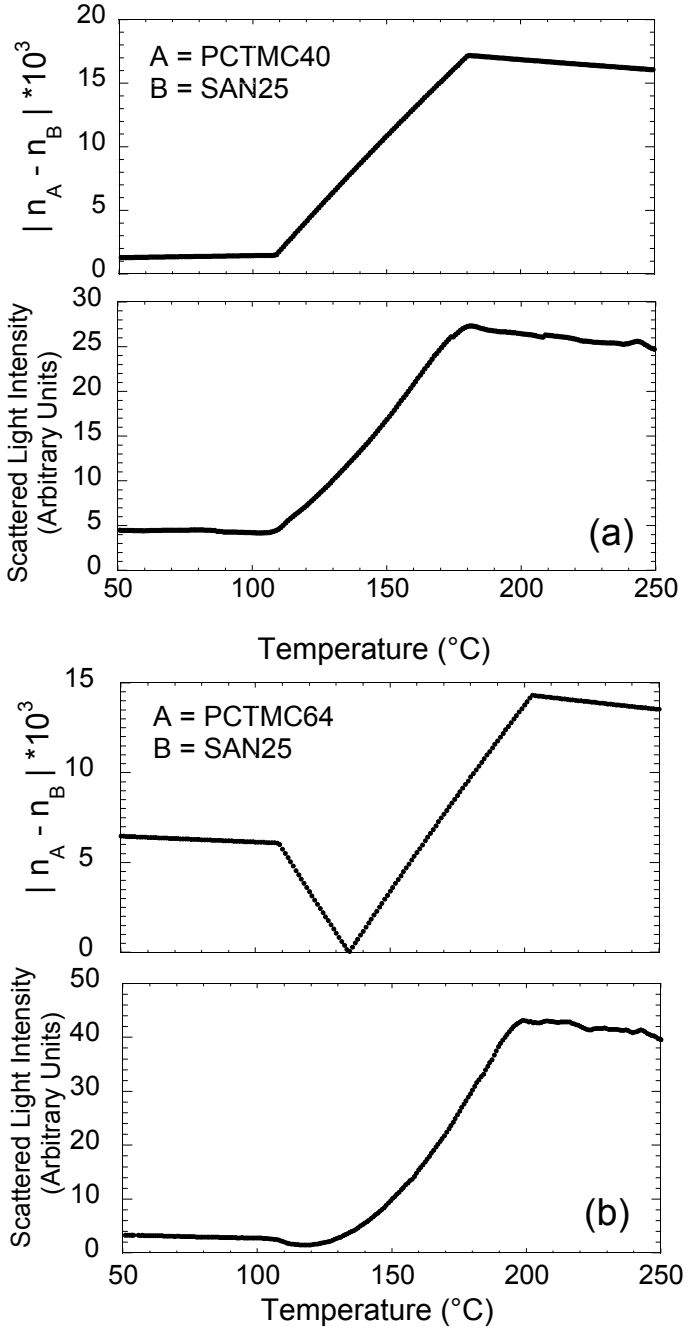

Figure 7.6 Scattered light intensity and index of refraction difference for (a) PCTMC40/SAN25 and (b) PCTMC64/SAN25 as a function of temperature. Scans were performed at 2 °C/min.

thermal expansion information estimated through group contribution methods[4, 17, 18]. Figure 7.5 illustrates how the refractive indices of the two TMC-PC copolymers and SAN25 change as a function of temperature. The clear to cloudy transitions observed with these blends are due to how the difference in the refractive indices of these polymers changes with temperature. If this is the case, then measured scattered light intensity should be directly correlated to the refractive index difference between the phases. Figure 7.6 shows the intensity of scattered light, which was determined by summing the light intensity over several fixed angles of scattering light, while the temperature was increased 2 °C per minute. One can see that the intensity of scattered light directly parallels the index of refraction difference calculated for these materials. Scattering profiles were also obtained during constant temperature conditions to confirm that the changes in scattered light intensity are not time dependant. The resulting scattering patterns for the PCTMC40/SAN25 and PCTMC64/SAN25 blends are shown in Figure 7.7. Identical curves were obtained by either increasing or decreasing the temperature between isothermal data collections. If one of the samples is held at 300 °C for several minutes and then rapidly quenched by liquid nitrogen, the sample then produces the same lower intensity scattering pattern observed before this thermal treatment. The rapid cooling caused by a quench in liquid nitrogen would prevent a change in morphology from occurring, leaving changes in scattering intensity to be explained by refractive index changes.

While it is apparent that the transparent to opaque transitions noted in the copolycarbonate blends are due to index of refraction changes, one is left with explaining the changes in scattered light intensity with time during a temperature jump experiment

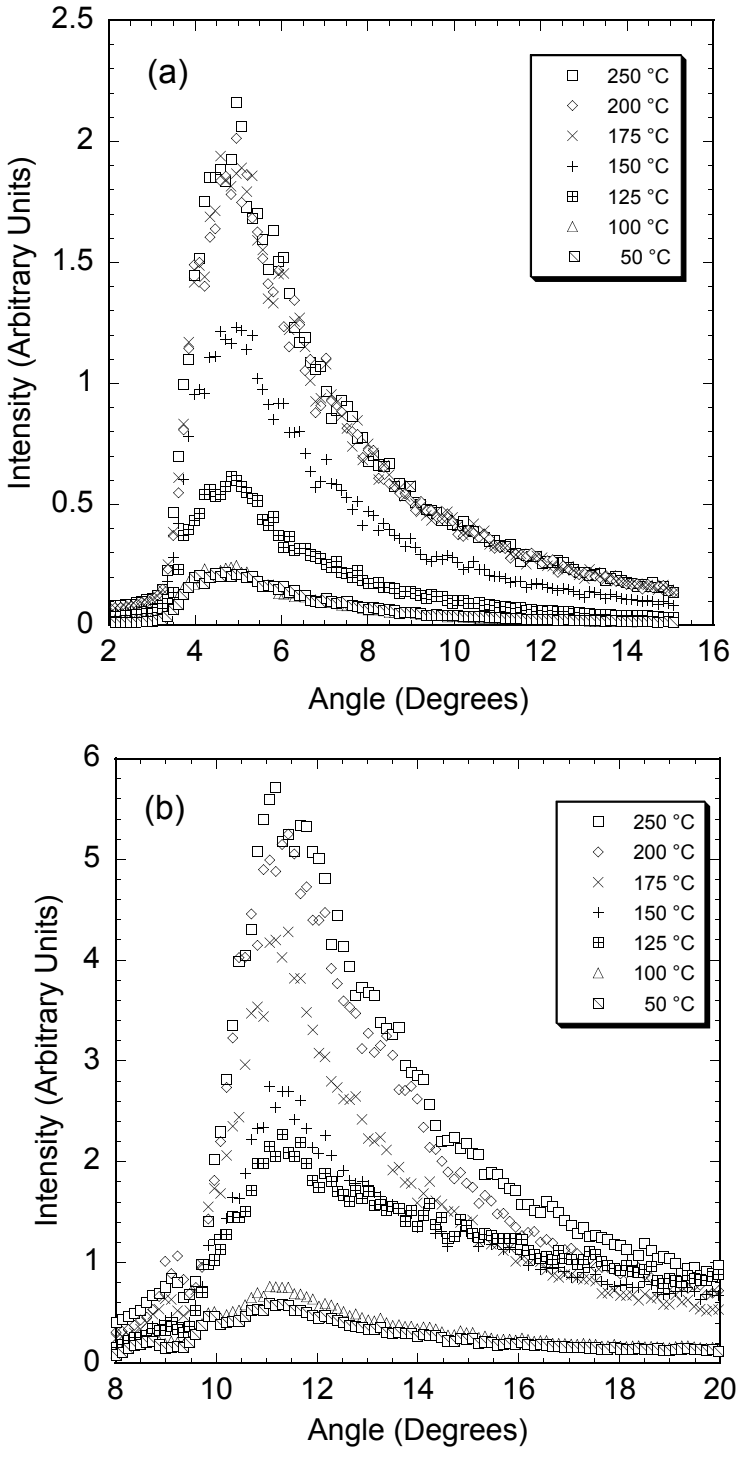

Figure 7.7 Scattered light intensity profiles for (a) PCTMC40/SAN25 and (b) PCTMC64/SAN25 blends measured at the indicated fixed temperatures.

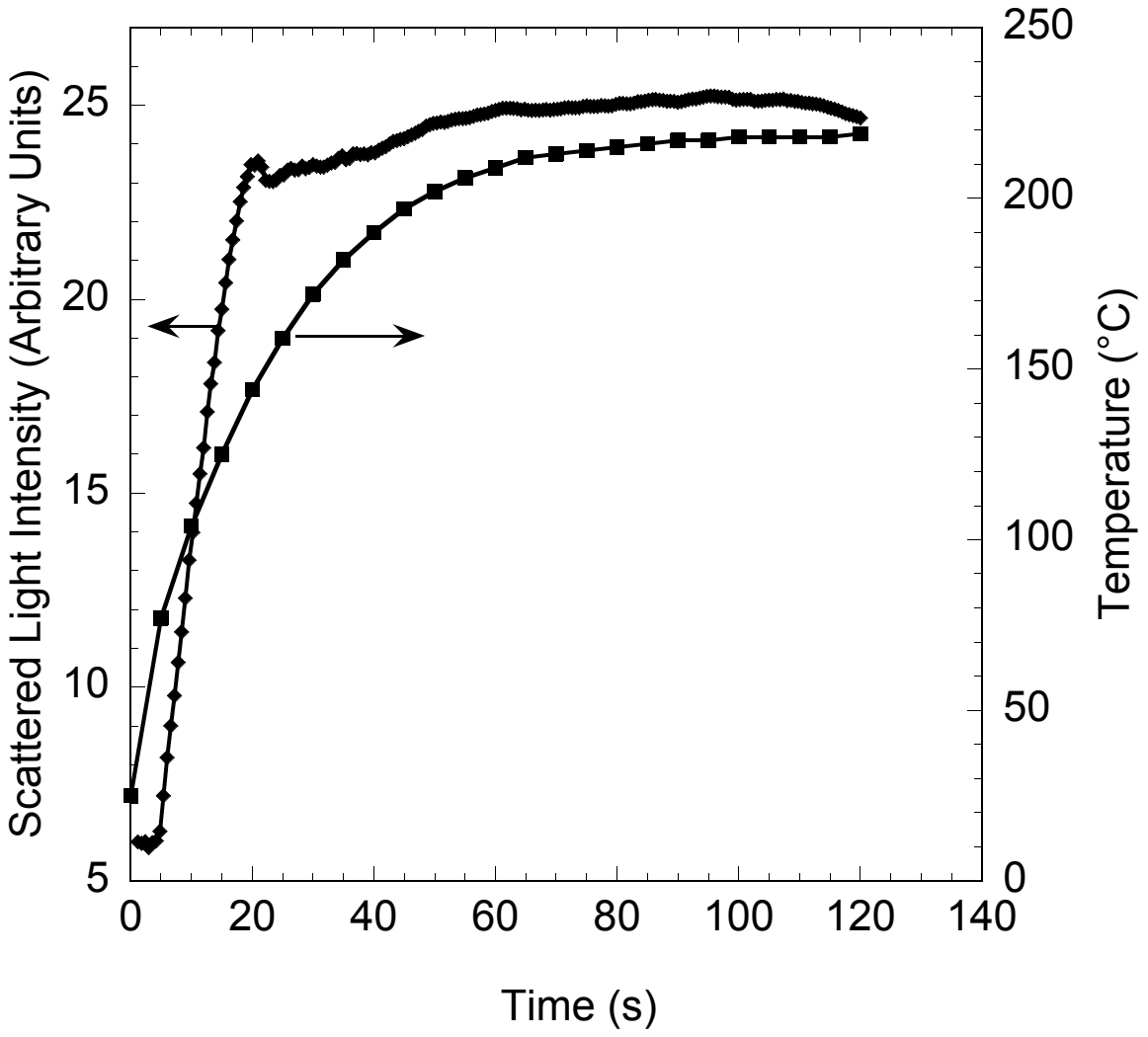

Figure 7.8 Temperature and scattered light intensity versus time for a PCTMC40/SAN25 blend during a temperature jump experiment.

reported by Okamoto et al[3]. The forgoing evidence suggests that any time dependent changes in scattered light intensity during a temperature jump experiment are related to the kinetics of heat transfer for the blends studied here. To determine if the heat transfer effects occur on the same time scale as the changes in scattered light intensity, a thermocouple was embedded in PCTMC64 on a glass slide and the temperature was recorded versus time during a temperature jump. Figure 7.8 shows the measured temperature versus time relation during the jump along with the scattered light intensity for PCTMC40/SAN25 as a function of time. The lower part of Figure 7.9 is a plot of the scattered light intensity versus the temperature implied by the temperature versus time data shown in Figure 7.8. The upper part of Figure 7.9 gives the index of refraction difference for the PCTMC40/SAN25 blend as a function of temperature. While the two plots in Figure 7.9 do not correlate as well as those shown for the temperature ramp experiments in Figure 7.6, it is apparent that the temperature change during a temperature jump experiment occurs on the same time scale as the observed changes in scattered light intensity. An increase in scattered light intensity may be evident sooner than indicated by the measured temperature because the latter does not fully reflect the gradient of temperature within the sample during the temperature jump. The scattered light intensity is a summation through the thickness of the sample and will be influenced by the temperature gradients. In addition, the thermal mass of the thermocouple may result in some time lag between the actual and the indicated temperature when attempting to measure rapid changes in temperature in a poor heat conductor.

Okamoto et al. [3] analyzed their light scattering results using the Cahn-Hillard

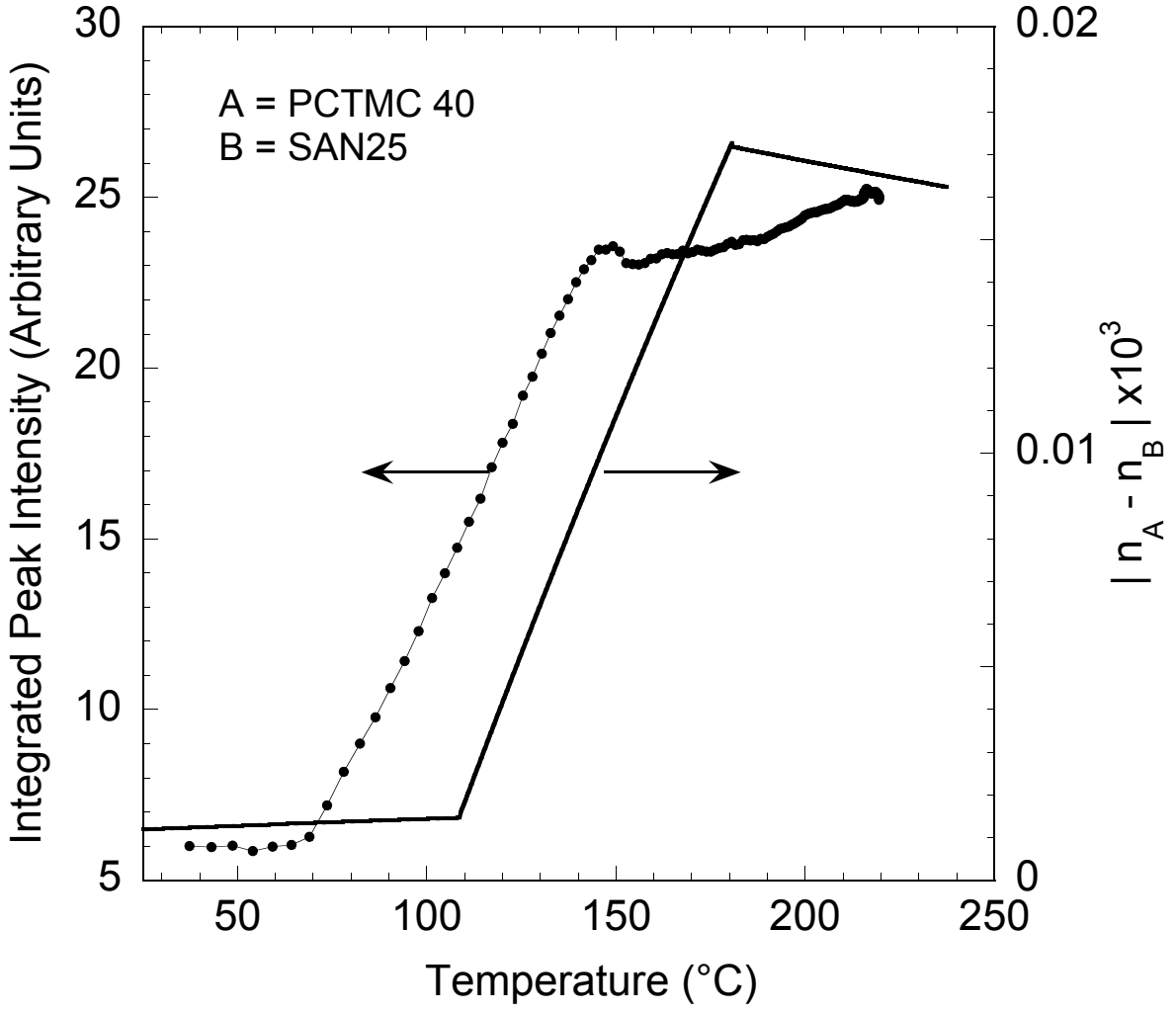

Figure 7.9 Scattering light intensity and index of refraction difference versus temperature for a PCTMC40/SAN25 blend during the temperature jump experiment shown in Figure 7.8.

diffusion model for spinodal decomposition[9, 10]. The data obtained here during temperature jump experiments were analyzed similarly to demonstrate that one could mistakenly assign a lower critical solution temperature to a blend not actually undergoing phase separation provided the rate of heat transfer is not adequate to give a near instantaneous temperature change. The growth rate, R(q), for a spinodal decomposition using the linearized Cahn-Hillard model is

$$R(q) = -Dq^2 - 2M\kappa q^2 \qquad (7.1)$$

where D is the apparent diffusion coefficient, q is the wavevector, κ is the interfacial free energy density, and M is the mobility. A plot of $R(q)/q^2$ versus q^2 for a given temperature has an intercept of D. Figure 7.10 shows this type of analysis for the current temperature jump experiments. The apparent diffusion coefficients are then plotted as a function of temperature and extrapolated to zero to determine the spinodal temperature. Figure 7.11 shows the apparent diffusion coefficients for the PCTMC40/SAN25 and PCTMC64/SAN25 blends.

While the data obtained during a clear to opaque transition in the TMC-PC copolycarbonate blends seems to be described fairly well by the linearized diffusion model for spinodal decomposition, there are several observations that indicate this is not an appropriate analysis. First, the apparent diffusion coefficient deduced is very large when compared to other blend systems. One might expect the kinetics of a TMC-PC copolycarbonate/SAN blend phase separation to be similar to that of tetramethyl polycarbonate/PS blends. Guo and Higgins have determined by light scattering analysis that the apparent diffusion coefficients for the TMPC/PS system are of the order of 10^{-15}

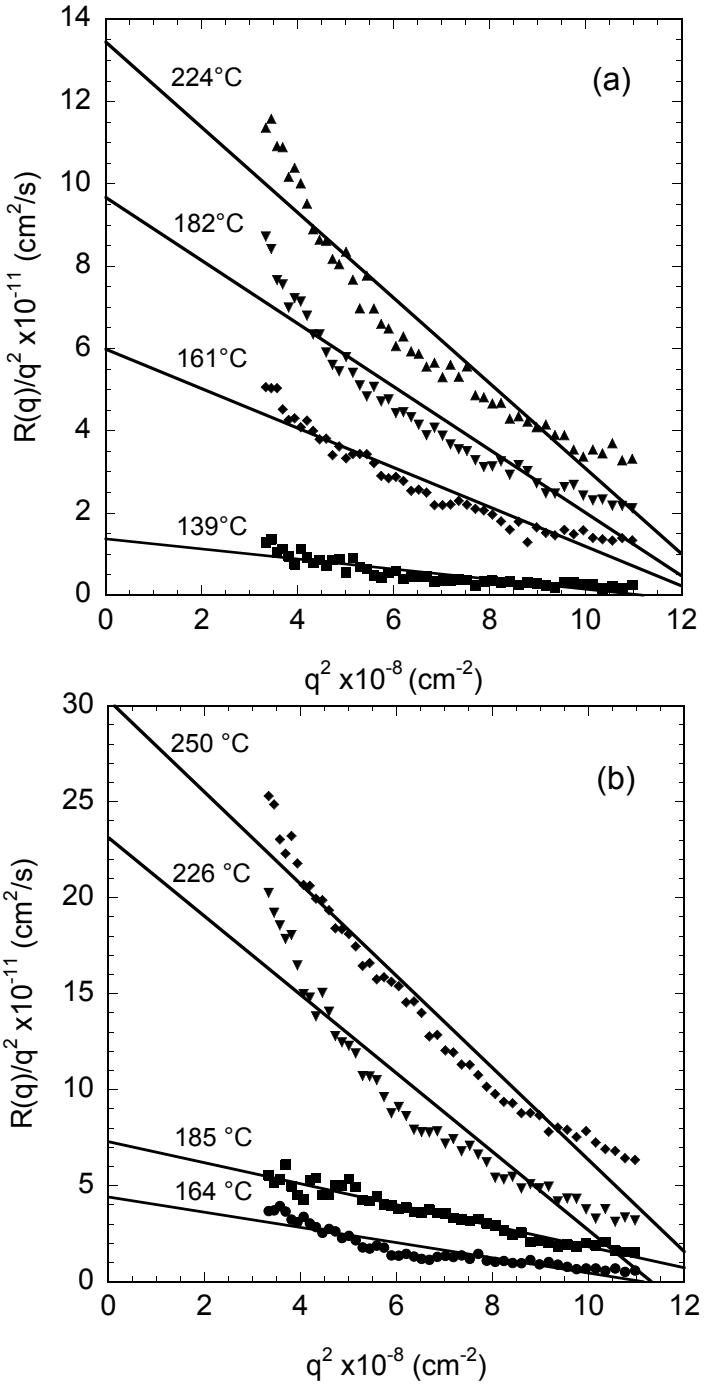

Figure 7.10 Plots of R/q^2 versus q^2 for (a) PCTMC40/SAN25 and (b) PCTMC64/SAN25 blends obtained during temperature jump experiments.

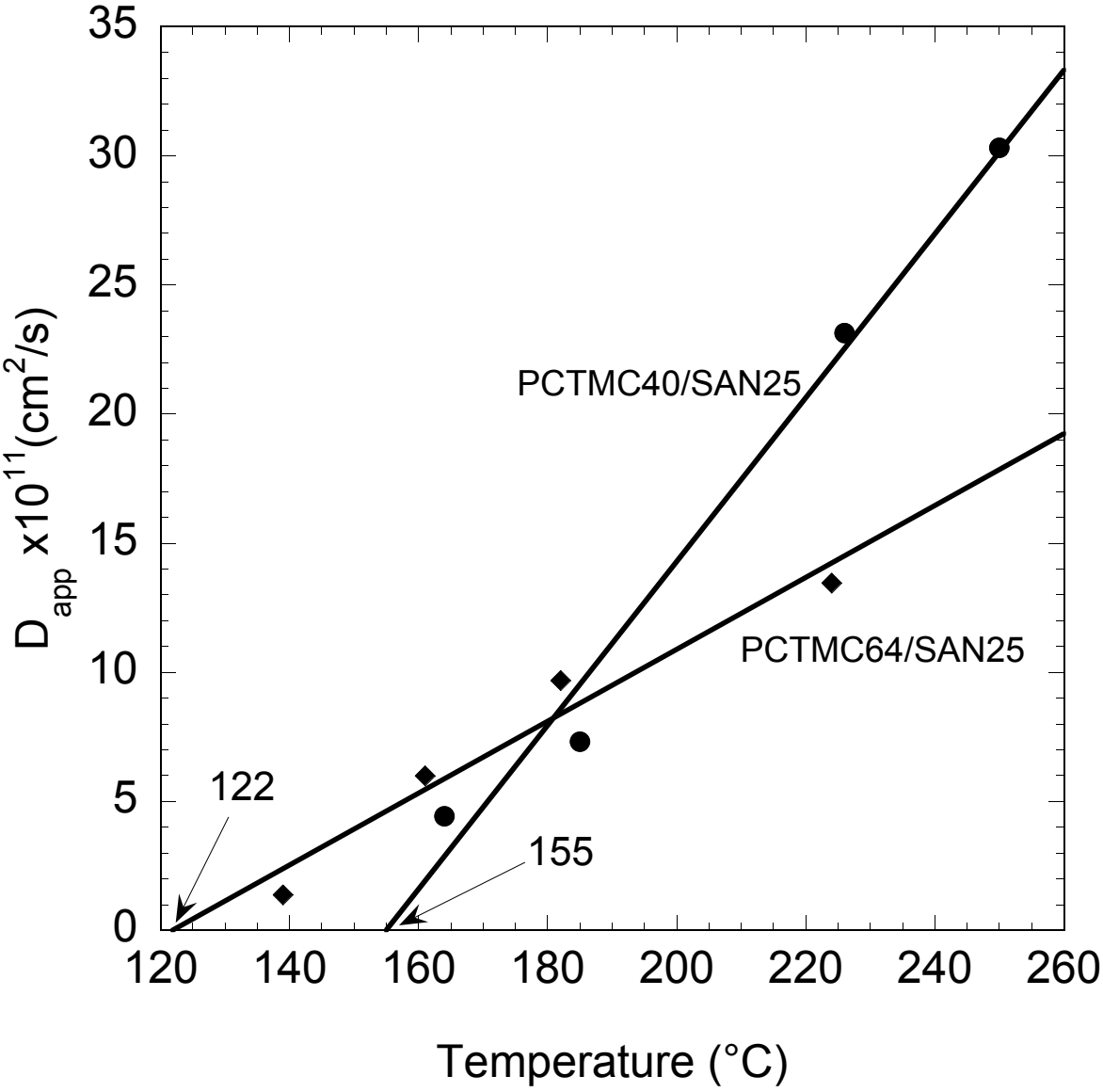

Figure 7.11 Apparent diffusion coefficients for PCTMC40/SAN25 and PCTMC64/SAN25 blends. According to the classical Cahn-Hillard analysis, the intercepts would correspond to the spinodal temperatures if the blends were undergoing phase separation.

cm^2/s within 10 °C of the spinodal temperature at 233 °C[19]. The apparent diffusion coefficients within 10 °C of the predicted zero apparent diffusion coefficient for the TMC-PC copolycarbonates /SAN25 blends (122 to 155 °C) deduced here are of the order of 10^{-11} cm^2/s. The apparent diffusion coefficients reported by Okamoto et al. are also on the order of 10^{-11} cm^2/s[3]. Another fundamental problem associated with fitting the kinetic data to the Cahn-Hillard model arises from the fact that only a small range of wavevectors were used to determine $R(q)/q^2$ versus q^2 plots as in Figure 7.12. The expanded region around these wavevectors identified in Figure 7.12 as open circles shows that the relationship between $R(q)/q^2$ and q^2 is quite nonlinear. This non-linearity is not consistent with the Cahn-Hillard diffusion model. Yet another discrepancy between the behavior expected during phase separation and that observed in this system is related to the shape of the curves of scattered light intensity versus wavevector. The angular position of the maximum in scattered light intensity in Figures 7.4 and 7.7 is invariant with time. The latter stages of phase separation involve an increase in the size of the phase domains resulting in a shift of the peak position[20-22]. The invariant peak position, therefore, suggests that the phase morphology is not changing during the clear to opaque transition for the cast blends studied.

CONCLUSIONS

Despite a suggestion of miscibility between a TMC-PC copolycarbonate and a SAN copolymer, the range of TMC-PC copolycarbonates and the TMC-PC homopolymer were found to be immiscible with several SAN materials. Due to the

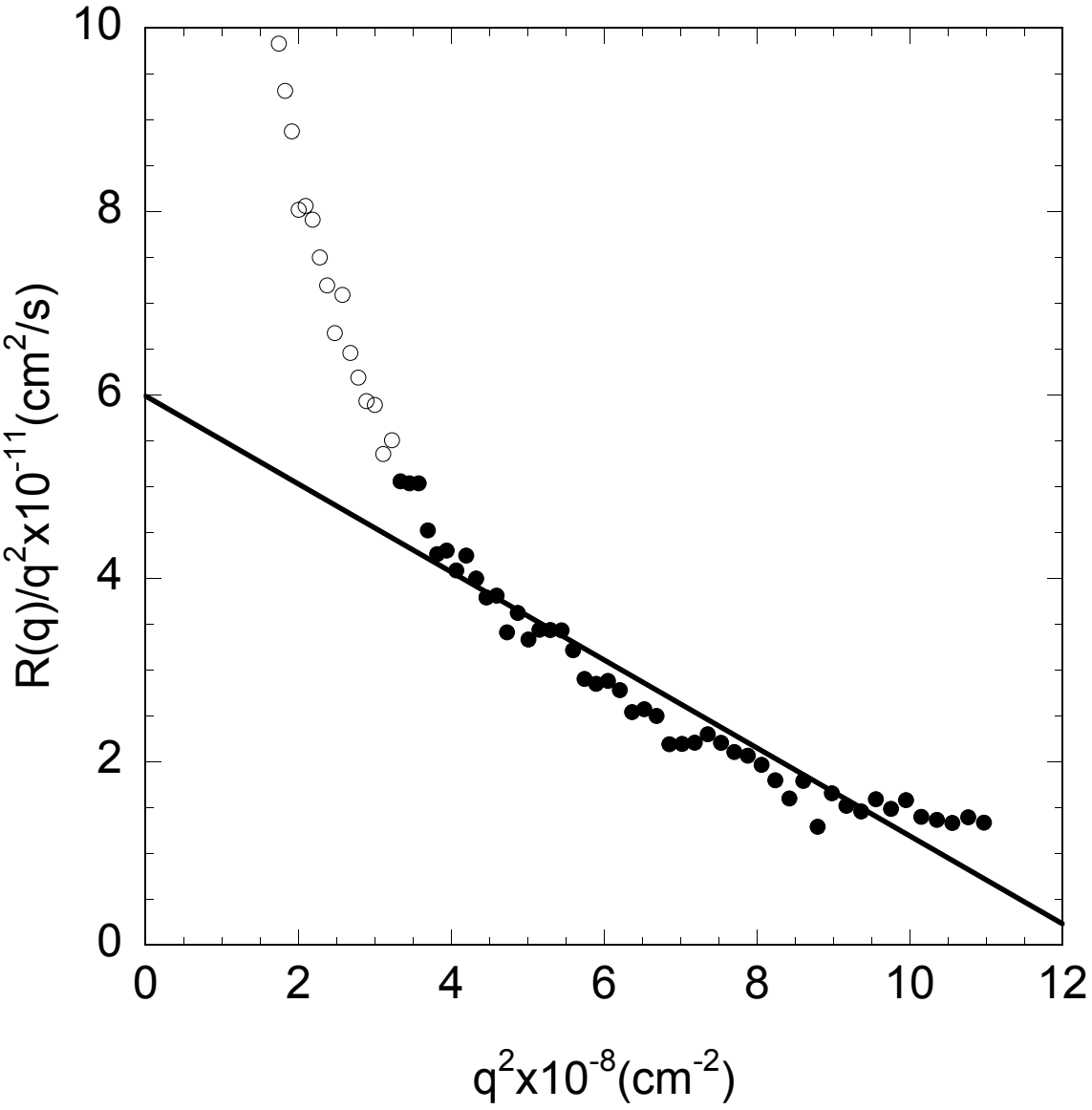

Figure 7.12 R/q^2 versus q^2 curve expanded over a larger range of q^2 values for the PCTMC40/SAN25 temperature jump to 161 °C. The filled markers represent data used in Figure 7.10 (a); the open circles were disregarded in the regression shown in Figure 7.10 (a).

temperature dependence of the refractive index difference between phases in these blends, a clear to cloudy transition occurs during heating even though no phase separation takes place. This assertion was proven through the analysis of glass transition behavior, the correlation between predicted refractive indices and scattered light, the kinetics of the changes in scattered light, scattered light peak position, and the angular dependence of the Cahn-Hillard growth factor. If the linearized Cahn-Hillard model is used to describe the changes during a temperature jump experiment, the corresponding analysis could lead one to assign a LCST temperature to these blends even though no phase transition actually occurs.

REFERENCES

1. Callaghan, T.A., et al. Polymer 1993;34:3796.
2. Merfeld, G.D. and Paul, D.R.'Polymer-Polymer Interactions Based on Mean Field Approximations', in Polymer Blends, Paul, D.R. and Bucknall, C.B. eds., John Wiley & Sons, Inc., New York. 2000;55.
3. Okamoto, M., K. Shiomi, and T. Inoue Polymer 1995;36:87.
4. van Krevelen, D.E., 'Properties of polymers'. 3 ed., Elsevier Pub. Co., Amsterdam, 1990.v
5. Lacombe, R.H. and Sanchez, I.C. J. Phys. Chem. 1976;80:2568.
6. Sanchez, I.C. and R.H. Lacombe J. Polym. Sci., Polym. Lett. Ed. 1977;15:71.
7. Merfeld, G.D. and Paul, D.R. Polymer 1999;41:649.
8. Bohn, L., 'Compatible Polymers', in 'Polymer Handbook', Brandrup J. and Immergut, E.H. eds, Wiley, New York, 1975.
9. Cahn, J.W. and Hillard, J.E. J. Chem. Phys. 1958;28:258.
10. Cahn, J.W. J. Chem. Phys. 1965;42:93.
11. Hindawi, I.A., Higgins, J.S. and Weiss, R.A. Polymer 1991;33:2522.
12. Fernandez, M.L. and Higgins, J.S. ACS Symp. Ser. 1995;597:106.
13. Fernandez, M.L., et al. Polymer 1995;36:149.
14. Chopra, D. and Vlassopoulos, D. J. Rheol 1998;42:1227.
15. Walsh, D.J., Lainghe, S. and Zhikuan, C. Polymer 1981;22:1005.
16. Walsh, D.J., Higgins, J.S. and Zhikuan, C. Polymer 1982;23:336.
17. Lorentz, H.A., Wied. Ann. Phys. 1880;9:641.

18. Lorenz, L.V., Wied. Ann. Phys. 1880;11:70.

19. Guo, W. and Higgins, J.S. Polymer 1990;31:699.

20. Binder, K. and Stauffer, D. Phys. Rev. Lett. 1974;33:1006.

21. Koberstein, J., Russell, T.P. and Stein, R.S. J. Poly. Sci. Polym. Phys. 1979;17:1719.

22. Hashimoto, T. Phase Transitions 1988;12:47.

Chapter 8: Blends of TMC Copolycarbonates with Poly(bisphenol-A-polycarbonate) and a Copolyester

The polycarbonate homopolymer derived from bisphenol-A (BPA-PC) is a transparent, amorphous material with excellent toughness and a relatively high glass transition temperature (T_g). In addition to its uses in neat form, blends of BPA-PC with other polymers have been of considerable practical and fundamental interest. Copolycarbonates of bisphenol-A combined with other bisphenol monomers have also attracted attention as a means of tuning specific physical properties. For example, a series of random copolycarbonates based on bisphenol-A (acetone) and 1,1-bis(4-hydroxyphenyl)-3,3,5-trimethylcyclohexanone (TMC-PC) has become available to meet the demand for amorphous materials with higher heat resistance, i.e., higher T_g than BPA-PC[1].

The availability of these materials and the long-term interest of this laboratory in blends based on polycarbonates, including the effects of structure on miscibility (or interactions) with other polymers, stimulated this study [2]. This chapter describes the miscibility of these copolycarbonates with BPA-PC, with each other, and with a copolyester based on 1,4-cyclohexanedimethanol and a mixture of terephthalic and isophthalic acids that is known to be miscible with BPA-PC[3-7].

MATERIALS AND PROCEDURES

The polymers used in this study, shown in Table 8.1, were used as received except for the TMC-PC homopolymer, which was precipitated in methanol three times from a dichloromethane solution to remove residual monomer. The copolyester molecular weight information was determined by viscometry [5].

The TMC-PC copolymers and homopolymer molecular weight information was obtained by gel permeation chromatography. When this work was previously published, polystyrene standards were used to calibrate the column[8]. However, it was later learned that when polycarbonates are tested, calibration with polystyrene indicates significantly larger molecular weights than when the column is calibrated with polycarbonates. To correct this problem, the three polydisperse polycarbonates from Dow Chemical Co. listed in Table 8.1, whose molecular weights have previously been determined by light scattering, were used to make a calibration curve. This curve is shown in Figure 8.1. The copolycarbonates, TMC-PC homopolymer, and BPA-PC(63) molecular weights have been adjusted accordingly. Therefore, the calculations of combinatorial entropy in this chapter will be different than those of the original publication[8]. However, the qualitative conclusions based on these calculations remain unchanged.

Polymer blends were made by both melt and solution methods. Melt blending was performed in a Brabender outfitted with a 50 cm^3 batch mixing head at a temperature 85 °C above the highest component glass transition temperature. Blends were also cast from approximately 10 wt% polymer in dichloromethane solutions onto glass slides at room temperature or precipitated into a non-solvent.

Table 8.1 Polymers used in this study.

Polymer	Source	Commercial Description	Composition (wt %)	M_w (Da)	M_w/M_n
PCTMC11	Bayer AG	Apec 9330	11.1%TMC[a]	29,800	2.4
PCTMC30	Bayer AG	Apec 9340	30.2%TMC[a]	33,200	2.5
PCTMC40	Bayer AG	Apec 9358	38.9%TMC[a]	35,900	2.2
PCTMC64	Bayer AG	Apec 9371	64.2%TMC[a]	38,300	2.7
TMC-PC	Bayer AG	N/A	Homopolymer	84,735	2.4
BPA-PC(63)	Mitsubishi Corp.	E-2000	Homopolymer	36,500	-
BPA-PC(46)	Dow Chemical Co.		Homopolymer	25,916	-
BPA-PC(31)	Dow Chemical Co.		Homopolymer	17,282	-
BPA-PC(19)	Dow Chemical Co.		Homopolymer	10,000	-
TMPC-PC	Bayer AG	N/A	Homopolymer	37,900[b]	3.6[b]
Copolyester[d]	Eastman Chemical Co.	Eastar A-150	80%Terephthalic 20%Isophthalic	-	22,000

[a] [29]
[b] [30]
[c] This commercial copolymer is formed from 1,4-cyclohexanedimethanol and the indicated mixtures of phthalic acids. The polymer was characterized previously [5]. This copolyester was formerly known as Kodar 150
* Note that the number in the notation of the PCTMC materials reflects the TMC content while the number in the notation for BPA-PC materials refers to their molecular weight.

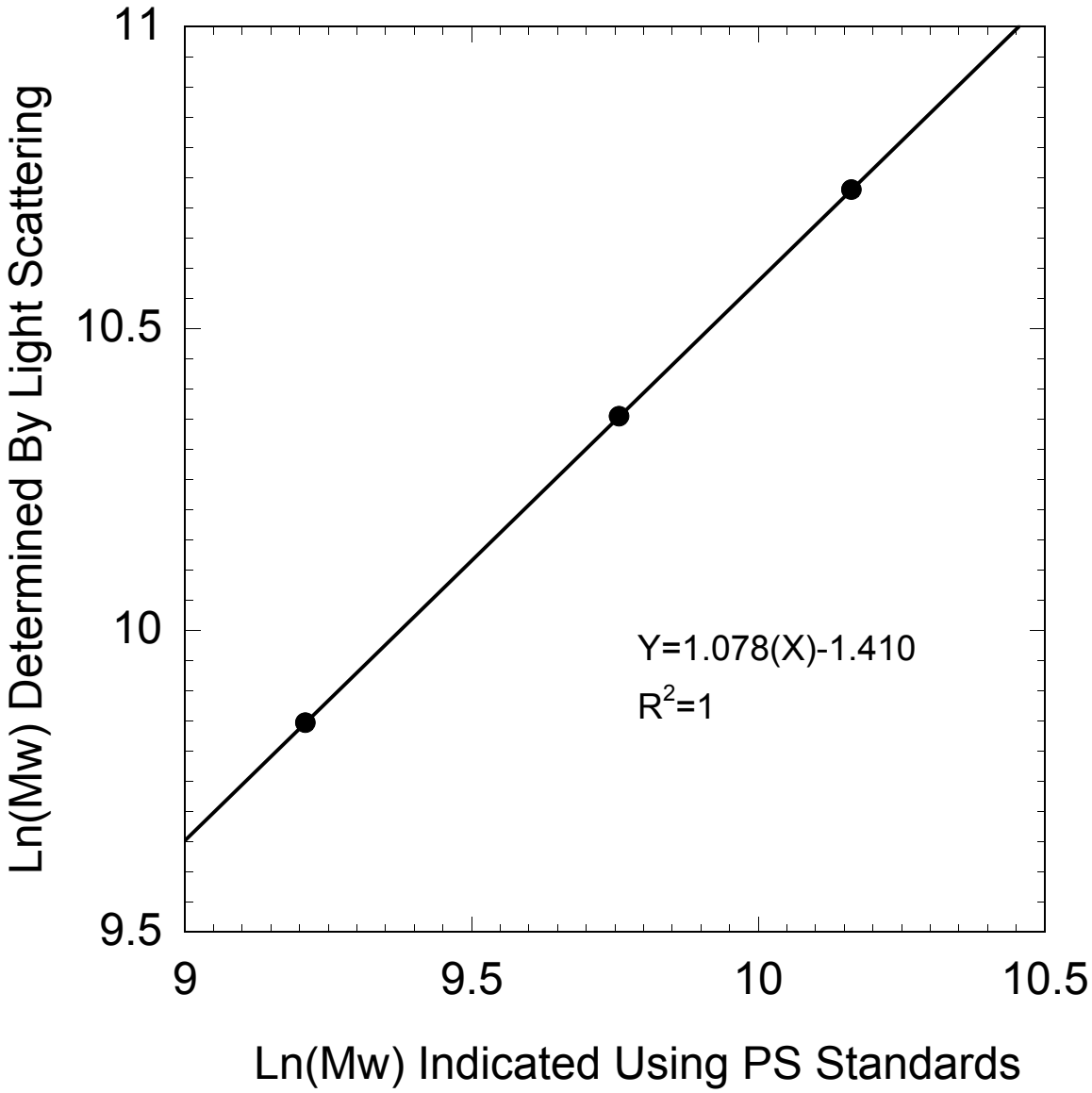

Figure 8.1 Calibration curve used to correct polycarbonate gel permeation chromatography data collected while using polystyrene standards.

The polycarbonate and polyester materials were dried for a minimum of 24 hours at 80°C in a vacuum oven prior to melt processing. A Killion single screw extruder (L/D = 30 D = 2.54 cm) operating at 60 rpm was used to disperse a catalyst deactivating agent, arsenic (III) oxide, into the copolyester[5]. Notched Izod bars 3.18 mm thick by 12.7 mm wide and ASTM D638 type I dogbone bars were formed in an Arburg Allrounder injection molder. The nozzle temperature was held 110 °C above the glass transition of the material, the injection pressure was 75 bar, and the holding pressure was 70 bar. Tensile testing was performed with a computerized Instron at a crosshead speed of 5.1 cm/min. Notched Izod impact tests were performed with a TMI tester using a 6.8 J hammer and 3.5 m/s impact velocity. The Izod impact specimens had the standard notch radius of 0.25 mm.

MECHANICAL PROPERTIES OF TMC-COPOLYCARBONATES

Since many applications of BPA-PC and associated blends depend on their modulus and ductility, we sought to investigate changes in these properties encountered upon the addition of TMC-PC units to form compolymers with BPA-PC. The mechanical properties of BPA-PC and the various copolycarbonates determined here are shown in Table 8.2. The elongation at break and the notched Izod impact energy, which are measures of ductility, are reduced by the addition of the TMC-PC monomer unit as shown in Figures 8.2a and 8.2b, respectively. It should be noted that a step decrease in the impact strength at a TMC-PC content between that of 11.1 and 30.2% is observed

Table 8.2 Polymer properties.

Polymer	T_g (°C)	Refractive Index (25°C)	Elongation at Break (%)	Tensile Modulus (GPa)	Notched Izod Impact Energy(J/m)	Yield Stress (MPa)
PCTMC11	156	1.581[a]	133	2.15	855	57.4
PCTMC30	167	1.578[a]	121	2.25	94.3	64.8
PCTMC40	180	1.572[a]	117	2.32	81.9	65.0
PCTMC64	203	1.565[a]	47.8	2.43	70.9	68.4
TMC-PC	237	1.554[b]	-	-	-	-
BPA-PC	149	1.586[a]	139	2.36	954	57.3
TMPC	190	1.602[a]	-	-	-	-
Copolyester[c]	87,	-	-	-	-	-

[a] (product literature)
[b] calculated[31]
[c] melting temperature = 265 °C crystallization temperature = 150°C

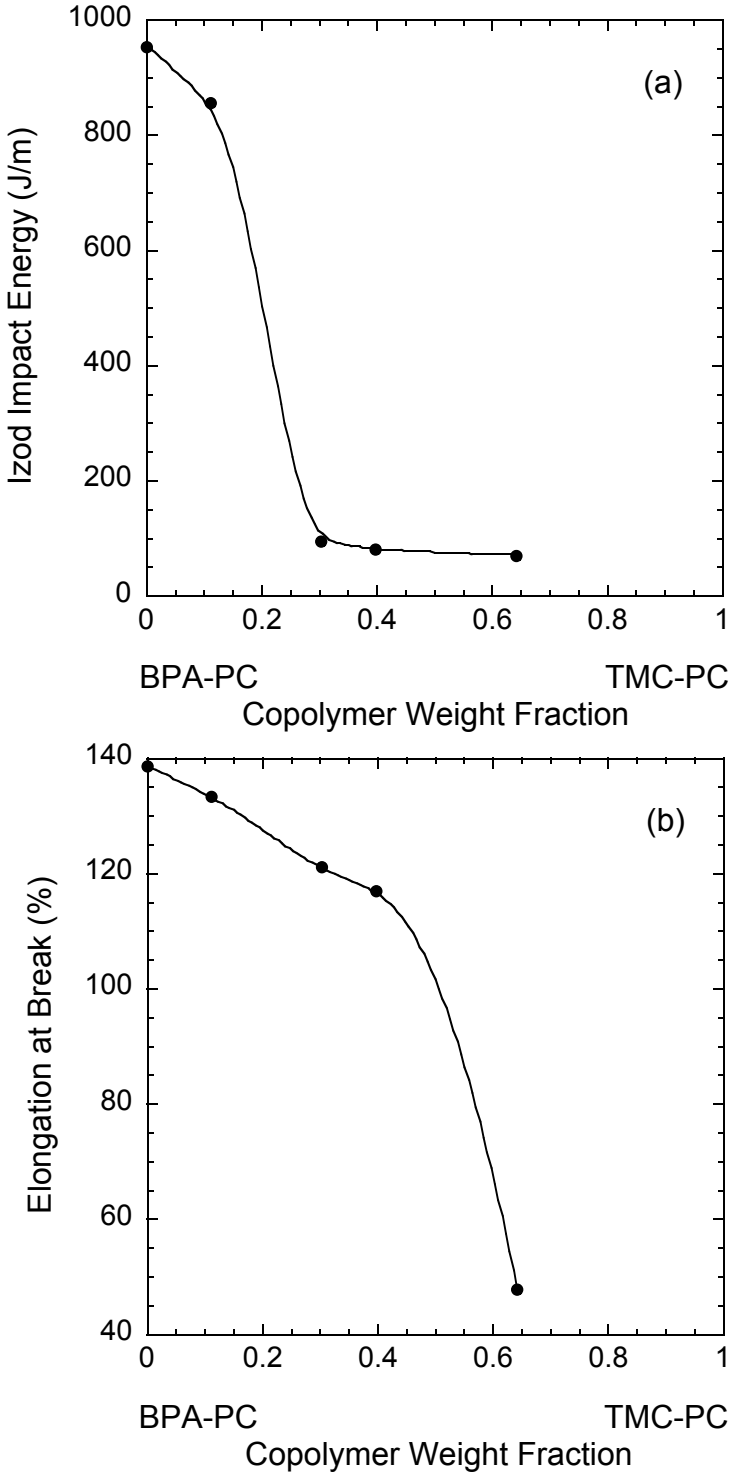

Figure 8.2 Mechanical properties of BPA/TMC copolycarbonates as a function of their composition. a) Notched Izod impact energy and b) % elongation at break.

here, while information from the manufacturer indicates a more gradual decrease. The modulus and yield stress increase slightly with an increase in TMC-PC content.

BLENDS WITH POLY(BISPHENOL-A-POLYCARBONATE)

Each of the four copolycarbonates shown in Table 8.1 were melt blended with the highest molecular weight Bispenol-A-Polycarbonate in Table 8.1, BPA-PC(63). All of the resulting mixtures were transparent and exhibited a single glass transition by DSC. The glass transition data for these blends are shown in Figure 8.3 along with the corresponding predictions of the Fox equation. These data are also plotted in Figure 8.4 as a function of the weight fraction of TMC-PC repeat units contained in the blend. The observed glass transition appears completely specified by the TMC-PC content in the blend. Blends of these components prepared by solution casting or precipitation in methanol also showed a single glass transition. These results suggest that physically miscible blends are formed and that either the copolymers interact favorably with BPA-PC or the entropy of mixing is able to offset any unfavorable interaction.

For a mixture of two copolymers based on the same two monomers, but with different compositions, Equation 2.10 reduces to

$$\mathbf{B} = \mathbf{B}_{12}\left(\phi_1^{'} - \phi_1^{''}\right)^2 \qquad (8.1)$$

where $\phi_1^{'}$ and $\phi_1^{''}$ represent the volume fractions of component 1 in the compositionally different copolymers. Changes in copolymer composition have a large effect on the calculated interaction energy since it is modulated by the square of the composition difference. The most extreme value of the interaction energy of mixing exists for blends of two homopolymers, as can be seen in Equation 8.1, since the difference between volume fractions are at a maximum. If B_{12} in Equation 8.1 were negative, then miscibility of the two homopolymers would be assured. However, if the

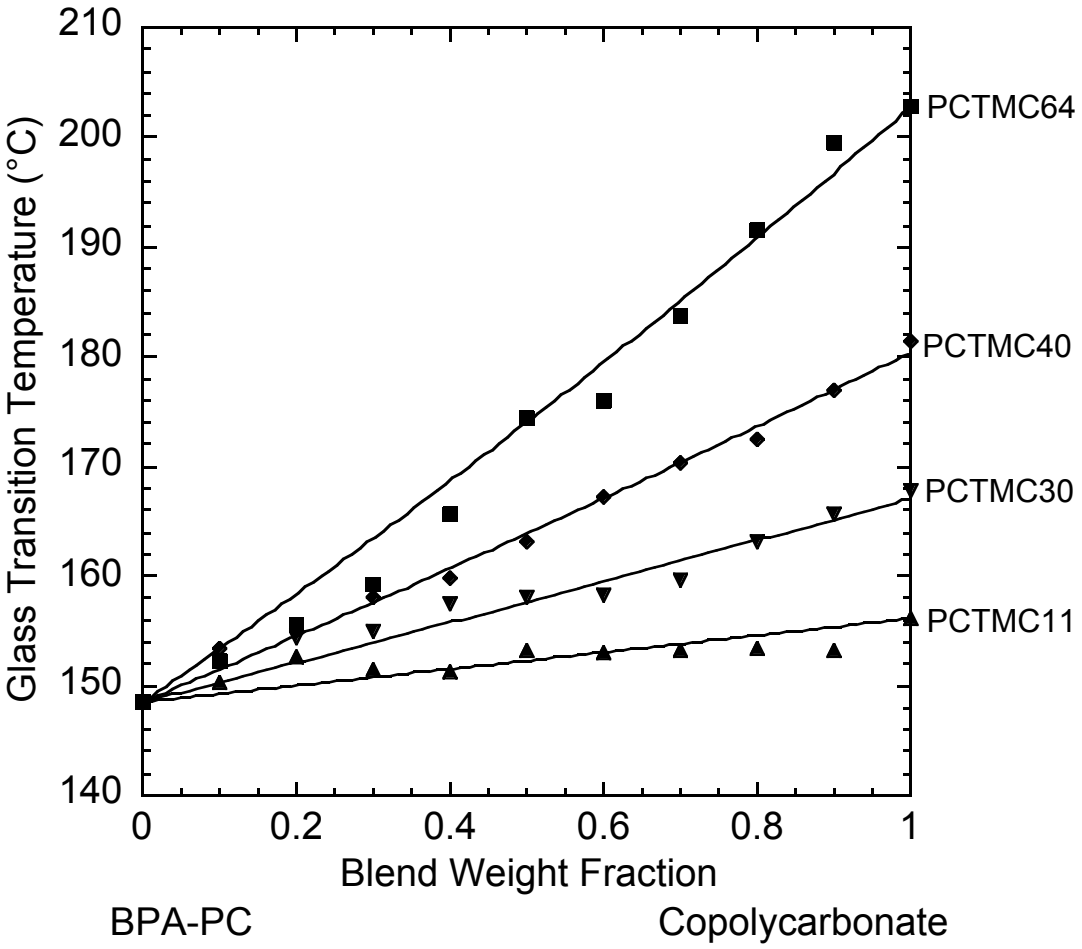

Figure 8.3 Glass transition temperatures versus composition for blends of Bisphenol-A polycarbonate (63) and the various copolycarbonates shown in Table 8.1 prepared blending in the melt. The curve shows the prediction by the Fox equation.

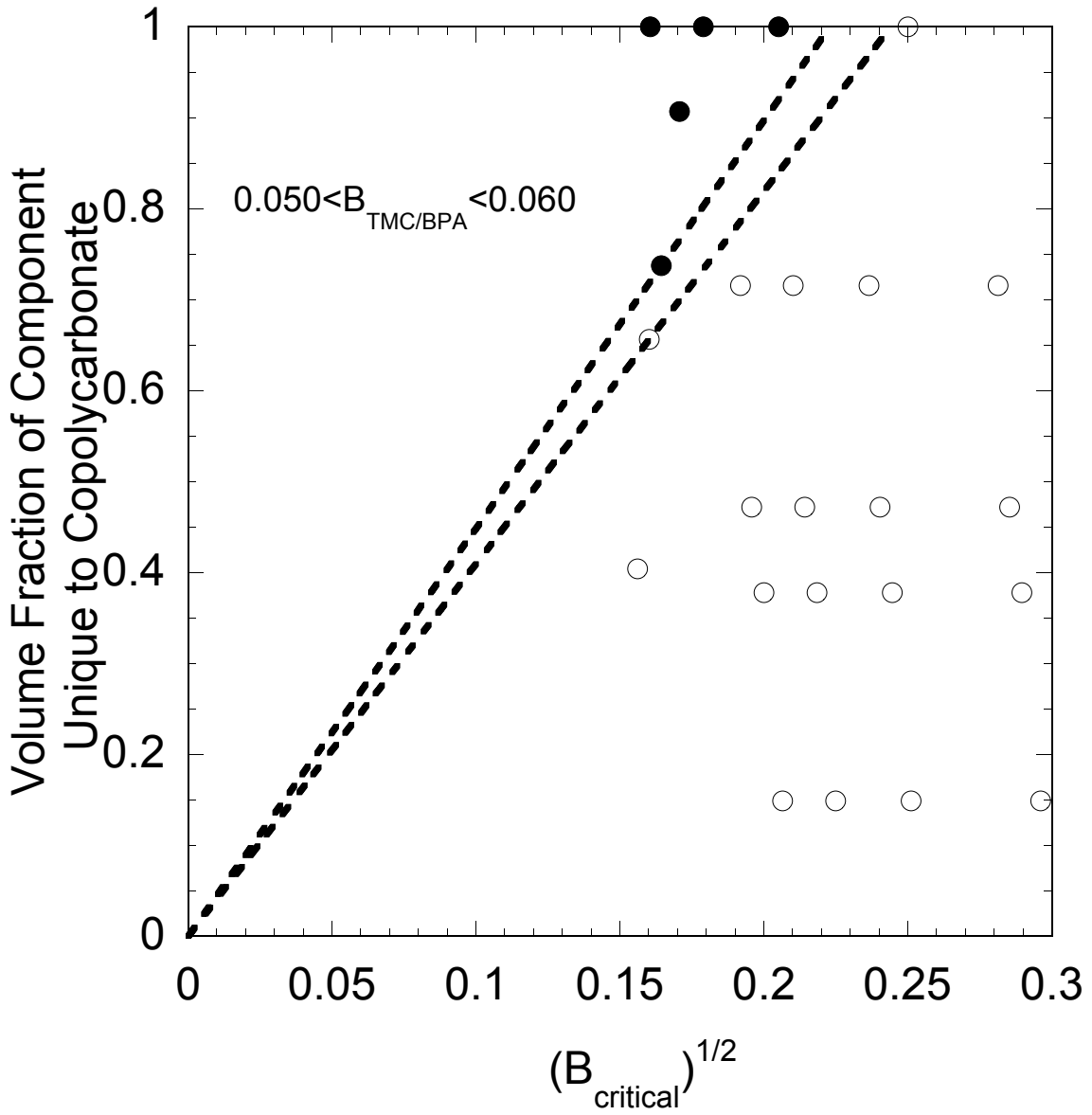

Figure 8.5 Phase behavior of blends solution cast and precipitated into methanol plotted such that the slope of the line separating single and two phase behavior is related to the TMC-PC/BPA-PC binary interaction energy as outlined in the text. Open circles represent single phase blends while closed circles represent two phase blends. The dashed lines shown correspond to binary interactions between TMC-PC and BPA-PC between 0.050 and 0.060 cal/cm^3.

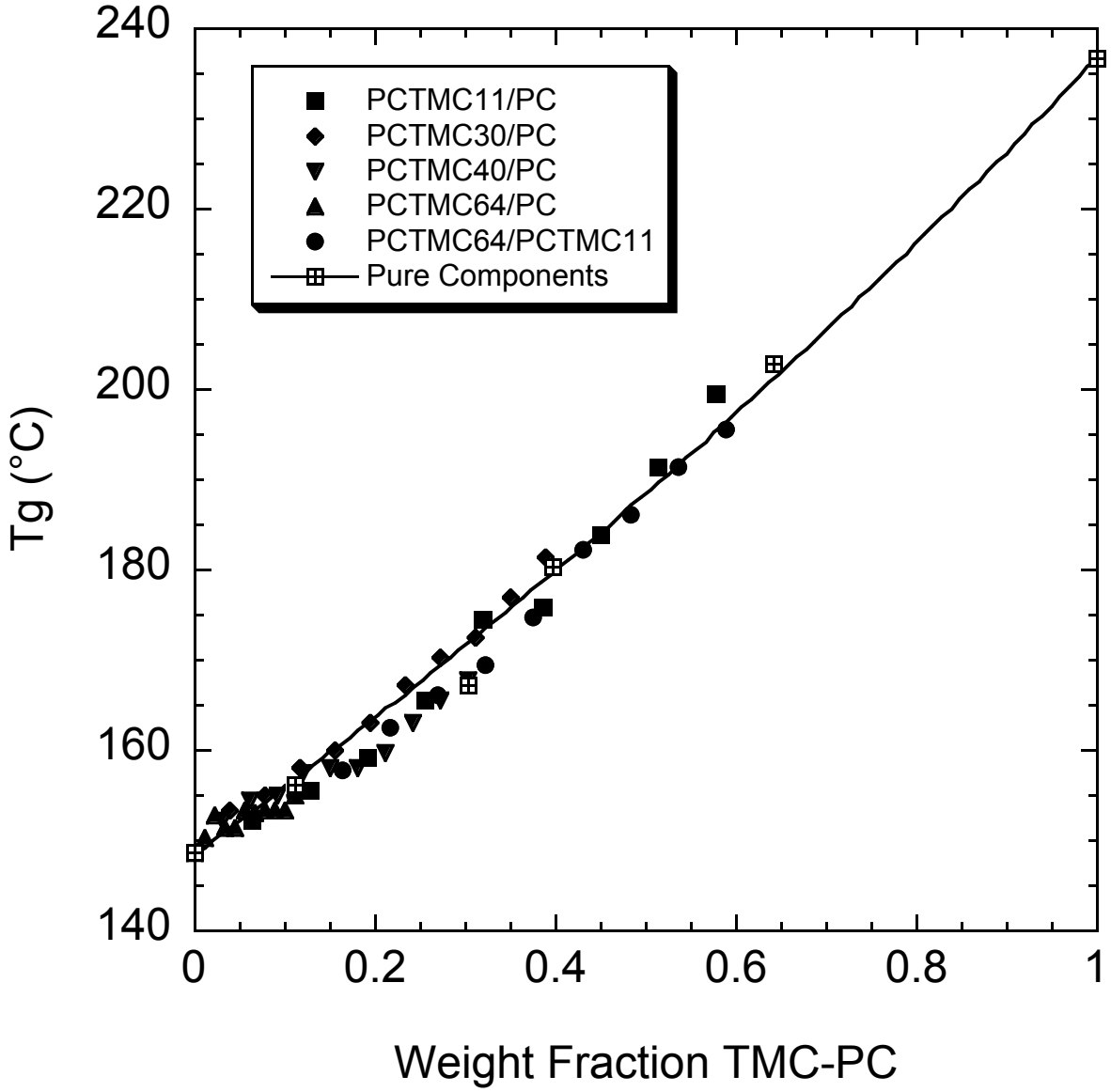

Figure 8.4 Glass transition data shown in Figure 8.3, re-plotted as a function of TMC-PC content. The curve shows the prediction by the Fox equation.

B_{12} is a positive quantity and the entropy of mixing drives miscibility, then miscibility of the two homopolymers is not assured since the value of Equation 8.1 is a maximum. The available supply of TMC-PC precluded melt mixing it with BPA-PC, so evaluation of these blends was limited to solution casting methods. It was found that the resulting phase behavior of the TMC-PC/BPA-PC homopolymer blends is strongly affected by the conditions of mixing and the thermal history of the blends.

It must be remembered that non-equilibrium effects may be encountered in preparing blends by solution casting methods. For example, a pair of polymers that are thermodynamically immiscible may become trapped in a homogenous state due to rapid solvent removal by hot casting or by precipitation with a non-solvent[9]. Alternatively, solution cast blends of polymer pairs that are thermodynamically miscible may become phase separated during solution casting due to the "$\Delta\chi$" effect[10-12]. The $\Delta\chi$ effect occurs because of a closed two phase region in the ternary phase diagram that results when the two polymers interact very differently with the solvent. When further solvent is removed, the polymers may not have enough mobility to re-form a single phase even though it is the condition of lowest free energy. This situation may be avoided by using a solvent that has similar interactions with both polymers. Blends of the TMC-PC homopolymers with the higher molecular weight BPA-PC homopolymers were phase separated when cast from dichloromethane, tetrahydrofuran, dioxane, bromobenzene or chloroform, and when precipitated from solution in an excess of methanol or n-heptane. It is unlikely that all of these observations stem from the $\Delta\chi$ effect. It seems reasonable to conclude that the interaction energy between the repeat unit pairs of the homopolymers is sufficiently repulsive to cause thermodynamic immiscibility of these homopolymers.

Blends of TMC-PC with the lower molecular weights of BPA-PC in Table 8.1 made by solution casting and precipitation into methanol produced single phase blends. Apparently, there is a repulsive interaction between the homopolymers that can be offset by the slightly larger entropy of mixing created by reducing the BPA-PC molecular weight.

To quantify the interaction between repeat units, it would be useful to anneal the blends above their glass transition temperatures to obtain physical equilibrium. However, if a phase separated TMC-PC/BPA-PC homopolymer blend is held at a temperature above its glass transition, interchange reactions, which have been noted in many polyester and polycarbonate systems, may occur. A useful way to confirm this is to redissolve and recast the blends. If no reaction occurred, then the original phase separated structure should reform again. Observation of a single phase in this experiment would indicate a permanent change in phase behavior due to interchange reactions.

A small number of interchange reactions can lead to homogenization through creating block copolymers at phase boundaries. With extended time, the interchange reactions essentially create random copolymers. The number of interchanges depends on the time at the elevated temperature[13]. Blends of TMC-PC with BPA-PC(63) have two glass transitions as cast, one transition after being held at 260°C for 10 minutes, and then two phases form again after the same sample is recast from heptane or methanol. The TMC-PC/BPA-PC(31) blends continued to have one glass transition after experiencing the same thermal treatment and then being recast into heptane or methanol. The number of interchanges should be similar for the two blends, with the difference in the recast solution behavior being due to the BPA-PC molecular weight difference.

All of the possible blend combinations were made by solution casting from dichloromethane, precipitation of these mixtures in heptane, and precipitation in methanol as shown in Table 8.3. As discussed in Chapter 2, a plot of the volume fraction of the monomer unique to the copolymer (ϕ_2) versus the square root of the entropy of mixing yields a line whose slope is $\sqrt{1/B_{TMC-PC/BPA-PC}}$ [14]. Thus, the phase behavior listed in Table 8.3 can be plotted in this manner, and the phase state boundary can be analyzed to extract an estimate for the binary interaction energy $B_{TMC\text{-}PC/BPA\text{-}PC}$. The entropy of mixing for these equal weight blends was approximated by the critical point entropy of mixing shown in Equation 2.16. Figure 8.5 shows the observed phase behavior of the BPA-PC/copolycarbonate and TMC-PC/copolycarbonate blends listed in Table 8.3 when they are precipitation cast into methanol or solution cast from dichloromethane at room temperature, plotted in the manner described above. In order to use phase state observations about the copolycarbonates blended with both homopolymers in Figure 8.5, plotting the volume fraction of the monomer unique to the copolymer, (ϕ_2), requires the ordinate to correspond to the volume fraction of TMC-PC in the copolymer with blends containing the homopolymer BPA-PC, and correspond to the BPA-PC content with blends containing the homopolymer TMC-PC. The phase state data shown in Figure 8.5 bounds the range of possible $B_{TMC\text{-}PC/BPA\text{-}PC}$ interaction energy densities between 0.050 and 0.060 cal/cm^3 as shown by the dashed lines. The phase behavior of blends solution cast into heptane at room temperature, plotted in the same way as Figure 8.5, is shown in Figure 8.6. A single line drawn through the origin will intersect observations of both single and two phases. An averaged fit of this data suggests an interaction energy density of 0.16 cal/cm^3.

The discrepancy between the two casting methods was probed by recasting a blend showing inconsistent phase behavior from the higher boiling point (156 °C) solvent

Table 8.3 Summary of blend phase behavior.

Blend	Solution Cast DSC / Optical	Precipitation n-Heptane	Precipitation Methanol
TMC-PC/BPA-PC(63)	2 T_g / Cloudy	2 T_g	2 T_g
TMC-PC/BPA-PC(46)	2 T_g / Cloudy	2 T_g	2 T_g
TMC-PC/BPA-PC(31)	2 T_g / Cloudy	2 T_g	2 T_g
TMC-PC/BPA-PC(19)	1 T_g / Hazy	2 T_g	1 T_g
TMC-PC/PCTMC64	1 T_g / Clear	1 T_g	1 T_g
TMC-PC/PCTMC40	1 T_g / Clear	2 T_g	1 T_g
TMC-PC/PCTMC30	2 T_g / Hazy	2 T_g	1 T_g
TMC-PC/PCTMC11	2 T_g / Cloudy	2 T_g	2 T_g
PCTMC64/BPA-PC(63)	1 T_g / Clear	2 T_g	1 T_g
PCTMC64/BPA-PC(46)	1 T_g / Clear	2 T_g	1 T_g
PCTMC64/BPA-PC(31)	1 T_g / Clear	2 T_g	1 T_g
PCTMC64/BPA-PC(19)	1 T_g / Clear	1 T_g	1 T_g
PCTMC40/BPA-PC(63)	1 T_g / Clear	2 T_g	1 T_g
PCTMC40/BPA-PC(46)	1 T_g / Clear	1 T_g	1 T_g
PCTMC40/BPA-PC(31)	1 T_g / Clear	1 T_g	1 T_g
PCTMC40/BPA-PC(19)	1 T_g / Clear	1 T_g	1 T_g
PCTMC30/BPA-PC(63)	1 T_g / Clear	1 T_g	1 T_g
PCTMC30/BPA-PC(46)	1 T_g / Clear	1 T_g	1 T_g
PCTMC30/BPA-PC(31)	1 T_g / Clear	1 T_g	1 T_g
PCTMC30/BPA-PC(19)	1 T_g / Clear	1 T_g	1 T_g
PCTMC11/BPA-PC(63)	1 T_g / Clear	1 T_g	1 T_g
PCTMC11/BPA-PC(46)	1 T_g / Clear	1 T_g	1 T_g
PCTMC11/BPA-PC(31)	1 T_g / Clear	1 T_g	1 T_g
PCTMC11/BPA-PC(19)	1 T_g / Clear	1 T_g	1 T_g
PCTMC64/TMPC	1 T_g	?	1 T_g
PCTMC40/TMPC	1 T_g	2 T_g	1 T_g
PCTMC30/TMPC	1 T_g	2 T_g	1 T_g
PCTMC11/TMPC	1 T_g	2 T_g	1 T_g
TMPC/BPA-PC(63)	2 T_g	2 T_g	2 T_g
TMPC/BPA-PC(46)	2 T_g	2 T_g	2 T_g
TMPC/BPA-PC(31)	1 T_g	2 T_g	1 T_g
TMPC/BPA-PC(19)	1 T_g	2 T_g	1 T_g

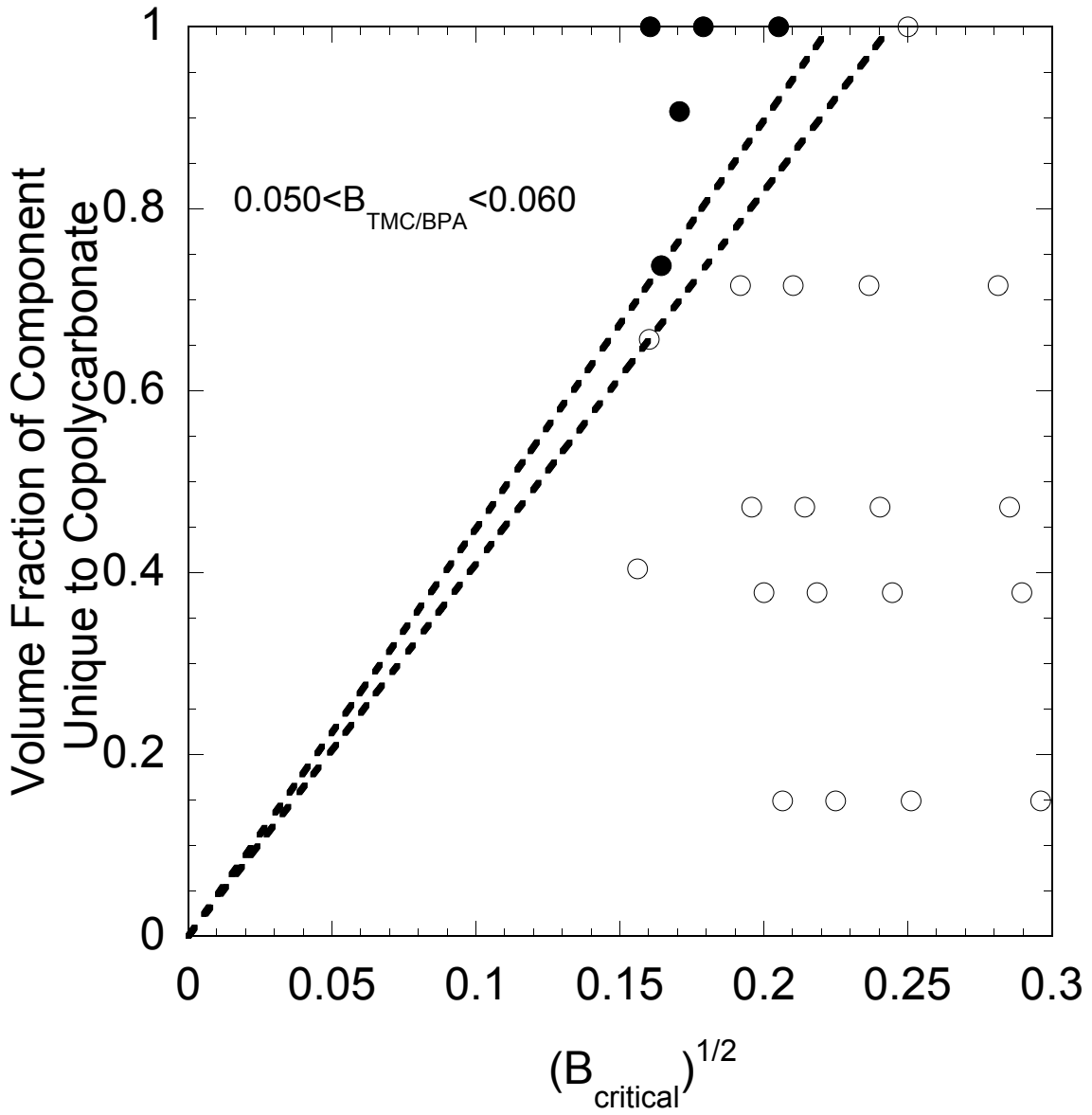

Figure 8.5 Phase behavior of blends solution cast and precipitated into methanol plotted such that the slope of the line separating single and two phase behavior is related to the TMC-PC/BPA-PC binary interaction energy as outlined in the text. Open circles represent single phase blends while closed circles represent two phase blends. The dashed lines shown correspond to binary interactions between TMC-PC and BPA-PC between 0.050 and 0.060 cal/cm^3.

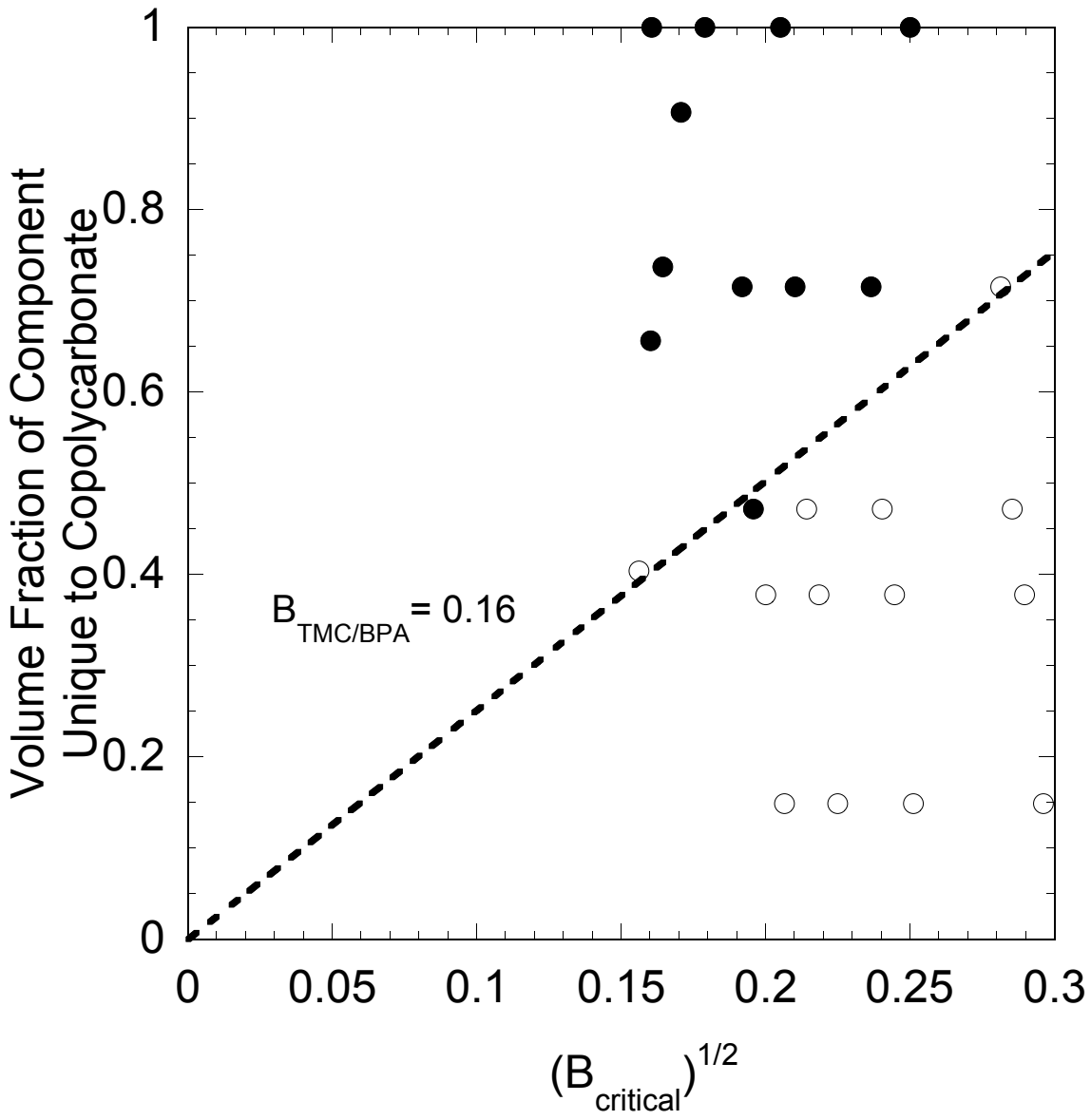

Figure 8.6 Phase behavior of blends precipitated into heptane plotted such that the slope of the line separating single and two phase behavior is related to the TMC-PC/BPA-PC binary interaction energy as outlined in the text. Open circles represent single phase blends while closed circles represent two phase blends. The dashed line represents a TMC-PC and BPA-PC interaction of 0.16 cal/cm^3.

bromobenzene at room temperature. It is unlikely that the observations from this method are biased towards phase homogeneity due to fast solvent removal. The resulting blend of TMC-PC/PCTMC40 produced the same phase behavior as the lower boiling point (40 °C) solvent dichloromethane. The blends prepared by solvent casting and precipitation into methanol show the same phase behavior; thus, we believe they represent the equilibrium phase behavior. We observed that the precipitation of the polycarbonates in the non-solvent occurred more rapidly in methanol than in heptane. The extra time during precipitation may have allowed for a metastable phase dissolution instead of the assumed spinodal one, which would account for the larger number of two phase blends observed while using heptane. The magnitude of the predicted interaction energies suggested by all blend preparation methods would preclude inducing miscible phase behavior due to the intramolecular repulsion as seen in blends containing stryrene/acrylonitrile copolymers which possess an intramolecular repulsion two orders of magnitude greater. The source of the discrepancy between precipitation in heptane and other methods is unknown; however, the difference in the estimated interaction energies between the two methods is not very significant in the context of designing polymer blends.

BLENDS WITH POLY(TETRAMETHYL BISPHENOL-A POLYCARBONATE)

Tetramethyl bisphenol-A polycarbonate (TMPC) is a unique polycarbonate because it is miscible with polystyrene[15-20]. Since BPA-PC blends with styrenic polymers are of considerable commercial interest, detailed studies of polycarbonate structure versus phase behavior with styrenic polymers have been conducted[2, 21]. One of the conclusions of these studies was that slight changes to monomer structure of either the styrene or polycarbonates had a large effect on the resulting blend phase behavior. In

continuing with the goal of these studies, the miscibility of TMPC with the TMC copolycarbonates was investigated.

As previously stated, the carbonate linkage allows interchange reactions that can alter the observation of physical miscibility. Therefore, the TMPC/TMC-PC copolycarbonate blends were made by the same casting procedures as the BPA-PC/TMC-PC copolycarbonate blends. The resulting phase behavior is shown in Table 8.3. Precipitation into heptane produced two phase blends with the TMC-PC copolycarbonates while solution casting and precipitation into dichloromethane did not. This is consistent with the observed tendency for this casting procedure to produce more immiscible blends as observed in the TMC-PC copolycarbonate/BPA-PC blends. It is also consistent with the agreement observed between casting procedures involving dichloromethane and precipitation into methanol.

TMPC was immiscible with the two higher molecular weight BPA-PC homopolymers by all casting methods as shown in Table 8.3. TMPC has been reported as being miscible with BPA-PC; however, these observations of miscibility were made after 24 hours of annealing at over 200°C[2]. The immiscible TMPC/BPA-PC blends were heated to 240°C at 20°C/min, then cooled, and reheated again in a series of steps. The two glass transitions eventually merged indicating a single phase. The dependence of miscibility on thermal history indicates the existence of interchange reactions between the polycarbonates. For the reasons discussed earlier, casting from dichloromethane or precipitation into methanol is likely to produce phase behavior more representative of physical miscibility than by precipitation into heptane for these blends. We can then conclude that the TMPC/BPA-PC enthalpic interaction is repulsive, but offset in some cases by the entropy of mixing. If we assume the entropy of mixing is that of the critical point, the TMPC/BPA-PC interaction can be bounded between 0.21 and 0.23 cal/cm^3.

Since the TMC-PC copolycarbonates are miscible with TMPC by solution casting from dichloromethane and precipitation in methanol, we can conclude that both the TMC-PC/BPA-PC intramolecular repulsion and the entropy of mixing offset the repulsive TMPC/BPA-PC interaction. Even though no TMPC/TMC-PC blends were made, and no boundary exists in the TMPC/TMC-PC copolycarbonate blends, we can still infer a maximum possible TMPC/TMC-PC interaction through the use of Equations 2.12 and 2.16. From this analysis, the TMPC/TMC-PC interaction cannot be more than -0.36 cal/cm^3.

BLENDS WITH A COPOLYESTER

The commercial polyester made from cyclohexanedimethanol and a mixture of about 80% terephthalic acid and 20% isophthalic acid are known to form miscible blends with BPA-PC[4-6, 22, 23]. An important benefit of blending these materials from a commercial point of view is that the copolyester retards the yellowing during radiation sterilization, which is a severe limitation for BPA-PC in some medical applications[24]. Blends of polyesters with TMC-PC copolycarbonates have been described as clear and miscible in the patent literature[25-28]. Thus, it is of interest here to examine in more depth the possible miscibility of the copolycarbonates in Table 8.1 with this commercial copolyester.

Blends of the copolyester with the various copolycarbonates were mixed in the melt with a Brabender batch mixing device. The total time spent in the mixer was less than 5 minutes for all blends and the temperature used was 85 °C above the T_g of the polycarbonate in the blend. The resulting blends were cooled rapidly after blending to reduce the thermal history and also to observe optical clarity without the interference of crystallinity. All of the copolyester/copolycarbonate blends were transparent, and their first heat DSC scans displayed a single glass transition indicating that all of the blends

exist as a single phase. To remove any possible effects of crystallinity, the blends were held above their melting temperature for one minute and then quenched at 200 °C/min to below their glass transition. The DSC scans after this thermal treatment also displayed a single glass transition temperature. The glass transition temperatures obtained after the thermal treatment in the DSC are shown in Figure 8.7. These glass transition temperatures are similar to the locations predicted for miscible blends using the Fox equation.

Blends of BPA-PC and this copolyester are known to undergo interchange reactions which are catalyzed by the residual titanium catalyst contained in the copolyester[5]. However, the residual titanium catalyst can be deactivated with additives like phosphite or arsenic compounds so that essentially no interchange reactions occur between BPA-PC and various polyesters like the copolyester of interest here. In an attempt to determine if the phase behavior observed here was due to physical miscibility or interchange reactions, 0.1 weight % arsenic (III) oxide was mixed with the copolyester prior to blending in equal weight fractions with the copolycarbonates. These blends were also clear when quenched to prevent crystallization and possessed a single glass transition. Figure 8.8 shows the heat of fusion (an indication of crystallinity) for blends containing equal parts by weight of copolycarbonates and the copolyester, with and without arsenic oxide, after being blended at 85°C above the copolycarbonate glass transition and annealed for 20 minutes at 177 °C. The interchange reactions in the uninhibited blends reduce the crystallizable segment length, and thus, reduce the heat of fusion after annealing. Figure 8.8 shows evidence of the interchange reactions in the uninhibited blends since the heat of fusion for the inhibited blends are consistently higher than those of the uninhibited blends. The heats of fusion for the inhibited blends, except

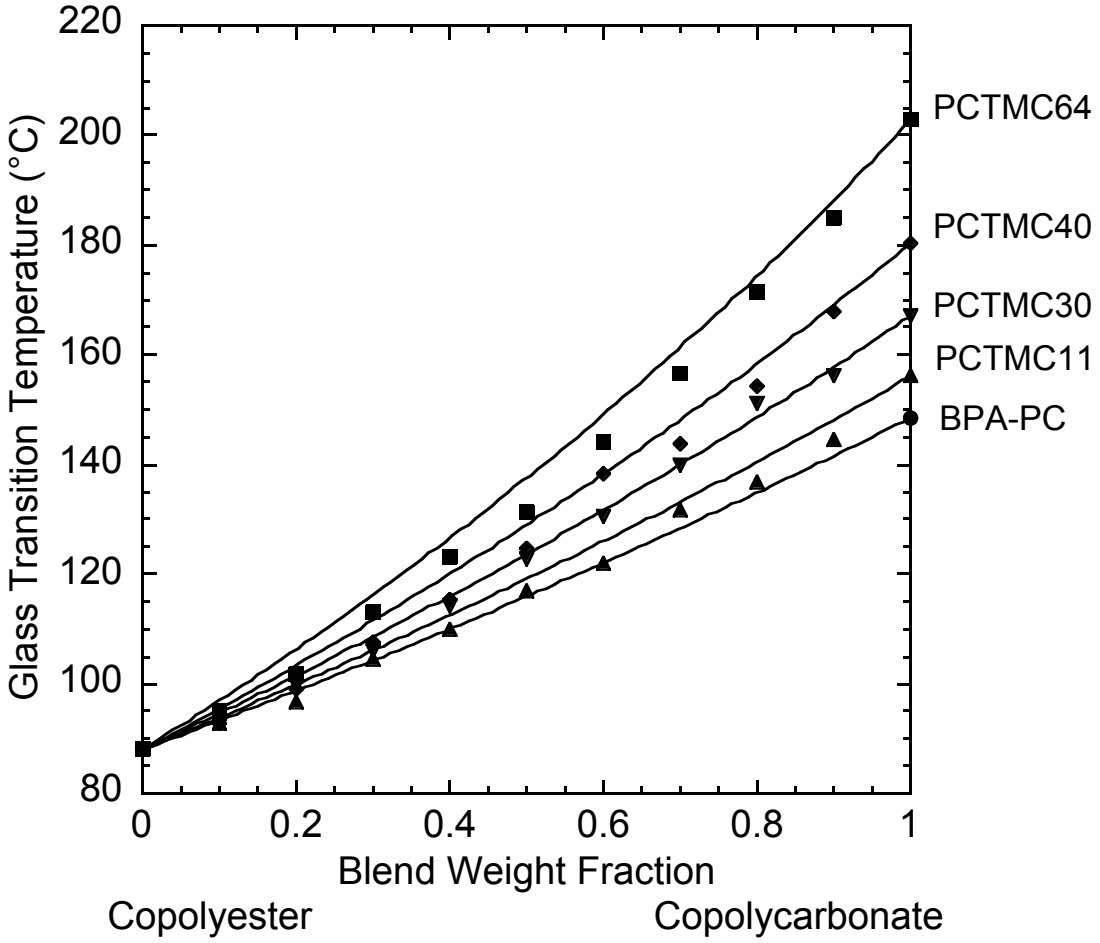

Figure 8.7 Glass transition temperatures of blends of the copolyester with the various copolycarbonates prepared by melt mixing. The curves show the prediction by the Fox equation.

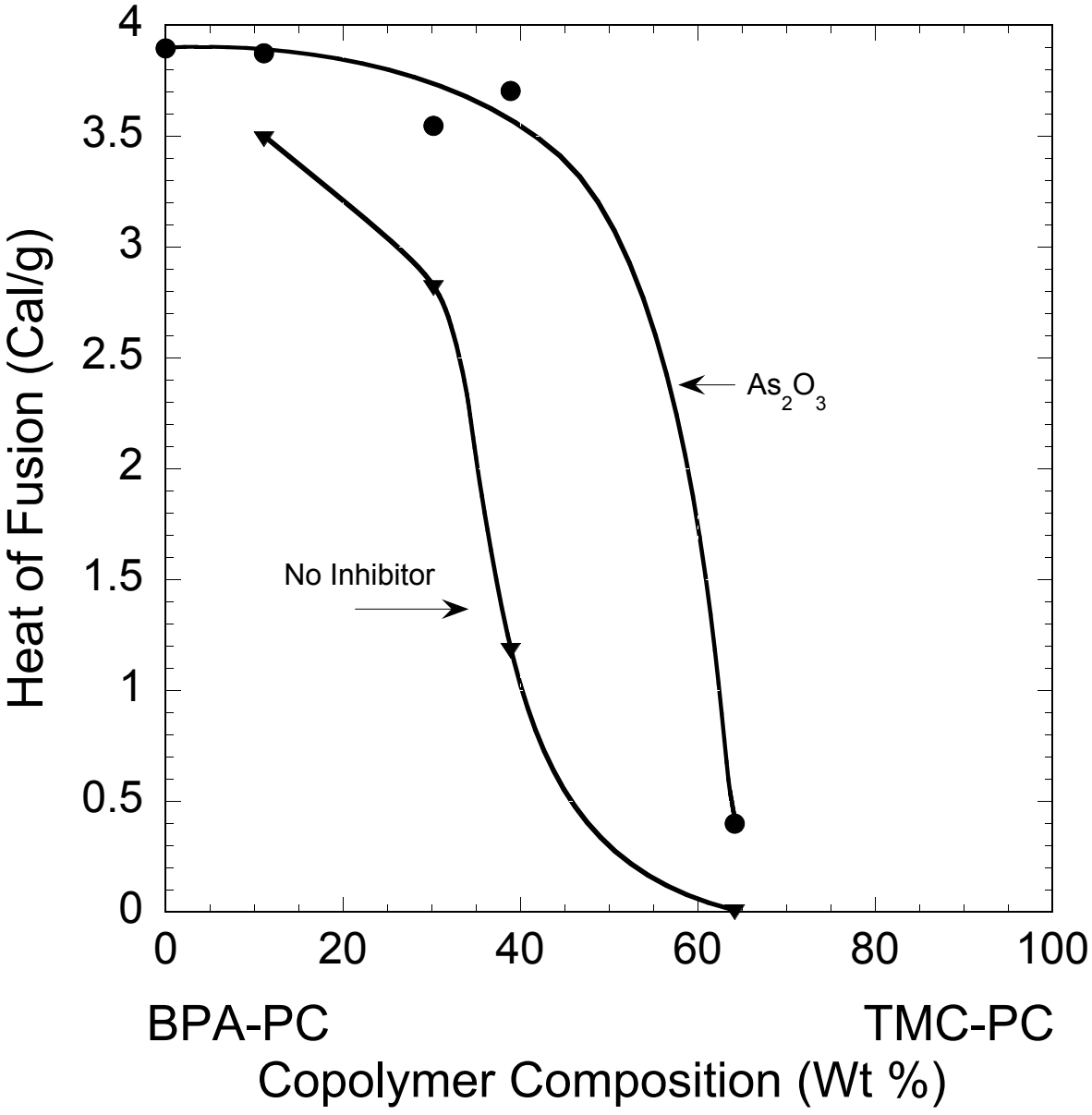

Figure 8.8 Heat of fusion versus copolymer composition for 50/50 weight % blends of copolycarbonates and the copolyester with and without 0.1weight % As_2O_3. Blends were annealed at 177 °C for 20 minutes prior to the assessment. The curves are drawn to aid the eye.

for the copolyester containing the highest amount of TMC-PC, are roughly equal to that of their pure copolyester content. This indicates that the interchange reactions are not significantly present in these one phase blends; thus, we conclude that these copolymers are physically miscible in the absence of interchange reactions.

CONCLUSIONS

All of the copolycarbonates based on bisphenol-A (BPA) and 1,1-bis(4-hydroxyphenyl)-3,3,5-trimethylcyclohexanone (TMC) were shown to be miscible with high molecular weight bisphenol-A-polycarbonate by solution casting and melt mixing methods. Two phase blends were observed between the homopolymer of TMC-PC and high molecular weight BPA-PC and also with copolycarbonates containing smaller amounts of TMC-PC. From these observations of phase behavior, it was estimated that the interaction energy between TMC-PC and BPA-PC units is between 0.053 and 0.063 cal/cm^3. The magnitude of this interaction precludes significant effects of intramolecular repulsion for inducing miscibility with other polymers.

We observed that the phase behavior of the copolycarbonate blends was a function of thermal history and method of mixing. The two phase homopolymer blends of TMC-PC and BPA-PC can be permanently homogenized through interchange reactions at elevated temperatures. Some copolycarbonate blends that were solution cast into heptane produced two phase blends that had a single phase when prepared by precipitation into methanol or cast from a variety of solvents. It is unlikely that solution casting from a high boiling point solvent would produce a non-equilibrium homogenized blend, therefore the solution casting and precipitation into methanol is believed to produce equilibrium phase behavior.

A similar study of phase behavior in blends of BPA-PC with tetramethyl bisphenol-A polycarbonate (TMPC) revealed a repulsive BPA-PC/TMPC interaction

between 0.21 and 0.23 cal/cm^3. A previous study observed miscibility between TMPC and a BPA-PC possessing a higher molecular weight than the BPA-PC materials used in this study[2]. This was probably due to interchange reactions whose effects were observed in this study. The TMC copolycarbonates were also miscible with TMPC. Miscibility with these copolymers requires that the TMC-PC/TMPC interaction be less than -0.36 cal/cm^3.

Blends of all of the copolycarbonates with a copolyester, based on 1,4-cyclohexanedimethanol with terephthalic and isophthalic acids, had a single phase when melt mixed. Because of the known tendency of these blends to undergo interchange reactions, the titanium catalyst in the copolyester was inhibited with arsenic (III) oxide prior to formation of selected blends with the polycarbonate. These blends were found to have a single glass transition. Heat of fusion data suggest that relatively few interchange reactions occur in the inhibited blends. This would indicate that the copolymers are physically miscible in the absence of the interchange reactions.

REFERENCES

1. Paul, W.G. and Bier, P.N. Annu. Tech. Conf.-Soc. Plast Eng. 1994;2:1759.
2. Kim, C.K. and Paul, D.R. Macromolecules 1992;25:3097.
3. Mohn, R.N., et al. J. Appl. Polym. Sci. 1979;23:575.
4. Cruz, C.A., Barlow, J.W. and Paul, D.R. Macromolecules 1979;12:726.
5. Smith, W.A., Barlow, J.W. and Paul, D.R. J. Appl. Polym. Sci. 1981;26:4233.
6. Barnum, R.S., Barlow, J.W. and Paul, D.R. J. of Appl. Polym. Sci. 1982;27:4065.
7. Campbell, J.A., Goodwin, A.A. and Simon, G.P. Polymer 2001;42:4731.
8. Haggard, K.W. and Paul, D.R. Polymer 2004;45:2313.
9. Nishimoto, M., Keskkula, H. and Paul, D.R. Polymer, 1991;32:272.
10. Zeman, L. and Patterson, D. Macromolecules 1972;5:513.
11. Nandi, A.K., Mandal, B.M. and Bhattacharyya, S.N. Macromolecules 1985;18:1454.
12. Woo, E.M., Barlow, J.W. and Paul, D.R. J. Polym. Sci., Polym. Symp. 1984;71:137.
13. Takeda, Y. and Paul, D.R. Polymer 1991;32:2771.
14. Chu, J.H., Tilakaratne, H.K. and Paul, D.R. Polymer 2000;41:5393.
15. Wisniewsky, C., Marin, G. and Monge, P. Eur. Polym. J. 1984;20:691.
16. Fernandes, A.C., Barlow, J.W. and Paul, D.R. Polymer 1986;27:1788.
17. Shaw, M.T. J. of Appl. Polym. Sci. 1974;18:449.
18. Casper, R. and Morbitzer, L. Angewandte Makromol. Chem. 1977;58-59:1.

19. Yee, A.F. and Maxwell, M.A. J. Macromol. Sci. Phys. 1980;B17:543.

20. Humme, G., Roehr, H. and Serini, V Angewandte Makromol. Chem. 1977;58-59:85.

21. Callaghan, T.A. and Paul, D.R. J. Polym. Sci. Polym. Phys. 1994;32:1813.

22. Joseph, E.A., et al. Polymer 1982;23:112.

23. Campbell, J.A., Goodwin, A.A., Simon, G.P. Polymer 2001;42:4731.

24. Avakian, R.W. and Allen, R.B. Polym. Eng. Sci. 1985;25:462.

25. Mason, J.P. Canada Patent No. 2113501; 1994. Assigned to Miles Laboratories, Inc., USA.

26. Mason, J.P. and Pyles, R.A. United States Patent No. 5461120; 1995. Assigned to Bayer A.-G., USA.

27. Massa, D.J., O'Reilly, J.M. and Chen, W.A. United States Patent No. 5925507; 1999. Assigned to Eastman Kodak Company, USA.

28. Scott, C.E., Bradley, J.C. and Rodney, J. United States Patent No. 6043322; 2000. Assigned to Eastman Chemical Co., USA.

29. Haggard, K.W. and Paul, D.R. Polymer. 2002;43;3727.

30. Merfeld, G.D. and Paul, D.R. Polymer 1999;41:649.

31. van Krevelen, D.E., 'Properties of polymers'. 3 ed., Elsevier Pub. Co., Amsterdam, 1990.

Chapter 9: Interactions with Copolymers Containing Benzyl Acrylate and Pentabromobenzyl Acrylate

In this study, the interaction of several polymer structures with benzyl acrylate (BA) are determined and compared to its brominated analogue, pentabromobenzyl acrylate (PBBA), which was the subject of a previous study[1].

MATERIALS AND PROCEDURES

Table 9.1 lists the BA and PBBA containing polymers used in this study. The BA polymers were synthesized by free radical polymerization in p-dioxane at 60°C using AIBN as the initiator. Conversions did not exceed 10% in order to limit composition drift. The resulting polymers were purified twice by reprecipitation from tetrahydrofuran into an excess of methanol. The synthesis and characterization of the PBBA containing polymers are described in detail elsewhere[1].

BA copolymer compositions were determined with proton NMR spectroscopy using tetramethyl silane as the shift reference. Poly(methyl methacrylate-co-benzyl acrylate) (MMABA) copolymer compositions were determined using the average ratio of the benzyl acrylate carbonyl and benzyl protons to the methyl methacrylate carbonyl protons. Poly(styrene-co-benzyl acrylate) (SBA) copolymer compositions were determined by the ratio of benzyl acrylate carbonyl protons to the total number of protons in the copolymer. The corresponding composition data and fit to Equation 3.1 is shown in Figure 9.1. The reactivity ratios for the BA copolymers used to construct the curves in Figure 9.1, and those previously reported for the PBBA copolymers are listed in Table 9.2.

Table 9.1 Polymers containing BA and PBBA

Polymer	Wt % BA	$\overline{M}_W$	$\overline{M}_W/\overline{M}_N$	Glass Transition (°C)
SBA10	15.2	126,000	1.9	85
SBA15	21.0	75,800	1.8	78
SBA20	25.5	176,400	1.8	77
SBA25	31.8	79,200	2.1	67
SBA30	36.5	202,500	1.6	69
SBA40	41.0	94,000	1.8	59
SBA50	48.5	83,000	1.6	49
SBA60	55.5	182,000	1.7	49
SBA70	58.4	203,000	1.6	42
SBA80	65.0	250,000	1.7	37
MMABA10	6.1	750,300	2	80
MMABA20	14.2	317,500	1.9	74
MMABA30	19.3	425,500	1.9	75
MMABA40	27.4	446,600	2.4	70
MMABA50	36.1	319,300	2.4	61
MMABA60	43.8	314,400	2.7	53
MMABA70	55.2	367,500	1.7	-
BA	1	300,000	5.4	6
SPBBA10	19.8	95,800	1.56	108
SPBBA 20	33.9	113,400	1.67	110
SPBBA 30	44.9	65,800	1.59	115
SPBBA 40	54.0	34,900	1.76	117
SPBBA 50	60.3	47,200	1.93	124
SPBBA 60	66.3	38,000	2.08	127
SPBBA 70	72.6	64,200	1.54	134
SPBBA 80	74.1	66,600	1.48	139
MMAPBBA10[a]	8.2	106,000	1.41	110
MMAPBBA20[a]	15.8	92,000	1.48	118
MMAPBBA30	23.7	92,000	1.44	123
MMAPBBA40	31.9	85,000	1.52	120
MMAPBBA50	39.8	87,000	1.50	124
MMAPBBA60	47.4	85,000	1.44	127
MMAPBBA70	58.4	87,000	1.85	125
MMAPBBA80	70.9	89,000	1.65	134
MMAPBBA90	80.5	62,000	1.68	146
PBBA	100			178

[a]5wt% ethyl acrylate was added to the reactant mixture during synthesis

*note that the copolymer name corresponds to the amount of BA or PBBA in the reactant mixture

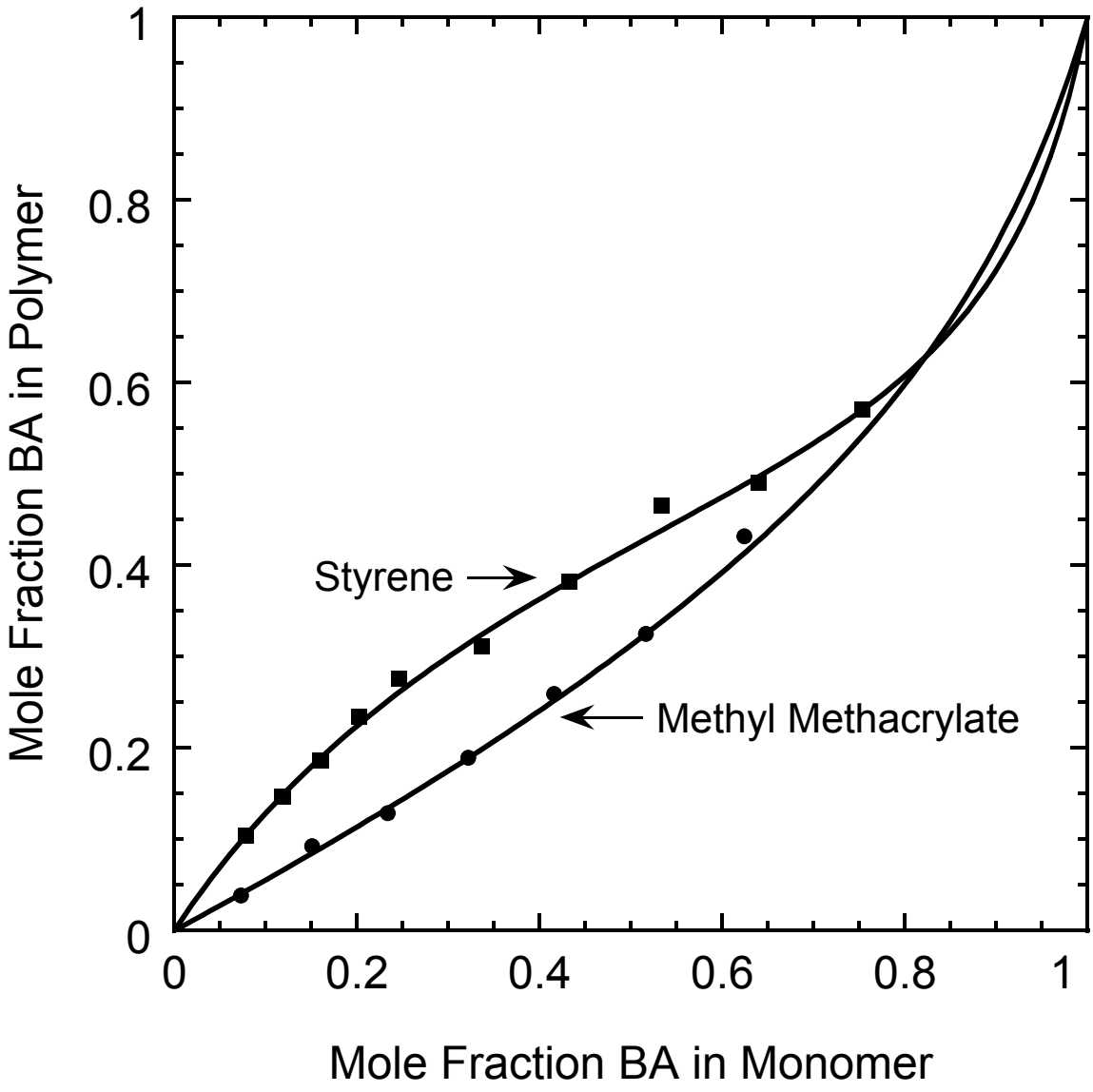

Figure 9.1 Concentration of BA in copolymers and reactant mixtures. The curves were constructed from the reactivity ratios stated in the text and Equation 3.1.

The molecular weights of the BA and PBBA containing polymers listed in Table 1 were determined by gel permeation chromatography. These molecular weights were calculated from a calibration curve using polystyrene standards and are, therefore, not absolute values.

Equation of state properties of Poly(benzyl acrylate) were determined using a pycnometer and mercury dilatometry. The data and Sanchez-Lacombe characteristic parameters for poly(benzyl acrylate) are listed in Appendix A. The Sanchez-Lacombe characteristic parameters for poly(pentabromobenzyl acrylate) were recalculated from reported data[2]. These parameters are also listed in Appendix A.

All blends made during this study were cast from dichloromethane, tetrahydrofuran, or bromobenzene from approximately 10 wt% solutions. These solutions were cast onto glass slides heated to 10°C below the boiling point of the solvent. These resulting blends were annealed at 150 °C for 48 hours.

INTERACTIONS WITH MONODISPERSE POLYSTYRENES AND POLY(METHYL METHACRYLATE)

Copolymers containing BA and PBBA were blended with monodisperse PS and PMMA, which are listed in Table 9.3, in their critical point compositions predicted by Equation 3.2. The resulting phase behaviors of selected blends whose compositions are near the phase behavior boundary at 150 °C are shown in Figure 9.2.

Table 9.2 Copolymer reactivity ratios

	S/BA	S/PBBA*	MMA/BA	MMA/PBBA *
r_1 (s or mma)	0.66	0.50	1.85	2
r_2 (ba or pbba)	0.15	0.40	0.29	0.9

* Previously reported values [1]

Table 9.3 Monodisperse PS and PMMA homopolymers.

Polymer	$\overline{M}_W$	$\overline{M}_W/\overline{M}_N$	Source
PS1.35	1,350	1.07	Polymer Laboratories
PS2	2,000	1.06	Pressure Chemical
PS4	4,000	<1.06	Pressure Chemical
PS7	7,000	1.03	Polymer Laboratories
PS9	9,000	<1.06	Pressure Chemical
PS12.9	12,900	1.02	Polymer Laboratories
PS17.5	17,500	1.04	Pressure Chemical
PS22	22,000	1.03	Polymer Laboratories
PS30.3	30,300	1.03	Polymer Laboratories
PS35	35,000	1.06	Pressure Chemical
PS52	52,000	1.03	Polymer Laboratories
PS100	100,000	1.06	Pressure Chemical
PMMA2.68	2,680	1.09	Polymer Laboratories
PMMA4.9	4,910	1.10	Polymer Laboratories
PMMA5.72	5,720	1.06	Polymer Laboratories
PMMA9.85	9,850	1.09	Polymer Source, Inc.
PMMA13	13,000	1.03	Polymer Laboratories
PMMA16.7	16,700	1.06	Polymer Source, Inc.
PMMA27.5	27,500	1.10	Polymer Source, Inc.
PMMA48.4	48,400	1.10	Polymer Source, Inc.
PMMA60	60,000	1.07	Polymer Laboratories
PMMA105.4	105,400	1.04	Polymer Source, Inc.
PMMA265.6	265,600	1.14	Pressure Chemcial

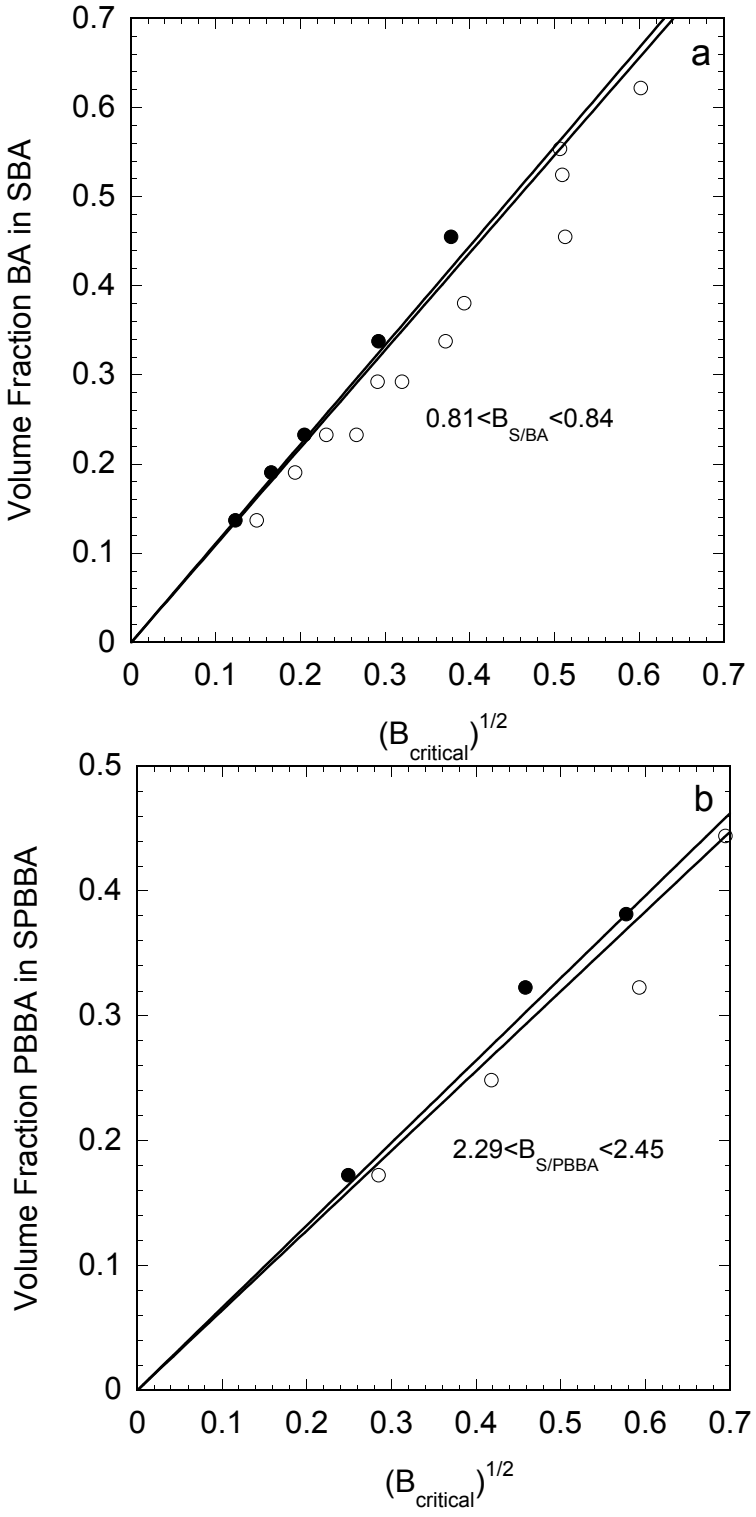
a
Volume Fraction BA in SBA
0.81<B S/BA <0.84
(B critical) 1/2
b
Volume Fraction PBBA in SPBBA
2.29<B S/PBBA <2.45
(B critical) 1/2

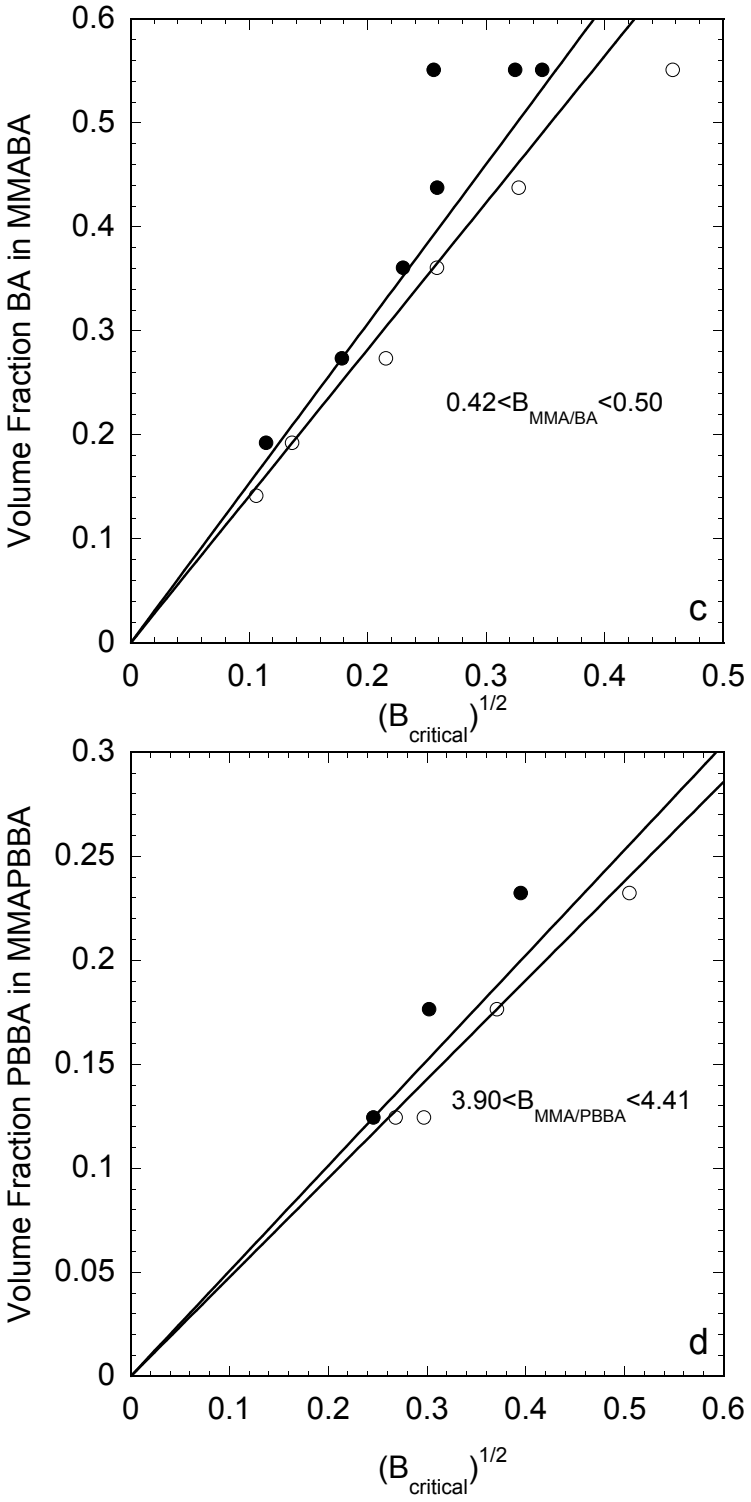

Figure 9.2 Phase behavior of BA and PBBA copolymer blends with monodisperse PS and PMMA at 150 °C. Open and closed circles represent single and two phase blends respectively.

The lines separating single and two phase regions in Figure 9.2 correspond to estimates of the binary interactions as discussed in Chapter 3. Estimates for the interactions, when analyzed in this way, are $0.81<B_{S/BA}<0.84$, $2.3<B_{S/PBBA}<2.5$, $0.42<B_{MMA/BA}<0.50$, and $3.9<B_{MMAPBBA}<4.4$ cal/cm^3. Note that the MMAPBBA10 and MMAPBBA20 copolymers were not used in this evaluation since they were synthesized with an ethyl acrylate comonomer.

EVALUATIONS OF COPOLYMER SELF COMPATIBILITY

The allowable difference in composition between copolymers having like repeat units, or self compatibility, of the BA and PBBA copolymers was determined using equal weight blends. The resulting observations of phase behavior are shown in Figure 9.3. Note that each data set shown in Figure 9.3 contains two points for each observation of phase behavior. Therefore, each data set is symmetric about the x-y axis. This was done to provide a better visual representation of the predicted and experimental regions of phase behavior.

The curves in Figure 9.3 are predicted miscibility regions using Equation 2.14 and an approximate critical point entropy of mixing based on the average densities and molecular weights of each set of copolymers. The interaction energies and average entropy of mixing for each predicted curve shown in Figure 9.3 is listed in Table 9.4. Each of the plots in Figure 9.3 contains two predicted areas of miscible blends to illustrate the range of interactions that could describe the observations of phase behavior.

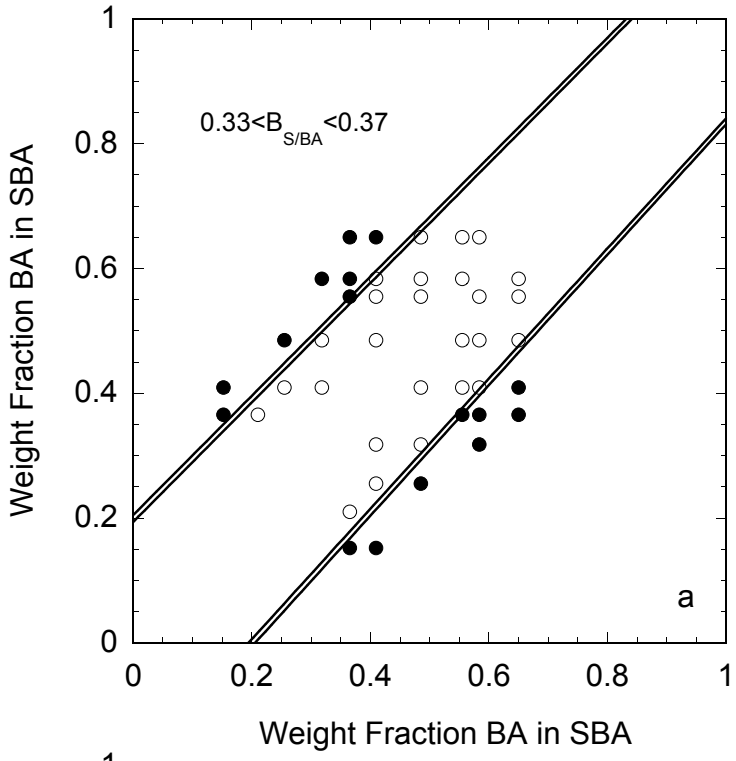
0.33<B_S/BA<0.37
Weight Fraction BA in SBA
Weight Fraction BA in SBA
a
0
0.2
0.4
0.6
0.8
1

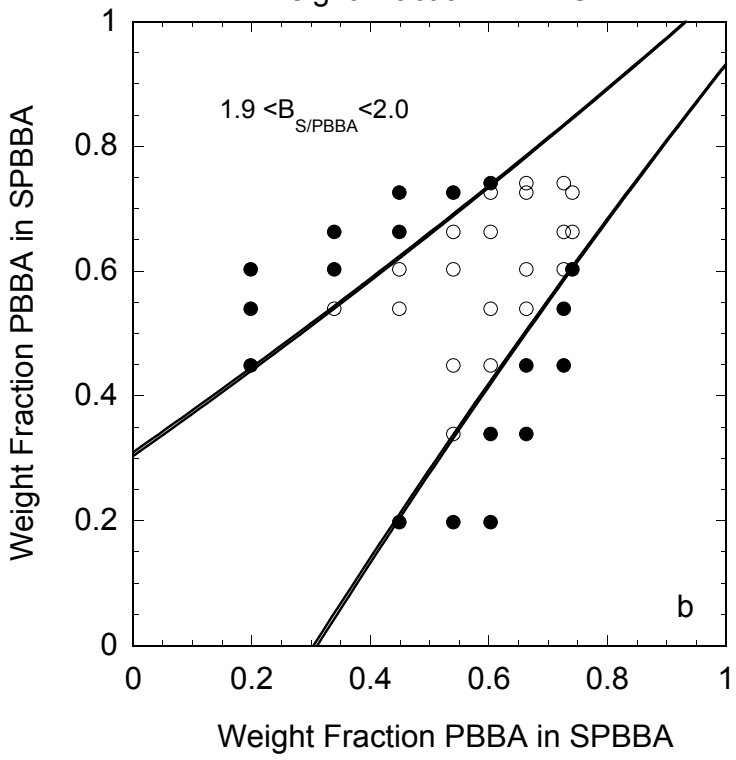
1.9 <B_S/PBBA<2.0
Weight Fraction PBBA in SPBBA
Weight Fraction PBBA in SPBBA
b
0
0.2
0.4
0.6
0.8
1

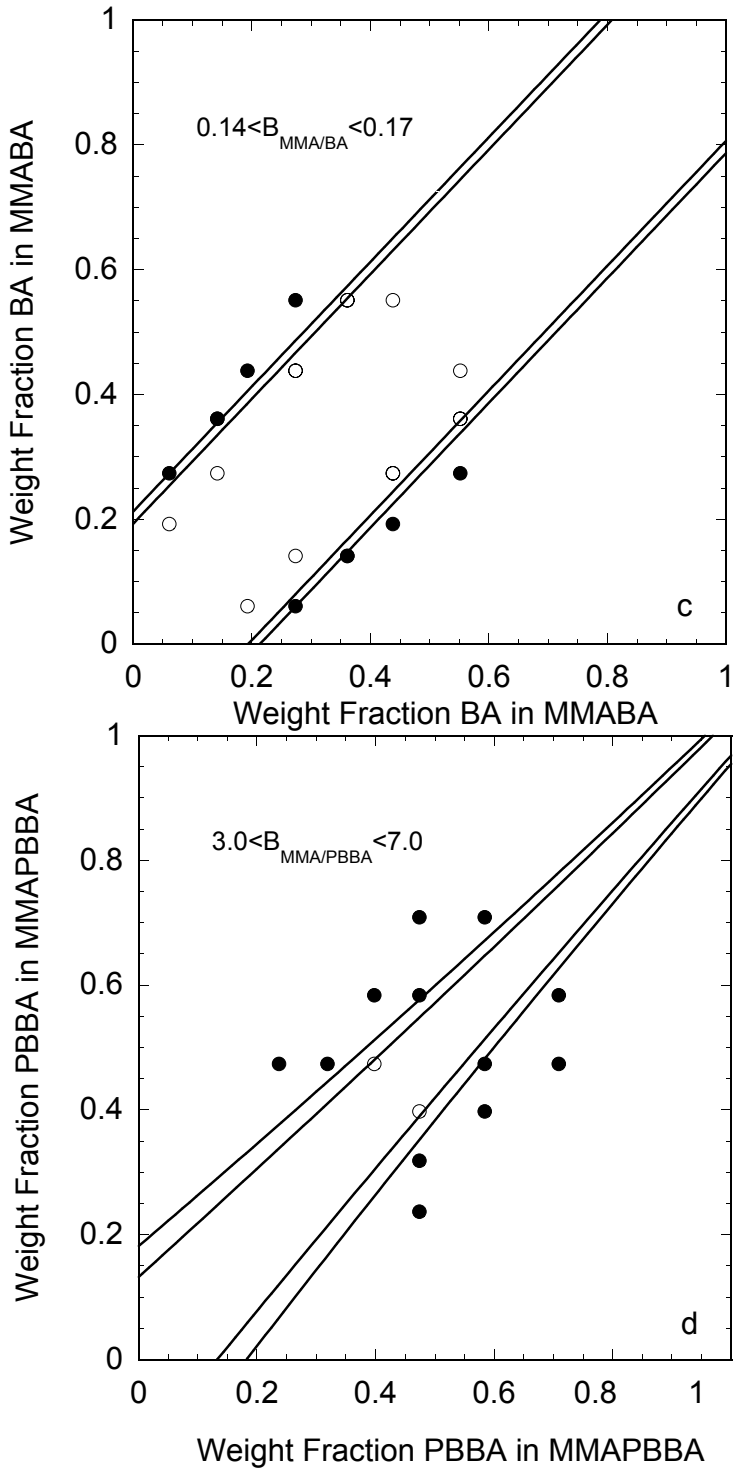

Figure 9.3 Self compatibility of the BA and PBBA copolymers. Open and closed circles represent single and two phase behavior respectively. The curves were drawn from the average critical point entropy of mixing and the binary interactions listed in Table 9.4.

Table 9.4 Estimated interactions in cal/cm^3.

Interaction Pair	Critical M_W	Self Compatibility	Copolymer-Copolymer	ΔP_{ij}	$(\delta_i-\delta_j)^2$	k_{ij}
S/BA	0.81-0.84	0.33-0.37	0.30	0.31	0.12	0.001
S/PBBA	2.3-2.5	1.9-2.0	1.95	1.51	2.2	-0.004
MMA/BA	0.42-0.50	0.14-0.17	0.27	0.22	0.05	0.001
MMA/PBBA	3.9-4.4	3.0-7.0	3.2	2.69	1.8	0.004
AN/BA			9.6	10.3	8.7	0.007
AN/PBBA			15.6	16.7	3.3	0.052
BA/PBBA			1.4	1.14	1.3	-0.001

MONODISPERSE PS/MMAPBBA BLENDS

If the intramolecular repulsion in the MMAPBBA copolymers were large enough, that interaction could induce miscibility with low molecular weight polystyrenes. However, none of the MMAPBBA copolymers were miscible with polystyrene having a molecular weight of 2000 Da when blended in their predicted critical point compositions. These observations suggest that the ratio of MMA/PBBA to S/PBBA interaction energies is less than that suggested by both the critical molecular weight and self compatibility experiments. Figure 9.4 shows the miscibility observations for PS2 and PS4, and a predicted miscibility boundary based on $B_{MMA/PBBA}$=3.2, B_{SMMA}=0.3, and $B_{S/PBBA}$=1.95 cal/cm^3.

COPOLYMER/COPOLYMER BLENDS

Interactions with Poly(styrene-co-acrylonitrile)

Merfeld described the PBBA/acrylonitrile interaction by evaluating the phase behavior equal weight blends of styrene-stat-acrylonitrile (SAN) and MMAPBBA copolymers at 150 °C. These equal weight blends were made and characterized again for the current study using the SAN copolymers listed in Table 4.2. In addition to those SAN copolymers, a SAN copolymer having an AN content of 6.3 wt% and a molecular weight of 343,000 Da was also used. The region of single phase behavior noted in that study was found to be slightly different than previously stated.

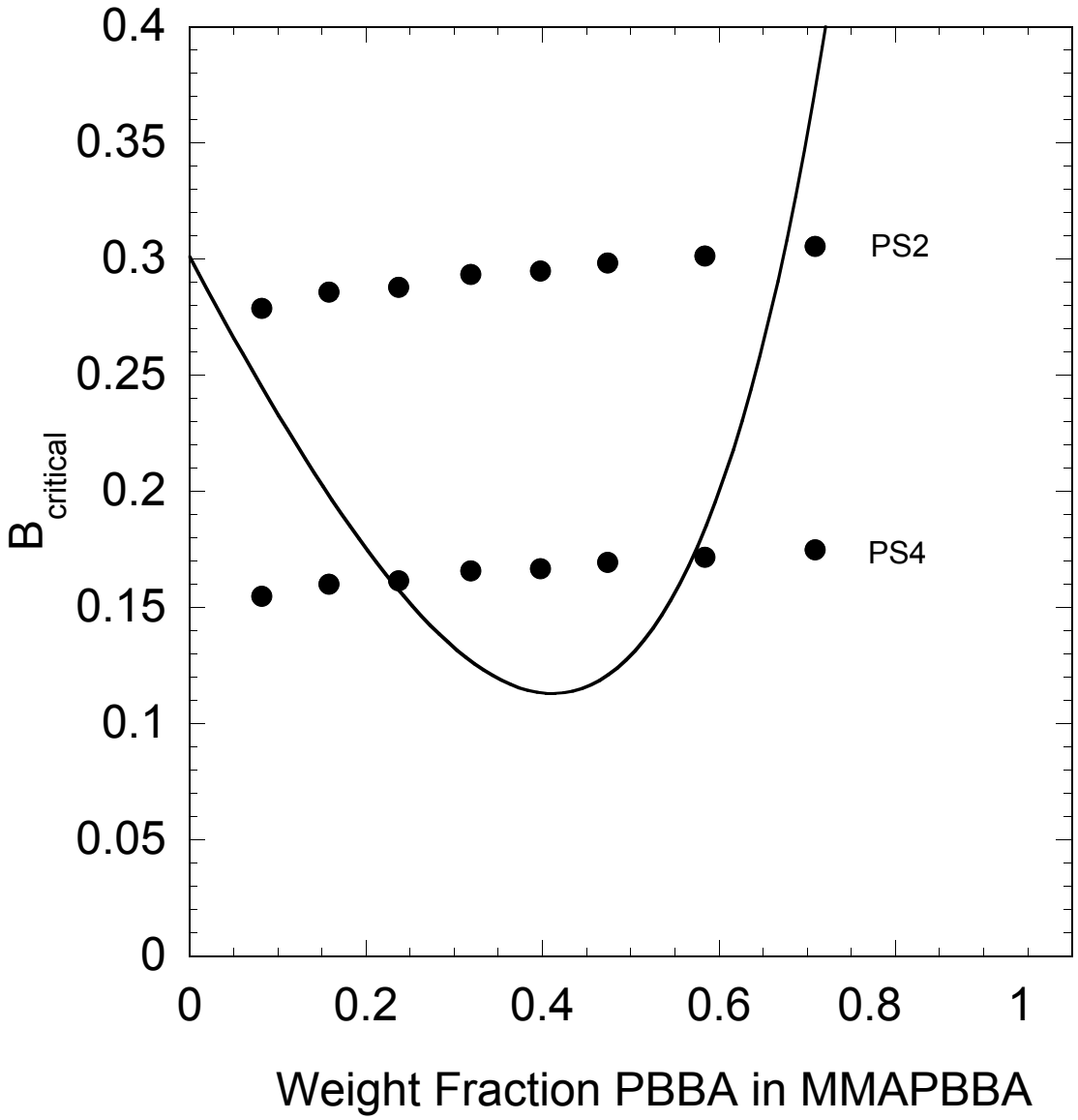

Figure 9.4 Phase behavior of monodisperse PS/MMAPBBA blends at the estimated critical point. All of the data corresponds to observations of two phase behavior. The curve was constructed using $B_{MMA/PBBA}$=3.2, $B_{S/MMA}$=0.30, and $B_{S/PBBA}$=1.95 cal/cm^3.

Figure 9.5 shows the phase behavior of the equal weight SAN/MMAPBBA blends. The curve was constructed from a best fit of the data, which corresponds to the copolymer-copolymer interactions listed in Table 9.4 and $B_{critical}$=0.01 cal/cm^3. The blends containing MMAPBBA10 and MMAPBBA20 were ignored when choosing interaction values since they contain ethyl acrylate.

Observations of equal weight blend phase behavior for SAN/MMABA blends are shown in Figure 9.6. The line was constructed using the copolymer-copolyemer interactions listed in Table 9.4 and $B_{critical}$=0.01 cal/cm^3. The MMA/BA, S/BA, and BA/AN interactions were varied such that a good fit of this and other copolymer-copolymer phase behavior containing these interactions was described well.

Figure 9.7 shows the phase behavior of equal weight SAN/SBA blends. The curve represents the copolymer-copolymer interactions listed in Table 9.4 and $B_{critical}$=0.01 cal/cm^3.

BA Copolymer/PBBA Copolymer Blends

The phase behavior of equal weight copolymer blends containing BA and PBBA were assessed to estimate the BA/PBBA interaction. In addition, these data sets allow further assessment of the interactions of S and MMA with BA and PBBA. Single phase blends were observed in SBA/MMAPBBA, MMABA/MMAPBBA, SBA/SPBBA and blends as shown in Figures 9.8-10. These figures also contain predicted miscibility regions using the copolymer-copolymer interactions listed in Table 9.4.

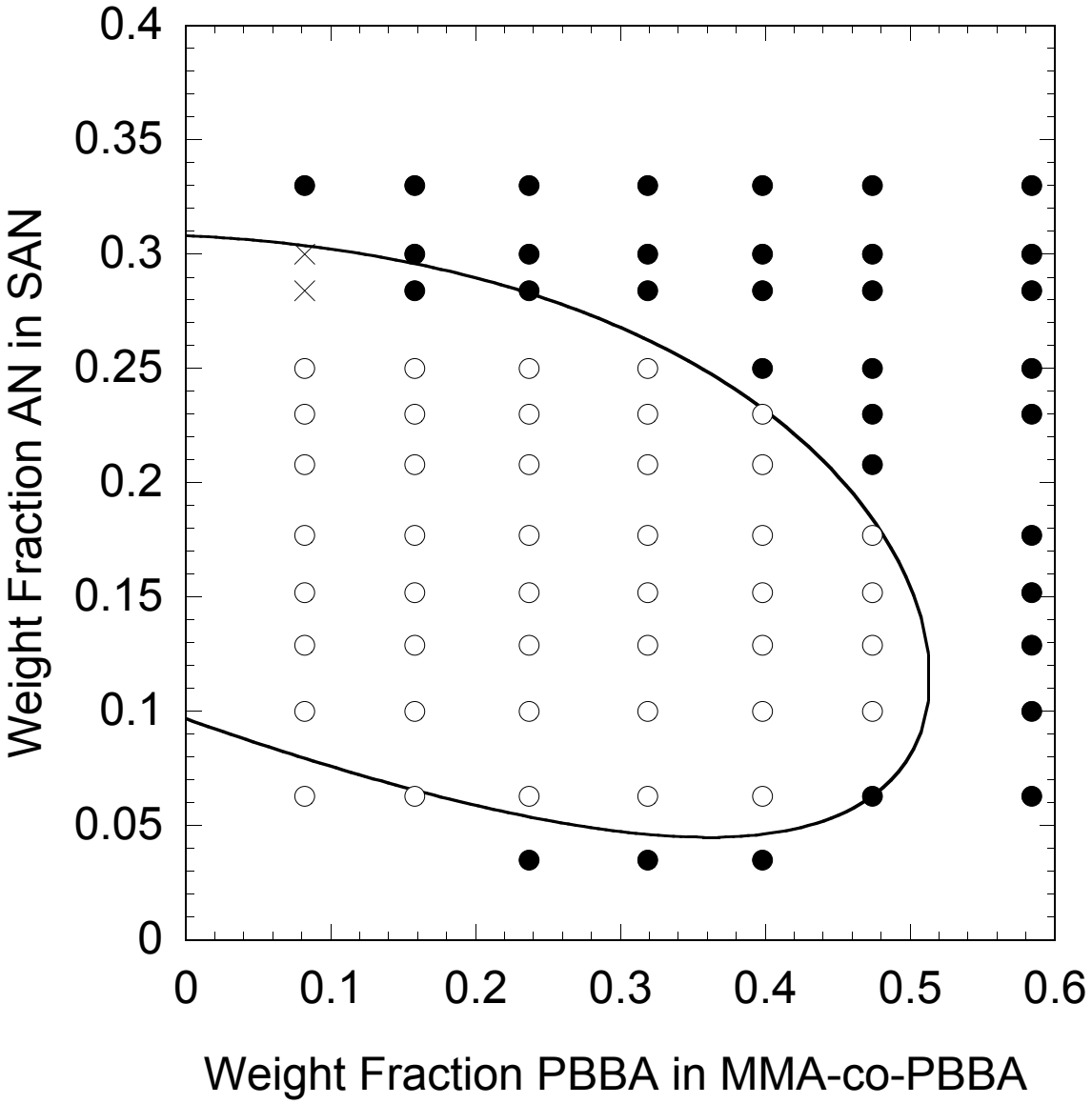

Figure 9.5 Phase behavior of equal weight SAN/MMAPBBA blends at 150°C. Open and closed circles represent single and two phase blends respectively. The two crosses indicate blends whose phase behavior could not be determined. The curve was constructed using $B_{MMA/PBBA}$=3.2, $B_{S/MMA}$=0.3, $B_{S/AN}$=12.1, $B_{PBBA/AN}$=15.6, $B_{S/PBBA}$=1.95, and $B_{critical}$=0.01 cal/cm^3.

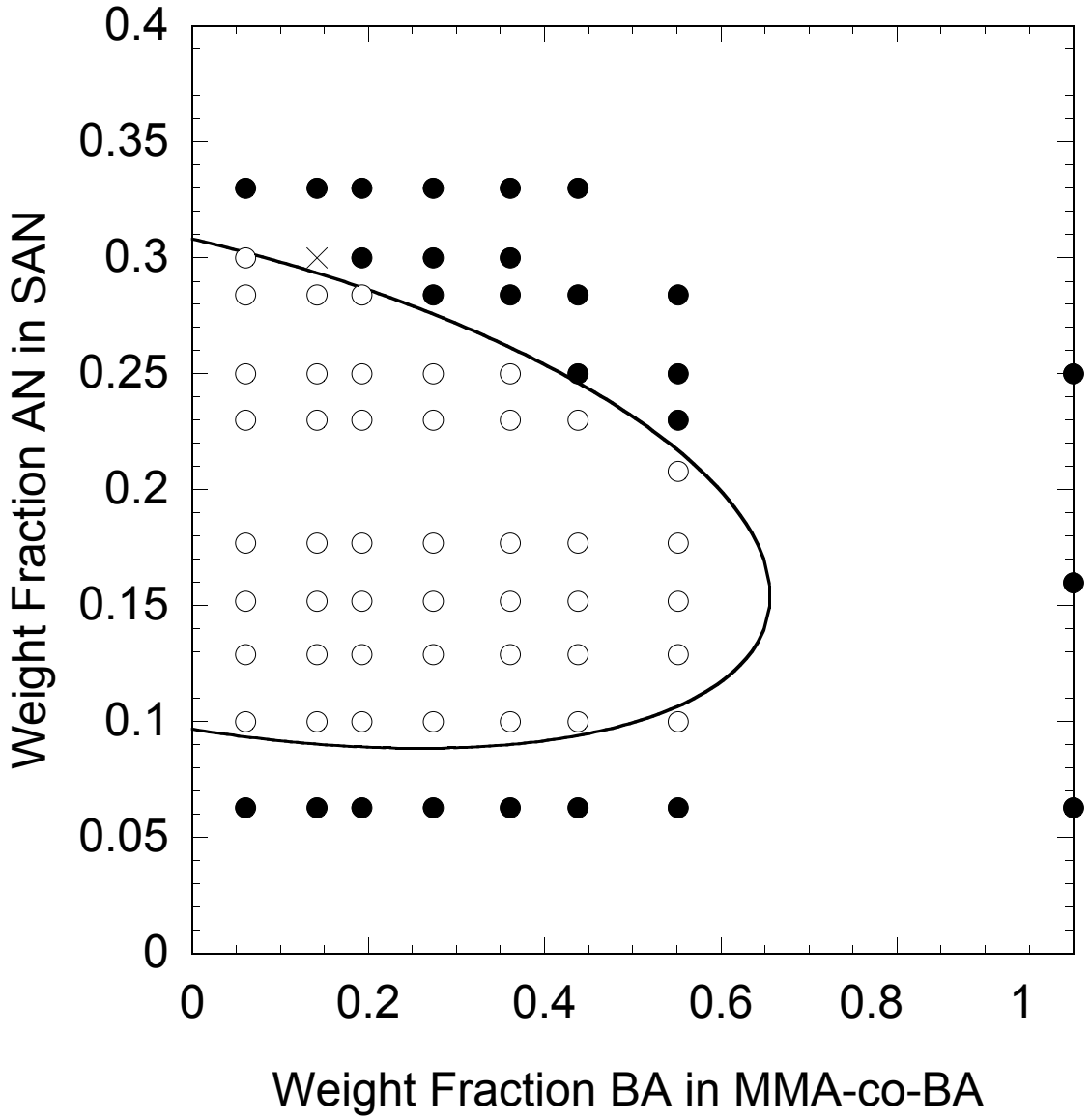

Figure 9.6 Observations of SAN/MMABA phase behavior. Open and closed circles represent single and two phase behavior respectively. The cross indicates a composition whose phase behavior could not be confidently assessed. The curve was constructed using $B_{MMA/BA}$=0.27, $B_{S/MMA}$=0.30, $B_{S/AN}$=12.1, $B_{BA/AN}$=9.6, $B_{S/BA}$=0.30, and $B_{critical}$=0.01 cal/cm^3.

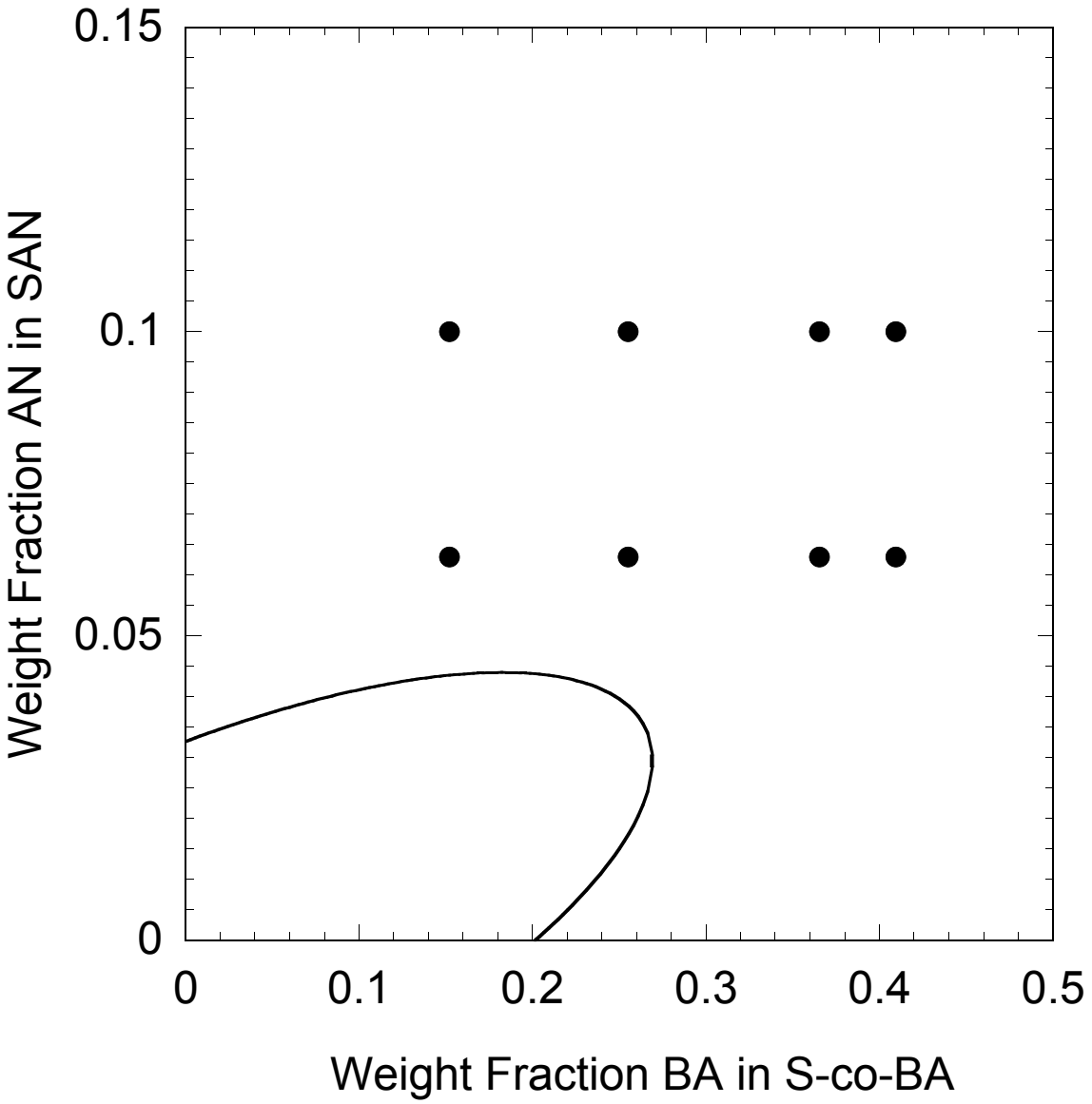

Figure 9.7 Observations of SAN/SBA phase behavior. Open and closed circles represent single and two phase behavior respectively. The curve was constructed using $B_{MMA/BA}$=0.27, $B_{S/MMA}$=0.30, $B_{S/AN}$=12.1, $B_{BA/AN}$=9.6, $B_{S/BA}$=0.30, and $B_{critical}$=0.01 cal/cm^3.

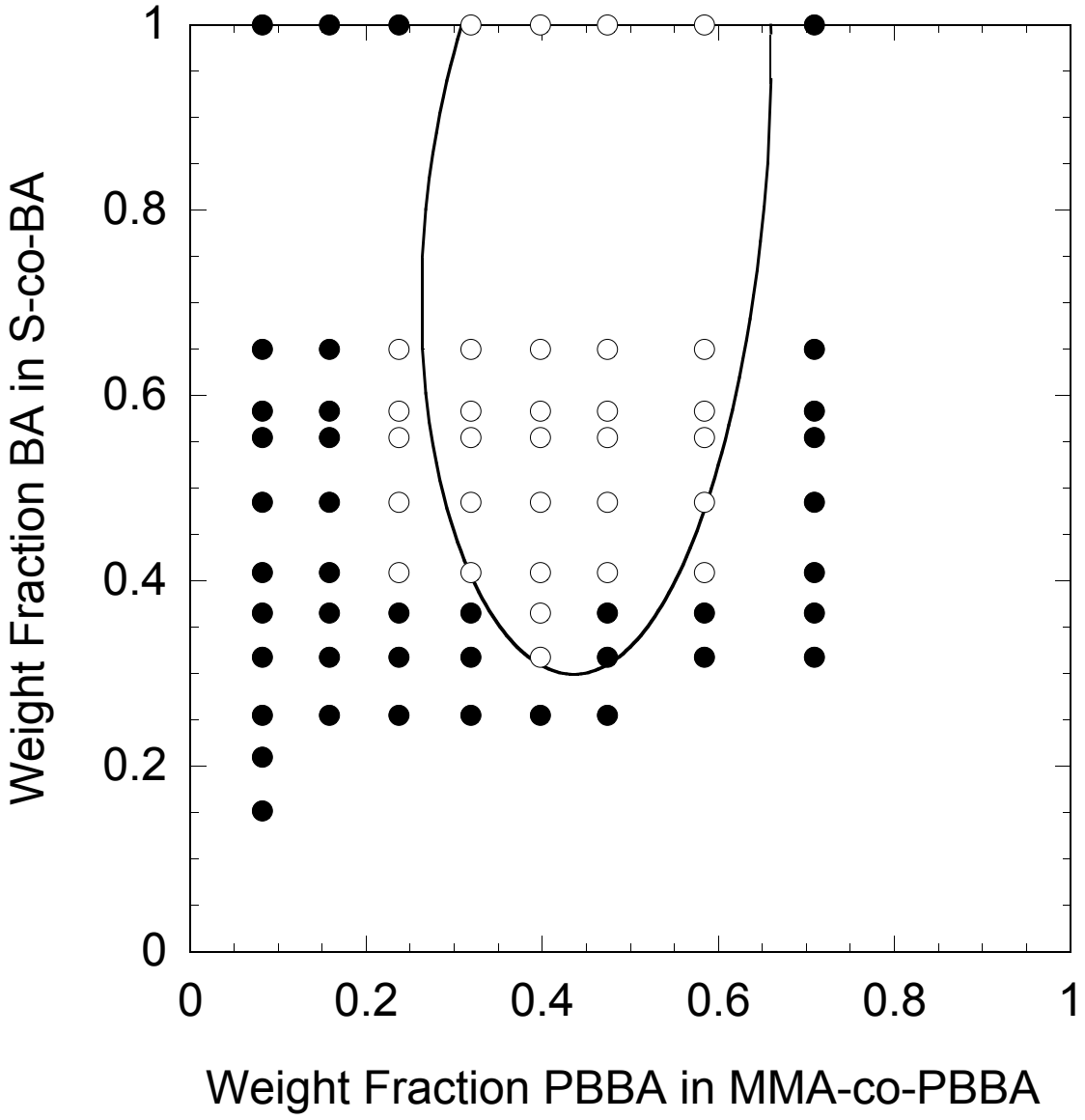

Figure 9.8 Observations of SBA/MMAPBBA phase behavior at 150 °C. Open and closed circles represent single and two phase behavior respectively. The curve was constructed using $B_{MMA/BA}$=0.27, $B_{S/MMA}$=0.30, $B_{S/PBBA}$=1.95, $B_{MMA/PBBA}$=3.2, $B_{S/BA}$=0.30, $B_{PBBA/BA}$=1.4, and $B_{critical}$=0.01 cal/cm^3.

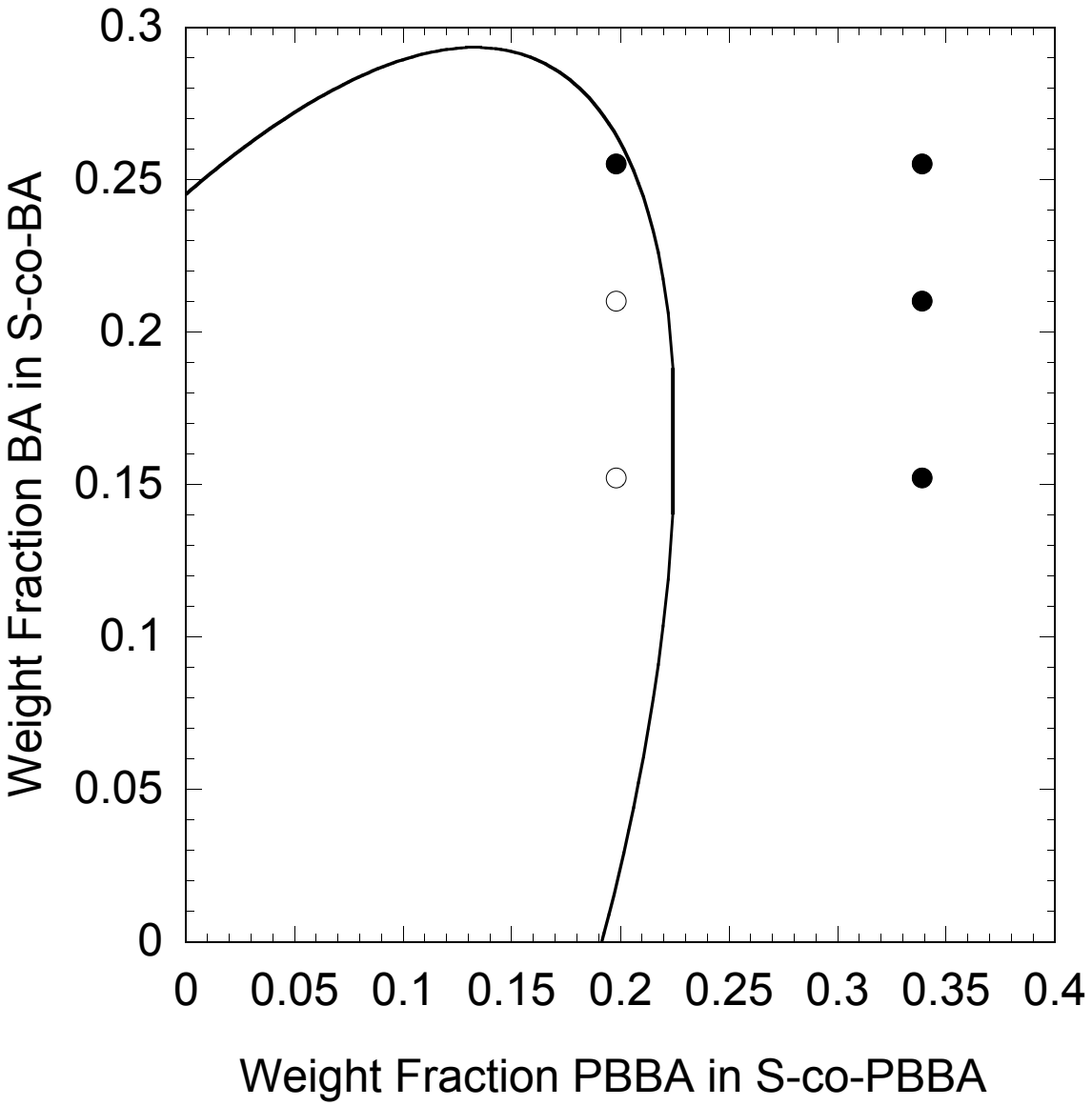

Figure 9.9 Observations of SBA/SPBBA phase behavior at 150 °C. Open and closed circles represent single and two phase behavior respectively. The curve was constructed using $B_{S/PBBA}$=1.95, $B_{S/BA}$=0.30, $B_{PBBA/BA}$=1.4, and $B_{critical}$=0.015 cal/cm^3.

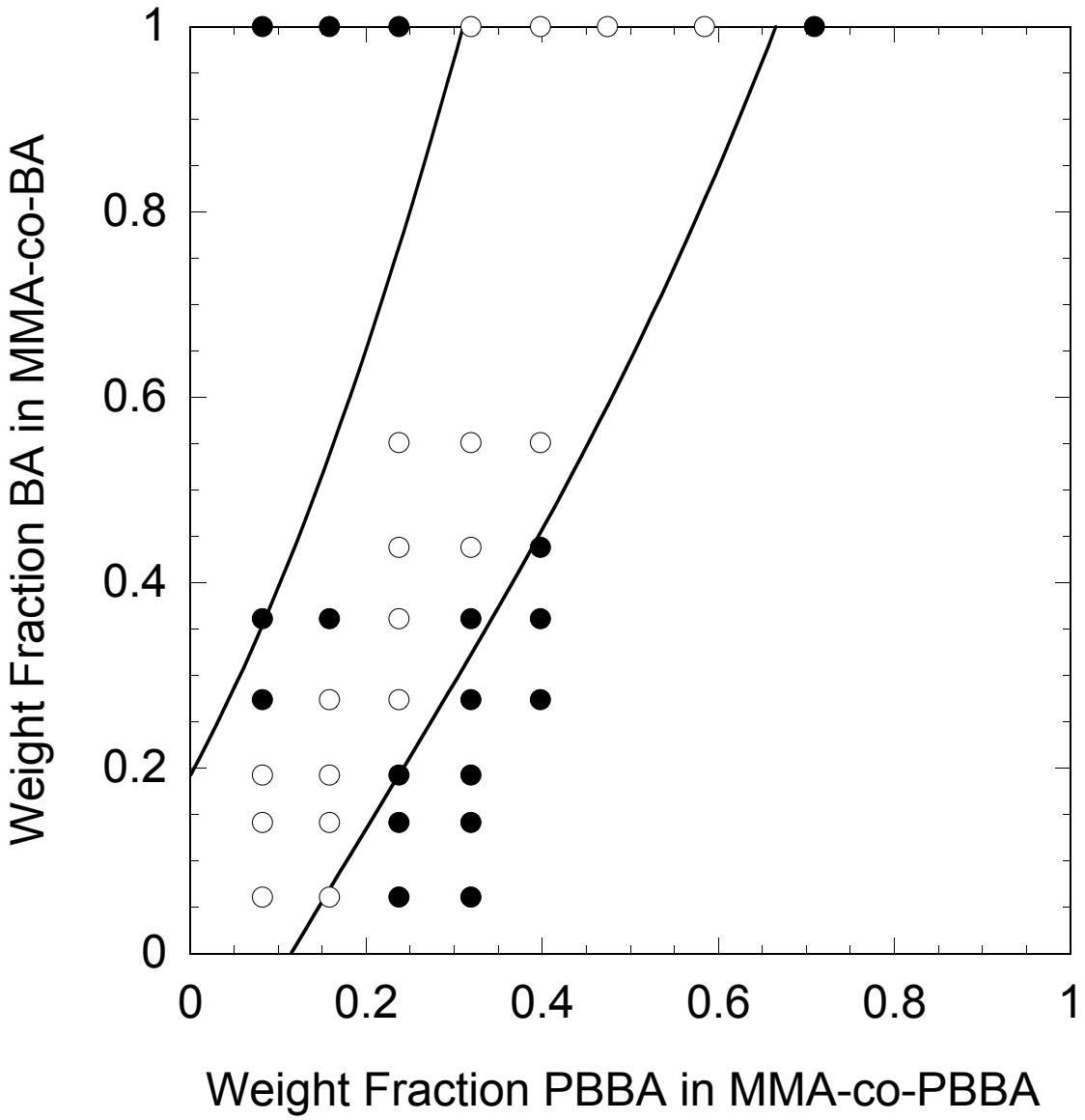

Figure 9.10 Observations of MMABA/MMAPBBA phase behavior at 150 °C. Open and closed circles represent single and two phase behavior respectively. The curve was constructed using $B_{MMA/BA}$=0.27, $B_{S/MMA}$=0.30, $B_{MMA/PBBA}$=3.2, $B_{PBBA/BA}$=1.4, and $B_{critical}$=0.01 cal/cm^3.

PREDICTED INTERACTIONS

Hoftzyer and van Krevelen and Fedors determined the effect of bromine substitution on cohesive energy density[3]. They determined that a single bromine substitution added 3708 and 3706 cal/mol respectively. The predictive capability of van Krevelen's group contribution methods for estimating cohesive energy densities of polymers is superior to that of Fedors. However, Fedor's study of bromine substitution was more detailed in that disubstitution and trisubstitution of bromine was studied. Fedors reported that disubstitution and trisubstitution resulted in the addition of 2950 and 2550 cal/mol to the cohesive energy density per bromine added. This data indicates a marginal decrease in cohesive energy addition per additional bromine substitution. If the group contributions are correlated to the number of bromine substitutions by a polynomial fit, there is a predicted minimum of 2479 cal/mol before the 4^{th} substitution. This value was used to calculate the cohesive energy densities of PBBA in conjunction with Hoftzyer and van Krevelen's group contribution method. The equation of state information in Appendix A was used to calculate the molar volume of PBBA at 150 °C. This information suggests that the solubility parameter for PBBA at 150 °C is 10.6 $(cal/cm^3)^{1/2}$.

This predicted PBBA solubility parameter was used in conjunction with others calculated by Hoftzyer and van Krevelen's group contribution methods to estimate the binary interactions as discussed in Chapter 2. The predicted interactions are listed in Table 9.3. The k_{ij} values were calculated based on these predictions and the bare interaction parameters listed in Table 9.3.

The bare interaction parameters determined from copolymer-copolymer miscibility were in reasonable agreement with interaction predictions with the exception

of the AN/PBBA interaction, which was much larger than predicted. The solubility parameters estimated through the framework of Hoftzyer and van Krevelen for PAN and PBBA, 12.3 and 10.6, are similar in magnitude. The addition of bromine increases the dispersion component of the solubility parameter, while the solubility parameter of PAN is composed primarily of its polar constituent. While the solubility parameters for PAN and PBBA are similar, they consist primarily of two different types of interaction components. The large disparity between predicted and inferred interactions may be due to the geometric mean assumption.

DISCUSSION

Differences in Interactions Deduced from Alternative Methods

There exists a large difference between the interactions derived by analysis of the homoplymer/copolymer and copolymer/copolymer blend phase behavior on a percentage basis. This is most noticeable between the two estimations of the S/BA interaction.

The molecular weights were determined by comparison of GPC elution volumes to polystyrene standards. An analysis of the predicted Mark-Houwink parameters for the BA homopolymer used in conjunction with the universal calibration curve indicates an underestimation of the BA homopolymer molecular weight if its elution volume is compared directly to that of polystyrene standards[3, 4]. An underestimation of molecular weights would result in a higher evaluation of the binary interactions by analysis of the phase behavior with monodisperse homopolymers. However, in the case of the monodisperse homopolymer/copolymer blends, the low molecular weight homopolymers are responsible for the greatest portion of the entropy of mixing. Even if the molecular weights of the SBA copolymers were doubled during the estimation of the

S/BA interaction from the PS/SBA phase behavior, the S/BA interaction would only change from 0.84 to 0.74 cal/cm^3. If the SBA molecular weights were doubled in the case of the self compatibility analysis, the implied S/BA interaction would change from 0.30 to 0.18 cal/cm^3. Therefore, the majority of the difference between the S/BA interactions derived from the PS/SBA and SBA/SBA phase behavior analysis is not likely to be caused by error in the estimation of SBA molecular weights.

The discrepancy between estimations of the S/BA interaction could also be related to the sequence distribution in the polymer chains. Chapter 6 illustrated an example of how treatment of a copolymer as having an alternating versus a random composition can result in different interactions when inferred through homopolymer/copolymer versus copolymer/copolymer blends. The discrepancy between interactions derived by homopolymer/copolymer and copolymer/copolymer blend analysis is the greatest for the S/BA interaction. Inspection of the reactivity ratios in Table 9.2 indicates that the BA monomer has a strong tendency towards alternation in the presence of styrene. Unlike the case of the purely alternating SMA copolymers, the alternation of the SBA copolymers is dependent on the copolymer composition. Hino et al. showed that a copolymer made from two unique monomers could be treated as terpolymer consisting of the three possible diad structures[5]. The terpolymer composition could be estimated from the copolymer reactivity ratios. Calculation of the predicted region of self miscibility for strongly alternating structures indicated a significant amount of curvature with respect to the copolymer/copolymer miscibility boundaries. The miscibility boundaries in Figure 9.3 have straight miscibility boundaries when viewed with respect to volume fractions. The limited data in Figure 9.3a suggests that curved miscibility boundaries are not needed to describe the experimentally determined self compatibility data. Unfortunately, SBA copolymers containing a high

amount of BA were not polymerized, and therefore ability to predict the self miscibility behavior cannot be evaluated over the full range of copolymer compositions.

Some of the discrepancy between interactions estimated by analysis of homopolymer/copolymer versus copolymer/copolymer studies may be related to assuming that the enthalpic interactions with low and high molecular weight homopolymers are equivalent. The lower molecular weight homopolymers have a larger volume fraction of end groups, which interact with other polymers differently than the rest of the polymer chain[6]. In addition, the equation of state properties may be significantly different between oligomers and high molecular weight polymers. These small differences may produce problems in estimating enthalpic interactions that are as small as the S/BA and MMA/BA interactions.

Dependency of the BA and PBBA Interactions on the S/AN Interaction

Difficulty in predicting the SAN/MMABA blend phase behavior while using the S/AN, S/MMA, and AN/MMA interactions of 6.98, 4.49, and 0.22 cal/cm^3 that had been used in the past prompted the investigation of the S/AN interaction presented in Chapters 4-6[1]. The S/BA and MMA/BA interactions required to accurately predict the experimentally determined phase behavior in SAN bends while using a lower S/AN interaction were not consistent with the trends in the predicted interactions or the interactions estimated from observations of hompolymer/copolymer, self compatibility, or copolymer/copolymer blends.

Three sets of binary interactions were used to predict the SAN/MMABA phase behavior shown in Figure 9.11. All three curves use the lower S/AN, S/MMA, and AN/MMA interactions. The first curve uses the S/BA, MMA/BA, and AN/BA interactions used previously to predict the SAN/MMABA phase behavior shown in

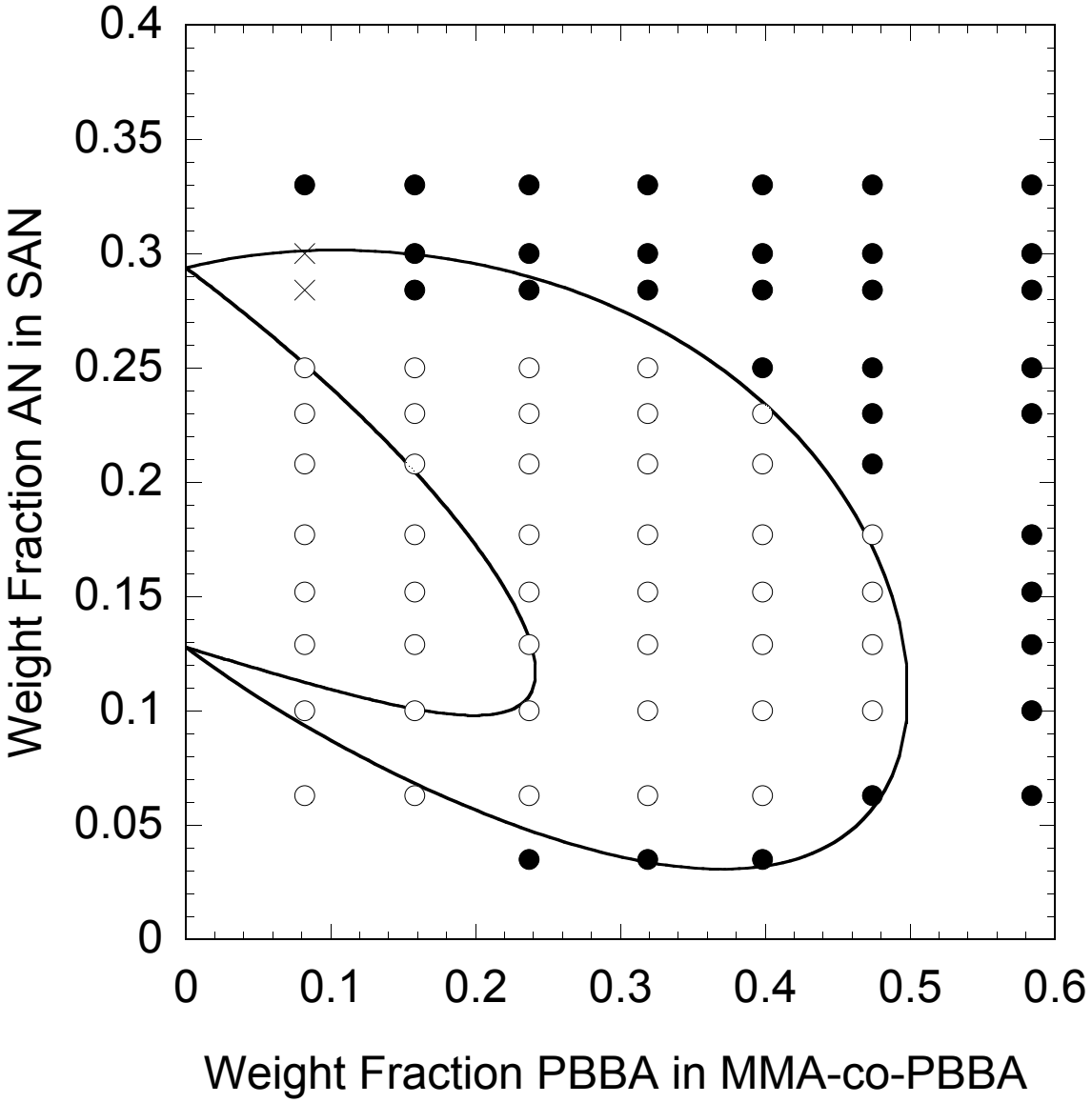

Figure 9.11 Observations of SAN/MMABA phase behavior at 150 °C. Open and closed circles represent single and two phase behavior respectively. The cross indicates a composition whose phase behavior could not be confidently assessed. The curve was constructed using $B_{S/AN}$=6.98, $B_{BA/AN}$=4.49, $B_{S/MMA}$=0.22, $B_{critical}$=0.01 cal/cm^3 and the interactions listed on the figure.

Figure 9.6. The second curve represents an adjustment of the AN/BA interaction such that the relative area of the experimentally determined miscibility region is represented. While the area of the single phase region is represented by those interactions, the curvature of the area with respect to increasing AN content is not well described. The third curve represents a change in the ratio of S/BA to MMA/BA interactions in addition to an adjustment in the AN/BA interaction such that the area of single phase behavior in addition to the curvature of the single phase area with respect to AN content is described. The resulting ratio of S/BA to MMA/BA interactions required for an accurate fit of this data indicates that the MMA/BA interaction is twice that of the S/BA interaction. Analysis of the predicted interactions and the homoplymer/copolymer, self compatibility, and copolymer-copolymer blend data all suggest that the S/BA interaction is higher than the MMA/BA interaction. These observations conflict with the S/BA to MMA/BA interaction ratio required to fit the SAN/MMABA blend phase behavior when using the lower S/AN, S/MMA, and AN/MMA interactions, but do not conflict with the S/BA to MMA/BA interaction ratios when using the S/AN and AN/MMA interactions estimated in Chapters 4 and 5.

The lower estimates of the S/AN, S/MMA, and AN/MMA interactions can be used in conjunction with the S/PBBA and MMA/PPBA interactions determined through self compatibility assessment to predict SAN/MMAPBBA phase behavior through modification of the AN/PBBA interaction. Figure 9.12 indicates the experimentally determined SAN/MMAPBBA phase behavior as shown in Figure9.5. The inner curve represents the prediction of phase behavior while using the lower S/AN, S/MMA, and AN/MMA interactions, and the MMA/PBBA, S/PBBA, and AN/PBBA interactions used

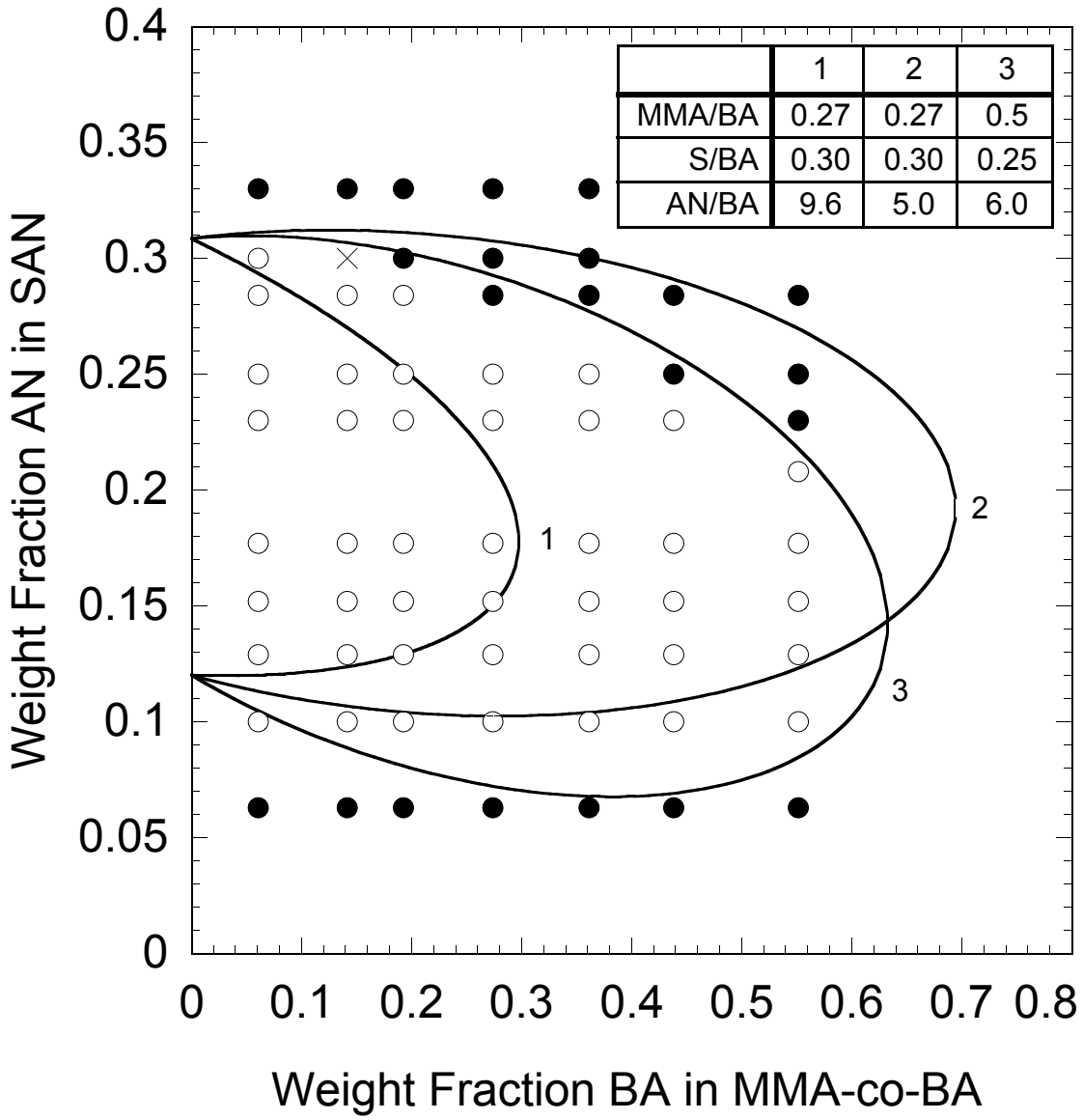

Figure 9.12 Observations of SAN/MMAPBBA phase behavior at 150 °C. Open and closed circles represent single and two phase behavior respectively. The crosses indicate compositions whose phase behavior could not be confidently assessed. The curve was constructed using $B_{MMA/PBBA}$=4.49, $B_{S/MMA}$=0.22, $B_{S/AN}$=6.98, $B_{PBBA/AN}$=15.6(inner curve) and 10.4(outer curve), $B_{S/PBBA}$=1.95, and $B_{critical}$=0.01 cal/cm^3.

to predict the phase behavior in Figure 9.5. The outer curve uses these same interactions except for the AN/PBBA interaction, which was changed to 10.4 cal/cm^3. A reasonable fit of this data is possible using the lower S/AN and accompanying values by the adjustment of the AN/PBBA interaction.

The two curves in Figure 9.13 represent predictions of miscible behavior in the SBA/MMAPBBA blends while using the BA and PBBA interactions determined from phase behavior of SAN blends while using the lower S/AN, S/MMA, and AN/MMA interactions. The inner and outer curves represent BA/PBBA interactions of 1.2 and 1.0 cal/cm^3 respectively. No choice of BA/PBBA interaction values results in an acceptable estimation of the SBA/MMAPBBA phase behavior. While some of the inability to predict the phase behavior may be a product of the error in estimating 6 interactions, the phase behavior between poly(benzyl acrylate) and the MMAPBBA copolymers, whose phase behavior is dictated by 3 binary interactions, is also poorly represented. Use of the BA/PBBA interaction that describes the PBA/MMAPBBA phase behavior well, 1.4 cal/cm^3, in conjunction with the interactions determined from the SAN blends while using the low S/AN interaction results in the prediction of no miscible SBA/MMAPBBA blends.

A set of S/BA and MMA/BA interactions can be used that satisfies the ratio requirement to fit the SAN/MMABA data, and a magnitude necessary to fit the SBA/MMAPBBA data. However, this set of interactions requires values for the S/BA and MMA/BA interactions that are substantially lower than the interactions implied by the self-miscibility and homopolymer/copolymer studies. These interactions also cannot be used to describe the SAN/SBA or SBA/MMAPBBA data. The only set of interactions that can be used to describe all of the copolymer-copolymer phase behavior as adequately

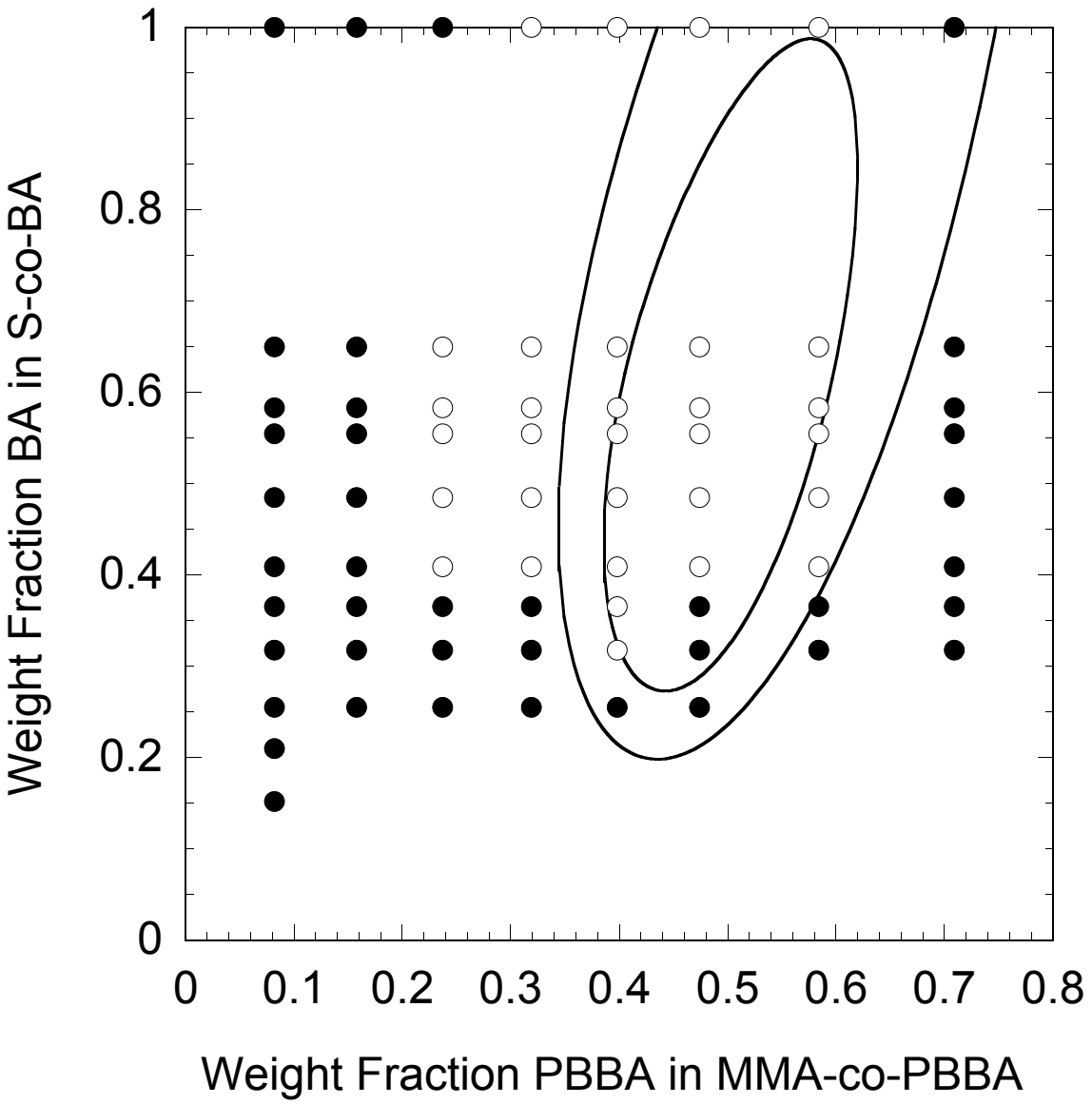

Figure 9.13 Observations of SBA/MMAPBBA phase behavior at 150 °C. Open and closed circles represent single and two phase behavior respectively. The curves were constructed using $B_{MMA/BA}$=0.5, $B_{S/MMA}$=0.22, $B_{S/PBBA}$=1.95, $B_{MMA/PBBA}$=3.2, $B_{S/BA}$=0.25, $B_{PBBA/BA}$=1.2(inner curve) and 1.0 (outer curve), and $B_{critical}$=0.01 cal/cm^3.

as shown in Figures 9.3 and 9.5-10, were those listed in Table 9.4. An adequate prediction of the observed phase behavior required that the S/BA interaction be greater than the MMA/BA interaction.

CONCLUSIONS

Copolymers containing benzyl acrylate (BA), styrene, and methyl methacrylate were synthesized and characterized. The phase behavior of these blends with monodisperse PS and PMMA, SAN, and with copolymers containing pentabromobenzyl acrylate (PBBA) was investigated. A set of interactions was determined that could be used to qualitatively predict the phase behavior in copolymer-copolymer blends containing benzyl acrylate and pentabromobenzyl acrylate(PBBA). These interactions were similar to the interactions predicted by the use of predicted solubility parameters and regular solution theory with the exception of the PBBA/AN interaction.

The S/BA and MMA/BA interactions determined from the analysis of copolymer-copolymer blend phase behavior conflicted with those obtained by the analysis of homopolymer/copolymer blend phase behavior. This discrepancy cannot be completely explained by error in copolymer molecular weight determination. The difference between these two inferred interactions correlates with the predicted amount of alternation in the copolymers. However, the available data for the self compatibility of the copolymers did not indicate that special treatment of the copolymers with respect to alternation was required. The source of the discrepancy between estimated interactions may be related to the assumption that the enthalpic interactions involving low or high molecular weight homopolymers are equivalent. Small errors due to any approximations may impair the ability to evaluate small enthalpic interactions such as the S/BA interaction.

REFERENCES

1. Merfeld, G.D., et al. Polymer 1999;41:663.
2. Merfeld, G.D., PhD Dissertation, 1998, University of Texas at Austin.
3. van Krevelen, D.E., 'Properties of polymers'. 3 ed., Elsevier Pub. Co., Amsterdam, 1990.
4. Barth, H.G. J. Polym. Sci. Polym. Phys. 1996;34:1705.
5. Hino, T., Y. Song, and J.M. Prausnitz, J.M. Macromolecules 1995;28:5709.
6. Callaghan, T.A. and Paul, D.R. J. Polym. Sci. Polym. Phys. 1994;32:1813.

Chapter 10: Conclusions and Recommendations

The following conclusions are summarized from the preceding chapters. Recommendations are then presented which offer some possible extensions of the work presented here.

CONCLUSIONS

The phase behavior of polymer blends was characterized with respect to binary interactions between monomer repeat units. This evaluation was conducted through the use of the Flory Huggins free energy model, mean field approximation, and attention to equation of state effects where appropriate. Estimations of binary interactions were compared to existing estimations, and predicted values when possible.

Experimental evidence presented in this work suggests that the repulsion between styrene (S) and acrylonitrile (AN) repeat units is significantly larger than previous estimates. The larger S/AN interaction that was introduced in Chapter 4 was successfully used in the prediction of phase behavior for numerous blends containing poly(styrene-co-acrylonitrile), as shown in Chapters 4, 5, 6, and 9. The S/AN interaction determined in this work is very close to the value predicted through regular solution theory using estimated solubility parameters. Binary interactions that were estimated from blend phase behavior while using the larger S/AN interaction were also much closer to their predicted values than those that had been previously reported.

Treatment of the repeating structure contained in poly(styrene-co-maleic anhydride) (SMA) played a significant role in the ability to predict the phase behavior in SMA blends. By treating copolymers of SMA as being comprised of styrene and (maleic

anhydride-styrene) (MA-S) repeat units, a single set of binary interactions can be used to accurately predict PS/SAN, PS/SMA, and SAN/SMA blend phase behavior. Analysis of the PS/SMA phase behavior conducted while treating the maleic anhydride repeat units as being randomly distributed throughout the polymer chain suggests a very large enthalpic interaction, which could not be used to accurately predict the SAN/SMA blend phase behavior.

Chapter 7 described a situation where changes light scattered by a polymer blend with changes temperature were associated with changes in the difference between blend component refractive indices rather than a phase transition. Several differences between the time resolved light scattering behavior in these blends versus the behavior expected during a phase transition were illustrated.

A set of binary interactions between benzyl acrylate (BA), pentabromobenzyl acrylate, methyl methacrylate, styrene and acrylonitrile repeat units was determined that could be used to qualitatively predict the observed phase behavior in several mixtures of copolymers containing these monomeric units. Significant differences between estimations of S/BA and MMA/BA binary interactions by interpretation of homopolymer/copolymer versus copolymer/copolymer blend phase behavior were observed. These differences may be related to monomer distribution or the error associated with estimations of small enthalpic interactions while using low molecular weight homopolymers.

RECOMMENDATIONS

To date, a large portion of our quantitative understanding of polymer-polymer interactions is based on significantly different interpretations of SAN and SMA phase behavior. A large body of polymer-polymer miscibility data exists that could be reanalyzed in the context of the larger S/AN interaction presented here. The adjusted

interactions deduced from these studies could be used to facilitate a correlation between chemical structures and deviations from predicted interaction values in terms of the k_{ij} values defined in Chapter 2.

The validity of the larger S/AN interaction presented in Chapter 4 could be further assessed through the evaluation of PS/SAN blend cloud point temperatures. Observation of reversible phase transitions would be useful in describing the equilibrium phase behavior of the PS/SAN blends. Polymer interfaces containing S/AN interactions have been probed by neutron reflectivity[1]. It would be interesting to see how the larger S/AN interaction would alter the analysis and conclusions associated with those projects.

The trends in n-alkyl acrylate interactions as a function of n-alkyl chain length discussed in Chapter 5 could be compared to trends in n-alkyl methacrylate interactions. This project would be also be beneficial in checking the predictive capability of the S/AN and S/methyl methacrylate interactions from Chapters 4 and 5.

The discrepancy between estimations of S/BA and methyl methacrylate (MMA)/BA interactions by assessment of homopolymer/copolymer versus copolymer/copolymer phase behavior could be investigated further. MMA/BA and S/BA copolymers containing larger amounts of BA could be synthesized so that the curvature of the self compatibility tests could be assessed more thoroughly. Cloud point temperatures associated with the self compatibility blends could also provide more information related to the phase behavior of these materials. This information could be used to assess whether the differences between methods of evaluating binary interactions are related to sequence distribution of the copolymers or the use of lower molecular weight homopolymers.

Tacticity has an effect on polymer-polymer miscibility, glass transition, permeation properties, and other physical parameters[2]. This is evident in several

industrially important blend systems such as PVC/PMMA and poly(ethylene oxide)/PMMA[3,4]. Atactic and syndiotactic PMMA have a more favorable interaction with PVC than does isotactic PMMA. Monodisperse PMMA samples are currently available in a range of molecular weights and tacticities. It is therefore possible to observe phase behavior of the PVC/PMMA blend system by changing the molecular weights of the constituents while maintaining a controlled tacticity. The Flory-Huggins-Staverman theory was developed to account for the effects of tacticity by evaluating the change in configurational entropy, surface area, and volume due to variation in tacticity[5]. It would be interesting to compare this approach to the treatment of the PMMA copolymer as being a terpolymer of diad structures which has been suggested by Hino to account for the effects of screening[6].

REFERENCES

1. Merfeld, G.D., *et al.* J. Polym. Sci. Polym. Phys. 1998;36:3115.
2. Min, K.E. and Paul, D.R., J. Polym. Sci. Polym. Phys. 1988;26:1021.
3. Vorenkamp, E.J., *et al*. Polymer 1985;26:1725.
4. Silvestre, C., *et al*. Polymer, 1987. 28: p. 1190.
5. Staverman, A.J., '*Integration of Fundamental Polymer Science and Technology'*, ed. Kleintjens, L.A. and Lemstra, P.J. 1986, London: Elsevier.
6. Hino, T., Song, Y. and Prausnitz, J.M. Macromolecules 1995;28:5709.

Appendix A – Equation of State Properties

Table A.1 Sanchez Lacombe Equation of State parameters

	Source	T* (K)	P* (MPa)	ρ* (g/cm3)	Temperature Range (°C)	Max. Pressure (Mpa)
Polyacrylonitrile (PAN)	[1]	853	535.7	1.2299	150-200	50
Polystyrene (PS)	[2]	751	397	1.109	150-200	50
Poly(methyl methacrylate) (PMMA)	[1]	728	503.0	1.2601	150-200	50
Poly(methyl acrylate) (PmeA)	[3]	664	558.1	1.2349	37-220	50
Poly(ethyl acrylate) (PEA)	[3]	640	401.4	1.1857	37-217	50
Poly(n-propyl acrylate) (PnPA)	[4]	702	339.5	1.1630	120-210	100
Poly(n-butyl acrylate) (PnBA)	[5]	646	378.8	1.1459	150-210	200
Poly(n-hexyl acrylate) (PnHA)	[4]	659	339.0	1.10914	120-210	100
Poly(n-decyl acrylate) (PnDA)	[4]	686	337.0	1.0340	120-210	100
Poly(styrene-co-maleic anhydride) 14wt%MA (SMA14)	[2]	754	422	1.171	150-200	50
Poly(styrene-co-maleic anhydride) 18wt%MA (SMA18)	[2]	757	457	1.186	150-200	50
Poly(styrene-co-maleic anhydride) 25 wt%MA (SMA25)	[2]	786	437	1.213	150-200	50
Hypothetical Poly(maleic anhydride)(MA)	[6]	832	656	1.540	180-230	
Combined (MA-S) (from extrapolation)		929	492	1.3064		
Poly (benzyl acrylate) (BA)		785	471	1.239	200-280	50
Poly (pentabromobenzyl acrylate) (PBBA) (recalculated from data)	[7]	937	540	2.614	200-280	50

Table A.1 Sources

1. Kim, C.K. and Paul, D.R. Polymer 1992;33:2089.
2. Gan, P.P. and Paul, D.R. J. of App. Polym. Sci. 1994;54:317.
3. Rodgers, P.A., J. App. Polym. Sci. 1993;48:1061.
4. Zhu, S. and Paul, D.R. Macromolecules 2002;35:8227.
5. Chu, J.H. and Paul, D.R. Polymer 1999;40:2687.
6. Merfeld, G.D. and Paul, D.R. Polymer 1998;39:1999.
7. Merfeld, G.D., PhD Dissertation. 1998, University of Texas at Austin.

Table A.2 PVT Data for Poly(benzyl acrylate)

Pressure (Mpa)	10	20	30	40	50	60	70	80	90	100
(°C)	30.5	30.6	30.6	30.6	30.6	30.7	30.8	30.9	30.9	30.9
$(cm^3/g)*10^4$	8222	8180	8150	8120	8091	8064	8038	8017	7989	7967
(°C)	56.4	56.6	56.6	56.7	56.6	56.6	56.7	56.7	56.7	56.6
$(cm^3/g)*10^4$	8350	8310	8273	8241	8210	8183	8153	8128	8102	8078
(°C)	81.1	81.5	81.4	81.5	81.5	81.6	81.7	81.7	81.8	81.8
$(cm^3/g)*10^4$	8453	8411	8373	8338	8306	8275	8246	8218	8191	8165
(°C)	100.8	101.0	100.9	101.1	101.0	101.1	101.1	101.2	101.2	101.3
$(cm^3/g)*10^4$	8540	8488	8450	8415	8379	8347	8315	8287	8259	8229
(°C)	120.2	120.3	120.4	120.7	120.8	121.0	121.0	121.0	121.0	121.2
$(cm^3/g)*10^4$	8620	8570	8528	8491	8453	8422	8389	8359	8328	8301
(°C)	139.3	139.6	139.6	139.4	139.5	139.4	139.4	139.7	139.7	139.6
$(cm^3/g)*10^4$	8711	8653	8607	8565	8529	8492	8458	8426	8394	8364
(°C)	157.8	158.3	158.4	158.5	158.5	158.8	158.9	159.0	159.0	159.2
$(cm^3/g)*10^4$	8801	8745	8694	8650	8611	8574	8539	8504	8471	8441
(°C)	176.5	176.8	177.1	177.2	177.5	177.7	177.8	177.8	178.0	178.4
$(cm^3/g)*10^4$	8893	8829	8778	8734	8692	8653	8616	8580	8547	8516
(°C)	203.9	204.4	204.6	204.4	204.1	204.2	204.4	204.6	204.7	204.8
$(cm^3/g)*10^4$	9040	8974	8914	8862	8811	8771	8729	8691	8655	8621
(°C)	222.2	222.3	222.3	222.5	222.8	222.8	223.1	223.4	223.2	223.3
$(cm^3/g)*10^4$	9140	9063	9002	8947	8900	8855	8814	8770	8733	8695
(°C)	240.5	241.2	241.2	240.8	240.8	241.1	241.4	241.5	241.8	241.9
$(cm^3/g)*10^4$	9243	9159	9094	9035	8983	8932	8887	8844	8805	8766
(°C)	259.1	259.6	260.0	260.2	260.2	260.3	260.4	260.5	260.5	260.7
$(cm^3/g)*10^4$	9343	9266	9189	9130	9072	9020	8971	8925	8881	8842
(°C)	277.3	278.1	278.2	278.0	278.0	278.5	278.8	278.9	279.2	279.5
$(cm^3/g)*10^4$	9447	9363	9277	9211	9153	9097	9046	8988	8955	8910

Table A.3 PVT Data for Poly(bisphenol-A-1,1-bis(4-hydroxyphenyl)-3,3,5-trimethylcyclohexanone)

Pressure (Mpa)	10	20	30	40	50	60	70	80	90	100
(°C)	30.0	30.2	30.2	30.4	30.5	30.5				
$(cm^3/g)*10^4$	9327	9293	9265	9238	9213	9188				
(°C)	53.0	53.2	53.2	53.3	53.5	53.6				
$(cm^3/g)*10^4$	9459	9424	9396	9369	9341	9312				
(°C)	71.7	72.1	72.4	72.6	72.7	72.8				
$(cm^3/g)*10^4$	9396	9364	9334	9308	9281	9254				
(°C)	99.9	100.3	100.7	100.9	101.0	101.1				
$(cm^3/g)*10^4$	9470	9437	9407	9379	9350	9322				
(°C)	127.7	128.2	128.6	128.9	129.1	129.3				
$(cm^3/g)*10^4$	9492	9455	9425	9395	9367	9339				
(°C)	154.3	155.0	155.3	155.8	156.1	156.1				
$(cm^3/g)*10^4$	9535	9513	9478	9449	9417	9450				
(°C)	181.2	181.5	182	182.4	182.6	182.9				
$(cm^3/g)*10^4$	9610	9562	9533	9504	9466	9444				
(°C)	207.2	207.7	208.1	208.6	208.6	208.8				
$(cm^3/g)*10^4$	9690	9632	9590	9557	9523	9490				
(°C)	232.8	233.1	233.8	234.2	234.4	234.7	234.9	235.2	235.2	235.4
$(cm^3/g)*10^4$	9823	9731	9673	9617	9568	9527	9491	9458	9428	9398
(°C)	250.6	251.4	251.7	252.1	252.3	252.6	252.8	252.9	253.1	253.3
$(cm^3/g)*10^4$	9936	9841	9772	9710	9650	9597	9547	9501	9461	9427
(°C)	269.2	270.0	270.4	270.8	271.0	271.3	271.6	271.8	272.0	272.1
$(cm^3/g)*10^4$	10059	9956	9880	9813	9750	9694	9639	9588	9540	9493
(°C)	287.7	288.4	288.9	289.1	289.5	289.6	289.9	290.0	290.1	290.3
$(cm^3/g)*10^4$	10201	10084	9999	9928	9860	9797	9740	9685	9634	9583

Bibliography

Aelmans, N.J.J., Reid V.M.C., and Higgins J.S. Polymer 1999;40:5051.

Aokj, Y., Macromolecules 1988;21:1277.

Avakian, R.W. and Allen, R.B. Polym. Eng. Sci. 1985;25:462.

Barnum, R.S., Barlow, J.W. and Paul, D.R. J. of Appl. Polym. Sci. 1982;27:4065.

Barth, H.G. J. Polym. Sci. Polym. Phys. 1996;34:1705.

Bell, S.Y., Cowie, J.M.G. and McEwen, I.J. Polymer 1994;35:786.

Bicerano, J., 'Prediction of Polymer Properties' Marcel Dekker, Inc., New York, 2002.

Bidkar, U.R. and Sanchez, I.C. Macromolecules, 1995;28:3963.

Binder, K. and D. Stauffer, Phys. Rev. Lett. 1974;33:1006.

Bogdanic, G., et al., Fluid Phase Equilibria 1997;139:277.

Bohn, L., 'Compatible Polymers', in 'Polymer Handbook', Brandrup J. and Immergut, E.H. eds, Wiley, New York, 1975.

Brannock, G.R., Barlow, J.W. and D.R. Paul, D.R. J. Polym. Sci. Polym. Phys. 1990;28:871.

Brannock, G.R. and Paul, D.R. Macromolecules 1990;23:5240.

Brinke, G.T., Karasz, F.E.,and MacKnight, W.J. Macromolecules 1983;16:1827.

Cahn, J.W. and J.E. Hillard J. Chem. Phys. 1958;28:258.

Cahn, J.W. J. Chem. Phys. 1965;42:93.

Callaghan, T.A., PhD Dissertation, 1992, The University of Texas at Austin.

Callaghan, T.A. and Paul, D.R. Macromolecules 1993;26:2439.

Callaghan, T.A., et al. Polymer 1993; 34:3796.

Callaghan, T.A. and Paul, D.R. J. Polym. Sci. Polym. Phys. 1994;32:1813.

Campbell, J.A., Goodwin, A.A. and Simon, G.P. Polymer 2001;42:4731.

Casper, R. and Morbitzer, L. Angewandte Makromol. Chem. 1977;58-59:1.

Chopra, D. and Vlassopoulos, D. J. Rheol. 1998;42:1227.

Chu, J.H. and Paul, D.R, Polymer 1999;40:2687.

Chu, J.H., Tilakaratne, H.K., and Paul, D.R. Polymer, 2000;41:5393.

Chu, J. and Paul, D.R. Polymer, 2000;41:7193.

Cowie, J.M.G. and D. Lath, Makromol. Chem. Macromol. Symp. 1988;16;103.

Cowie, J.M.G., et al. Polym. Comm. 1991;32:293.

Cowie, J.M.G., Harris, J.H. and McEwen, I.J. Macromolecules 1992;25:5287.

Cruz, C.A., Barlow, J.W. and Paul, D.R. Macromolecules 1979;12:726.

Dodgson, K. and Ebdon, J.R. Eur. Polym. J. 1977;13:791.

Fernandes, A.C., Barlow, J.W. and Paul, D.R. Polymer 1986;27:1788.

Fernandez, M.L. and Higgins J.S., ACS Symp. Ser. 1995;597:106.

Fernandez, M.L., et al., Polymer, 1995;36:149.

Gan, P.P., Paul, D.R. and Padwa, A.R. Polymer 1994;35:1487.

Gan, P.P. and Paul D.R. J. App. Polym. Sci., 1994;54:317.

Guo, W. and J.S. Higgins Polymer 1990;31:699.

Flory, P.J., J. Chem. Phys. 1942;10:51.

Haggard, K.W. and Paul, D.R. Polymer. 2002;43;3727.

Haggard, K.W. and Paul, D.R. Polymer 2004;45:2313.

Hall, W.J., et al., Prepr. Am. Chem. Soc. Div. Org. Coatings Plast. Chem., 1982;47:298.

Hall, W.J., et al., Am. Chem. Soc. Symp. Ser. 1983;49:229.

Hashimoto, T. Phase Transitions 1988;12:47.

Hildebrand, J.H. and Scott, R.L., 'The Solubility of Nonelectrolytes'. 3 ed. 1950.

Hindawi, I.A., Higgins J.S., and. Weiss, R.A. Polymer 1991;33:2522.

Hino, T., Song, Y. and Prausnitz, J.M. Macromolecules 1995;28:5709.

Huggins, M.L., J. Chem. Phys. 1941;9:440.

Humme, G., Roehr, H. and Serini, V Angewandte Makromol. Chem. 1977;58-59:85.

Joseph, E.A., et al.Polymer 1982;23:112.

Kambour, R.P., Bendler, J.T., and Bopp, R.C., Macromolecules 1983; 16:753.

Kim, J.H., Barlow, J.W., and Paul, D.R. J. Polym. Sci. Polym. Phys. 1989;27:223.

Kim, C.K. and Paul, D.R. Polymer 1992;33:1630.

Kim, C.K. and Paul, D.R. Polymer, 1992;33:2089.

Kim, C.K. and Paul, D.R. Macromolecules 1992;25:3097.

Koberstein, J., Russell, T.P. and Stein, R.S. J. Poly. Sci. Polym. Phys. 1979;17:1719.

Koningsveld, R. and Kleintjens, L.A. J. Polym. Sci. Polym. Sym. 1977;61:221.

Lacombe, R.H. and Sanchez, I.C. J. Phys. Chem. 1976;80:2568.

Lorentz, H.A., Wied. Ann. Phys. 1880;9:641.

Lorenz, L.V., Wied. Ann. Phys. 1880;11:70.

Luengo, G., et al., Macromol. Chem. Phys. 1994;195:1043.

Mason, J.P. Canada Patent No. 2113501; 1994. Assigned to Miles Laboratories, Inc., USA.

Mason, J.P. and Pyles, R.A. United States Patent No. 5461120; 1995. Assigned to Bayer A.-G., USA.

Massa, D.J., O'Reilly, J.M. and Chen, W.A. United States Patent No. 5925507; 1999. Assigned to Eastman Kodak Company, USA.

Merfeld, G.D. and Paul, D.R. Polymer, 1998. 39:1999.

Merfeld, G.D., *et al.* J. Polym. Sci. Polym. Phys. 1998;**36**:3115.

Merfeld, G.D. and Paul, D.R. Polymer 1999;41:649.

Merfeld, G.D., et al. Polymer 1999;41:663.

Merfeld, G.D., Chan, K. and Paul, D.R. Macromolecules, 1999;32:429.

Merfeld, G.D., PhD Dissertation, 1998, University of Texas at Austin.

Merfeld, G.D. and Paul, D.R.'Polymer-Polymer Interactions Based on Mean Field Approximations', in Polymer Blends, Paul, D.R. and Bucknall, C.B. eds., John Wiley & Sons, Inc., New York. 2000;55.

Min, K.E. and Paul, D.R., J. Polym. Sci. Polym. Phys. 1988;**26**:1021.

Mohn, R.N., et al. J. Appl. Polym. Sci. 1979;23:575.

Nandi, A.K., Mandal, B.M. and Bhattacharyya, S.N. Macromolecules 1985;18:1454.

Nishimoto, M., Keskkula, H., and Paul, D.R. Polymer 1991;32:272.

Okamoto, M., K. Shiomi, and T. Inoue Polymer 1995;36:87.

Panayiotou, C. and Sanchez, I.C. Macromolecules 1991;24:6231.

Panayiotou, C. and Sanchez, I.C. Polym. Pre. 1992;33:567.

Paul, D.R. and Barlow, J.W. Polymer 1984;25:487.

Paul, D.R. and Bucknall, C.B. eds. 'Polymer Blends' 2 ed. Volume 1, Vol. 1. John Wiley & Sons, Inc., New York, 2000.

Paul, W.G. and Bier, P.N. Annu. Tech. Conf.-Soc. Plast Eng. 1994;2:1759.

Prausnitz, J.M., Lichtenthaler, R.N. and Gomez de Azevedo, E., 'Molecular Thermodynamics of Fluid-Phase Equilibria' 2 Ed. Prentice-Hall, Englewood Cliffs, N.J., 1986.

Rodgers, P.A., J. App. Polym. Sci. 1993;48:1061.

Sanchez, I.C. and Lacombe, R.H. J. Chem. Phys. 1976;80:2353.

Sanchez, I.C. and Lacombe, R.H. J. Polym. Sci., Polym. Lett. Ed. 1977;15:71.

Sanchez, I.C. and Lacombe, R.H. Macromolecules 1978;1:1145.

Scott, C.E., Bradley, J.C. and Rodney, J. United States Patent No. 6043322; 2000. Assigned to Eastman Chemical Co., USA.

Shaw, M.T., J. of Appl. Polym. Sci. 1974;18:449.

Silvestre, C., *et al*. Polymer, 1987. **28**: p. 1190.

Smith, W.A., Barlow, J.W. and Paul, D.R. J. Appl. Polym. Sci., 1981;26:4233.

Staverman, A.J., 'Integration of Fundamental Polymer Science and Technology', ed. Kleintjens, L.A. and Lemstra, P.J. Elsevier Pub. Co., London, 1986.

Takeda, Y. and Paul, D.R. Polymer 1991;32:2771.

van Krevelen, D.E., 'Properties of polymers'. 3 ed., Elsevier Pub. Co., Amsterdam, 1990.

van Laar, J.J. Baarn., Z. physik. Chem., 1910;72:723.

Vanhee, S., et al. Macromolecules 2000;33:3924.

Vorenkamp, E.J., *et al*. Polymer 1985;**26**:1725.

Walsh, D.J., Lainghe, S, and Zhikuan, C. Polymer 1981;22:1005.

Walsh, D.J., Higgins, J.S., and Zhikuan, C. Polymer 1982;23:336.

Wisniewsky, C., Marin, G. and Monge, P. Eur. Polym. J. 1984;20:691.

Woo, E.M., Barlow, J.W. and Paul, D.R. J. Polym. Sci., Polym. Symp. 1984;71:137.

Yee, A.F. and Maxwell, M.A. J. Macromol. Sci. Phys. 1980;B17:543.

Zeman, L. and Patterson, D. Macromolecules 1972;5:513.

Ziaee, PhD Dissertation, 1995, The University of Texas at Austin.

Zhu, S. and Paul, D.R. Macromolecules 2002;35:2078.

Zhu, S. and Paul, D.R. Macromolecules 2002;35:8227.

Zhu, S. and Paul, D.R. Polymer 2003;44:3009.

Zhu, S. and Paul, D.R., Polymer 2003;44:5671.

Zhu, S. PhD Dissertation, 2003, The University of Texas at Austin.

Vita

Kris Wilcox Haggard was born in Wilmington, North Carolina on February 26, 1976, the son of Robert Howard Haggard and Rachael Ann Haggard. After graduation from Lovell High School in Lovell, Wyoming in 1994, he entered New Mexico Institute of Mining and Technology in Socorro, New Mexico. During the summer of 1997, he was an intern at the research division of Shell Chemical Company in Houston, Texas. He received the degree of Bachelor of Science from New Mexico Institute of Mining and Technology in May of 1998. In August of 1998 he entered the Graduate School of The University of Texas at Austin.

Permanent address: 3338 West Mesquite St., Phoenix, AZ 85086

This dissertation was typed by the author.